University of Bath

PHD

The role of alpha-lactones and cognate species in organic reactivity

Robinson, James Justin

Award date:
2005

Awarding institution:
University of Bath

Link to publication

General rights
Copyright and moral rights for the publications made accessible in the public portal are retained by the authors and/or other copyright owners and it is a condition of accessing publications that users recognise and abide by the legal requirements associated with these rights.

- Users may download and print one copy of any publication from the public portal for the purpose of private study or research.
- You may not further distribute the material or use it for any profit-making activity or commercial gain
- You may freely distribute the URL identifying the publication in the public portal ?

Take down policy
If you believe that this document breaches copyright please contact us providing details, and we will remove access to the work immediately and investigate your claim.

Download date: 13. May. 2019

The role of α-lactones and cognate species in organic reactivity

Submitted by

James Justin Robinson BSc(HONS) MRSC

For the degree of PhD of the University of Bath

2005

COPYRIGHT

Attention is drawn to the fact that copyright of this thesis rests with its author. This copy of the thesis has been supplied on condition that anyone who consults it is understood to recognise that its copyright rests with its author and that no quotation from the thesis and no information derived from it may be published without the prior written consent of the author.

This thesis may be made available for consultation within the University Library and may be photocopied or lent to other libraries for the purpose of consultation.

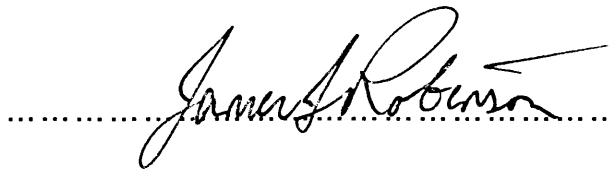

Dr James Justin Robinson BSc(HONS) PhD MRSC

UMI Number: U193247

All rights reserved

INFORMATION TO ALL USERS
The quality of this reproduction is dependent upon the quality of the copy submitted.

In the unlikely event that the author did not send a complete manuscript
and there are missing pages, these will be noted. Also, if material had to be removed,
a note will indicate the deletion.

UMI U193247
Published by ProQuest LLC 2013. Copyright in the Dissertation held by the Author.
Microform Edition © ProQuest LLC.
All rights reserved. This work is protected against
unauthorized copying under Title 17, United States Code.

ProQuest LLC
789 East Eisenhower Parkway
P.O. Box 1346
Ann Arbor, MI 48106-1346

30 - 4 AUG
Ph.D.

Ph.D. Thesis

The role of α-lactones and cognate species in organic reactivity.

Supervised by Professor Ian H. Williams and Professor. J. Grant Buchanan, Department of Chemistry, The University of Bath, Bath, UK.

2005.

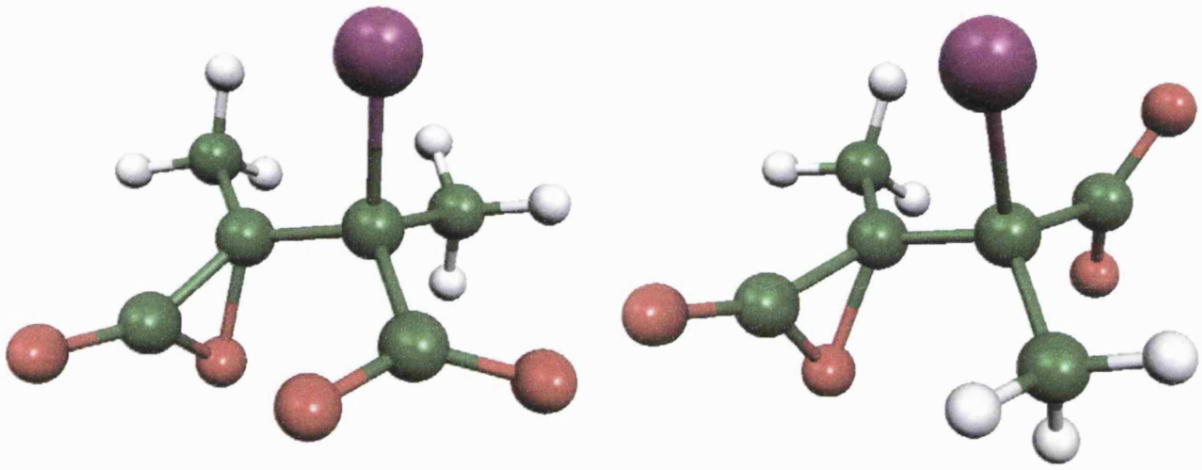

α-lactone [2-bromo-2-(methyl-3-oxiranyl)-propionate] anion structures obtained spontaneously from PCM/rB3LYP/6-31+G(d) calculations for relaxation of symmetrical bromonium structures from disodium salts of 2,3-dimethylmaleic and 2,3-dimethylfumaric acids.

Index of contents

1. Summary

Crystallographic analysis of the bromo-β-lactones obtained by addition of bromine to aqueous solutions of disodium 2,3-dimethylmaleic acid and the disodium salt of 2,3-dimethylfumaric acid, reveals stereochemistries opposite to those originally assigned.[I,II] The bromination of disodium 2,3-dimethylmaleate leads to [3S(3R),4S(4R)]-3-bromo-4-carboxy-3,4-dimethyloxetan-2-one (a). The bromination of disodium 2,3-dimethylfumarate leads to [3R(3S),4S(4R)]-3-bromo-4-carboxy-3,4-dimethyloxetan-2-one (b).

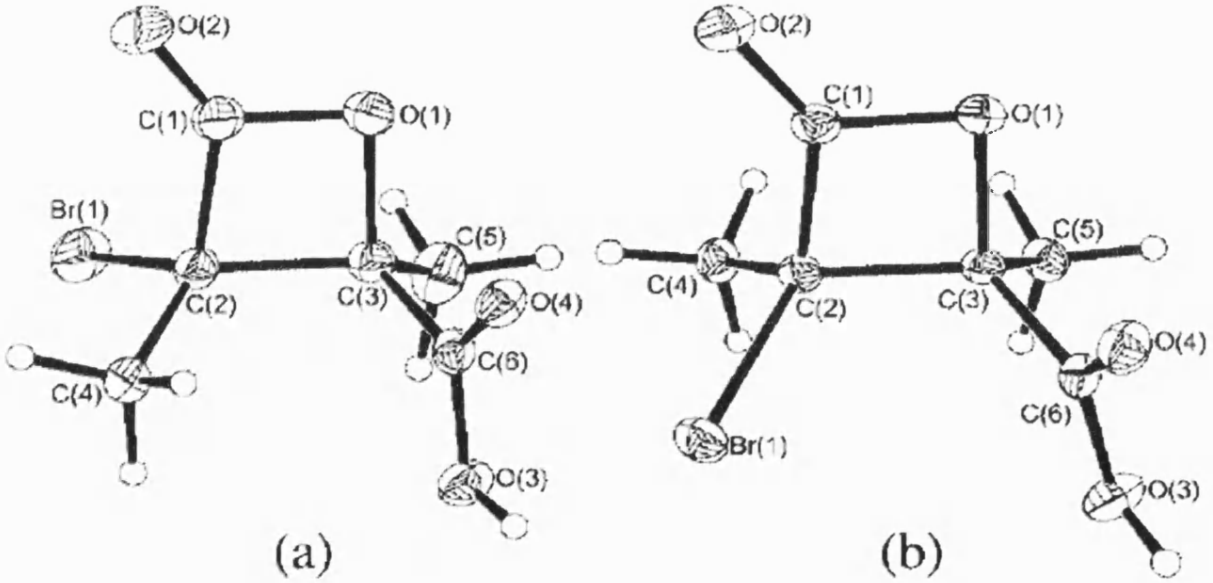

To account for this observation, it has been suggested that the first-formed intermediate in each case is an α-lactone.[II,III] Calculations with PCM/B3LYP/6-31+G(d) indicate that the cyclic symmetrical bromonium adducts of 2,3-dimethylmaleate and 2,3-dimethyfumarate dianion are not intermediates but transition structures that spontaneously relax to 2R*(*3S*)*-bromo-2R(2S*)*-(2R(2S*)*-methyl-3S(3R)-oxo-oxiranyl)-propionate anion from the cyclic bromonium ion of 2,3-dimethylmaleate dianion and 2S(2R*)*-bromo-2S(2R)-(2S(2R)-methyl-3S(3R*)*-oxo-oxiranyl)-propionate anion from the cyclic bromonium for 2,3-dimethylfumarate dianion, by 3-*Exo-Tet* ring closure. Rotation about the central carbon-carbon bonds facilitates further 4-*Exo-Tet* ring closure to yield the bromo-β-lactone

products. Two inversion steps are involved. Calculation of potential single step bromo-β-lactone 4-*Endo-Tet* ring closure of the carboxyl group oxygen on the cyclic bromonium, as proposed by Tarbell and Bartlett, indicate that such pathways involve zwitterionic transition states and are higher in energy compared to reaction paths involving α-lactone formation by 3-*Exo-Tet* ring closure.

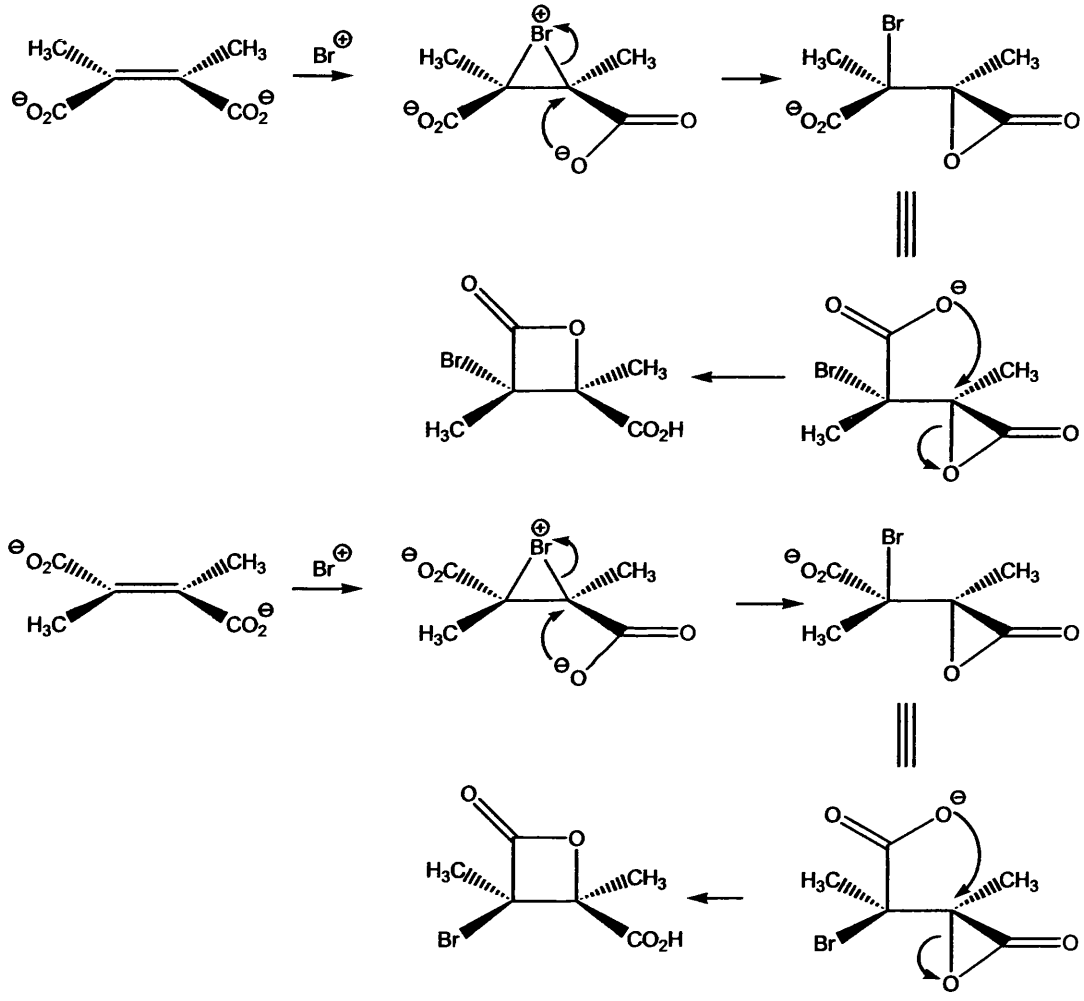

Calculations with bromine molecules and unsaturated dianions suggest a reaction pathway without cyclic bromonium transition states for bromination of 2,3-dimethylmaleate disodium salt. The bromine molecules initially associate with a carboxyl group that is more electron rich compared to the central double bond. Removing the peripheral bromine atom, α-lactones are once again optimised.

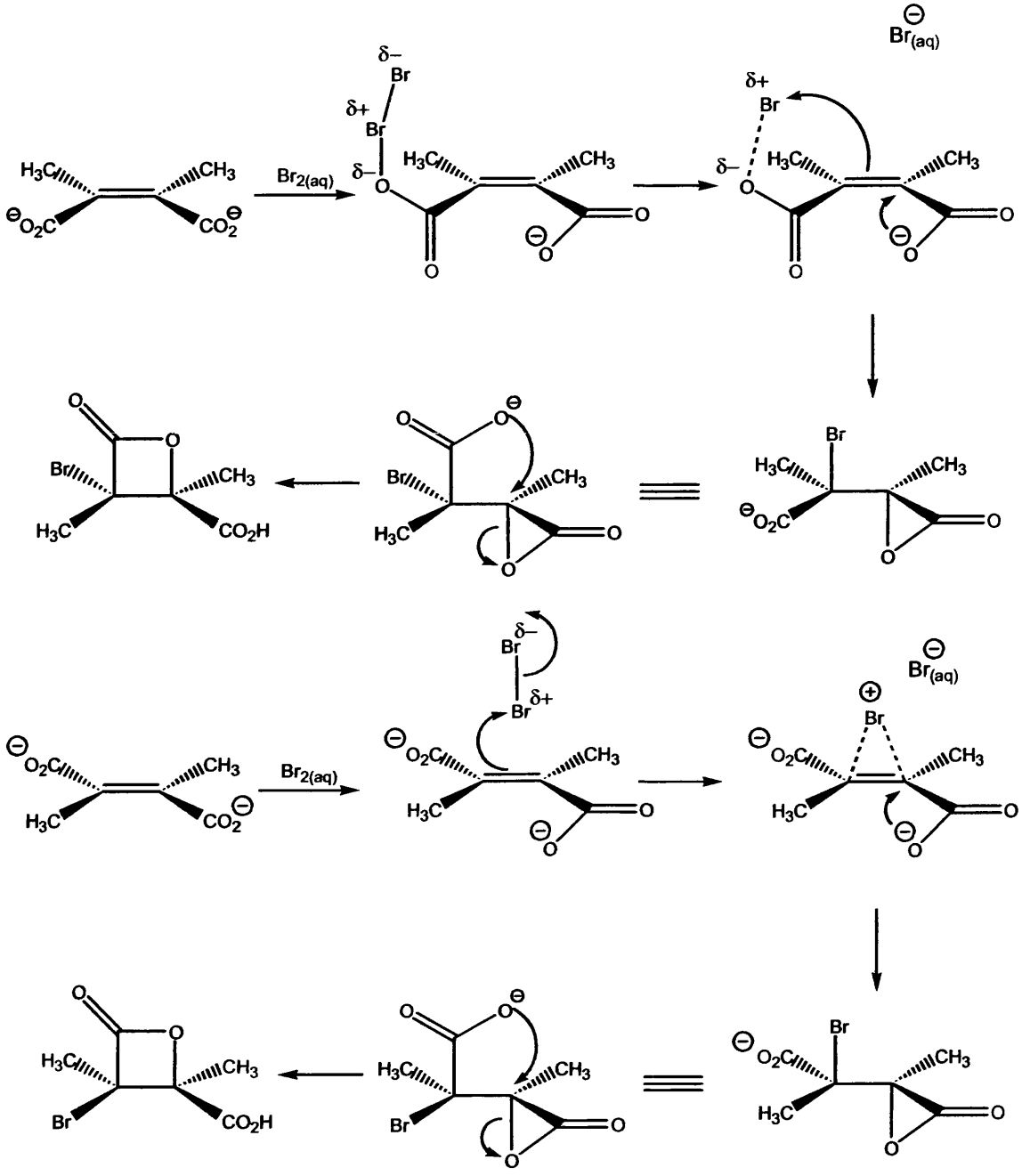

In both proposed mechanisms α-lactones are initial intermediates that are sufficiently stable in aqueous solution to undergo conformational change to facilitate the 4-*Exo-Tet* ring closure to bromo-β-lactone.

I. D. S. Tarbell and P. D. Bartlett, *J. Amer. Chem. Soc.*, 1937, 59, 407.

II. J. J. Robinson, J. G. Buchanan, M. H. Charlton, R. G. Kinsman, M. F. Mahon and I. H. Williams, *J. Chem. Soc., Chem. Comm.*, 2001, 5, 485.

III. J. G. Buchanan, M. H. Carlton, M. F. Mahon, J. J. Robinson, G. D. Ruggiero and I. H. Williams, *J. Phys. Org. Chem.*, 2002, 15, 9, 642.

2. Chemistry Introduction

2.1. Historical background

Advances in the understanding of the mechanism of chemical reactions have been aided by studies of reaction kinetics and stereochemical relationships. The study of reaction stereochemistry has allowed general mechanisms to be proposed for reactions such as electrophilic addition, nucleophilic substitution and other classes of reactions that account for observed stereoselectivity of reactions. At the beginning of the 20th century, the topic of nucleophilic substitution was at the forefront of research in chemistry. Methods of analysis were mainly limited to classical properties such as melting point, boiling point, refractive index, and optical rotation.

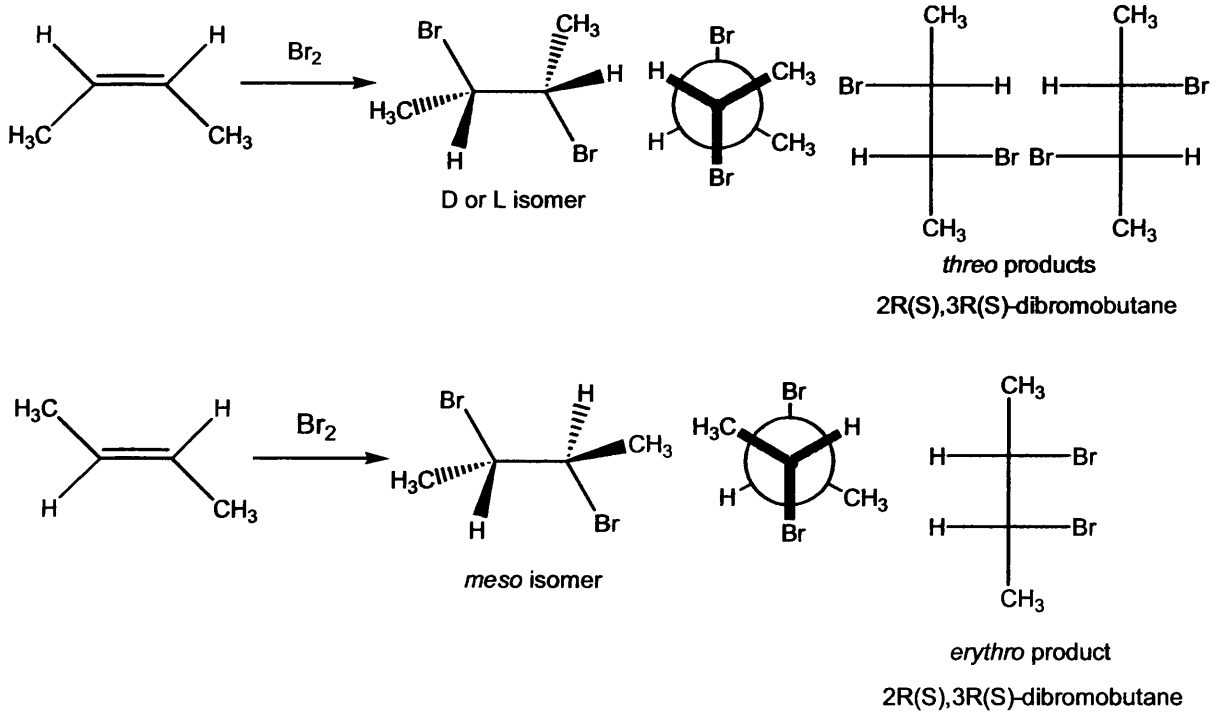

Fig. 1. Stereospecific addition of bromine to but-2-ene.[2]

Describing the stereochemical features of a reaction involves distinguishing between two types: stereospecific and stereoselective reactions. A stereospecific reaction involves stereoisomeric reactants

yielding stereoisomerically different products under the same reaction conditions. A stereoselective reaction involves a single reactant having the potential to yield two or more stereoisomeric products but one is formed preferentially.[1] An example of a stereospecific reaction is the addition of bromine to *cis*-but-2-ene and *trans*-but-2-ene.[2]

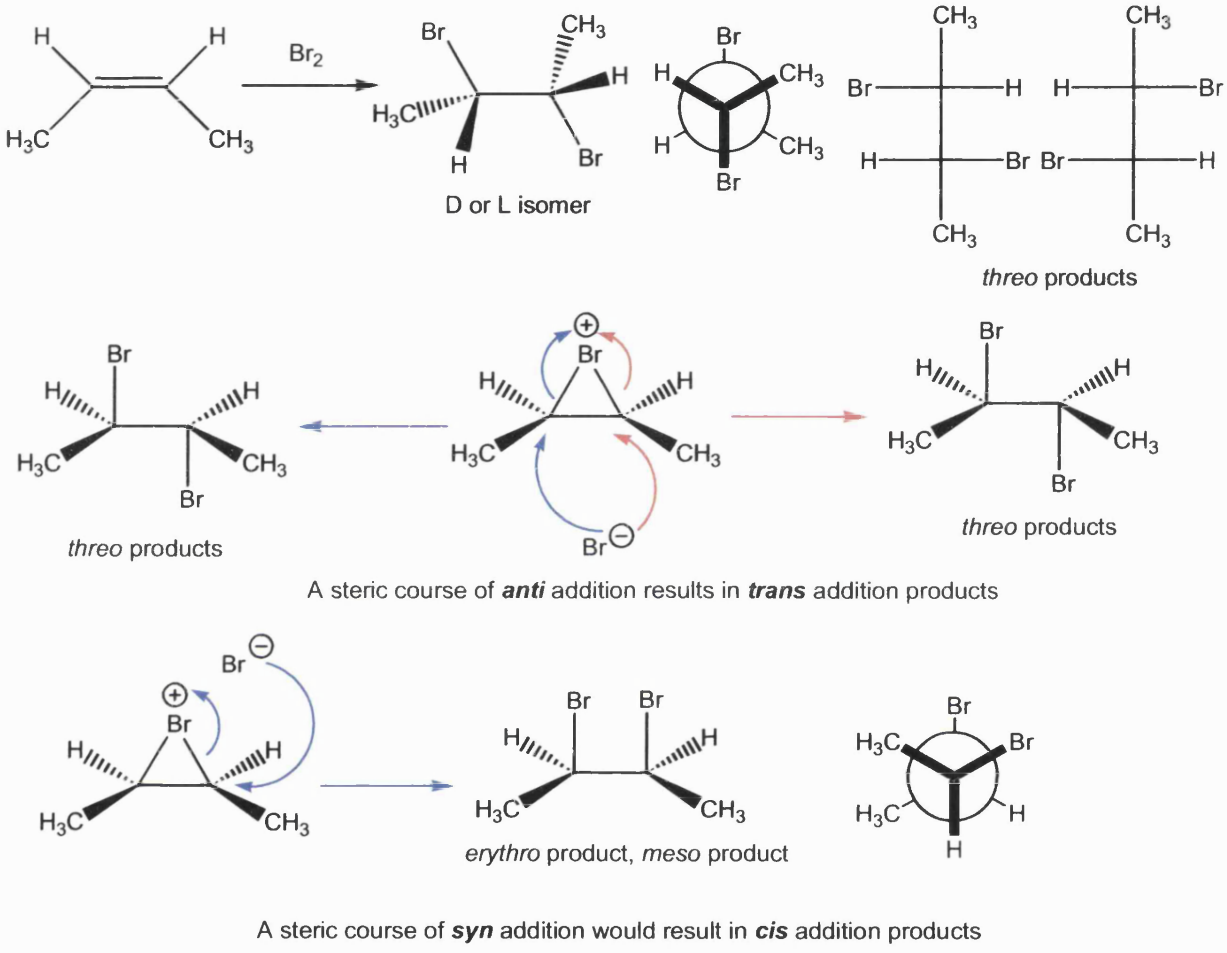

Fig. 2. Mechanism of attack on bromonium ions showing different mechanism for addition reaction.

The reaction mechanism in figure 2, serves to illustrate frequently used term describing addition reactions, such as steric course of *anti* and *syn* addition and *trans* and *cis* addition products. A steric course of *syn* addition to yield *cis* addition products often occurs with anchimeric assistance, neighbouring group assistance, and is shown to illustrate the

terms used. An example of a stereoselective reaction is the reduction of a hindered ketone with lithium aluminium hydride.[3]

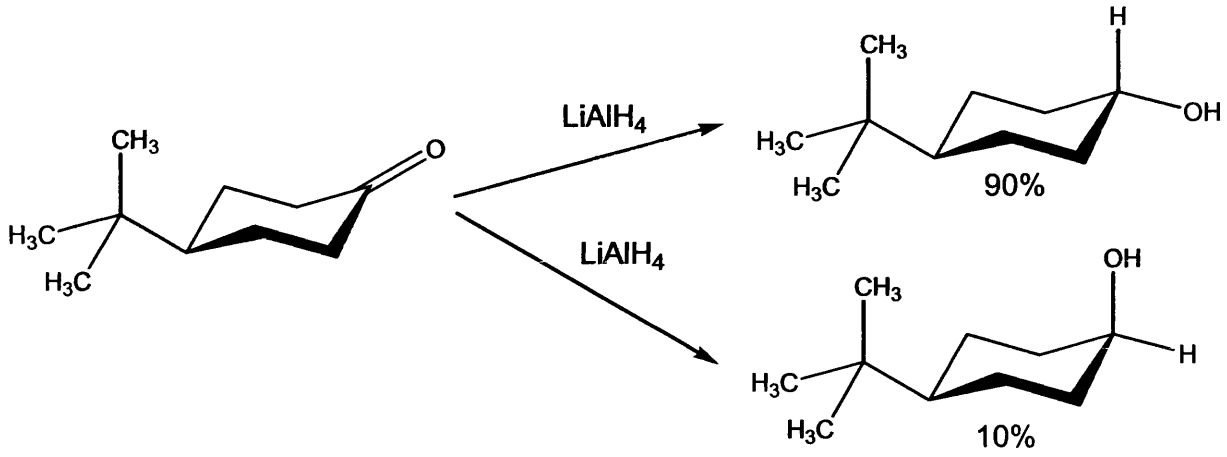

Fig. 3. Stereoselective reduction with $LiAlH_4$.[3]

Nucleophilic substitution reactions have probably been the most intensely studied of all reactions.[4,5,6] It has since been established that nucleophilic substitution reactions can have essentially three outcomes:

- Racemisation results when a substitution reaction generates both possible enantiomers of a product from a single enantiomer of reactant.
- Inversion results when the configuration of the substitution site in the product has a mirror image relationship with the reactant.
- Retention of configuration applies to a reaction when the relative spatial arrangement at the reaction centre is the same in the reactant and product.[7]

In practice however, complete racemisation is rarely observed. Substitution reactions that are expected to afford racemic mixtures are often accompanied by some degree of inversion.[8] The stereochemical relationship between reactants and products for a studied reaction will often provide the initial starting points for mechanistic considerations of a reaction.

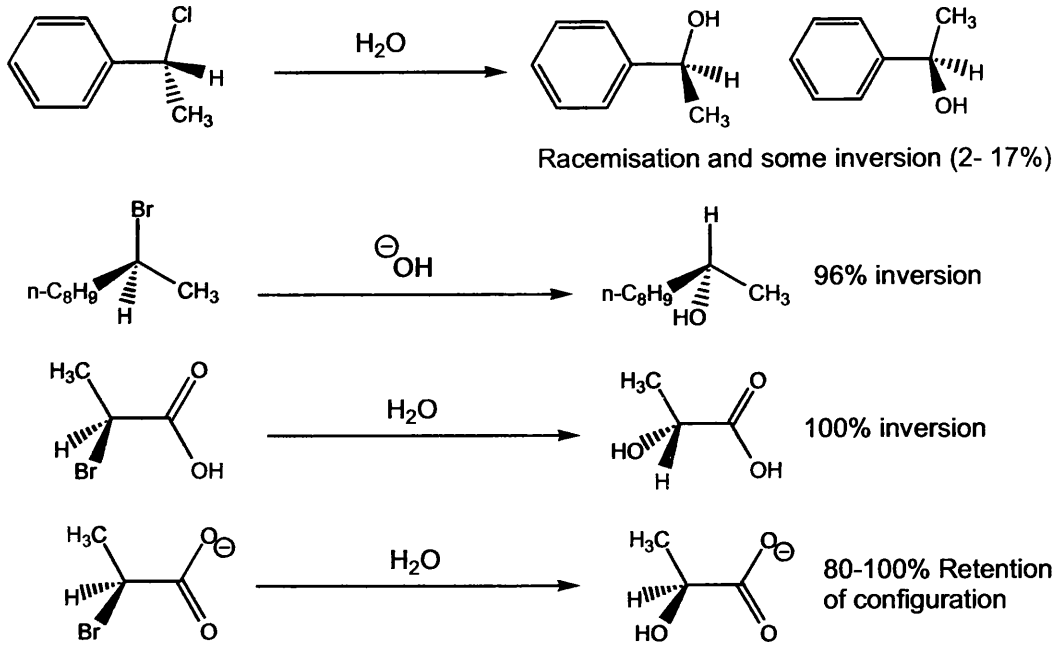

Fig. 4. Reactions resulting in inversion, racemisation and retention of configuration.[9]

That some substitution reactions result in retention of configuration and some result in inversion of configuration is dependent upon mechanism. Research to rationalise the mechanism of substitution reactions is still a heavily researched subject area. Substitution reactions were initially thought to proceed with retention of configuration. Substitution reactions that were attended with retention of configuration were referred to as normal and substitution reactions that were attended by inversion as abnormal.[10,11,12] Until the late 19th century, this was a commonly held belief. The primitive concept that all substitution reactions proceed homofacially was dispelled by Walden. During studies of optically active compounds by P. Walden, a reaction was reported in 1896 whereby optically active starting materials reacted to give optically active products with opposite configuration.[10]

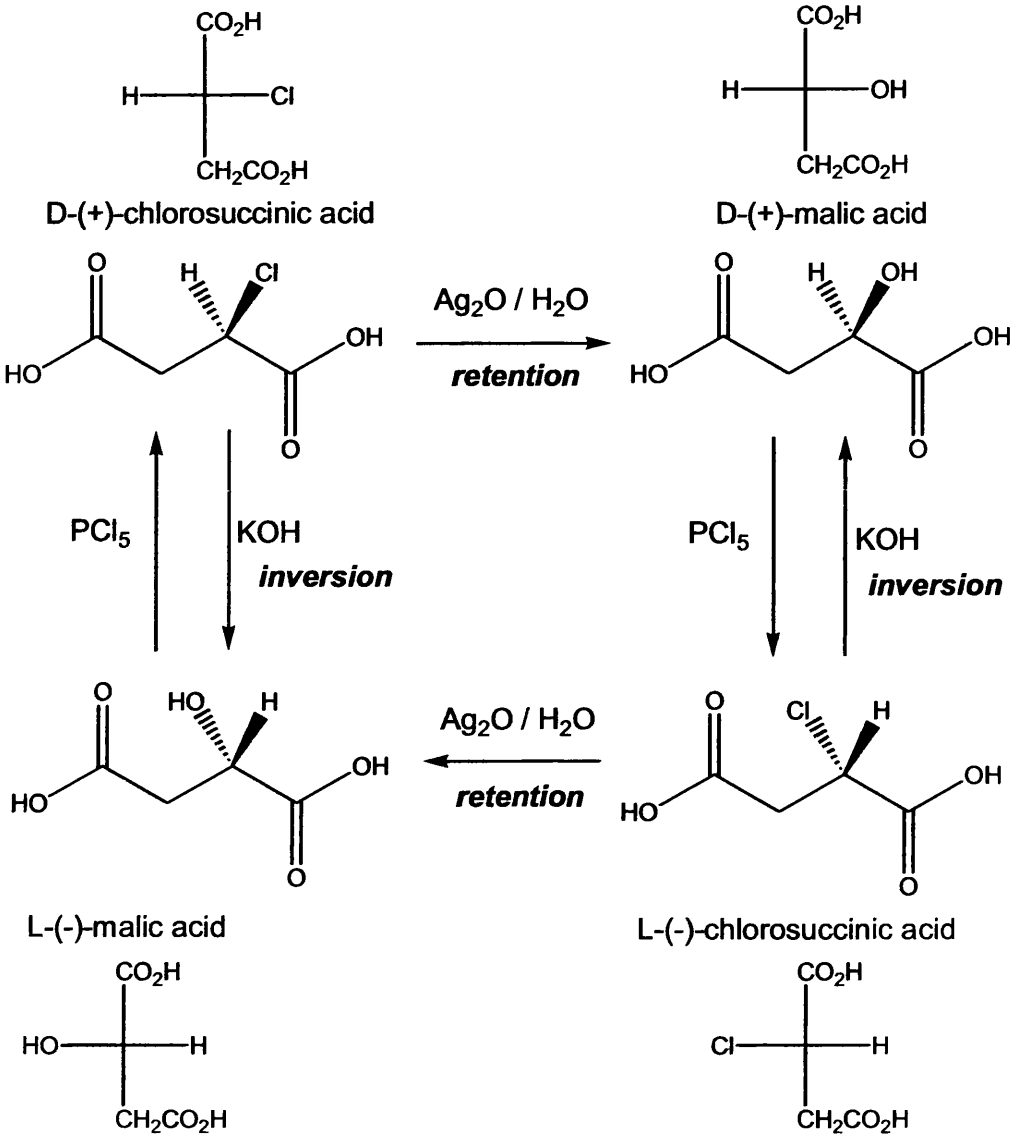

Fig. 5. Reaction scheme of the classic stereospecific Walden inversion cycle.[10,11,12]

The enantiomers (-)-chlorosuccinic and (+)-chlorosuccinic acids have different configurations. If the reaction with moist silver oxide proceeds with retention configuration, then the reactions with KOH/PCl_5 must proceed with inversion of configuration. However, should the reaction with moist silver oxide proceed with inversion of configuration then the reaction with KOH/PCl_5 must proceed with retention of configuration. Two inversion processes would result in net retention of configuration for the substitution reactions examined by Walden. At the time, Walden

was unable to determine which conditions were responsible for the inversion of configuration.[12]

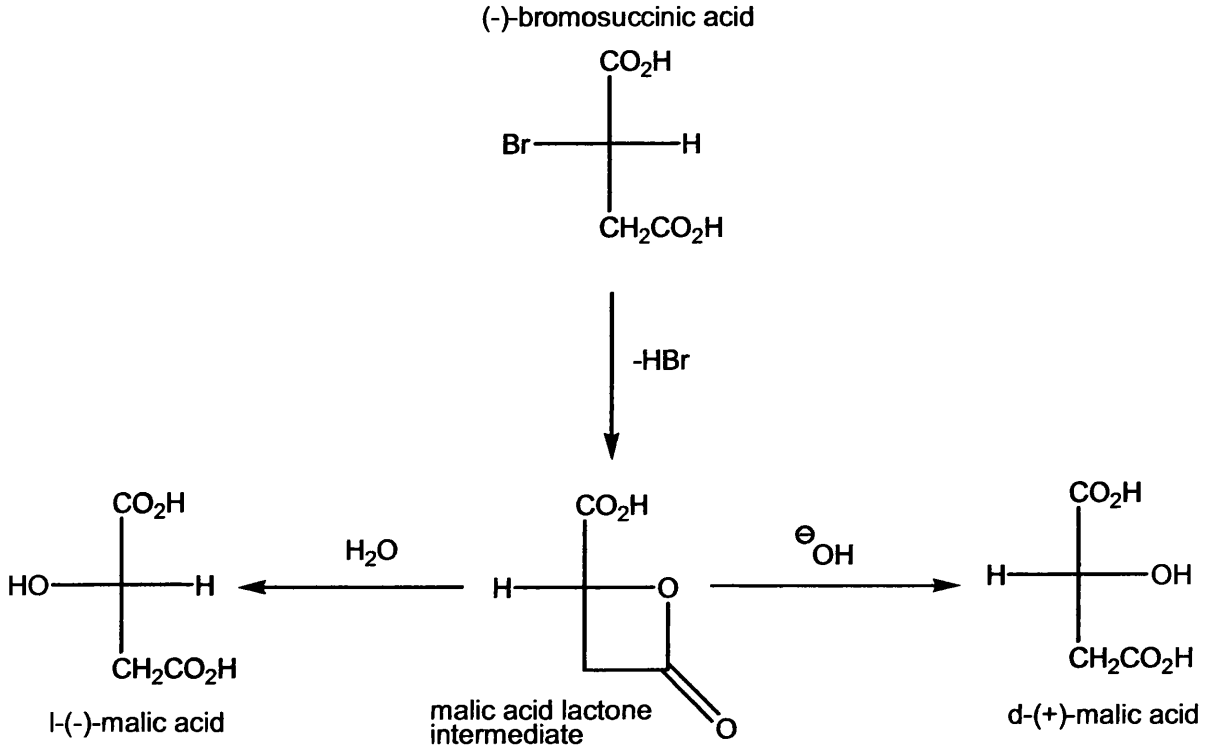

Fig. 6. Hydrolysis of bromosuccinic acid to yield two enantiomers of malic acid.[13]

Holmberg studied the hydrolysis of bromosuccinic acid. Holmberg discovered that there was an intermediate in the hydrolysis that was monobasic. Holmberg was unable to actually isolate and crystallise the intermediate. However, aqueous solutions of the intermediate were available, so studied were made of the hydrolysis of the intermediate at different pH and malic acids were isolated. The reaction intermediate was suggested to be malic acid lactone, obtained from (-)-bromosuccinic acid and gave predominantly (+)-malic acid in alkaline medium whilst acid hydrolysis of the malic acid lactone resulted in (-)-malic acid to be in excess. In one of the hydrolysis steps of malic acid lactone, inversion must have occurred.[13] The work of Holmberg proved that β-lactones were intermediates in the original Walden cycle.

Olson and Miller studied the hydrolysis of β-butyrolactone and found results similar to those found by Holmberg. The hydrolysis of β-butyrolactone is catalysed by acid and base and gave an optically active 2-hydroxybutanoic acid. The carbonyl bond in the ester is attacked. However, hydrolysis of β-butyrolactone at neutral pH gave 2-hydroxybutanoic acid that had opposite optical activity to the 2-hydroxybutanoic acid formed from acid or base catalysed hydrolysis, the carbonyl bond is not attacked.[14]

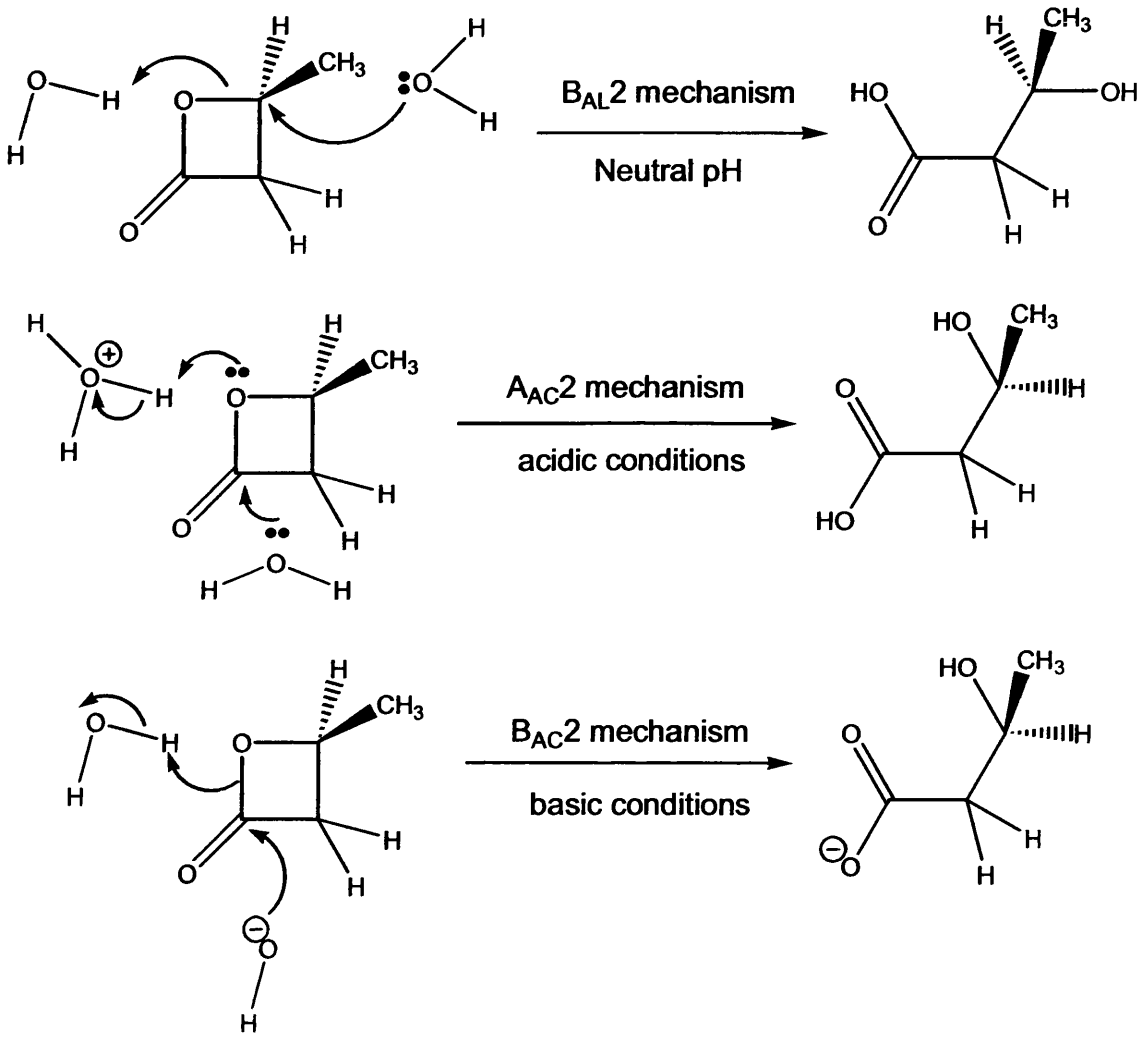

Fig. 7. Hydrolysis of β-lactones studied by Olson and co-workers.[14]

The results suggested a mechanism in which water would attacks the alkyl C-O bond from a back-side approach under neutral conditions.

These results were later supported by the results obtained from hydrolysis of a β-lactone in $H_2{}^{18}O$ solvent.[15]

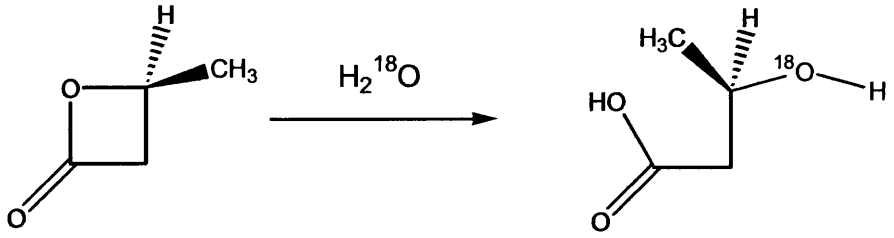

Fig. 8. Isotopic labelled water used to follow hydrolysis of β-lactone.[15]

The work of Kenyon and Philips clearly illustrated a cycle in which some substitution reactions involved inversion and retention of configuration. An optically active alcohol with only one chiral centre, with $[\alpha]^{23}{}_D$ of +33.02°, was converted to an enantiomer with $[\alpha]^{23}{}_D$ of −32.18°.[16]

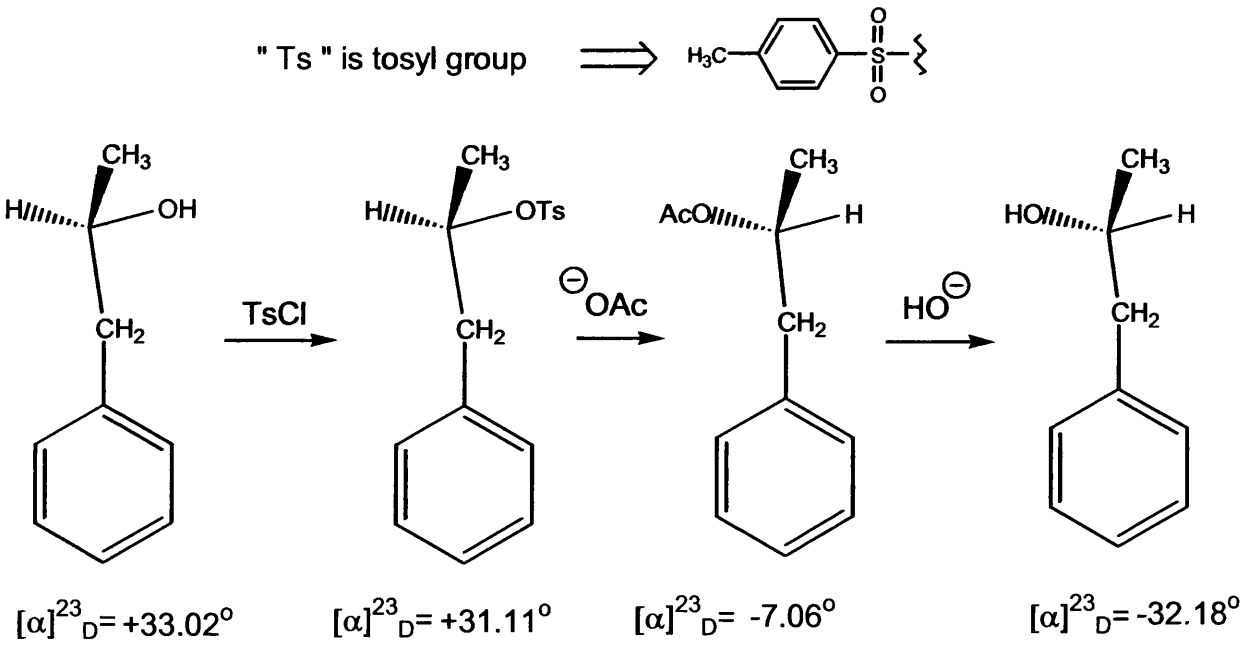

Fig. 9. Conversion from one enantiomer to another in discrete steps.[16]

The first step converts the alcohol to a tosylate derivative. The reaction occurs at the oxygen centre and not the asymmetric carbon atom. There is in this instance no net change in configuration. In the third step, the basic hydrolysis of the acetate ester, involves cleavage of acyl-oxygen

and not alkyl-oxygen bond. The carbonyl group of the ester is attack by base. The third step must also involve no net change in configuration; the stereochemistry is retained. As the enantiomer is formed in step three, the second step in the reaction must involve an inversion of configuration. The tosylate group is an excellent leaving group; the acetate anion attacks the asymmetric carbon centre resulting in inversion of configuration.[16]

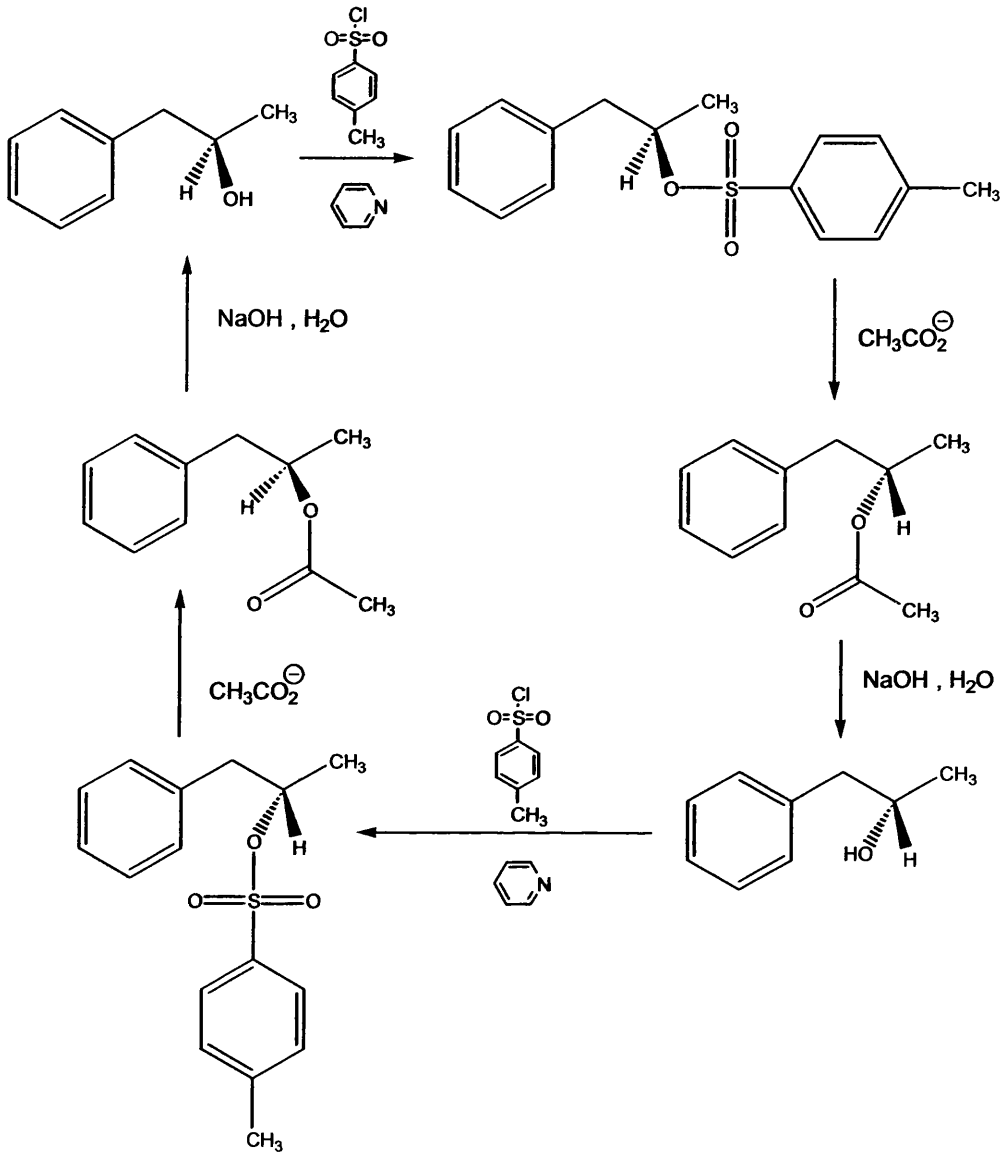

Fig. 10. The work of Kenyon and Phillips shown as a Walden cycle.[16]

2.2. Reaction mechanism for substitution reactions: S_N2 and S_N1

The work of Walden and Holmberg demonstrates substitution reactions can result in inversion of configuration. However, the work of Kenyon and Phillips demonstrates that substitution reaction can result in retention of configuration. Substitution reactions are often referred to as operating by S_N1 or S_N2 mechanisms. The terms S_N1 and S_N2 are designations of non-observable mechanism and not of observable experimental reaction kinetics. The two terms are useful in describing substitution reactions and were suggested by Ingold and co workers.[17]

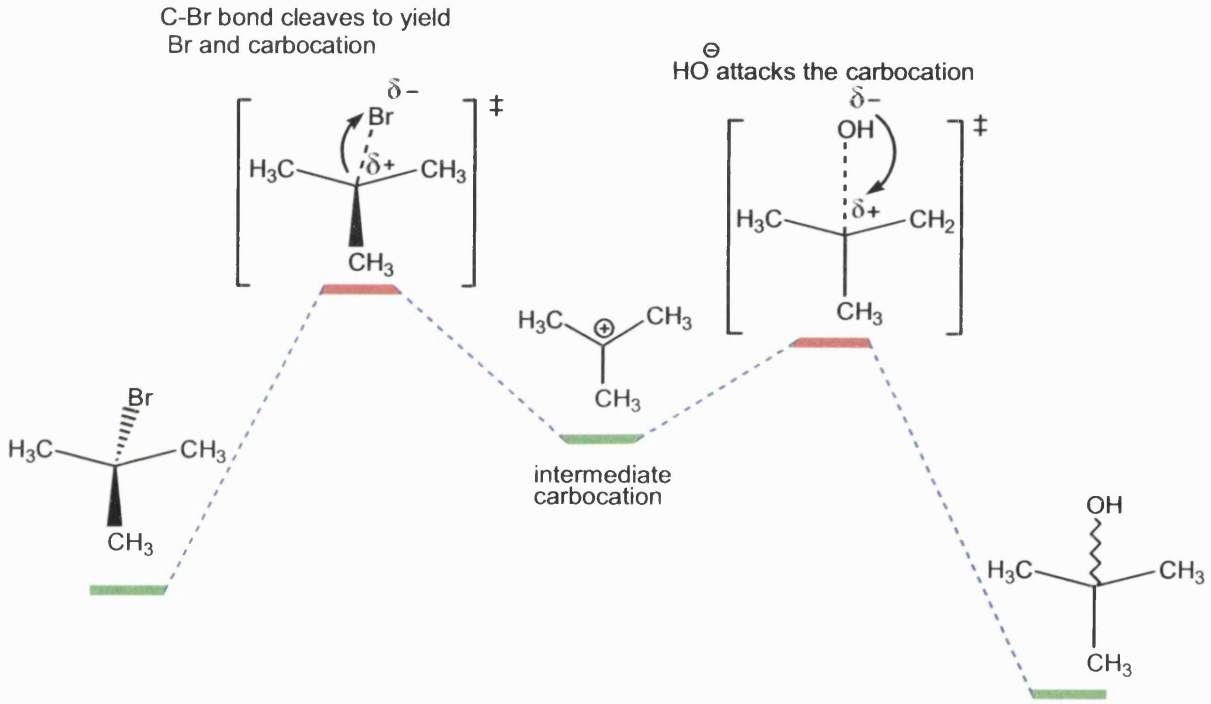

Fig. 11. Energetics of S_N1 reaction scheme.[18]

Consider two substitution reactions. Reacting 2-bromo-2-methylpropane with sodium hydroxide produces a corresponding alcohol; 2-hydroxy-2-methylpropane. With a solvent system of 80% ethanol and 20% water by volume and at 55°C the reaction rate is proportional to the amount of the bromoalkane reactant and is independent of the hydroxyl ion concentration.[19] That is the rate of reaction = k_1 [RBr]. The reaction is unimolecular; the reaction involves an intermediate carbocation and is

designated as S_N1. The stereochemistry of a S_N1 process is complex. Carbocations prefer a geometry that is trigonal coplanar. An optically active reactant adopting the trigonal coplanar arrangement would have a plane of symmetry as a carbocation so it is no longer chiral. There is an equal probability of nucleophilic attack from both sides on the intermediate carbocation, hence such reactions often result in racemisation.

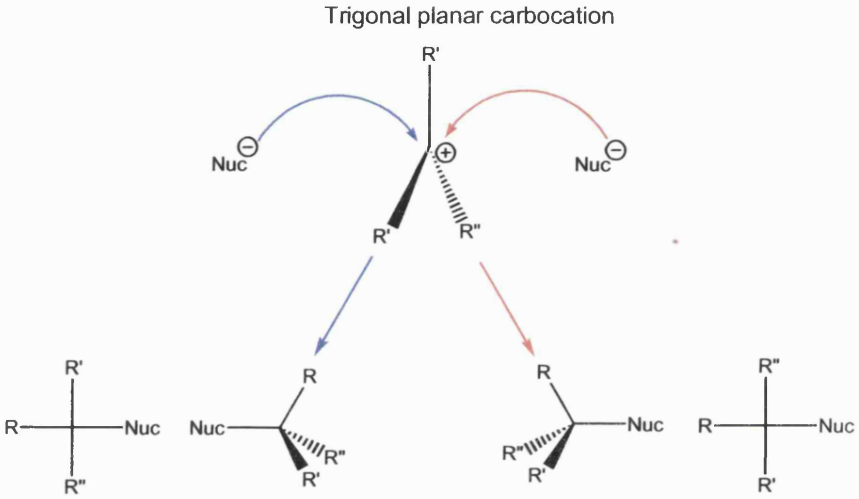

Fig. 12. Planar carbocation can be attacked from either side during S_N1 substitution.[20]

A classic example of a reaction proceeding by S_N1 reaction is illustrated by the reaction of 1-phenylethylchloride with acetate anions in acetic acid, the isolated 1-phenylethylacetate is partly racemised and partly inverted. Addition of acetate anions to the reaction does not increase the rate of reaction.[21]

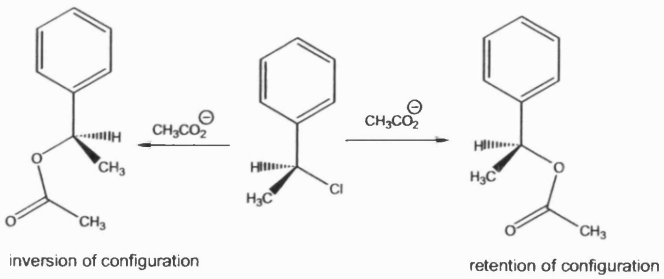

Fig. 13. Solvolysis of 1-phenylethylchloride in acetic acid.[21]

Reacting methyl bromide with sodium hydroxide under similar conditions as the substitution reaction of 2-bromo-2-methylpropane, 80% ethanol and 20% water at 55°C, the reaction rate for formation of methanol is proportional to the amount of the methyl bromide and the amount of sodium hydroxide used. The rate of reaction = k_2 [RBr][NaOH].

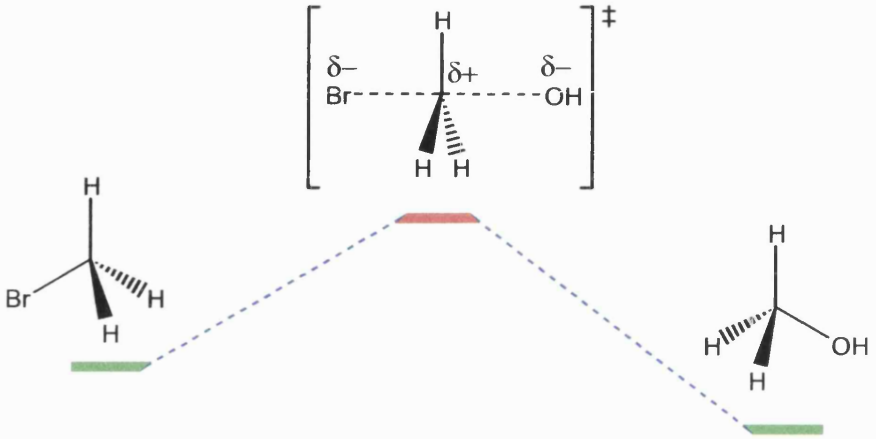

Fig. 14. Energetics of S_N2 reaction scheme.[18]

The reaction depends upon the concentration of methyl bromide and sodium hydroxide; the reaction is bimolecular. The reaction does not involve an intermediate carbocation. The reaction mechanism is classed as a S_N2 reaction.[19]

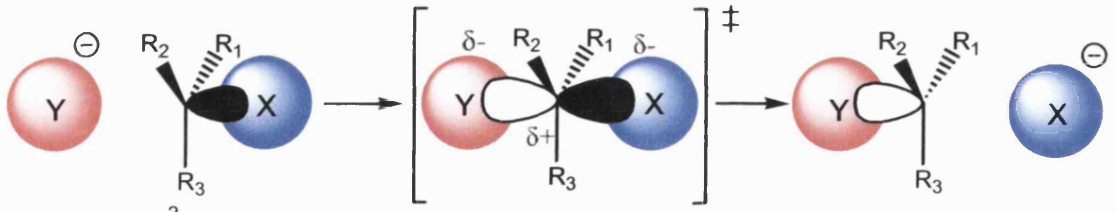

sp^3 tetrahedral reactant

carbon has sp^2 hydridisation as transition state has partial bonds for Y-C-X

sp^3 tetrahedral product - inversion results from back-side attack of Y on the C-X

Fig. 15. No charged intermediates in S_N2 processes, inversion results.

Another important experiment that established S_N2 reactions were responsible for inversion of configuration was the radio-labelled iodine (^{128}I) exchange reaction with optically active 2-iodooctane.[22]

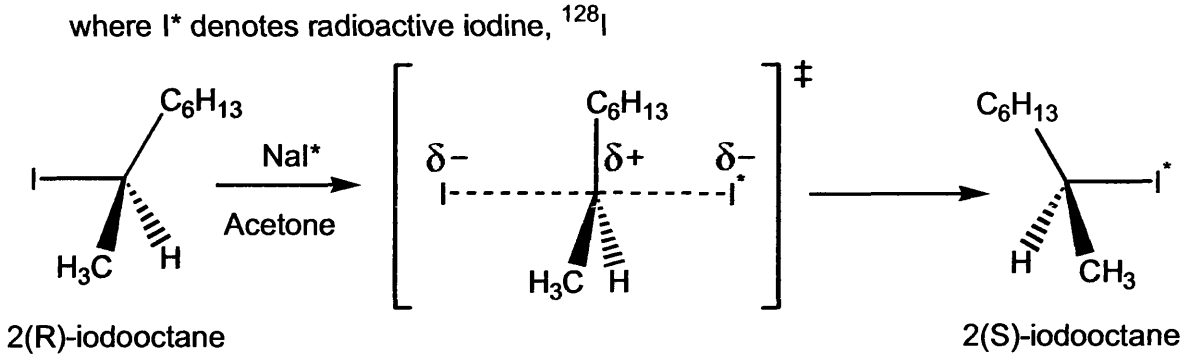

Fig. 16. Radioactive iodide exchange with 2-iodooctane.[22]

Hughes and co-workers found that the exchange reaction to be bimolecular from measurements of kinetics, first order for both the iodide anion and 2-iodooctane. The rate of reaction = k_2[Iodide][2-iodooctane]. The rate of racemisation, as 2(R)-iodooctane would react to yield 2(S)-iodooctane and 2(S)-iodooctane would yield 2(R)-iodooctane upon iodine exchange, was found to be twice the rate the of incorporation of radioactive iodine. Thus, 100% of 2(R)-iodooctane had been racemised when only 50% of has been converted to 2(S)-iodooctane. This led to the hypothesis that each attacking iodide ion was responsible for an act of inversion of 2-iodooctane.[22,23]

Alkyl chain branching will increase the stability of a carbocation intermediates through inductive effects and promote S_N1 type processes.[24] Steric bulk may mean that some substituents prevent attack of a nucleophile from a particular face of the carbocation. However, nucleophilic concentrations will also influence the mechanism of substitution reactions.

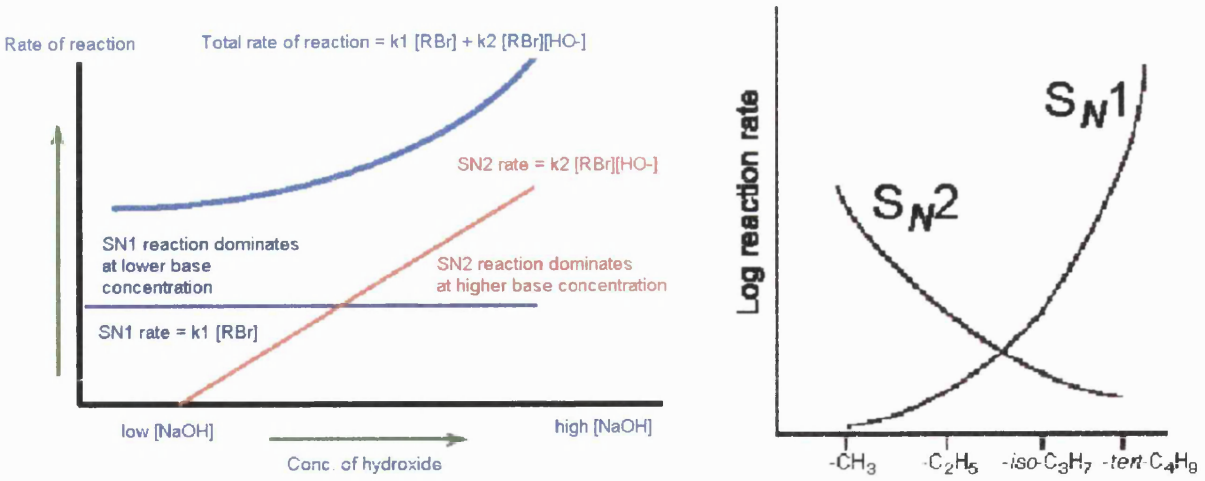

Fig. 17. Mechanistic change with increasing nucleophile concentration and changes with increasing alkyl group size.[24]

The blue curve for the total reaction rate in figure 17 is a qualitative illustration and does not represent the sum of the S_N2 (red) and S_N1 (dark blue) reaction rates. Increasing nucleophile concentrations will increase the rate of reaction but not in linearly dependent manner. High concentrations of nucleophile will actually promote S_N2 type substitution and will retard S_N1 type substitution. Increases in base concentration, hence increase in nucleophile concentration, will also change the characteristic of the reacting medium.[25]

2.3. S_Ni mechanism and neighbouring group affects

The table below shows results of nucleophilic substitutions of a set of organohalides and the relationships with mechanism and reactants. The substitution reactions that occur by S_N2 mechanism demonstrate inversion of configuration. The substitution reactions that occur by S_N1 mechanism demonstrate racemisation and some inversion.

The Walden cycle contains substitution steps that result in retention of configuration, shown by Holmberg to be the result of lactone ring formation and lactone ring opening. The formation of the lactone arises from anchimeric assistance or neighbouring group effect. Neighbouring

group effects give rise to S_Ni, substitution nucleophilic internal, unimolecular processes and these demonstrate first order kinetics, like S_N1 processes and retention of configuration, unlike S_N2 processes.

Organohalide	Reagent	Mechanism	Net effect upon configuration
$n\text{-}C_6H_{13}CH(CH_3)Br$	HO^-	S_N2	Inversion (96%)
$n\text{-}C_6H_{13}CH(CH_3)Br$	H_2O	S_N1	Inversion (66%) and racemisation
$C_6H_5CH(CH_3)Cl$	H_2O	S_N1	Racemisation and inversion (2-17%)
$C_6H_5CH(CH_3)Cl$	CH_3O^-	S_N2	Inversion
$C_6H_5CH(CH_3)Cl$	CH_3OH	S_N1	Racemisation and some inversion
$CH_3CH(CO_2H)Br$	H_2O	S_N2	Inversion
$CH_3CH(CO_2CH_3)Br$	CH_3O^-	S_N2	Inversion
$CH_3CH(CO_2^-)Br$	HO^-	S_N2	Inversion (80-100%)
$CH_3CH(CO_2^-)Br$	*H_2O*	S_Ni	*Retention (80-100%)*
$CH_3CH(CO_2^-)Br$	*CH_3OH*	S_Ni	*Retention (90-100%)*
$CH_3CH(OH)CH(CH_3)Br$	*HBr*	S_Ni	*Retention (80-90%)*

Fig. 18. Relationship between mechanism and stereochemical outcome.[25]

However, unlike S_N1 processes, S_Ni processes do not involve charged intermediates, the energetics resemble S_N2 processes. To illustrate an early example of a S_Ni reaction, consider the hydrolysis of 2-bromopropionate carried out in a dilute basic solution, 2-hydroxy-propionate is formed with retention of configuration.[26]

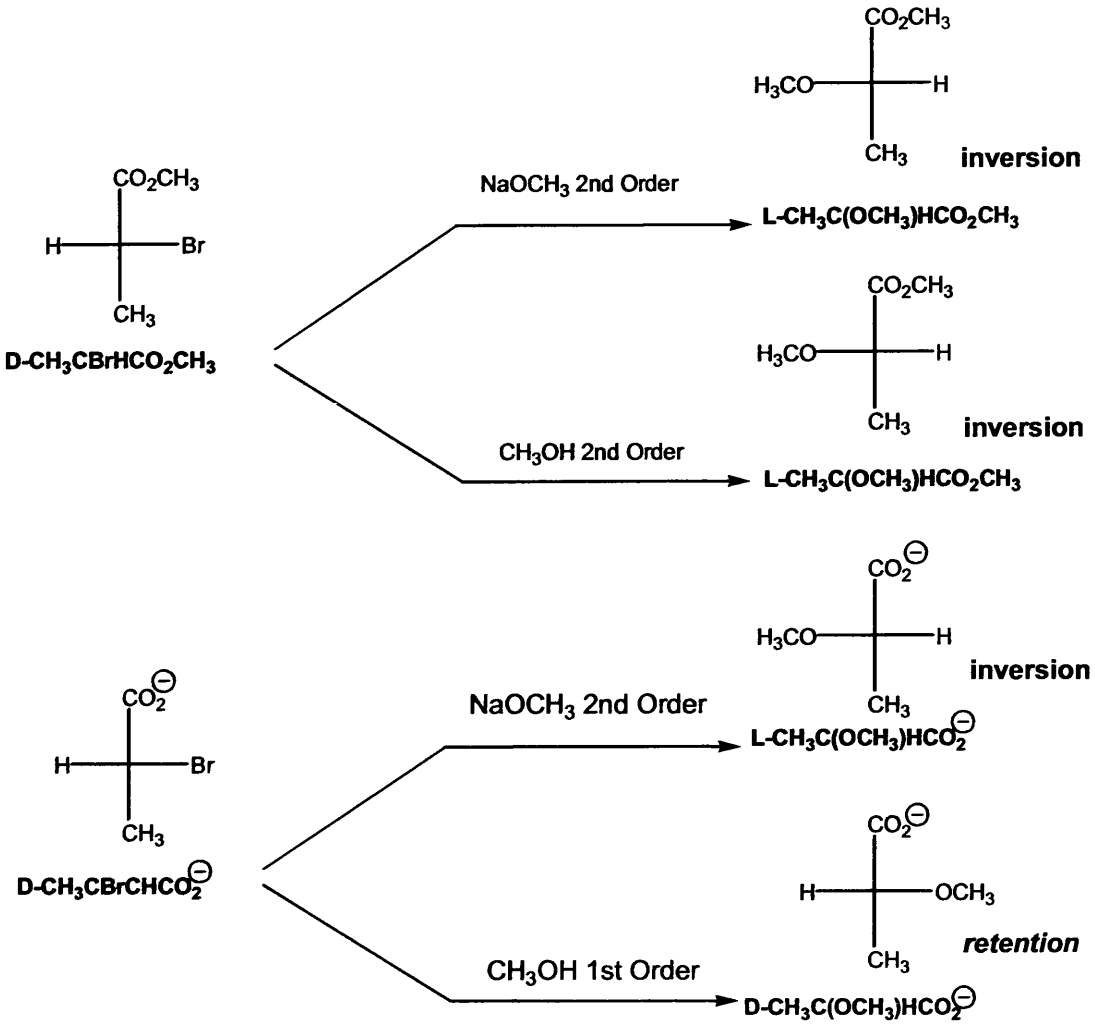

Fig. 19. Ingold and co worker examined solvolysis of haloacids and haloesters.[26,27]

Cowdrey, Hughes and Ingold found that substitution reactions with optically active α-bromopropionate methyl esters were as expected. The 2nd order and 1st order reactions with sodium methoxide giving inversion of configuration in methanol. In concentrated sodium methoxide solution, in methanol, the optically active α-bromopropionate anion undergoes a 2nd order substitution reaction to yield α-methoxypropionate with inversion of configuration.

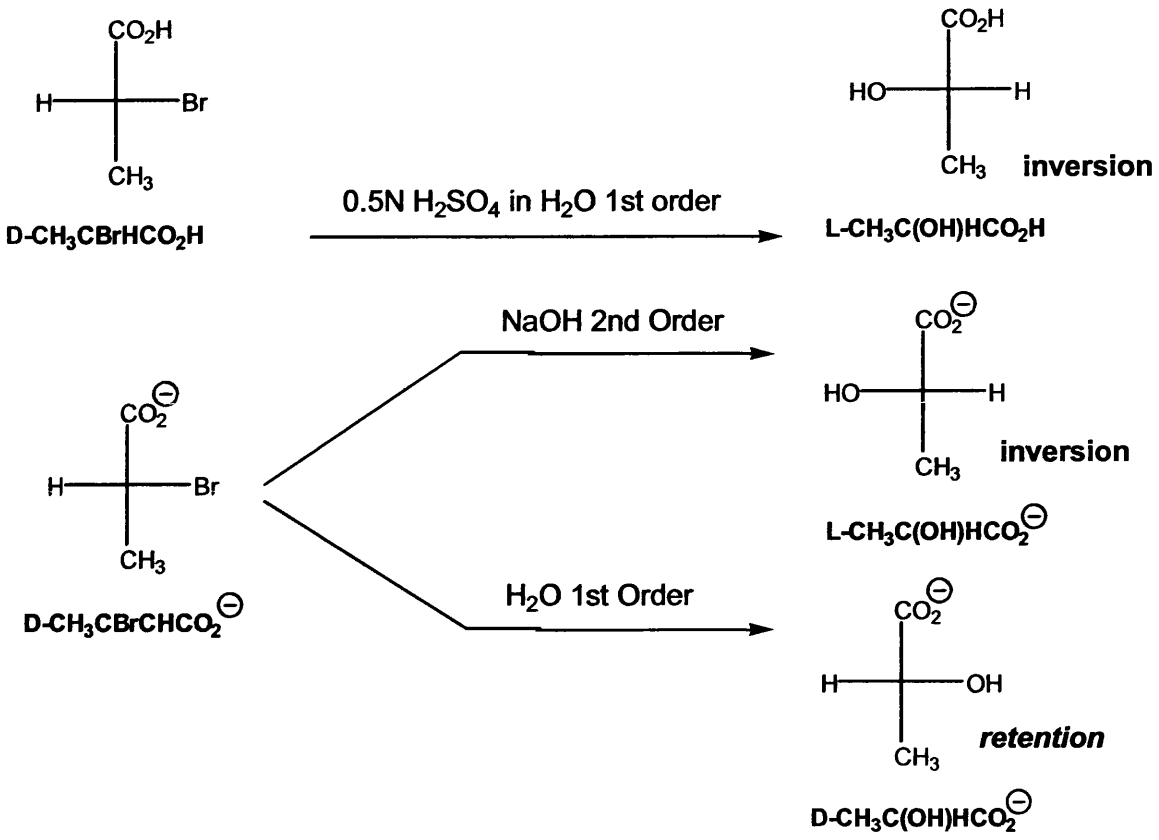

Fig. 20. Hydrolysis of carboxylate anion studied by Cowdrey, Hughes, and Ingold.[26,27]

However, in dilute alkali methanol solution, the decomposition of optically active α-bromopropionate anion is 1st order and α-methoxypropionate anion is formed with retention of configuration. The 1st order hydrolysis of α-bromopropionate with retention of configuration was not expected and could not proceed by a S_N2 mechanism that would result in inversion of configuration. The reaction had to proceed by a S_Ni mechanism, with anchimeric assistance from the carboxylate group affording retention of configuration.

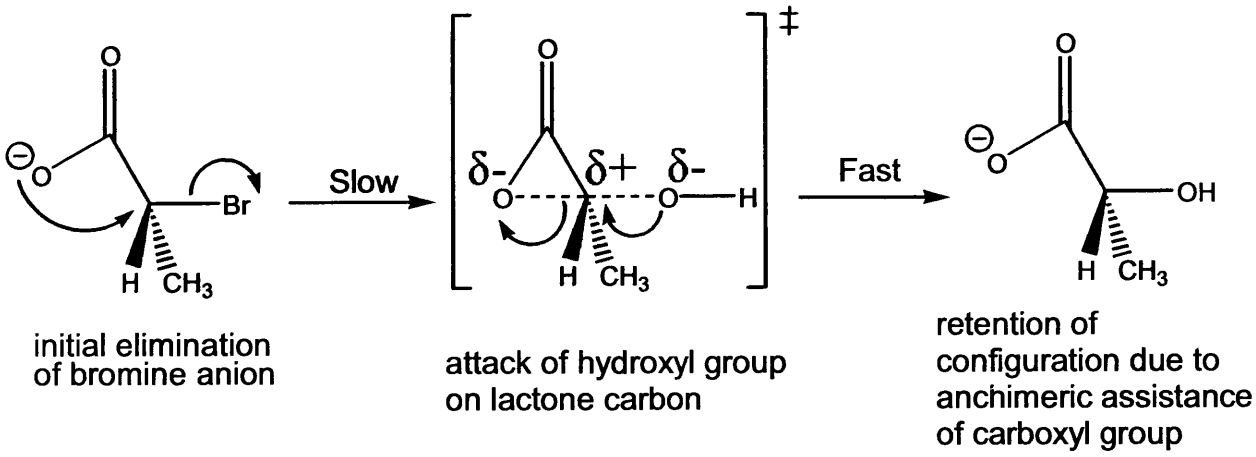

Fig. 21. Scheme proposed by Ingold.[26,28]

Ingold and co-workers explained the effect of the α-carboxylate ion group as being due to the presence of the negatively charged group in an alkyl cation, thus stabilizing the ion in a pyramidal configuration.[26,28] A similar mechanism had been proposed by Bean and co-workers.[29] The presence of an inductive geminal-exocyclic-alkyl group donating electrons to the greatly charged polarised α-carbon atom in the transition state also promotes ring closure as suggested by the Thorpe-Ingold effect.[30]

The Thorpe-Ingold effect arises as the presence of geminal alkyl group substitution on the α-carbon of a nucleophilic chain, will decrease the C-C-C angle slightly and promote ring closure when compared to geminal hydrogens in the same moiety, where there is no steric clash from geminal alkyl hydrogen's. During the formation of small rings, a reduction of the C-C-C bond angle must occur to facilitate intramolecular nucleophilic attack. Consider the rate of ring closure of a set of chlorohydrins. Epoxide rings are formed from chlorohydrins by the action of base. The rate of reaction shows a trend with alkyl substitution.

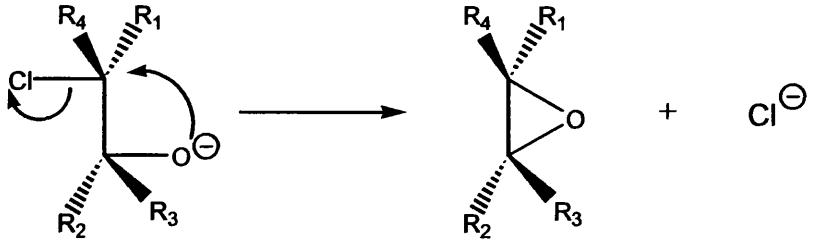

Chlorohydrin reactant anion	Relative rate of reaction
$^{-}O\text{-}CH_2CH_2\text{-}Cl$	1
$^{-}O\text{-}CH_2CH(CH_3)\text{-}Cl$	5.5
$^{-}O\text{-}C(CH_3)HCH_2\text{-}Cl$	21
$^{-}O\text{-}CH_2C(CH_3)_2\text{-}Cl$	248
$^{-}O\text{-}C(CH_3)_2CH_2\text{-}Cl$	252
$^{-}O\text{-}C(CH_3)_2CH(CH_3)\text{-}Cl$	1360
$^{-}O\text{-}C(CH_3)HC(CH_3)_2\text{-}Cl$	2040
$^{-}O\text{-}C(CH_3)_2C(CH_3)_2\text{-}Cl$	11,600

Fig. 22. Rate of ring closure increase with geminal exocyclic methyl substitution, carried out under basic conditions.[30]

Returning to the hydrolysis of 2-bromopropionate anion, two pathways are possible. The carboxyl group could attack the carbon-bromine bond by backside attack to give an α-lactone intermediate. Alternatively, the carbon-bromine bond could cleave to yield a bromine anion and a zwitterionic carbocation.

Anchimeric assistance was also noted for reactions of bromobutanols.[31] The formation of an intermediate in the reaction of α-bromopropionate anion was also examined by Grunwald and Winstein.[32] A mass-law effect was found upon addition of inert salts to the reaction, such as perchlorate and bromide anion. The rate of reaction was found to increase with addition of perchlorate anion but the rate of reaction was retarded by the addition of bromide anions. Addition of excess bromide anion would increase the likelihood of the intermediate α-lactone being attacked by bromide anion to reform the reactants. The discovery of a

mass-law effect itself did not disprove or indeed prove the hypothesis of that an intermediate α-lactone was participating in the reaction. Similar effects upon reaction rate by addition of inert salts were noted by Chadwick and Pacsu.[33]

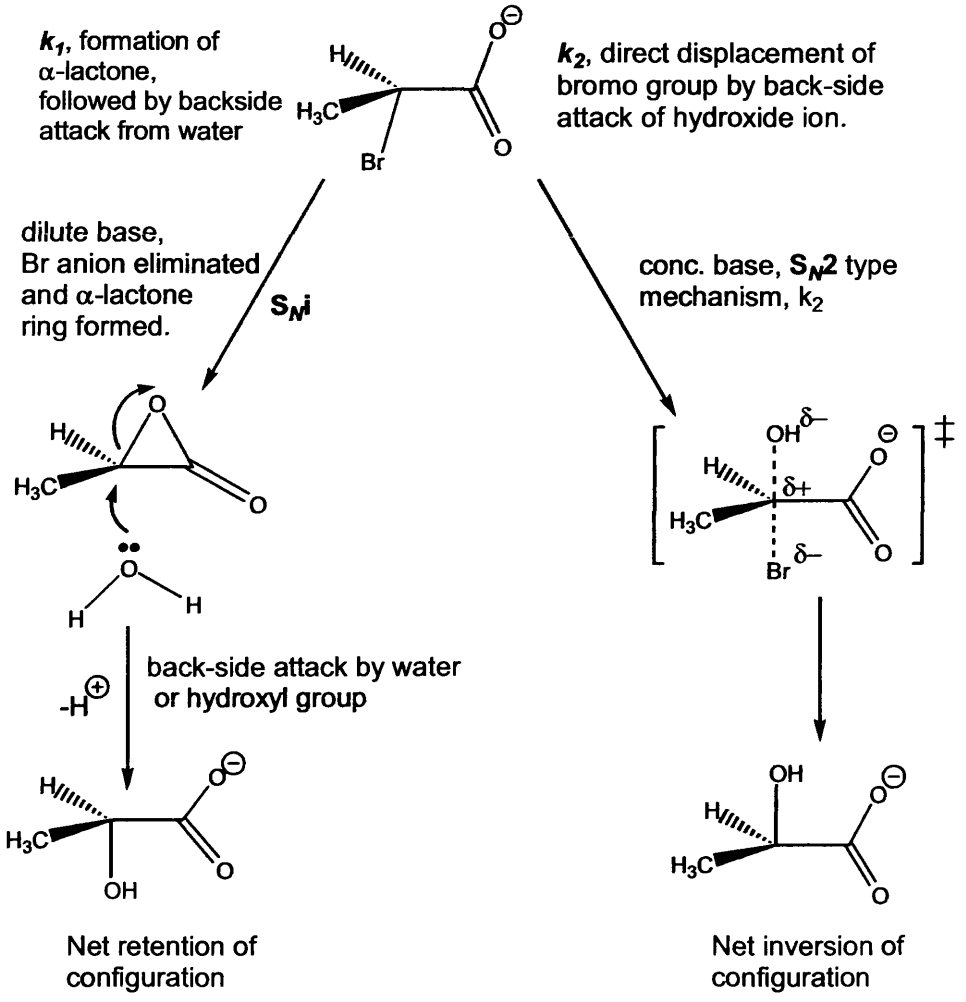

Fig. 23. Grunwald and Winstein added inert salts to reactant mixtures to see if the two mechanisms were competing.[32]

Studying the rate of solvolysis (hydrolysis and methanolysis) of α-bromopropionate cannot indicate whether the formation of the three-membered ring α-lactone occurs synchronously, with breakage of the C-Br bond, or indeed whether the C-Br bond is broken first, since in either case first order kinetics should be expected. As Grunwald and Winstein had shown a positive salt effect for the reaction that indicates that

formation of the transition state requires separation of unlike charges, as opposed to dispersal of charges, this may mean that C-Br bond fission is a slower process compared to formation of the O-C acyl α-lactone bond. It was many years after the work of Grunwald and Winstein that α-lactones were finally isolated, so early researchers, such as Ingold, preferred the intermediate to be described as a zwitterion in which electrostatic bond from the carboxylate group holds the carbocation in the correct geometric arrangement to facilitate back-side attack from solvents. Hydrolysis of α-lactones that results in retention of configuration must involve cleavage of the alkyl-oxygen bond and not the acyl-oxygen bond. Some β-lactones will cleave in this manner but most esters do not cleave in this manner.[34]

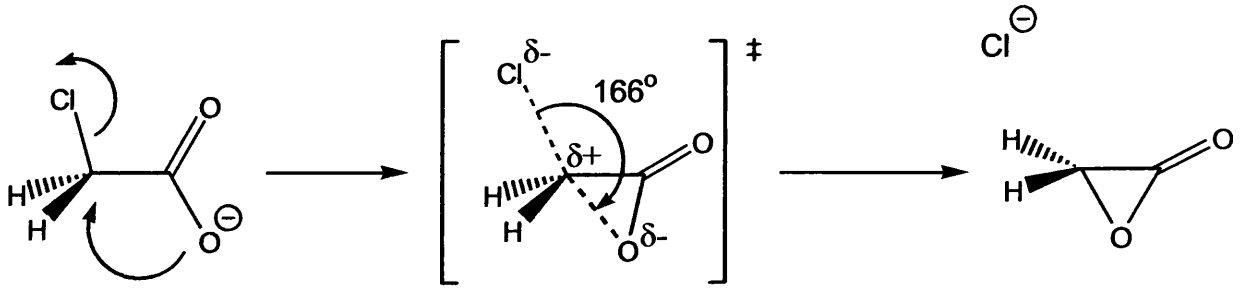

Fig. 24. Calculated pathway and structures for elimination of Cl^- from α-chloroacetate anion.[35]

Some early theoretical work, using MNDO computational calculations, on the α-chloroacetate ion was conducted by Davidson and co workers.[35] The elimination of a chloride anion and ring closure to an α-lactone was considered. The theoretical calculations performed supported the hypothesis that an α-lactone has a role in the elimination of chloride anions from chloroacetate ions.[35] In the calculated transition-state shown in figure 24, the Cl-C-O angle is 166°.

2.4. The nature of α-lactones (substituted oxiranone)

Lactones are cyclic species, intramolecular esters. Oxiranones (α-lactones) are strained and usually unstable three membered internal

esters. It had been assumed by Winstein and other researchers that α-lactones could not be isolated.[28] The simplest possible α-lactone is oxiranone and theoretical calculations have been performed upon the oxiranone moiety.[36,37]

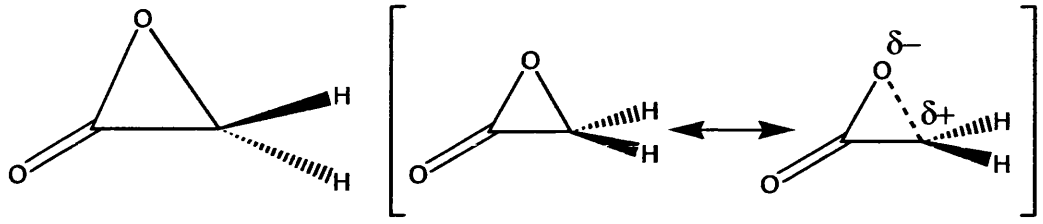

Fig. 25. Oxiranone, the simplest α-lactone.[37]

Oxiranone has been calculated to have an *in vacuo* enthalpy of formation ($\Delta H^{\theta}_{f,298}$) of -45.4 kcal mol^{-1} and a conventional ring strain energy of 40.4 kcal mol^{-1} as calculated with a level of theory corresponding to QCISD(T)=full/6-311G(2df,p)//MP2=full/6-311G(d,p).[37] Oxiranone has been implicated as an intermediate in the reaction between methylene carbene and carbon dioxide, see below.[36,38] There has been debate about the nature of the bonding in α-lactones; is there a formal bond between the O-CH_2 moiety in oxiranone or is this bond highly polar or indeed charge separated as in a zwitterion?[28,37] The QCISD(T) calculated enthalpy of formation of cyclopropanone is 1.5 kcal mol^{-1}. The oxiranone ring is probably slightly less strained than the cyclopropanone ring. Calculated electron density, using MP2/6-31+G(d), in the gas-phase for oxiranone indicate a covalent like structure, with a polarised bond between C_α and O_n. However, implicit solvation, SCI-PCM/MP2/6-31+(d), indicates that the C_α and O_n bond is so polarised that the bond is best described as being an electrostatic interaction.[37]

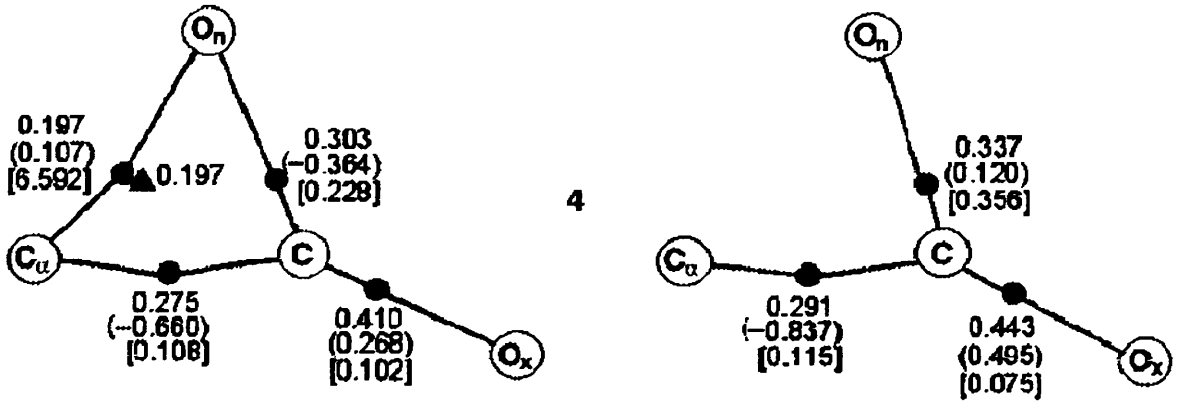

Gas phase SCI-PCM water

Fig. 26. MP2/6-31+G(d) calculations, • refers to bond critical point and ▲ refers to ring critical point, with associated electron densities.[37]

Mass spectra experiments have been used to derive an estimated the heat of formation of oxiranone, sometimes called acetolactone, as -47.3 +/- 4.7 kcal mol^{-1} from chloride anion elimination from chloroacetate anions.[39] Earlier calculations reported by Liebman and Greenberg calculated the heat of formation of oxiranone to be -31 kcal mol^{-1}.[40]

Studies of isolated α-lactones have been made and spectroscopic data has been used to assign structural features. Studies of α-lactones have shown them to undergo decarbonylation even at low temperatures and/or polymerise to polyesters.[37,41]

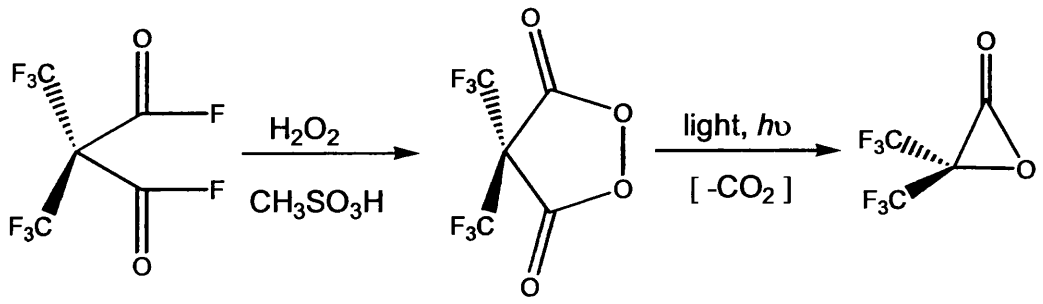

Fig. 27. 2,2-dimethyloxiranone prepared by photolysis.[42]

Photolysis of bis(trifluoromethyl)malonyl peroxide at 77K led to immediate loss of C=O i.r. bands at 1870-1825 cm^{-1} and simultaneous

appearance of a C=O i.r. band at 1970 cm^{-1} and CO_2 band at 2350 cm^{-1}. Also photolysis of a 0.32M solution of bis(trifluoromethyl) malonyl peroxide in carbon tetrachloride at -15°C results in an 87% yield after 1 hour of 2,2-bis(trifluoromethyl)-oxiranone. At 24°C the 2,2-bis(trifluoromethyl)-oxiranone is a gas with a C=O i.r. band at 1980 cm^{-1} and mass spectroscopy shows the parent ion [m/e^+ 194 a.u.] persisting with a decay rate that corresponds to a half-life of 8 hours.[42]

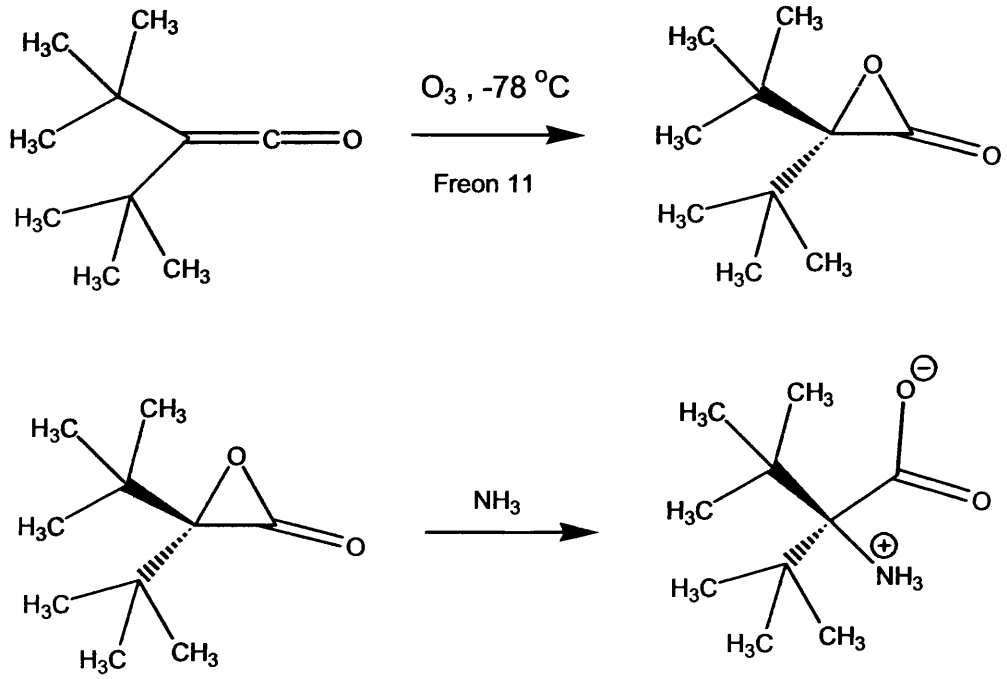

Fig. 28. Bartlett preparation of *di-tert*-butylacetolactone.[43]

Wheland and Bartlett studied the formation of polyesters from ketenes and characterized an intermediate α-lactone.[43] Wheland and Bartlett reasoned that a hindered α-lactone would be less likely to exist in an open dipolar/zwitterion form. Ozonolysis of di-*tert*-butylketene in freon11 at -78°C followed by the addition of ammonia resulted in a white precipitate; found to be *di-tert*-butyl-glycine. The ^1H NMR spectrum of the *di-tert*-butyl-glycine, in concentrated hydrochloric acid showed a singlet at 2.0 ppm corresponding to *tert*-butyl groups being equivalent in the zwitterionic product. The ^1H NMR spectrum of *di-tert*-butylacetolactone, at -60°C, showed a singlet at 1.2 ppm for the *di-tert*-

butyl groups which was identical to the starting materials, *di-tert*-butyl ketene and *di-tert*-butylketone. Warming the solution of *di-tert*-butylacetolactone to -20°C in the presence of hexafluoroacetone resulted in an alkene (29%) and a β-lactone (21%) product.[44]

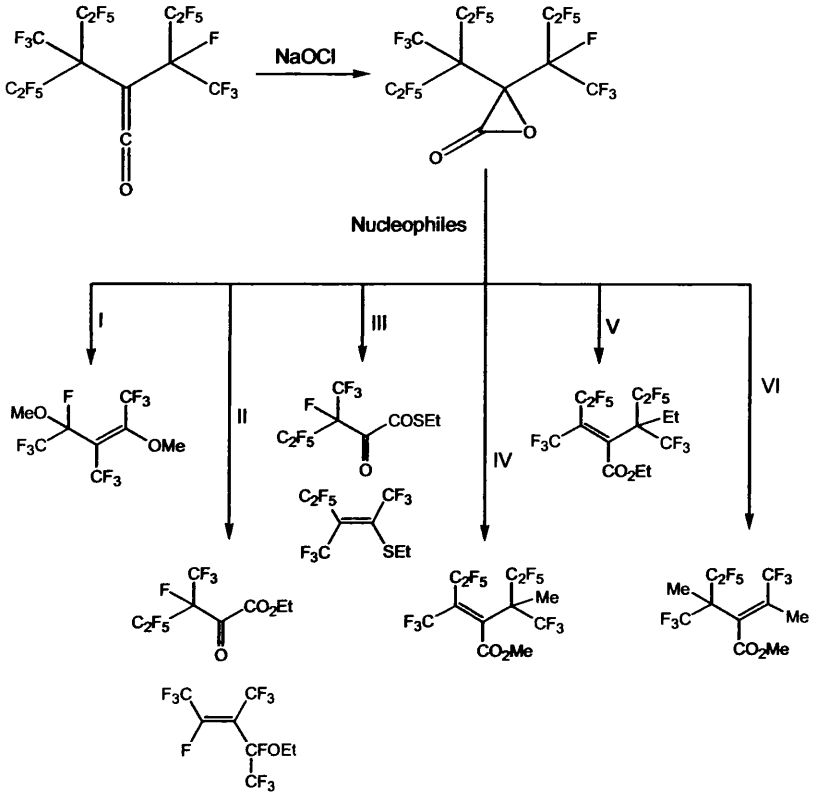

Fig. 29. More reactions with previously prepared α-lactone. i, MeO^-; ii, EtO^-; iii, EtS^-; iv, MeMgI; v, EtMgI; vi, MeLi.[44]

Reacting a perfluoroketene with sodium hypochlorite has enabled the isolation of 3-(1,2,2,3,3,3-hexafluoro-1-trifluoromethyl-propyl)-3-(2,2,3,3,3-pentafluoro-1-pentafluoroethyl-1-trifluoromethylpropyl)-oxiran-2-one, as shown in figure 29.[44] Most of the reaction products of the perfluorinated α-lactone with nucleophiles have resulted from rearrangement and fragmentation after nucleophilic attack. The results did suggest that relatively small nucleophiles attack the carbonyl carbon. Slightly larger nucleophiles attack the acyl oxygen, in the α-lactone.[44]

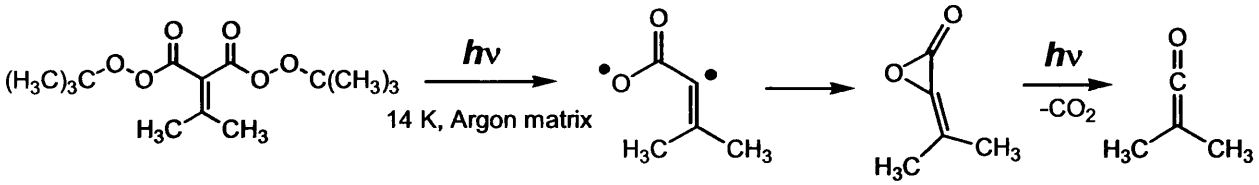

Fig. 30. Irradiation of a bisperoxyester to yield a diradical (singlet) and an α-lactone, with further decay to a ketene.[42]

Reed and co-workers studied the low temperature infra-red irradiation of a bisperoxyester and characterised dimethylvinlydene [$(CH_3)_2C{=}C{:}$] generated within an argon matrix at 14K.[45] Additional products were identified, including an α-lactone and vibrational spectra were compared with calculated vibrational frequencies. The α-lactone, 3-isopropylidene-oxiran-2-one, has experimental infra-red absorptions at 1924 cm^{-1}, 1695 cm^{-1}, 1148 cm^{-1} and 1050 cm^{-1}. These were compared to computed B3LYP/6-31G(d) vibrational frequencies of 2013 cm^{-1}, 1710 cm^{-1}, 1156 cm^{-1} and 1051 cm^{-1}. However, a calculated vibrational frequency at 707 cm^{-1} could not be reconciled with experimental data.[38] Chapman and Adam reported the formation of α-lactone, see figure 27, at 77K with reported C=O absorption data at 1900 cm^{-1} and 1935 cm^{-1}. Reed and co-workers performed calculations on 3-isopropylidene-oxiran-2-one with B3LYP/6-31G(d) and vibrational frequencies indicate the C=O stretches occur at 1932 cm^{-1} and 1966 cm^{-1}.

Due to the internal ring strain associated with α-lactones, they often have a role as intermediates, ring opening leading to relief of ring strain.

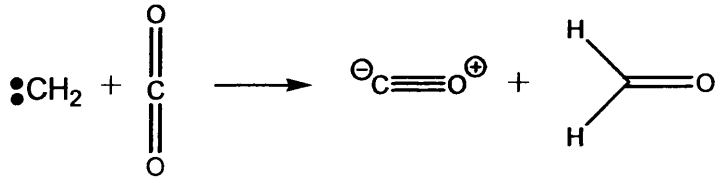

Fig. 31. Reaction of carbon dioxide to yield formaldehyde (glyoxal) and carbon monoxide.[38]

Oxiranone itself, the simplest α-lactone, has been implicated as an intermediate in the reaction between methylene carbene and carbon dioxide.[38] Three reaction paths were considered by Kovac and co-workers for the reaction of carbene with carbon dioxide.[38] The second path, shown as b in figure 32, considered cycloaddition to a carbonyl π-bond leading to the formation of oxiranone.

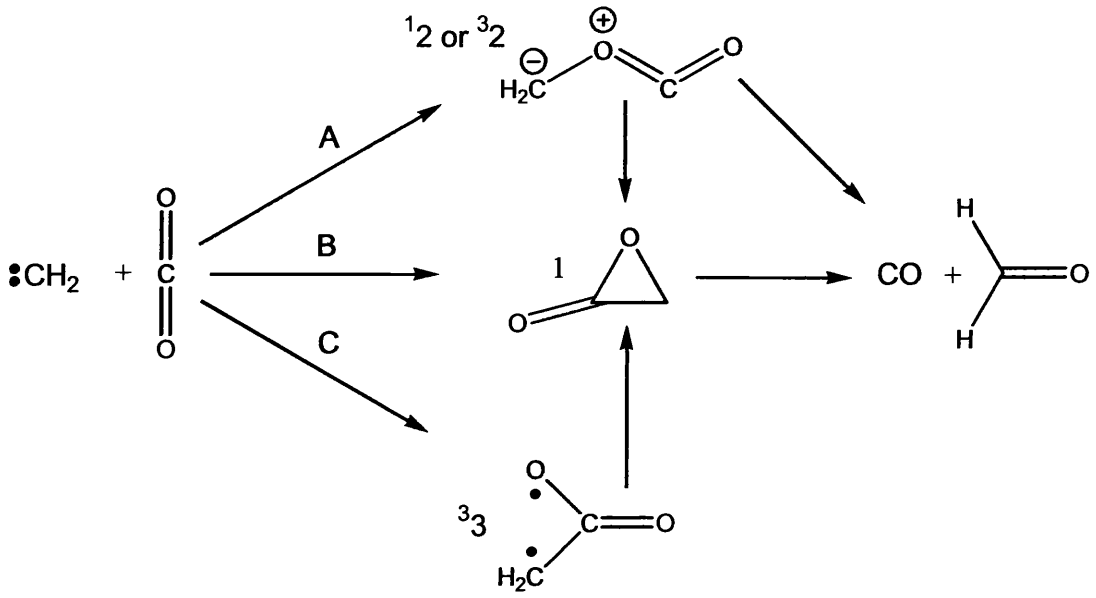

Fig. 32. Reactions pathways considered by Kovac.[38]

Fragmentation and dissociation of the oxiranone then led to the formation of carbon monoxide and formaldehyde. Kovac and co-workers also used computational chemistry calculations, HF/6-31+G(d) and G2, to provide a quantitative test of ideas and found that oxiranone intermediate pathway was energetically preferable to pathways involving ylide-like intermediates or acetoxyl diradicals.[38]

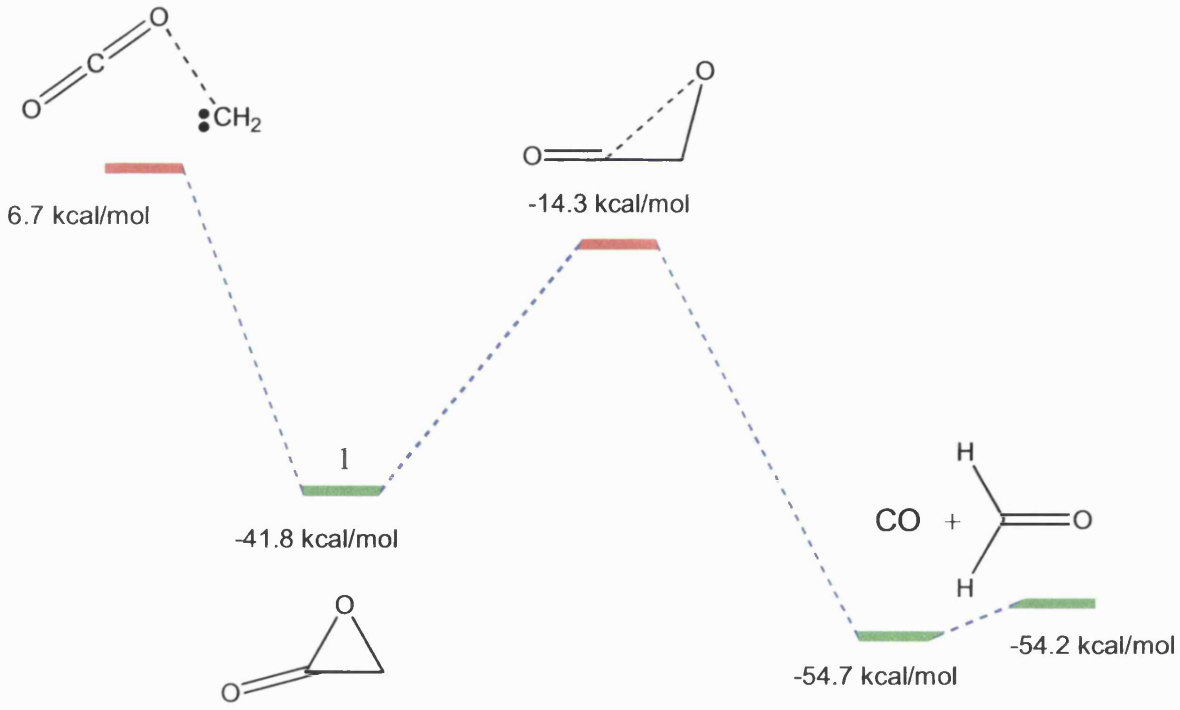

Fig. 33. Reaction of singlet methylene carbene [^{1}:CH_2] with CO_2 and calculated energetics (G2) for path "B" studied by Kovac.[38]

The intermediacy of α-lactones and intermediate carbene diradicals has also been investigated by Toscano and co-workers at John Hopkin's University.[46] During the nitrosation and alkylation of amino acid, α-lactones have been suggested as intermediates.[47]

2.5. β-lactone and larger ring formation.

As hydrolysis of α-haloacids involves α-lactone participation, this could be extended to hydrolysis of a β-haloacids and participation of β-lactones. Work on the hydrolysis of β-bromo and α,β-dibromo-β-arylpropionate ions by Bordwell and Knipe also found relationships with neighbouring groups and involving ring-closure; β-lactones could be prepared.[48]

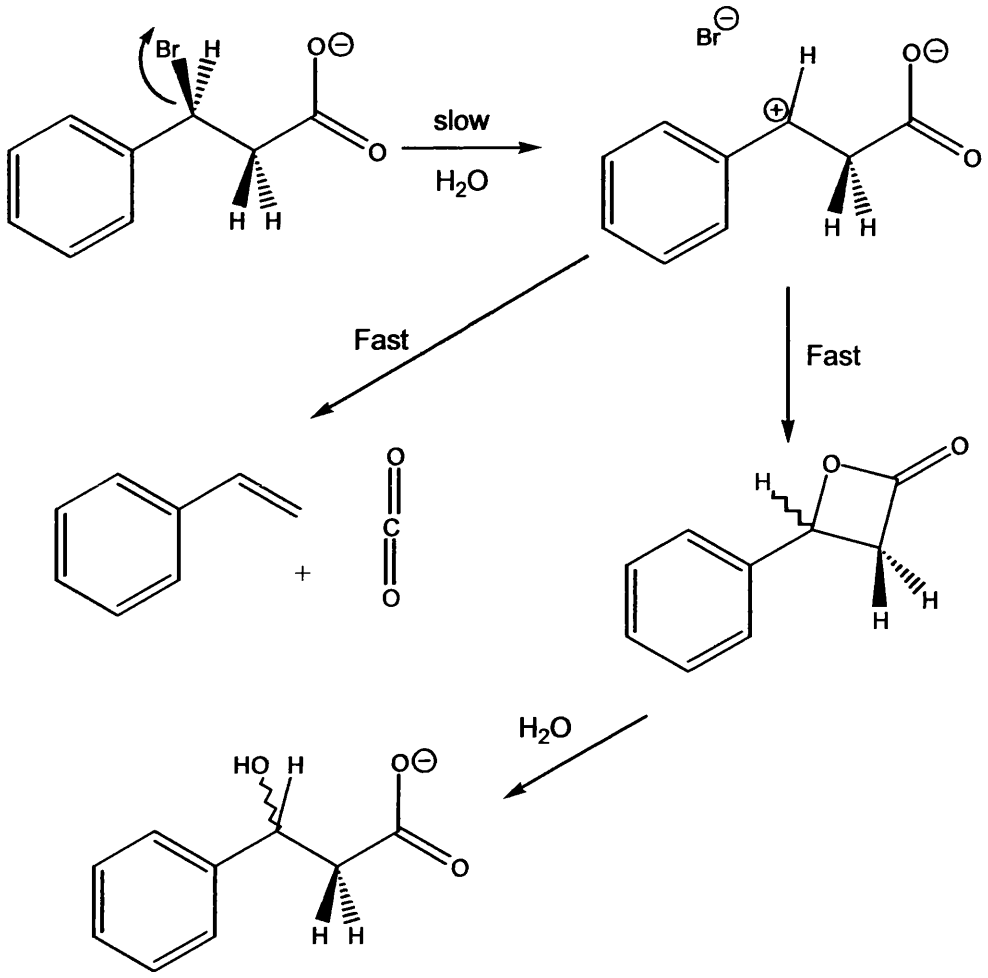

Fig. 34. Bordwell and Knipe scheme for $ArCHBrCH_2CO_2^-$ hydrolysis.[48]

Halo-lactonisation rarely involves chlorination, however examples are reported. Guthrie and co workers reported the isolation of γ-chloro-β-lactones by chlorination of the sodium salts of (Z)-aconitic acid and (E)-aconitic acid in water.[49]

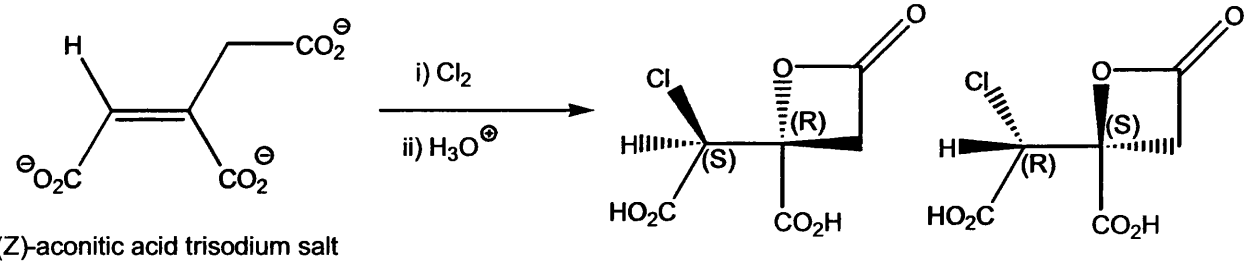

(Z)-aconitic acid trisodium salt

2S(R)-(carboxy-chloro-methyl)-4R(S)-oxo-oxetane-2-carboxylic acids

γ–chloro-β-lactone

Fig. 35 4-*Exo-Tet* halolactonisation of (*Z*)-aconitic acid with chlorine.[49]

Completely stereospecific cyclisation to yield β-lactones by bromolactonisation of α-substituted-β,γ-unsaturated acids under basic conditions, using $NaHCO_3$, has been reported.[50] The stereochemistry of an isolated β-lactones, 4S-bromoethyl-3R-methyl-oxetan-2-one, was confirmed by reduction with tri-*n*-butyltin hydride in the presence of AIBN which allowed the isolation of a de-brominated β-lactone, 3R,4R-dimethyl-oxetan-2-one, in 89% yield. Examining the ^1H NMR spectra indicated that coupling constant between ring methine hydrogen's was 3.9Hz. No *cis* isomers were detected.[50]

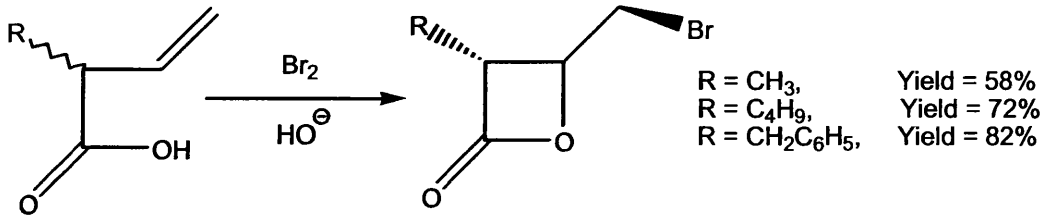

Fig. 36. Bromolactonisation to yield *trans* β-lactones.[50]

Terashima and Jew reported the stereoselective preparation of α-hydroxy-acids in which the stereochemistry was established by bromo-lactonisation.[51]

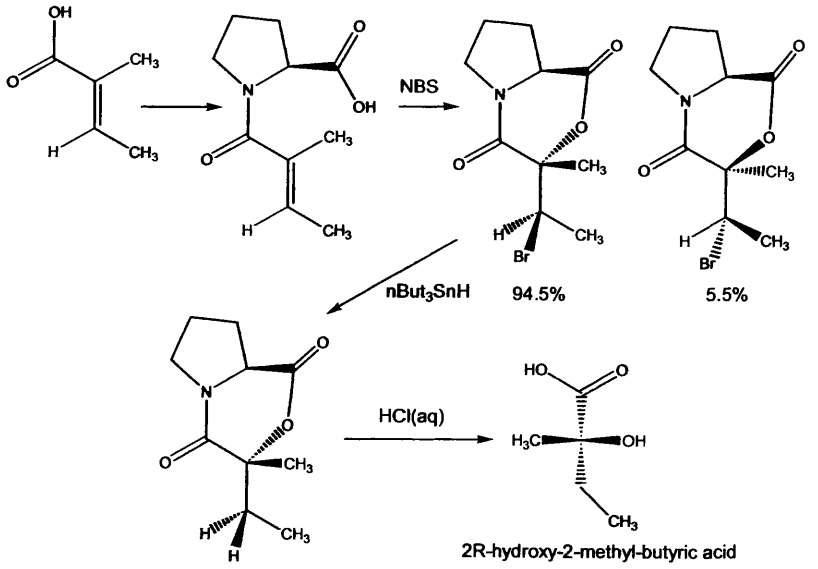

Fig. 37.Stereospecific synthesis of α-hydroxyacid.[51]

Backside attack (S_Ni) on a bromonium ion has been utilised in synthetic work. Terashima and Jew proposed that carboxyl group attack on a bromonium was responsible for exclusive formation of one of the two diastereomers in the asymmetric synthesis of optically active α-hydroxy acids.[51] The interesting question was posed that intramolecular attack of the carboxylate anion to the incipiently formed bromonium ion would either occur from the α-side of the s-*cis*-conformer (I) or from the β-side in the s-*trans*-conformer (II), as shown in figure 38. Examination of the resultant stereochemistry of the resultant bromo-β-lactone however does not suffice to offer an answer. It is a good example of back-side attack of a carboxylate anion upon a bromonium ion species leading to formation of a lactone.

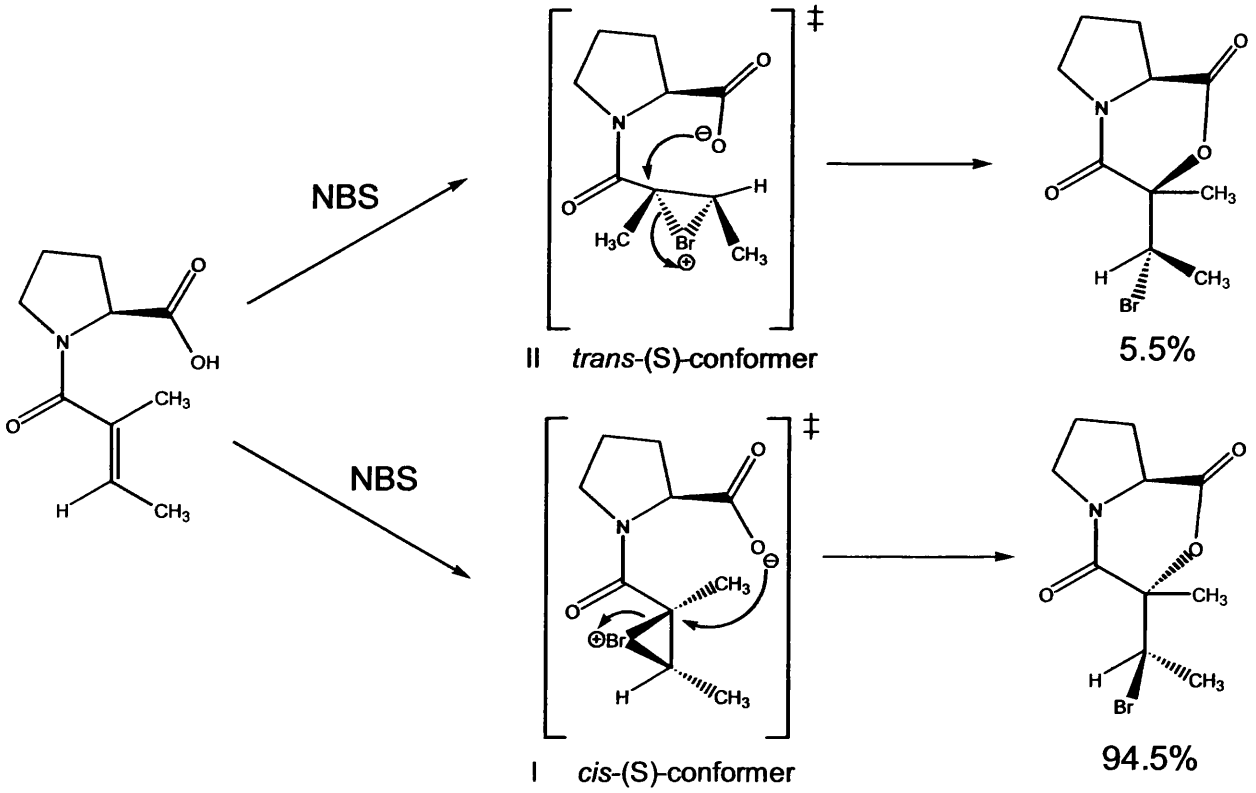

Fig. 38. Attack on a bromonium as proposed by Terashima and Jew.[51]

Bromination and ring formation has been utilised in synthetic work. The preparation of methyl *trans*-4-(*tert*-butoxycarbonylamino)-3-oxo-1-cyclohexanecarboxylate was desired to provide mimic of peptide bonds

in a drug design program. The 3-Cyclohexene-1-carboxylic acid was brominated with bromine in chloroform. The bromination gave a diastereoisomeric mixture of a minor product, 10% of 3S,4R-dibromo-cyclohexane-1S-carboxylic acid and a major product, 90% 3R,4R-dibromo-cyclohexane-1S-carboxylic acid. Addition of aqueous sodium hydroxide then caused base induced ring closure to yield a β-lactone 4R-bromo-6-oxa-bicyclo[3.2.1]octan-7-one, structure 3 in figure 39. Only the major product, shown as 2 in figure 39 will ring close to a β-lactone. It was noted that the minor product from bromination, 3R,4R-dibromo-1S-cyclohexanecarboxylic acid did not undergo base induced ring closure. The β-lactone was then ring opened with sodium hydrogen carbonate in methanol to yield a bromohydrin 4R-bromo-3S-hydroxy-cyclohexane-1S-carboxylic acid, structure 4 in figure 39. The yield of the bromohydrin was 95%.[52]

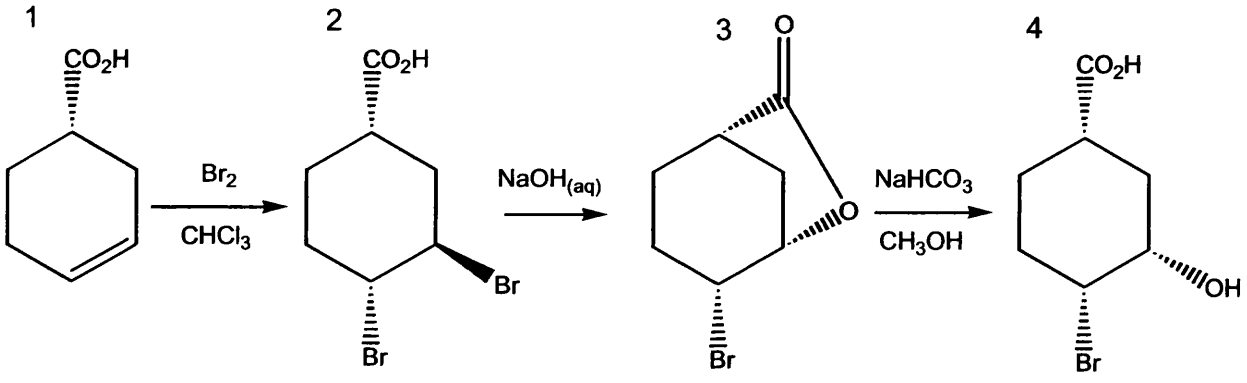

Fig. 39. Bromination, ring-closure and ring-opening implemented in synthesis.[52]

Halolactonisation has been used to form larger rings and allow study of the mechanism of ring closure. The rates of ring closure of ω-bromo-alkylcarboxylates to lactones has been studied.[53]

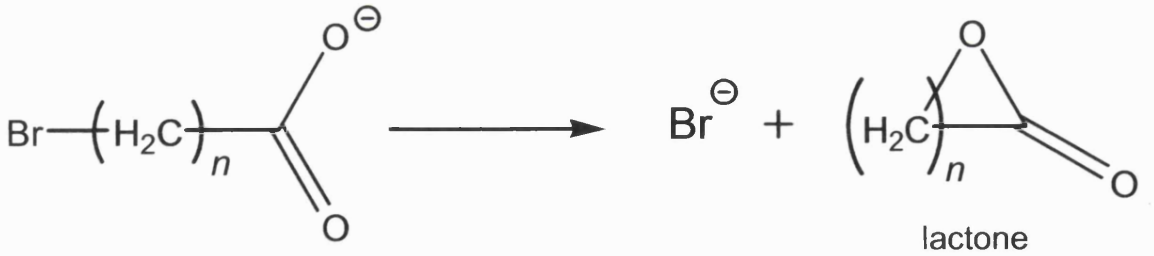

bromo-*n*-alkyl carboxylate

lactone

Ring Size	3	4	5	6	7	8
Relative Rates of ring closure	8.3×10^{-4}	0.31	90	1	0.0052	6×10^{-5}

Fig. 40. Rate of formation of lactone.[53]

Figure 40 shows the relative rates of formation for the formation of lactones from ω-bromoalkanecarboxylates.[53] The enthalpy of the formation of the TS, $\Delta H^{\ddagger}$, for three and four membered rings is normally greater than that seven membered rings. The $\Delta H^{\ddagger}$ terms also reflect the ring strain associated with smaller rings. However, $\Delta S^{\ddagger}$ is less negative for formation of three-membered rings relative to $\Delta S^{\ddagger}$ four, five and six membered rings.[53]

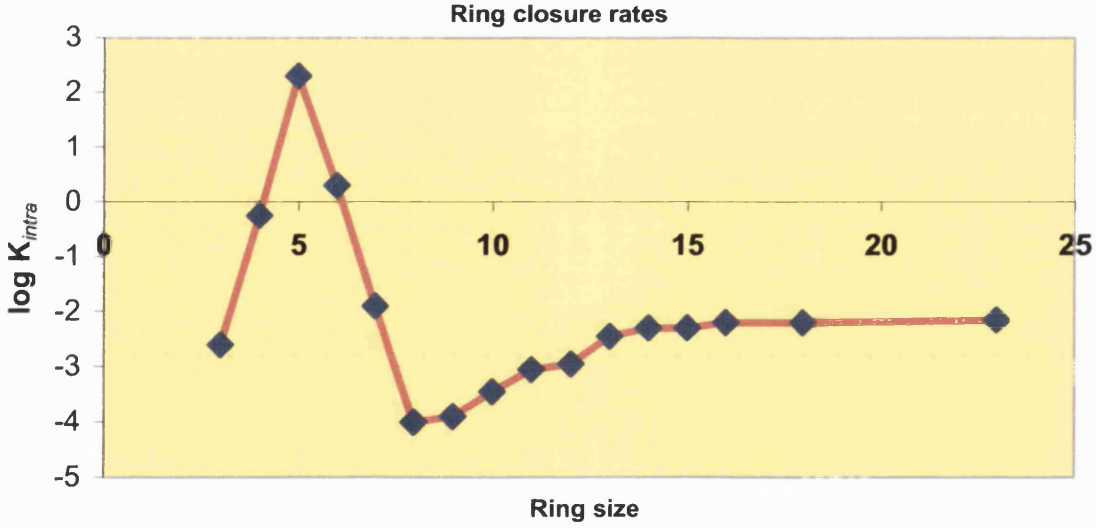

Fig. 41. Rates of ring closure for bromocarboxylates.[53]

The large negative entropy, $\Delta S^{\ddagger}$, is associated with the improbability of the achieving the required molecular conformation for ring closure as chain length increases. Hence formation of five and six membered rings is favourable. Stereoelectronic considerations of the ring closure must also be taken into account.[54] Different intramolecular nucleophilic attacks have different modes of attack. In figure 42, one ring species is shown, with the two potential routes for intramolecular attack. Baldwin and co-workers have developed systematic rules relating to ring formation, where the heteroatom X is a first row element as shown in figure 42.[54] Three considerations are made:-

- The ring size.
- The hybridisation of the carbon at the reactive centre.
- The relationship between; *Endo*-cyclic or *Exo*-cyclic, attack of the reacting bond to the formation of the ring.

The following table summarises these relationships.

EXOCYCLIC BONDS				ENDOCYCLIC BONDS		
Ring Size	sp (dig)	sp2 (trig)	sp3(tet)	sp (dig)	sp2 (trig)	sp3 (tet)
3	unfav	fav	fav	fav	unfav	rare
4	unfav	fav	fav	fav	unfav	rare
5	fav	fav	fav	fav	unfav	rare
6	fav	fav	fav	fav	fav	rare

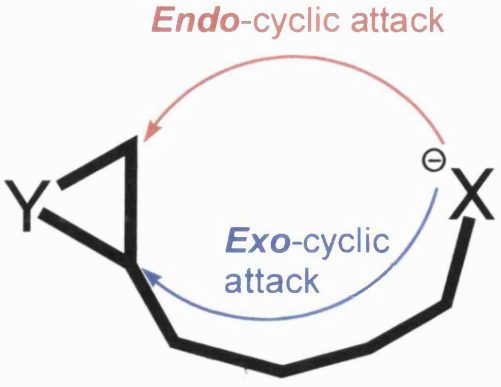

Fig. 42. Different modes of attack for ring opening/closure for an epoxide.[54]

The enzyme fumarase is responsible for the hydrolysis of fumaric acid to S-(-)-malic acid. The addition takes a steric course of *syn* addition resulting in *cis* addition product.[55,56] This is a good example of specificity of enzyme catalysis, as hydration of fumaric acid will only yield S-(-)-malic acid and maleic acid hydration is not catalysed. This emphasises the fact that many biochemical reactions do not necessarily follow expected stereochemical pathways as enzymes may use internal structure to attack substrates in a manner that is quite distinct from reaction occurring in a locally ordered solvent such as water.

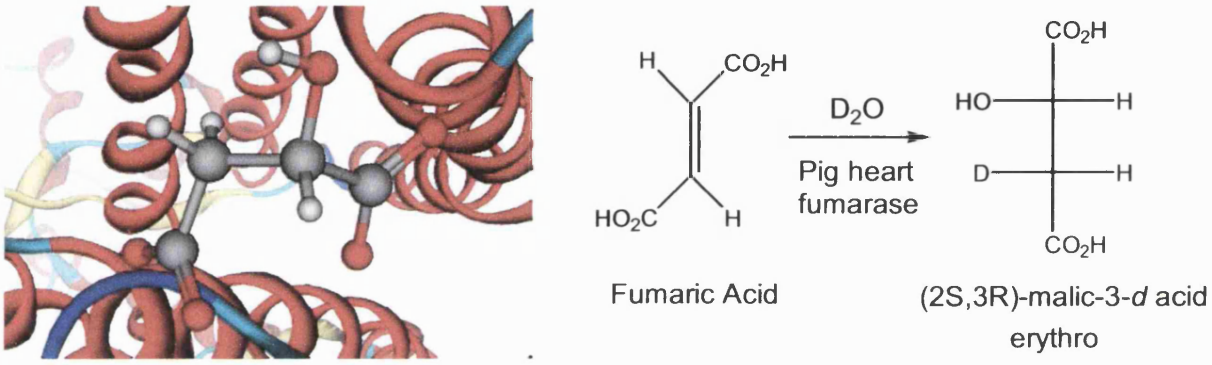

Fig. 43. Close-up view of fumarase active site with S-(-)-malic acid product.[55]

The dehalogenase enzymes also exhibit stereospecificity that is quite distinct from classical behaviour.[57] The enzymes use internal structure such as serine and aspartic acid amino acid residues to hold the carboxylate group, then Arginine amino acid residue removes the α-chloro atom and an ester intermediate results.

Hydrolysis of the ester intermediate results in inversion of configuration, neighbouring group assistance from the carboxyl group is not observed. A proposed reaction mechanism for the completion of the Walden inversion is illustrated in the figure 44. There are two possible routes from the transition state to the ester intermediate, however hydrolysis results in inversion of configuration.[57,58]

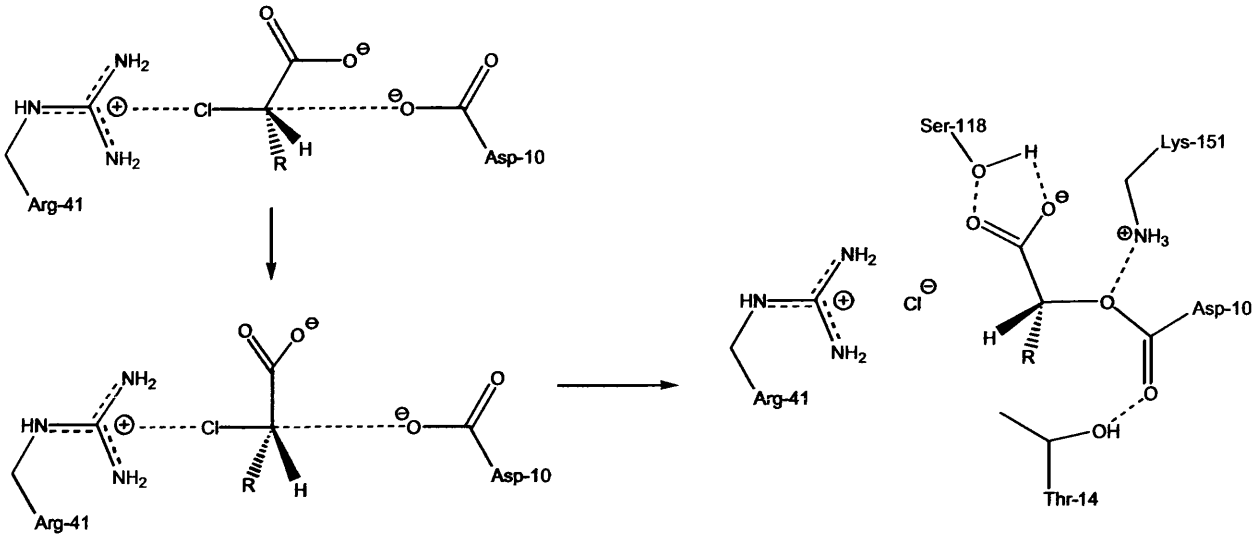

Fig.44. dehalogenase enzymes eliminate halides from α-haloacids with inversion of configuration.[57]

Bromination of unsaturated species will also yield lactones, through ring closure of carboxyl groups attacking bromonium ions by back-side attack. Homsi and Rousseau prepared 2-oxetanones, 2-azetidines and oxetanes from the reaction of bis(collidine)bromine hexafluorophosphate with α,β-unsaturated acids, α,β-unsaturated N-sulfonamides and allylic alcohols, in dichloromethane.[59]

Homsi and Rousseau reported ring closures occurred by unusual 4-*Endo-Trig* processes. Many electrophilic ring closures occur by *Exo*-mode as noted by Baldwin, these are favoured over *Endo* processes normally.[54,59] In figure 45, Homsi and Rousseau have assumed that the formation of β-lactones is a single step process.[59] In figure 45 the term *Trig* implies that there is no formal bond between the bromine and the unsaturated compound in the bromonium ion. There is thus an ambiguity in relation to the use of the terms *Tet* or *Trig* in the ring closure processes concerning bromonium species.

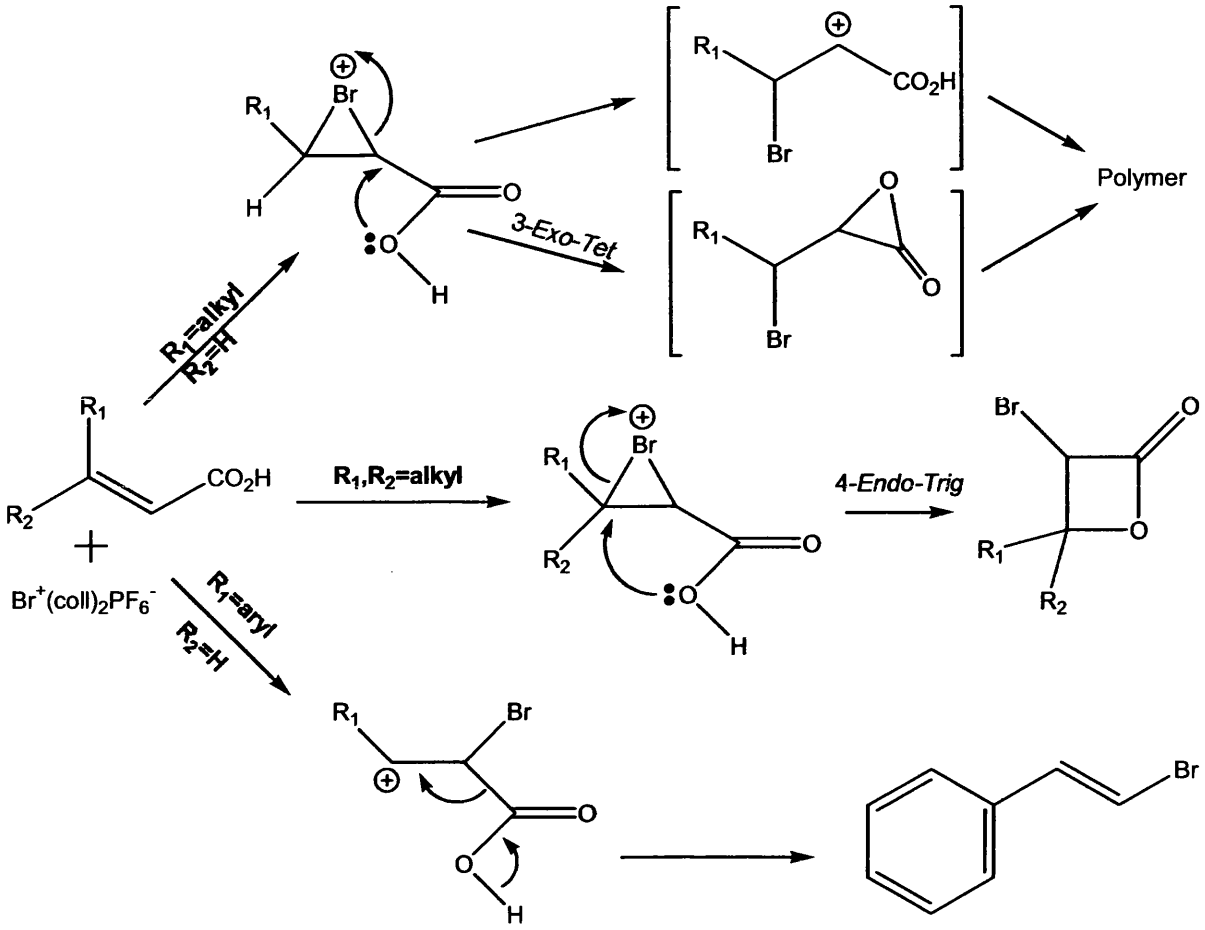

Fig. 45. Possible fates for bromonium species.[59]

The term *Tet* has been used in this thesis to describe ring closure on halonium ions, since modelling has been performed assuming that there are bonds between the bromine and the alkenes in the bromonium species.[54,59,60]

2.6. Addition of halogens to substituted alkenes.

Roberts and Kimball discussed the fact that work by Tarbell and Bartlett showed that the first step in the reaction of a halogen with an alkene leads initially to a negatively charged halide ion and a positively charged organic ion.[61]

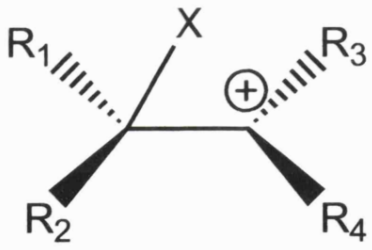

Fig. 46. Structure proposed by R. Robinson for halogen-alkene cation.[61]

Robinson proposed a structure as shown above in figure 46. However, the ion as shown is quite capable of rotation about the central carbon-carbon bond. Such potential rotation would not account for the fact that homogenous, non-photochemical, halogenations give rise to either *cis* or *trans* addition products, usually accounting for at least 80% of the stereo selectivity of the reaction. Roberts and Kimball suggested that as the C+ atom has a vacant orbital and the halide atom, X, has three orbitals occupied by pairs of electrons, a co-ordinate link should form from donation of electrons from the halide atom to the C+ cation atom. Roberts and Kimball suggested the following structure, a cyclic intermediate cation, as the structure for halogen-alkene intermediate, a cyclic halonium ion.

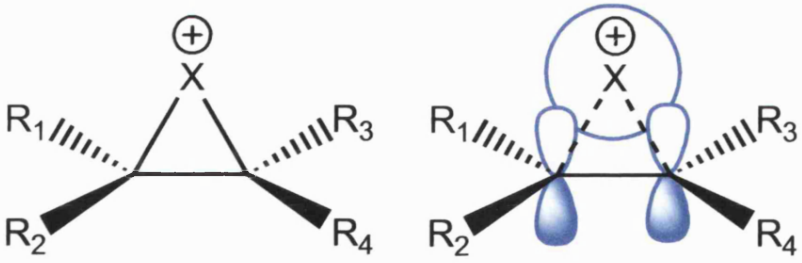

Fig. 47.Cyclic halonium ion suggested by Roberts and Kimball.[61]

The first ionisation potentials for carbon and bromine are similar; 259.6 kcal mol^{-1} for carbon and 272.5 kcal mol^{-1} for bromine.[61] Roberts and Kimball suggested that the small difference in the ionisation potentials means that the initially formed complex is intermediate between the structures shown in figure 46 and figure 47. Interestingly though Roberts and Kimball did suggest that charged groups for R1 and R3 (and/or R3

and R4) may provide sufficient repulsion to overcome the cyclic halonium bonds and allow rotation to the opposite *trans* isomer. Computational studies conducted on halonium ions have supported the suggestion of Roberts and Kimball.[63]

Empirical data has also supported the suggestion of Roberts and Kimball, including the isolation of a stable bromonium ion with corresponding crystallographic data.[64] Heats of formation of bromonium ions have been determined experimentally at -60 °C in fluorosulfonic (FSO_3H) acid containing 11.5% moles SbF_5. The relative stabilities were measured by calorimetry and compared to N.M.R data.[65]

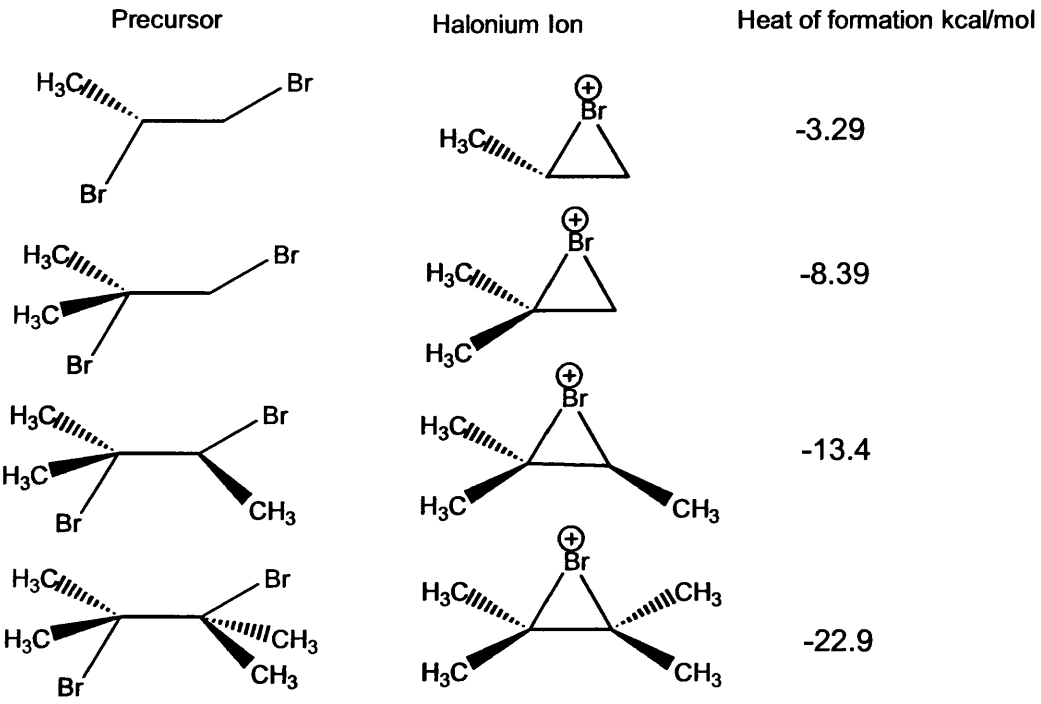

Fig. 48. Bromonium ion heats of formation at -60°C.[65]

As the formation of halonium ions involves the donation of electrons from the alkene to the approaching halogen moiety, the ionisation potential of the alkene should be related to the ease of formation of the halonium intermediate. For simple alkenes, the rate-determining step in the addition reaction is the formation of halonium ions. Relationships between ionisation potential of alkenes and the rate of reaction of

halogenation have been examined.[66] Halonium ion formations with aromatic rings adjacent to the alkene double bonds are less stable than the alkyl counterparts. Aromatic rings, such as a phenyl ring, can stabilise the formation of carbocations, bridged species are not so stable as alkyl counterparts. The carbocation is susceptible to nucleophilic attack from a solvent molecule. This is one of the reasons why bromination of stilbene results in formation of 1-methoxy-bromo-stilbene when conducted in methanol.[67]

Chlorination of alkenes tends to result in a similar stereochemical outcome as bromination, however chloronium ions are less stable compared to bromonium ions. Rearrangement during the course of a reaction may result in overall *cis* addition products, though the initial addition was *anti* to the reactant double bond.[68] A classical test for unsaturation is to dissolve bromine in carbon tetrachloride and to observe decolourisation upon adding an alkene. Chlorine will readily dissolve in water forming hypochlorite ions, an oxidising agent that detonates with methanol, and chloride ions. Heavier halogens will not so readily dissolve in water, bromine has poor aqueous solubility compared to chlorine, but will dissolve in organic solvents readily. Iodine, I_2, will only dissolve readily in water in the presence of iodide salts like KI. Addition of bromine to alkenes usually results in *trans* addition products resulting from a steric course of *anti*-addition. Classic examples of such addition reactions include the bromination of *cis*-butene, *trans*-2-butene, a number of cycloalkenes and maleic and fumaric acid.[69]

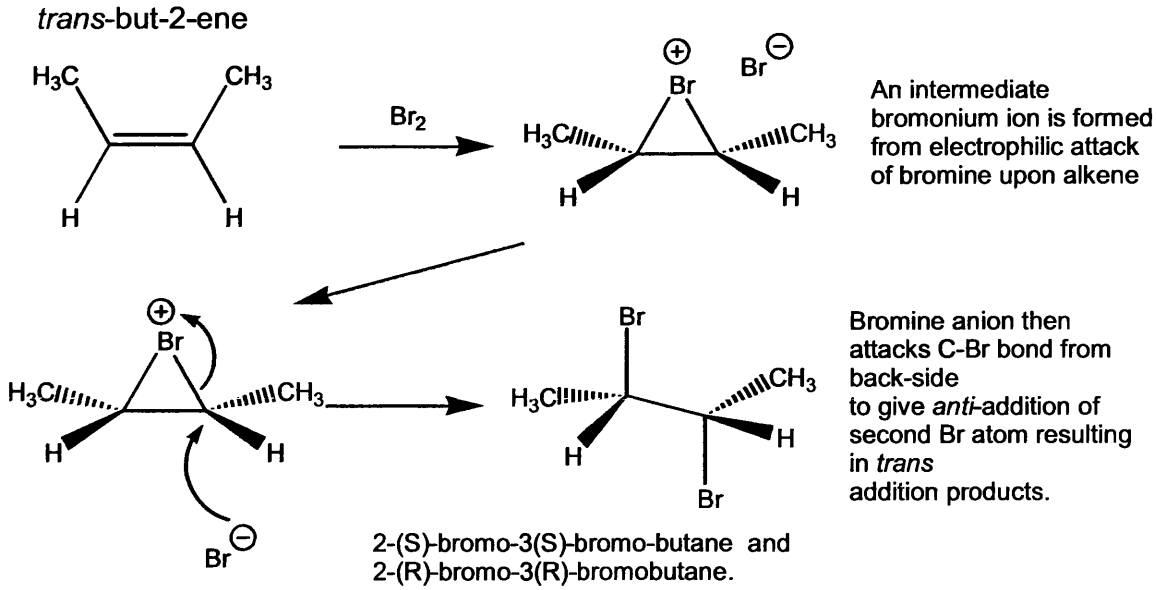

Fig. 49. Addition of bromine to *cis*-but-2-ene.[69]

Bromination of *cis*-but-2-ene yields a racemic mixture of 2-R(S)-bromo-3-S(R)-butane. Most additions of molecular bromine do yield *trans* addition products from a steric course of *anti* addition. Halogenation to yield *cis* addition has also been recently reported, albeit with little success and with bulky hydrocarbons only to facilitate favourable steric reaction course.[70] Halogenation to yield *cis* addition products would have to occur by a steric course of *syn* addition, yielding *cis* addition products as shown in figure 2.

Alkene	Relative Rate
Ethylene	1
1,1-dimethylethylene	5.5
Tetramethylethylene	14
Styrene	3.2
Acrolein	1.5
Acrylic Acid	< 0.03
Crotonic Acid	0.26
Vinyl bromide	< 0.03

Table. 50. Relative rate of bromination of some alkenes.[72]

The decolourisation of bromine in chloroform will test for unsaturation, Iodolactonisation has been used to locate the position of double bonds in α,β-unsaturated moieties.[70,71] Substituents attached to double bonds will affect the rate of bromination, as illustrated by the table above, cf. table 50. The mechanism of bromination of alkenes appears to a complex process, kinetic isotope measurements indicate that some processes are in competition and polymeric bromine species are involved. Bromination of alkenes is accelerated by electron-releasing substituents and retarded by electron-withdrawing substituents, see table 50.[73]

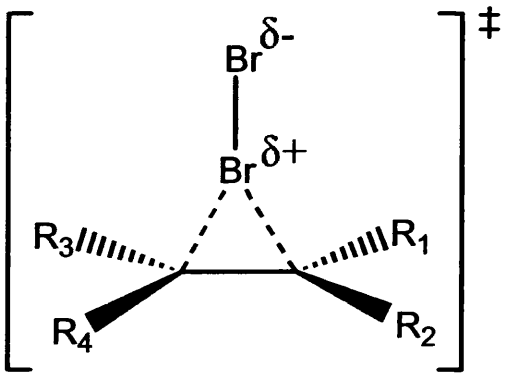

Fig. 51. TS corresponding to Ad_E2 mechanism.[73]

Consider the reaction between a simple alkene and bromine. The rate of bromination is first order for alkene, however, first or second order for molecular bromine. At low concentration of molecular bromine and in water or alcoholic solvents, the rate of reaction is second order overall, first order for both alkene and bromine. Under these conditions, the reaction proceeds via Ad_E2 mechanism, the reaction rate is expressed

$$\text{Rate} = k_1[\text{alkene}][Br_2]$$

In less polar solvents, e.g. acetic acid, and/or with higher bromine concentrations the kinetics is complex, often with three terms making a contribution to the rate expression: [73,74]

$$\text{Rate} = k_1[\text{alkene}][Br_2] + k_2[\text{alkene}][Br_2]^2 + k_3[\text{alkene}][Br_2][Br^-]$$

The mechanism for more complex brominations is best described as Ad_E3 processes. In methanol, pseudo-second order kinetics are observed when excess bromide ion is present. In such instances, the third term becomes the most significant.[74]

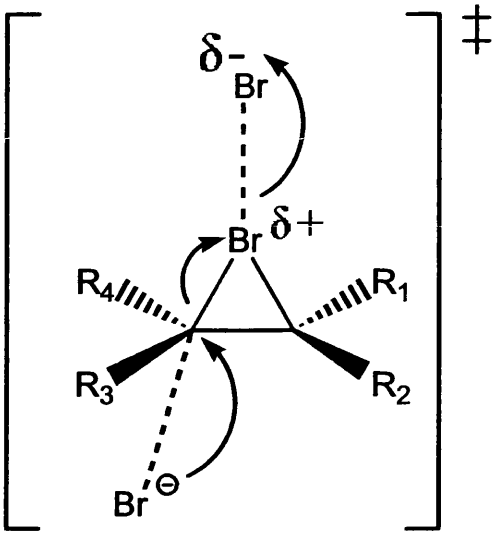

Fig. 52. TS corresponding to Ad_E3 mechanism.[73,74]

This leads to kinetic expressions similar to Ad_E3 mechanism for addition of hydrogen halides to alkenes, attack of halide ion on alkene-halogen complex is significant. In non-polar solvents the kinetics are often found to correspond to the first two terms, this is interpreted as the collapse of an alkene-halogen complex to an ion-pair. Chlorination generally exhibits second-order kinetics, first order for both alkene and chlorine. Various species for the brominating species have been suggest, including Br_6, Br_2, and solvent-bromine complexes.[73] However the KIE data does suggest that the major mechanistic process involves rate-limiting bromonium ion formation.[75,163]

2.6. Electrophilic addition to Maleic and Fumaric acids and salts.

The addition of bromine to maleic and fumaric acids was studied by McKenzie, using ether as a solvent.[76] Previous researchers had used aqueous solutions and some erroneous results recorded due to the

isomerisation of maleic acid to fumaric acid catalysed by hydrochloric or hydrobromic acid.[76] Bases will also catalyse the isomerisation of maleic to fumaric acid.[77] Co-crystallisation of maleic and 4,4'-bipyridine, in DMSO or DMF, solvent with high polarity and dielectric constants that disrupt hydrogen-bonding, will result in crystals of fumaric acid and 4,4'-bipyridine adduct. The same is not achieved when using acetone, methanol, chloroform and ethyl acetate. Refluxing maleic acid in DMF or DMSO alone does not result in isomerisation to fumaric acid.[77] The preparation of esters using sulphuric acid catalyst does not result in isomerisation of maleic acid to fumaric acid.

McKenzie discovered that the addition of bromine products to maleic acid yielded *iso*-dibromosuccinic acid and fumaric acid yielded *meso*-dibromosuccinic acid.[76] Holmberg independently and at the same time, also concluded that bromine added to maleic acid would yield *iso*-dibromosuccinic acid. This indicated that addition reactions tended to yield *trans* addition products but did not solve the problem of Walden inversions.

Derivatives of succinic acid provided the initial starting point for research into the Walden inversion. The configuration of substituted succinic acids would shed light on which isolated acid was formed in the Walden inversion. The study of addition reactions was conducted a few years later and this also help to shed light on stereospecific reactions. Oxidation of maleic acid by potassium permanganate yields *meso*-tartaric acid, and oxidation of fumaric acid by potassium permanganate yields racemic mixture of tartaric acid, in accordance with the concept of *cis*-addition as proposed by Wislicenus.[76,78]

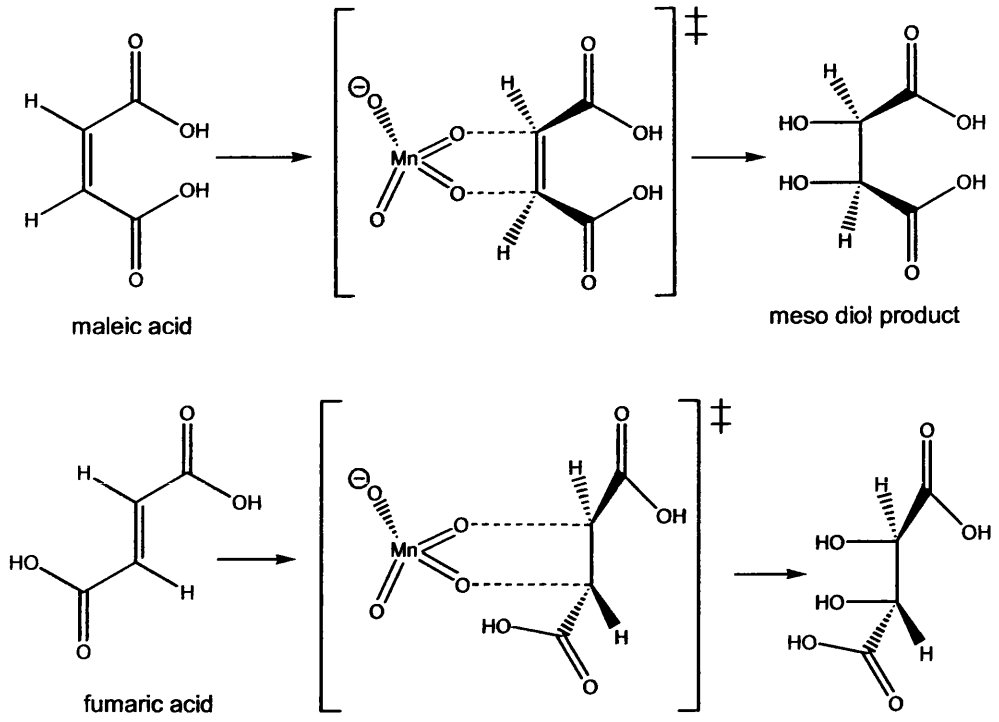

Fig. 53. Oxidation of maleic and fumaric acids by $KMnO_4$.[76]

However, Pasteur and Jungfleisch had shown that a racemic mixture of tartaric acid and *meso*-tartaric acid could be isolated by hydrolysis of silver salts of dibromosuccinic acids.[76] Both Anschütz and Kekule isolated *meso*-tartrate salts from boiling dibromosuccinic acid in water. Demuth and Meyer obtained racemic tartaric acid from *iso*-dibromosuccinic acid. The conversion of dibromosuccinic acid into *meso*-tartaric acid and the conversion of *iso*-dibromosuccinic acid into racemic tartaric acid did not present a simple story.[76]

Frankland had also presented work that shows *trans* addition to acetylenic and ethylenic compounds was the rule and not the exception.[12] McKenzie considered the nature of fumaric and maleic acid should show a relationship with the dibromosuccinic acids prepared from the acids by addition of bromine. One set of dibromosuccinic acids prepared should be of the *meso*-type and the other should be resolvable into *d*- or *l*- forms.[76]

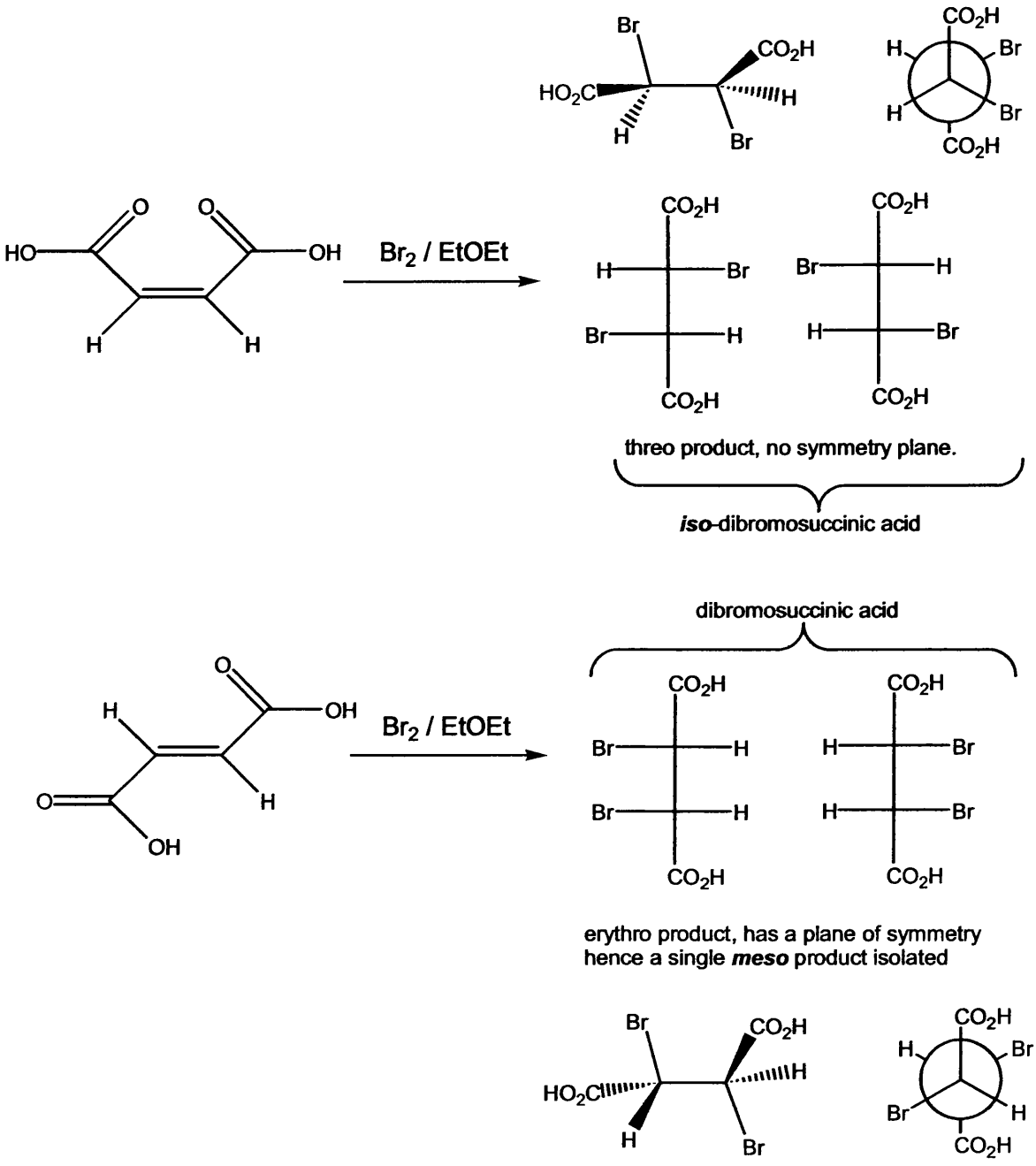

Fig. 54. Bromination of maleic and fumaric acids reported by McKenzie.[76]

McKenzie found that the *iso*-dibromosuccinic acid resulting from bromination of maleic acid in ether, consisted of two *threo*-dibromosuccinic acids and could be resolved with morphine salts. McKenzie also found that the dibromosuccinic acid prepared from bromine addition to fumaric acid in ether, an *erythro* product, could not

be resolved.[76] Holmberg at the same time and independently, concluded that *iso*-dibromosuccinic acid could be resolved, he measured the optical rotation of his most active product and found $[\alpha]_D$ -137.6° in ethyl acetate. McKenzie obtained a value of $[\alpha]_D^{13}$ of -148° for l-1,2-dibromosuccinic acid in ethyl acetate.[13]

Addition of halogens to unsaturated diacid dianions result in stereochemical outcomes quite different from those observed by MacKenzie. In 1925 it was shown that the disodium salt of maleic acid reacts with hypochlorous acid, chlorine dissolved in water, under aqueous conditions to give mainly chlorohydrins as *cis* addition products.[79]

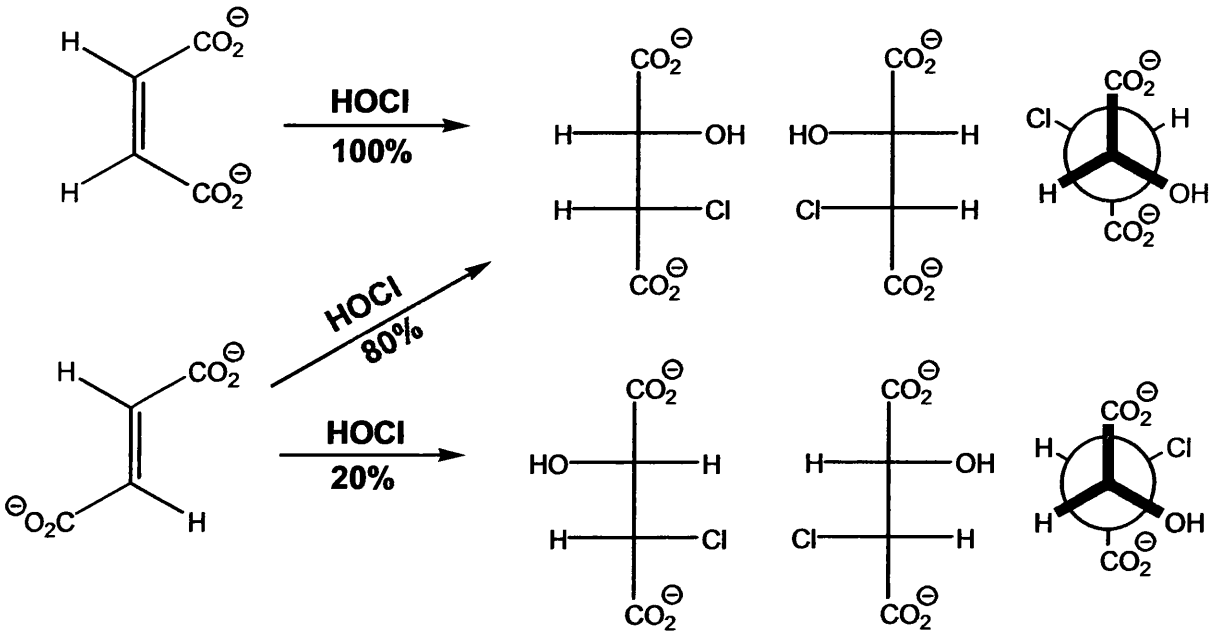

Fig. 55. Kuhn and Ebel preparation of 1R(S)-chloro-2R(S)-hydroxy-succinic acid dianion, yielding a racemic addition product.[79]

Kuhn and Ebel found that addition of hypochlorous acid (HOCl) to the disodium salt of maleic and fumaric acids gave *syn* addition products for disodium maleate and mainly 80% *anti* addition for disodium fumarate. The addition of hypochlorous acid to the disodium salt of fumaric acid

also yields *syn* addition products (20%) resulting in some overall *cis* addition products.[79]

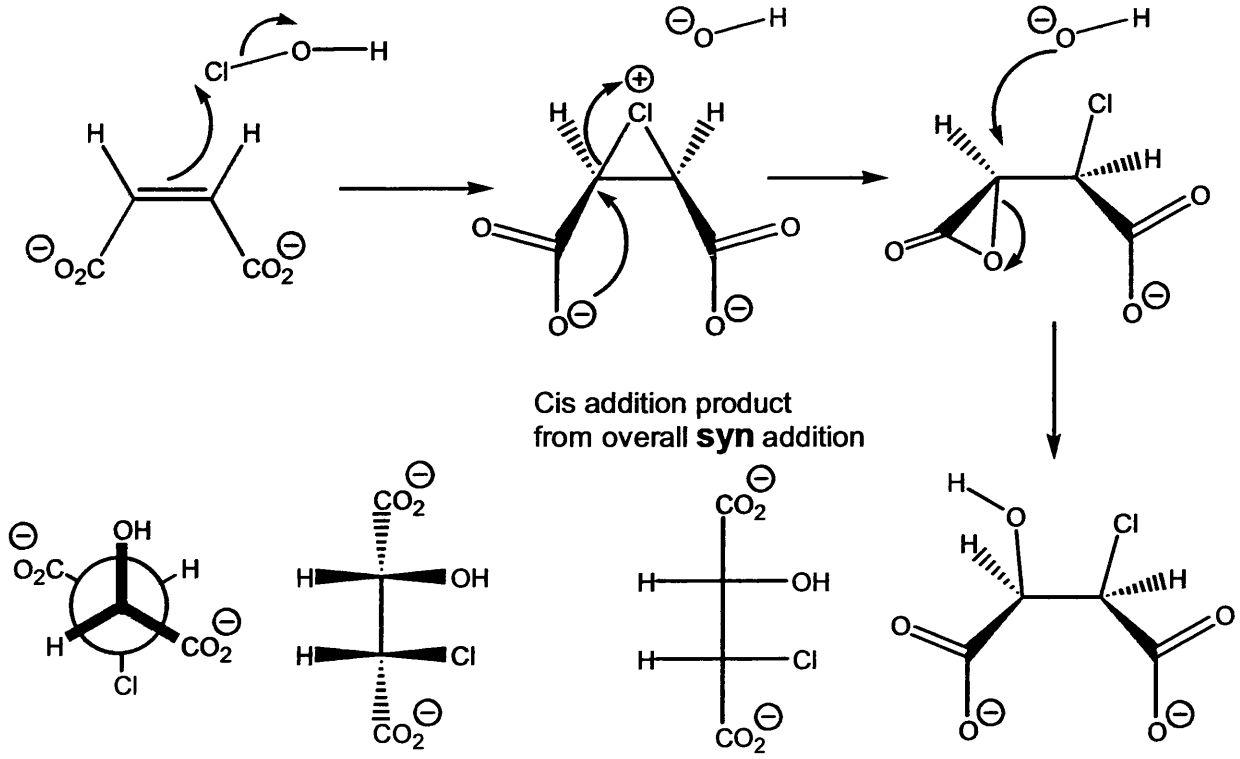

Fig. 56. Badea proposed mechanism for chlorohydrin formation from disodium salt of maleic acid by hydrolysis of α-lactone.[80]

These result were claimed by Badea to be result of the participation of carboxylate groups in causing ring opening of the intermediate chloronium ions. Badea also claims that with substituted maleic acids, mono-methyl-maleic and 2,3-dimethylmaleic acids, there is no *syn* addition in basic solutions.[80] Badea also claims that participation of the carboxyl groups in the chlorination of disodium maleic and fumaric acid is also in agreement with solvolysis of α-halogenated acids and the Walden inversion. Badea did not present empirical evidence.[80]

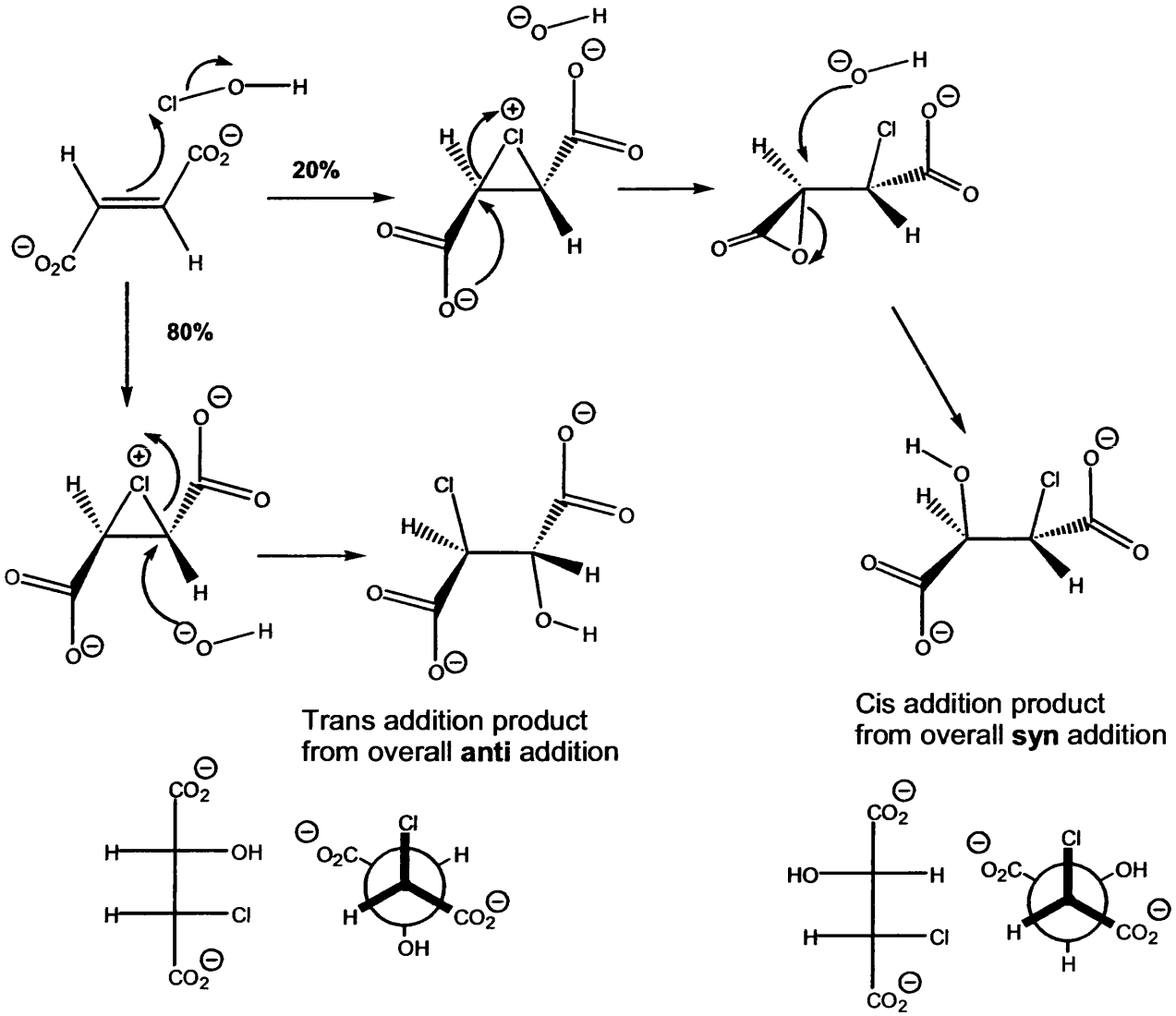

Fig. 57. Badea proposed mechanism for chlorohydrin formation from disodium salt of fumaric acid by hydrolysis of α-lactone and chloronium ions.[80]

Terry and Eichelberger, also in 1925 and therefore independently, did similar work studying the addition of hypochlorous acid to disodium salts of maleic acid and fumaric acid, however with additional chloride ions from added sodium chloride. Terry and Eichelberger however isolated dichlorocompounds instead of chlorohydrins.[81] Terry and Eichelberger isolated *syn* addition products from addition of chlorine to disodium maleate, in agreement with earlier work by Kuhn and Ebel. However, Terry and Eichelberger isolated *syn* addition products from addition of chlorine to disodium fumarate.[81]

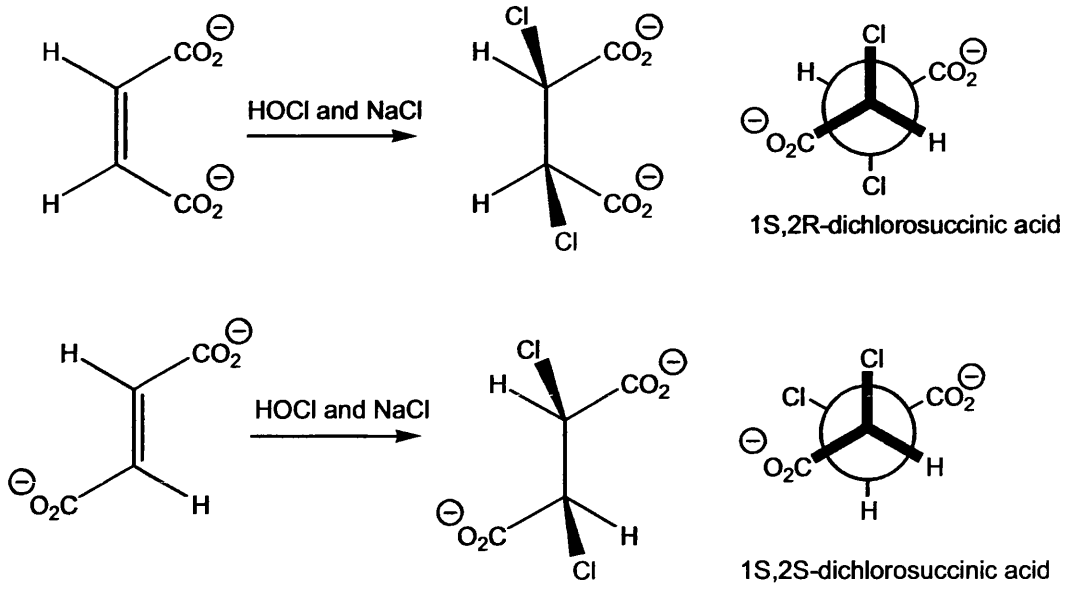

Fig. 58. Summary of reported work by Terry and Eichelberger.[81]

In 1928 Kuhn and Wagner-Jauregg repeated the work of Terry and Eichelberger and showed that Terry and Eichelberger were mistaken in the case of halogenation of disodium fumarate, which actually gave mostly 82% yield of *meso*-dichlorosuccinic acid, the *anti* addition product.[82]

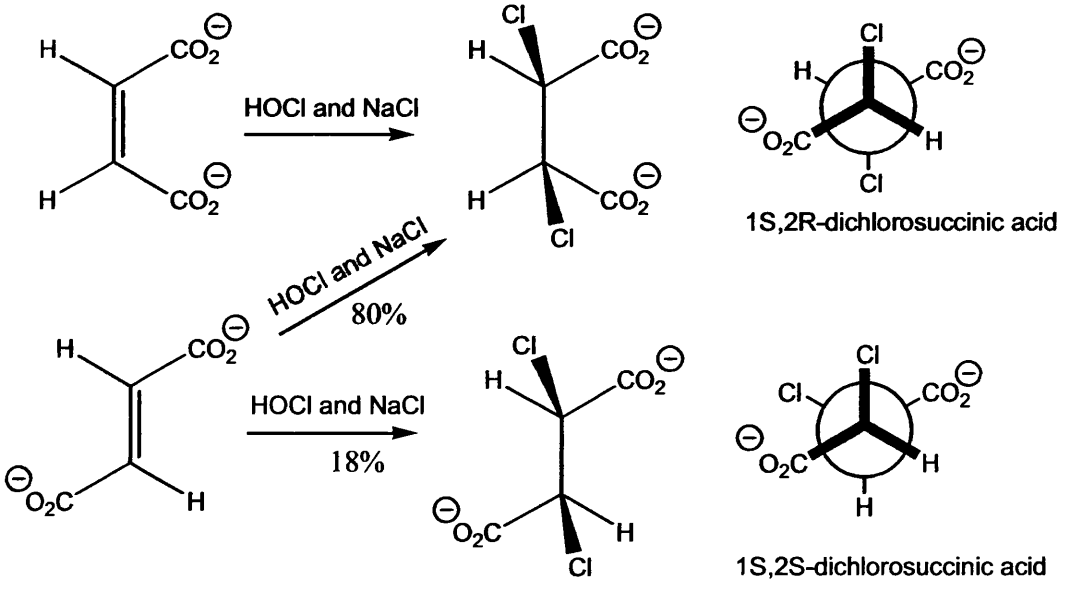

Fig. 59. The results of Kuhn and Wagner-Jauregg.[82]

Also isolated was, at most 18% racemic-dichlorosuccinic acid in agreement with Kuhn and Ebel's earlier work where chlorohydrins were isolated.[82] Addition of chlorine to sodium maleate in the presence of sodium chloride yields almost exclusively *meso*-dichlorosuccinic acid, whereas sodium fumarate under similar conditions gives at most 18% of *racemic*-dichlorosuccinic acid and more than 80% of *meso*-dichlorosuccinic acid.[82]

The initial explanation for these findings was attributed by Weiss to the instability of the bromonium ion of maleate dianion, as the two eclipsed carboxyl group would repel each other.[83] Weiss took the opinion that the two groups would repel each to such an extent as to initiate ring opening of the bromonium and rotation of the central carbon-carbon single bond and subsequent formation of the *meso*-1,2-dibromide product.[83]

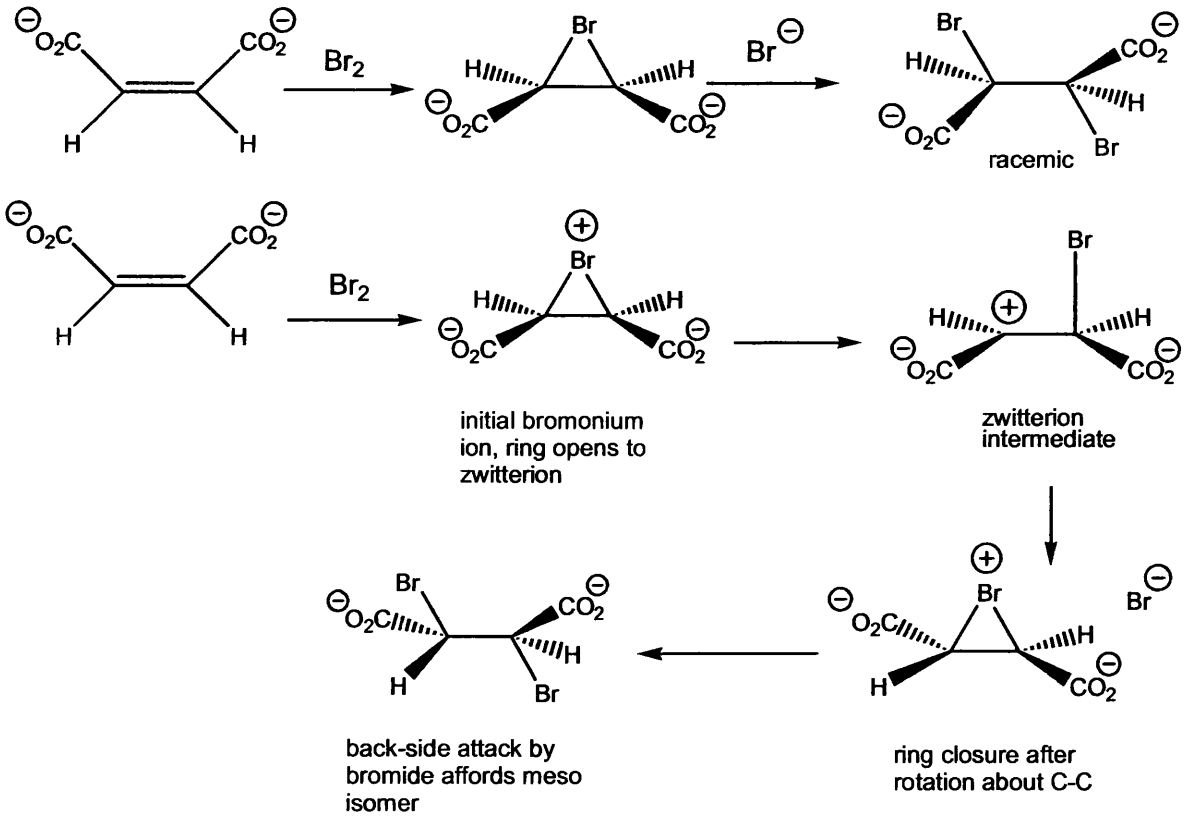

Fig. 60. Weiss suggested mechanism for formation of *racemic* and *meso*-dibromosuccinate.[83]

Weiss found that bromination of disodium maleate gave primarily 78% *meso* dibromide adducts. Weiss also found that bromination of fumarate at various temperatures and bromide concentrations always led to a mixture of products, which contained 93% *meso* dibromide. Weiss proposed that the initial cyclic bromonium ion would be difficult to form and may hydrolyse to yield bromohydrin, however, no bromohydrin was isolated.[83]

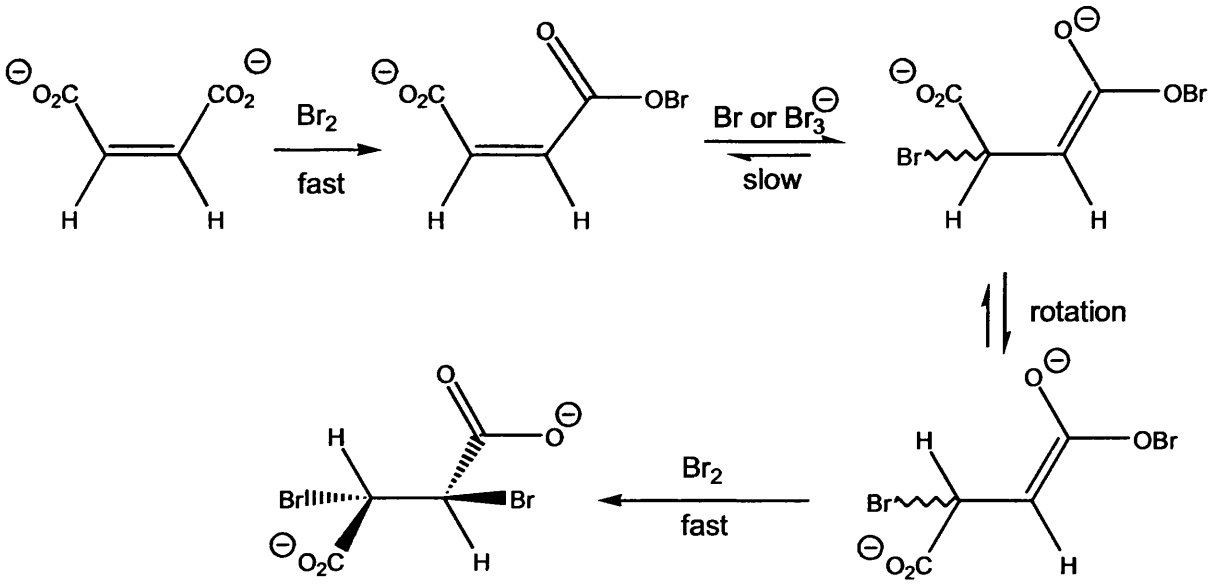

Fig. 61. Weiss suggested mechanism for formation of *meso*-dibromosuccinate.[83]

Attack of bromine upon carboxyl groups to yield acyl hypobromite intermediate, yielding products from 1,4-addition. Water is not sufficiently nucleophilic to attack the hypobromite. Weiss therefore proposed that two mechanisms were operating in the bromination of maleic and fumaric salts. The higher energy bromonium mechanism, which effects a trans addition product and the lower energy 1,4-addition mechanism which produces primarily a *meso* product. The mechanism that proposes the initial formation of a cyclic bromonium ion followed by back-side attack by of bromine anion has been accepted as a general mechanism for bromination of alkenes. Bell and Pring have pointed out that "The main evidence adduced to support the bromonium ion

hypothesis is the preponderance of *trans* addition, though an exception has to be made for addition to the doubly charged maleate ion."[84] The suggested mechanism of Weiss does not involve neighbouring group participation of the carboxylate groups, α-lactone formation is not involved.[83]

Kingsbury treated mesaconic acid with potassium carbonate in deuterium oxide with dropwise addition of bromine accompanied by intermittent cooling. From following ^{1}H NMR spectra he claimed to have formed a β-lactone.[85]

2.8. Halogenation of 2,3-dimethylmaleate and 2,3-dimethylfumarate salts.

Tarbell and Bartlett had investigated the bromination of stilbene in methanol to investigate non-photochemical halogenation. The product was not dibromostilbene, 1-bromo-2-methoxy-stilbene was isolated and it was concluded that a charged intermediate was involved in the bromination reaction.[67]

The reaction scheme for aqueous halogenation of 2,3-dimethylmaleate and 2,3-dimethylfumarate disodium salts proposed by Tarbell and Bartlett is illustrated below in figure 62.[86] Although the reaction is illustrated with chlorine, the assumption was made that bromine would behave in a similar manner as chlorine.[86]

The reaction of 2,3-dimethylmaleate and 2,3-dimethylfumarate salts with chlorine or bromine in aqueous solution follows exactly the same course. The products of reaction with chlorine or bromine will yield β-lactones. Acid hydrolysis of the β-lactones will result in halohydrins, which melt with decomposition.[86]

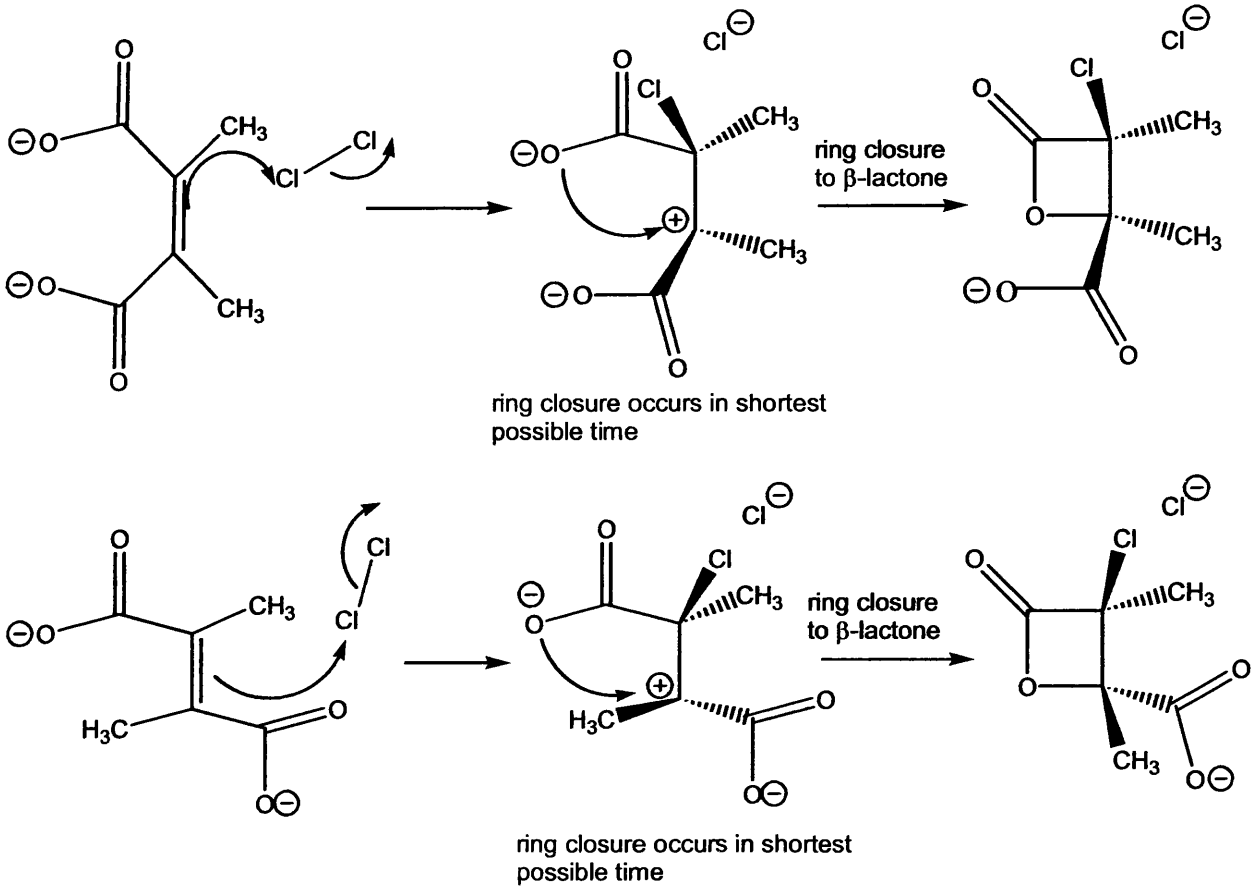

Fig. 62. Tarbell Bartlett reaction scheme for formation of β-lactones from aqueous halogenation of diacid salts.[86]

The thermal decomposition of some β-lactones to alkenes has been shown to be a stereospecific *cis* elimination.

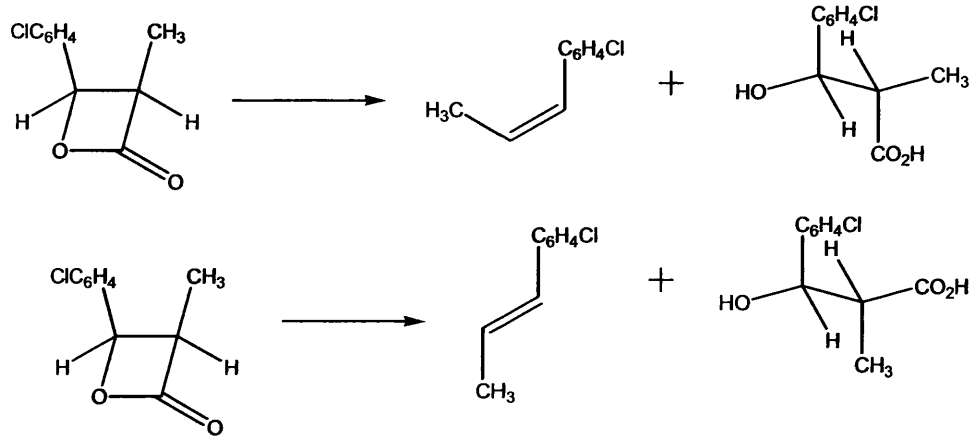

Fig. 63. Decarboxylation of p-chlorophenyl-β-lactones.[48,86]

In water at pH 6.2, 75% of *cis*-α-methyl-β-(p-chlorophenyl)-β-propiolactone will undergo decarboxylation with retention of configuration at 25°C or 100°C, to yield a *cis*-propene. The remaining lactone, 25% will hydrolyse to yield a *threo*-hydroxy-acid.[48,86] However, β-lactones cannot be prepared from halohydrins. So whereas aqueous halogenation of maleic and fumaric salts will yield halohydrins as found by Kuhn, Ebel and Wagner-Jauregg, Tarbell and Bartlett did not find halohydrins from aqueous halogenation of 2,3-dimethylmaleate and 2,3-dimethylfumarate disodium salts.[86] If single-step addition of chlorine molecule yield a dichloro-adduct, elimination of sodium chloride might yield chlorolactone. An initial dichloro-adduct would have to be symmetrical dichlorodimethylsuccinate. Only one form the two possible acids of dichlorodimethylsuccinic acid was noted by Kuhn and Ebel, and as two β-lactones were prepared, the dichlorodimethylsuccinate noted by Kuhn and Ebel should yield a β-lactone if the dichlorodimethylsuccinate was an intermediate.[86,79] When the dichlorodimethylsuccinic acid was neutralised with sodium bicarbonate and left at ambient for 2 days, only chlorotiglic acid with a m.p. of 66-68°C and some starting material were isolated. No β-lactone was isolated. Also quantitative elimination of sodium chloride from dichlorodimethylsuccinate required about 24 hours at 25°C, whereas aqueous halogenation of 2,3-dimethylfumarate and 2,3-dimethylmaleate disodium salts yield β-lactones in less than 30 minutes.[86]

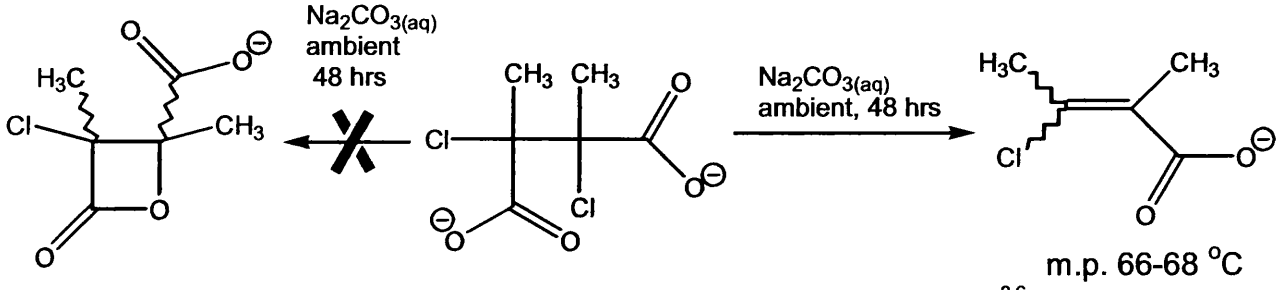

Fig. 64. Elimination to yield chlorotiglic acid.[86]

The formation of a zwitterion intermediate was discounted as this would allow for rotation about the C-C central bond and thus identical products

from both reactants would be possible. Tarbell and Bartlett further argued that synchronous attack by halogens and carboxyl group oxygen would present stereochemical difficulty, due to the rigidity of the central carbon-carbon double bond, either a methyl group or a carboxyl group will hinder any attacking carboxylate oxygen atom. Therefore, Tarbell and Bartlett took the opinion that the reaction steps occurred in the quickest possible succession. The presence of methyl groups in the 2,3-dimethylmaleate and 2,3-dimethyfumarate should also assist in ring formation.[86]

Free 2,3-dimethylmaleic acid is unknown, acidification in aqueous solution gives rise to the spontaneous formation of a stable anhydride that is inert towards bromination or chlorination, even with chloroform with solvent. The reaction of stilbene with bromine results in addition products arising from addition of bromine and/or solvent methanol. The reaction of 2,3-dimethylmaleic acid disodium salt and 2,3-dimethylfumaric acid disodium salt with aqueous bromine results initially in the formation of β-lactones, not substituted succinic acids or bromohydrins.

Substitution reactions with phenylhaloacetic and halosuccinic acids do not result in β-lactones.[86,87,88] Stilbene has phenyl groups attached to the double bond and the bromine addition is similar to the halogenation of *cis* and *trans*-2-butene.[68,69,86] The carboxyl groups must therefore account for the mechanistic differences.

Tarbell and Bartlett were of the opinion that any intermediates were short lived and that ring closure by attack of a carboxyl group occurred in the quickest possible succession following electrophilic attack by chlorine. Tarbell and Bartlett also assumed that identical bromohydrin formed from acid catalysed hydrolysis of both β-lactones formed. As the halohydrins melt with decomposition, to check stereochemical purity and identity, the rate of reaction of the chlorohydrins with sodium hydroxide was studied. For maleic and fumaric chlorohydrins, the rate of reaction

with sodium hydroxide is dependent upon configuration.[79,82] However, Tarbell and Bartlett found that both chlorohydrins, from chlorination of 2,3-dimethylmaleate and 2,3-dimethylfumarate, reacted as single substances and with similar rates. Reaction of the chlorohydrins with aqueous sodium hydroxide resulted in liberation of chloride ions.[86]

The β-lactone from the reaction with 2,3-dimethylmaleate disodium salt and aqueous bromine gave a β-lactone with a m.p. of 95–96°C. The β-lactone formed from the reaction of 2,3-dimethylfumarate disodium salt and bromine gave a β-lactone with a m.p. of 148–150°C. Tarbell and Bartlett were examining the nature of electrophilic addition and were interested in rationalising the kinetic data previously obtained for electrophilic addition of bromine to stilbene in methanol.[67] A dibromo adduct was not formed, 1-bromo-2-methoxystilbene was the major isolated product. This led Tarbell and Bartlett to conclude that a mechanism as illustrated in figure 65 was responsible for halogen addition to an alkene.

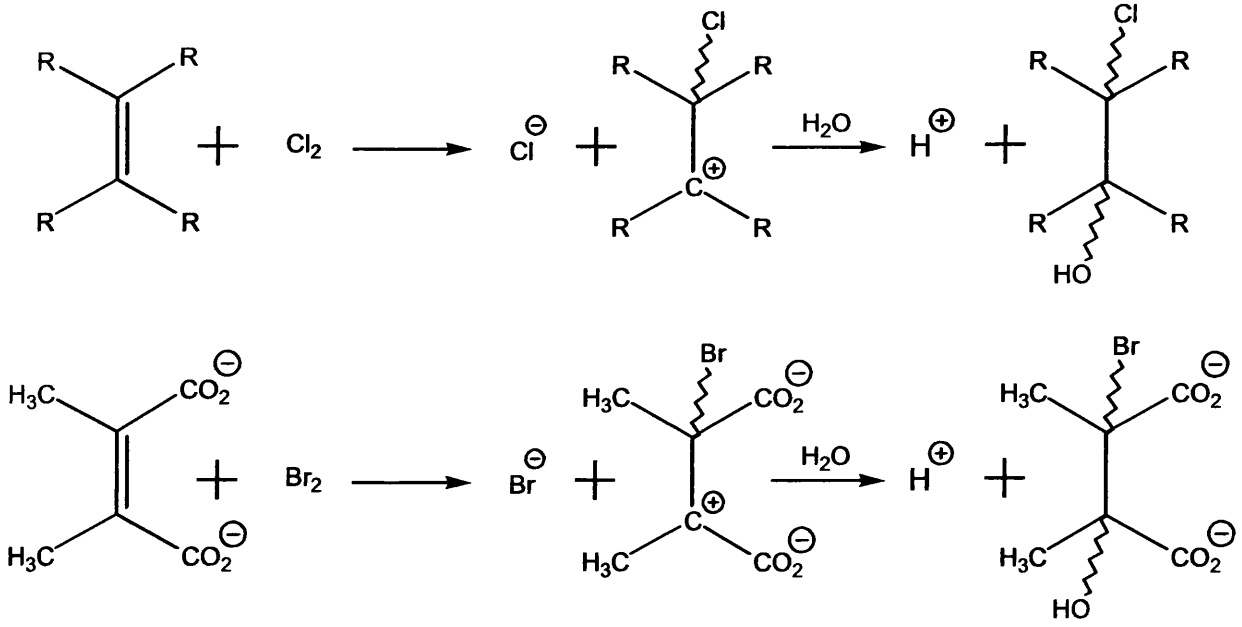

Fig. 65. Tarbell and Bartlett proposed mechanism for chlorohydrin and bromohydrin formation.[86]

3. Experimental Section

The bromination of 2,3-dimethylmaleate and 2,3-dimethylfumarate disodium salts was repeated to facilitate unambiguous stereospecific assignment using spectroscopic techniques for isolated bromo-β-lactones.[91]

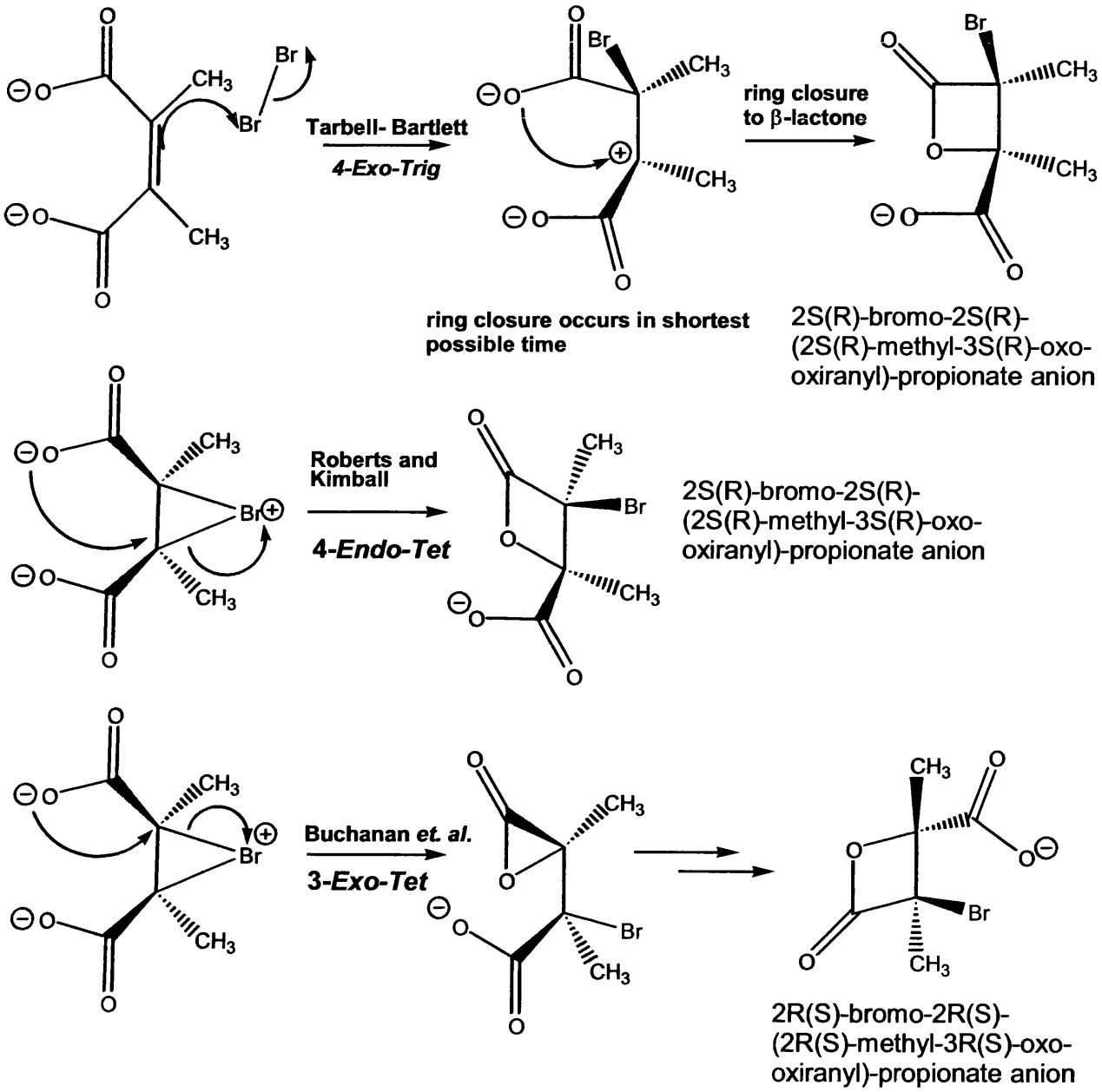

Fig. 66. A number of mechanisms have been proposed.[91]

The β-lactone prepared by Tarbell and Bartlett had different melting points and were monobasic lactones. No structural assignment could be made in 1937. In light of the fact that different mechanisms have been proposed by Tarbell and Bartlett, Roberts and Kimball, Badea and Buchanan and co-workers, repeating the experiment would allow structural assignment to be made.[91]

3.1 Procedure for aqueous bromination of 2,3-dimethylmaleate disodium salt.

The bromination of 2,3-dimethyl-maleate was carried out according to the method of Tarbell and Bartlett[86].

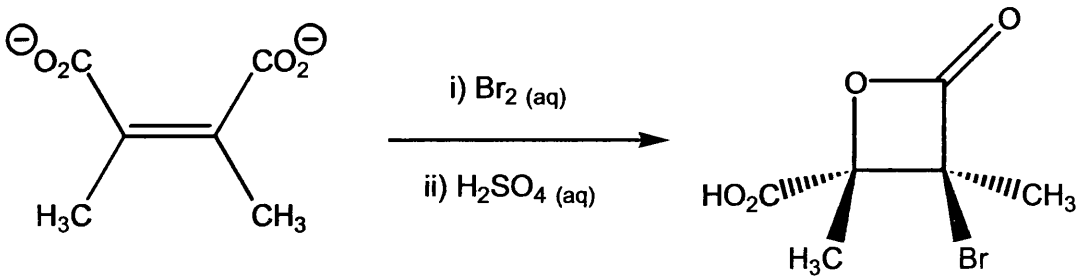

2,3-dimethylmaleic anhydride (5g, 39.64mmol) was added to water (40ml) with sodium hydroxide (3.2g, 80.00mmol) and stirred to effect solution. Bromine (6.4g, 40.04mmol) was suspended in water (400ml) with stirring. The bromine suspension was added to the 2,3-dimethylmaleate dianion solution dropwise with stirring over a period of about 20 minutes. The bromine colour disappeared after a few minutes.

The aqueous solution was extracted with ethyl acetate (3×100ml). The combined ethyl acetate was dried with anhydrous sodium sulphate, filtered and evaporated in *vacuo* at ambient temperature to remove the ethyl acetate. The residue was thick oil with some crystals on the flask sides. The organic residue was dissolved in toluene (30ml). Dropwise addition of petroleum ether [40-60°, ≤5ml] caused turbidity and crystals were allowed to form. More petroleum ether [40-60°, 35ml] was added. The crystals were collected and the fractional crystallisation repeated a

further two times from toluene and petroleum ether [40-60°] to yield the [3S(3R),4S(4R)]–3-bromo-4-carboxy-3,4-dimethyloxetan-2-one.

The aqueous layer was acidified with sulphuric acid, sulphuric acid (0.7g, 7.14mmol) in water (20ml). This was extracted with ethyl acetate (3×100ml). The combined ethyl acetate was washed with water (50ml) to remove excess acid and the organic phase was dried with anhydrous sodium sulphate. Then filtered and evaporated in *vacuo* at ambient. This left acidified organic crude product. The acidified crude product was fractionally recrystallised from toluene and petroleum ether [40-60°] as with the non-acidified product, see above. The crystallised product was dried with gentle vacuum.

Yield of [3S(3R),4S(4R)]–3-bromo-4-carboxy-3,4-dimethyloxetan-2-one as crude yield was 2g (22%). Recrystallised yield was 0.9g (10%). Measured m.p. 92-94°C, the literature value is 95-96°C.[86,91]

3.2 Procedure for preparation of 2,3-dimethylfumaric diacid from 2,3-dimethylmaleic anhydride

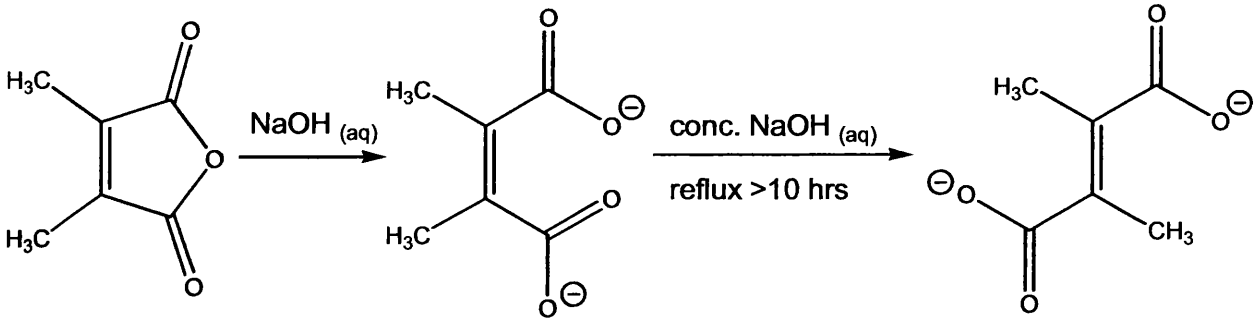

The 2,3-dimethylfumaric acid was prepared from the method of Ott.[90] 2,3-dimethyl-maleic anhydride (30g, 237.8mmol) was added to sodium hydroxide (80g, 2mol) in water (200ml). The mixture was heated to reflux for 10 hours. Once cooled, conc. hydrochloric acid (ca 32%, 155ml) was added to bring pH to neutral and causes solid to precipitate. More concentrated hydrochloric acid (20ml) was added and a thick white solid separated out, pH was 3. Ethyl acetate (200ml) was added and the mixture allowed to separate. To aid separation water (500ml) was added.

Further extractions with ethyl acetate (4×200ml) were made. The combined ethyl acetate portion was evaporated in *vacuo* at 40°C. The organic residue was dried in *vacuo* and the yielded 4.15g and m.p. 235°C, recovered starting material. The aqueous layer was then extracted with chloroform (4×200ml). The organic product from the chloroform was dried with in *vacuo*, yield 10.25g. Crude product was recrystallised, hot, from chloroform (60ml), dried in *vacuo*, with a yield of 2,3-dimethyl-fumaric acid of 3.4g (9.9%) and m.p. 247.8°C.

3.3 Procedure for aqueous bromination of 2,3-dimethylfumarate disodium salt.

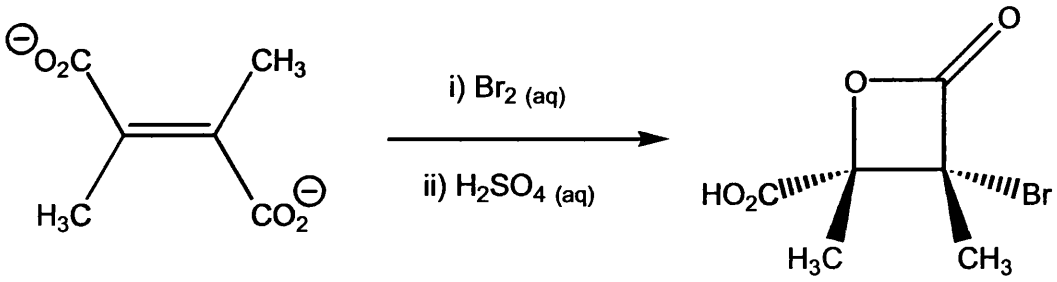

The bromination of the fumarate species was carried out in a similar manner to that for the maleate species. 2,3-dimethylfumaric acid (3g, 21.1mmol) was added to water (24ml) and sodium hydroxide (1.66g, 41.5mmol). Bromine (3.3g, 20.65mmol) was suspended in water (240ml) with stirring. The bromine suspension was added to the 2,3-dimethylfumarate dianion solution dropwise with stirring over a period of about 20 minutes. The bromine colour disappeared after a few minutes. The aqueous mixture was extracted with ethyl acetate (4×30ml). The ethyl acetate was evaporated at ambient in *vacuo*. The crude product from ethyl acetate phase was fractionally recrystallised from toluene (15ml) and Pet Ether [40-60°, 7ml], three times. The yield of [(3R(3S), 4S(4R)]-3-bromo-4-carboxy-3,4-dimethyloxetan-2-one was 0.82g, m.p. 148.7°C, literature value is 148-150°C.[86]

The bromohydrins have been characterised by other researchers from hydrolysis of the bromo-β-lactone isolated.[89]

4. Spectroscopic Results

Isolated recrystallised bromo-β-lactones were examined with X-ray crystallography. As both crude and recrystallised material was also isolated, ^{13}C NMR and ^{1}H NMR, infra red spectra and m.p. data were obtained. No bromohydrins or dibromoadducts were isolated, only bromo-β-lactones and 2,3-dimethylmaleic anhydride was isolated.

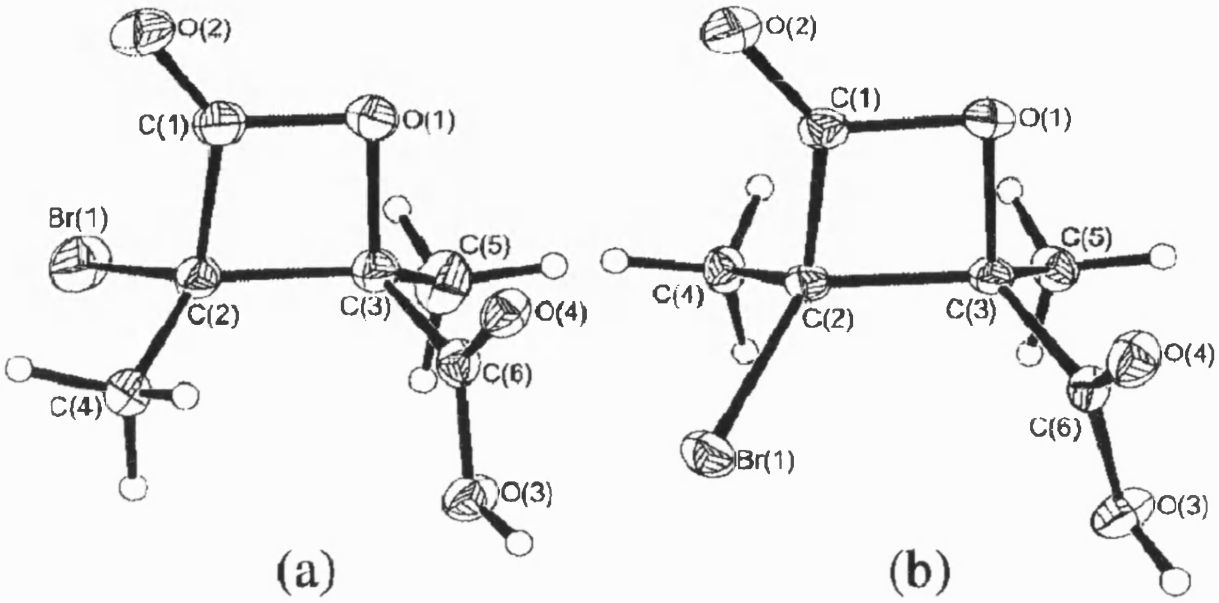

Fig. 67. Crystal structures of isolated products.[91]

4.1 Product from bromination of 2,3-dimethylmaleate disodium salt

For [3S(3R),4S(4R)]-3-bromo-4-carboxy-3,4-dimethyloxetan-2-one (M8x) isolated from aqueous bromination of 2,3-dimethylmaleate disodium salt, shown as S1 on page 71. The literature value for m.p. is 95-96°C, a value of 92-94°C was measured. The ^{1}H NMR (400 MHz) data obtained in $(CD_3)_2SO$, shown as S2 on page 72, was 1.81 ppm singlet for methyl protons adjacent to carboxylic acid group and 1.93 ppm was singlet for other methyl protons adjacent to bromine atom. The ^{13}C NMR (100 MHz) obtained in $(CD_3)_2SO$, shown as S3 on page 73, was 22.9 ppm for methyl carbon atom adjacent to carboxylic acid group, 23.1 ppm for the other methyl carbon atom adjacent to bromine, 66.4 ppm for the C-3 carbon

atom attached to bromine, 83.6 ppm for the C-4 carbon atom attached to carboxylic acid, 166.5 ppm for the β-lactone ring C=O carbonyl and 168.2 ppm the other carboxylic acid C=O atom. See figure 67 for crystal structures and atom numbering.[91] The COSY spectrum for the recrystallised material M8x is shown in S4 on page 74. An infra-red spectrum of the isolated [3S(3R),4S(4R)]–3-bromo-4-carboxy-3,4-dimethyloxetan-2-one as a nujol mull was obtained and is shown as S9 on page 79. The nujol blank is shown as S10 on page 80. The nujol mull IR spectrum of [3S(3R),4S(4R)]-3-bromo-4-carboxy-3,4-dimethyloxetan-2-one shows two intense bands at 1835.2cm^{-1} is a C=O (β-lactone) stretch and 1722.7cm^{-1} is normally associated with C=O (acid $-CO_2H$) stretch.

For the crude acidified product from aqueous bromination of 2,3-dimethylmaleate disodium salt, [3S(3R),4S(4R)]–3-bromo-4-carboxy-3,4-dimethyloxetan-2-one, shown as S11 and expanded sections S12, S13, S14 and S15 on pages 81 to 85, the ^{13}C NMR (100 MHz) obtained in $(CD_3)_2SO$ was 23.6ppm for methyl carbon atom adjacent to carboxylic acid group, 23.8 ppm for the other methyl carbon atom adjacent to bromine, 65.2 ppm for the C-3 carbon atom attached to bromine, 84.5 ppm for the C-4 carbon atom attached to carboxylic acid, 167.5 ppm for the β-lactone ring C=O carbonyl and 169.3 ppm the other carboxylic acid C=O atom. The 2,3-dimethylmaleic anhydride appears at 9.9 ppm (-CH3), 141.2 ppm (C=C) and 174.4 ppm (C=O).[91,89] There is no [3R(3S),4S(4R)]–3-bromo-4-carboxy-3,4-dimethyloxetan-2-one present in the crude maleate-bromo-β-lactone, so only one diastereomer of bromo-β-lactone is present in the crude product before the [3S(3R),4S(4R)]–3-bromo-4-carboxy-3,4-dimethyloxetan-2-one is isolated by recrystallisation.

4.2 Product from bromination of 2,3-dimethylfumarate disodium salt

For the bromo-β-lactone isolated from aqueous bromination of 2,3-dimethylfumarate disodium salt, [3R(3S),4S(4R)]–3-bromo-4-carboxy-

3,4-dimethyloxetan-2-one (F8x), structure shown as S5 on page 75 from X-ray crystallography. The literature value for m.p. is 148-150°C, a value of 148.7°C was measured. The ^{1}H NMR (400 MHz) data obtained in $(CD_3)_2SO$, S6 on page 76, was 1.77 ppm a singlet for methyl protons on C-5, 1.99 ppm for methyl protons on C-4. The ^{13}C NMR (100 MHz) obtained in $(CD_3)_2SO$, shown as S7 on page 77, was 18.3 ppm for methyl group C-5, 21.0 ppm for methyl group C-4, 61.4 ppm for the C-2 carbon atoms, 85.0 ppm for the C-3 carbon atoms, 166.7 ppm for the β-lactone C1 carbonyl group and 168.9 ppm for the C-6 carboxyl group. See reference 91 for crystallographic data.

The crude acidified product from aqueous bromination of 2,3-dimethylfumarate disodium salt, shown as S16 and expanded as S17, S18, S19 and S20 on pages 86 to 90, the ^{13}C NMR (100 MHz) obtained in $(CD_3)SO$ was 19.1 ppm for methyl group C-5, 21.8 ppm for methyl group C-4, 62.2 ppm for the C-2 carbon atoms, 85.9 ppm for the C-3 carbon atoms, 167.8 ppm for the β-lactone C1 carbonyl group and 169.9 ppm for the C-6 carboxyl group. Relatively small amounts of the bromo-β-lactone from bromination of 2,3-dimethylmaleate, [3S(3R),4S(4R)]–3-bromo-4-carboxy-3,4-dimethyloxetan-2-one, were present too, 23.6ppm for methyl carbon atom adjacent to carboxylic acid group, 23.8 ppm for the other methyl carbon atom adjacent to bromine, 65.2 ppm for the C-3 carbon atom attached to bromine, 84.6 ppm for the C-4 carbon atom attached to carboxylic acid, 167.6 ppm for the β-lactone ring C=O carbonyl and 169.4 ppm the other carboxylic acid C=O atom. Maleic anhydride was also present 174.4 (C=O), 141.2 ppm (C=C) and 10.0 ppm ($-CH_3$). The 2,3-dimethylfumarate salt was prepared from 2,3-dimethylmaleic anhydride, so 2,3-dimethylmaleate salt was also present in small amounts. Thus, the aqueous bromination of the 2,3-dimethylfumarate disodium salt also produced the bromo-β-lactone of bromination of 2,3-dimethylmaleate disodium salt from the relatively small amount of anhydride in the reactant salts.

S1. M8x maleate bromo-β-lactone as isolated from crystallography

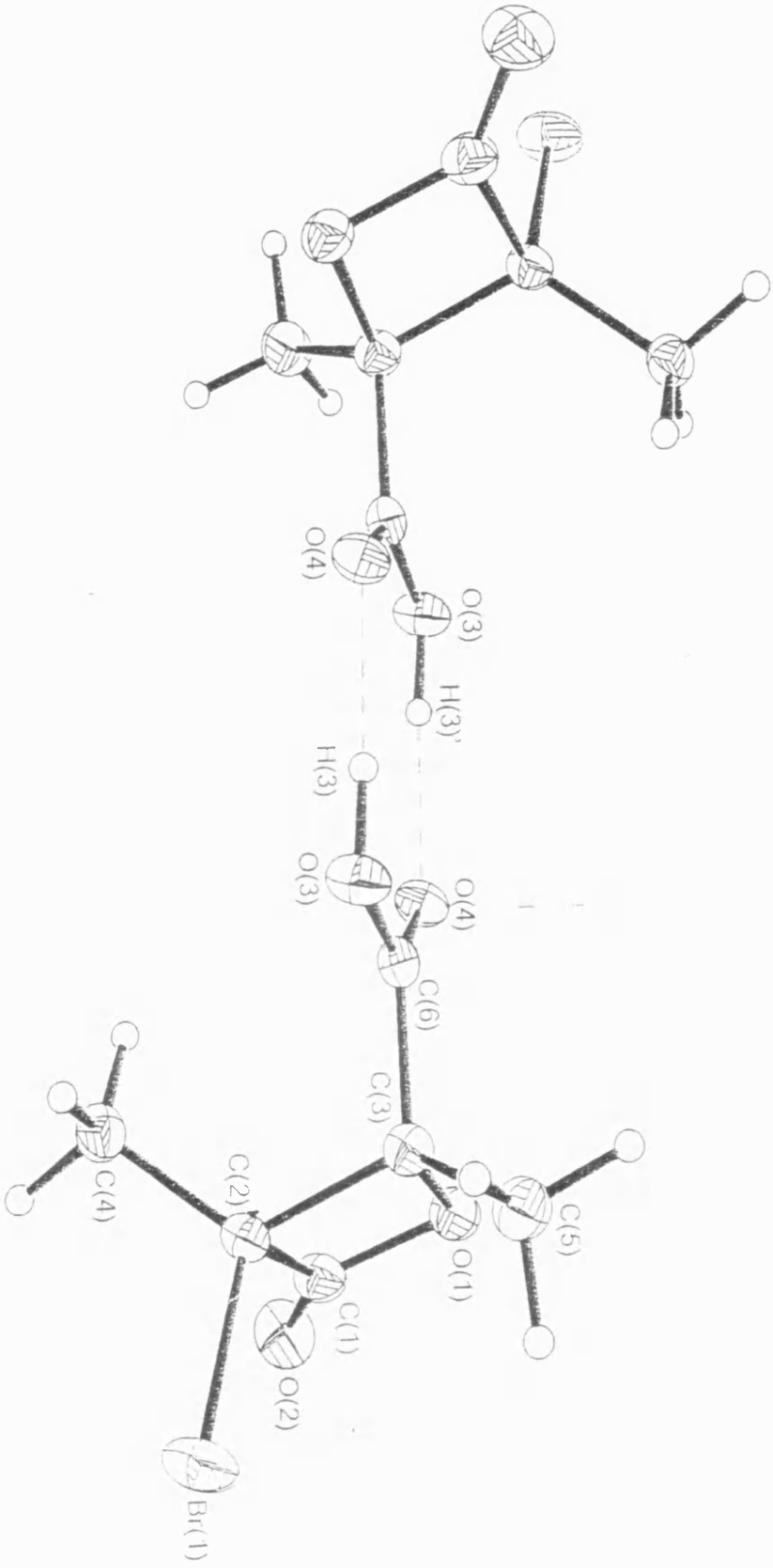

S2. Maleate bromo-β–lactone after recrystallisation ^{1}H NMR

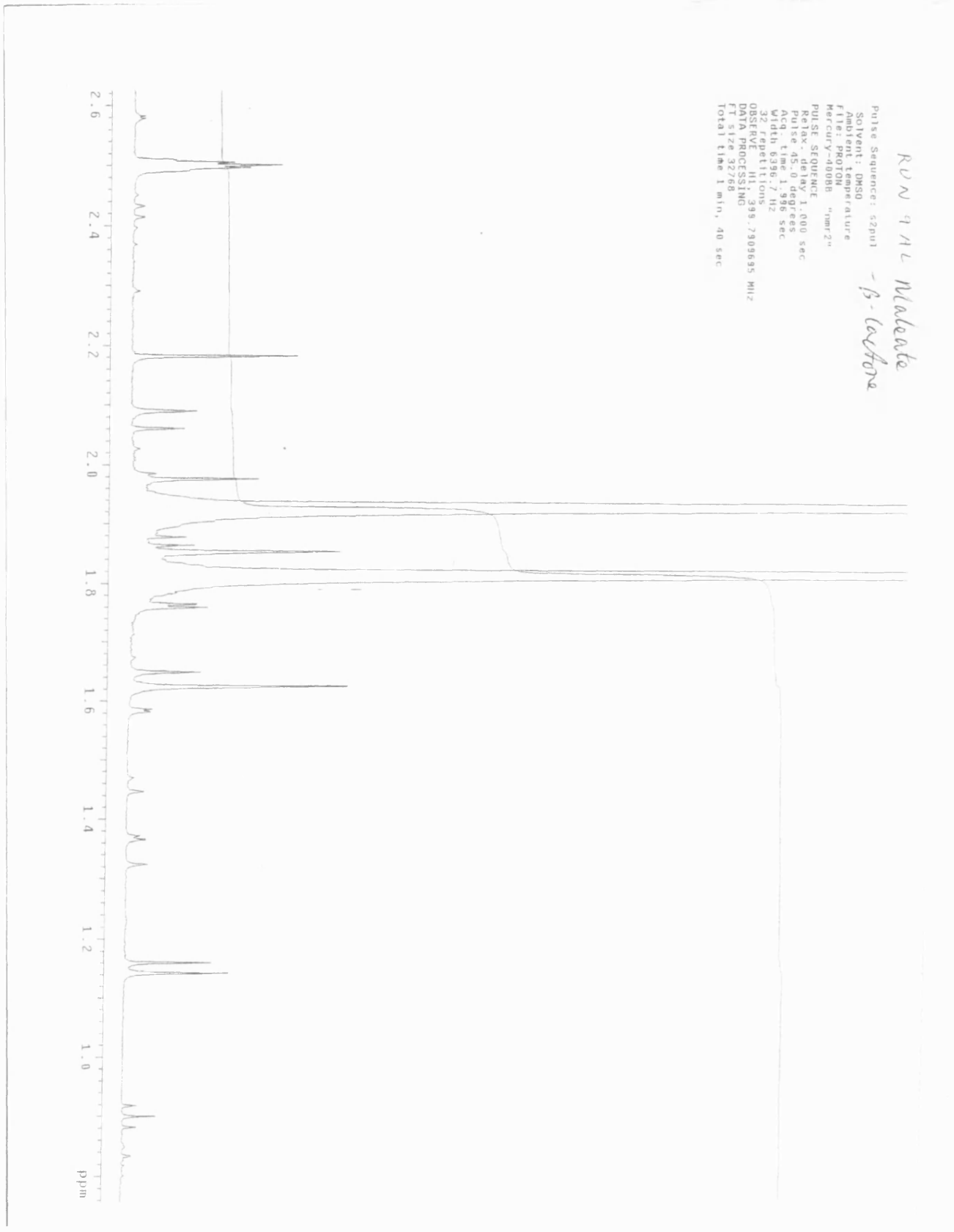

S3. Maleate bromo-β-lactone after recrystallisation ^{13}C NMR

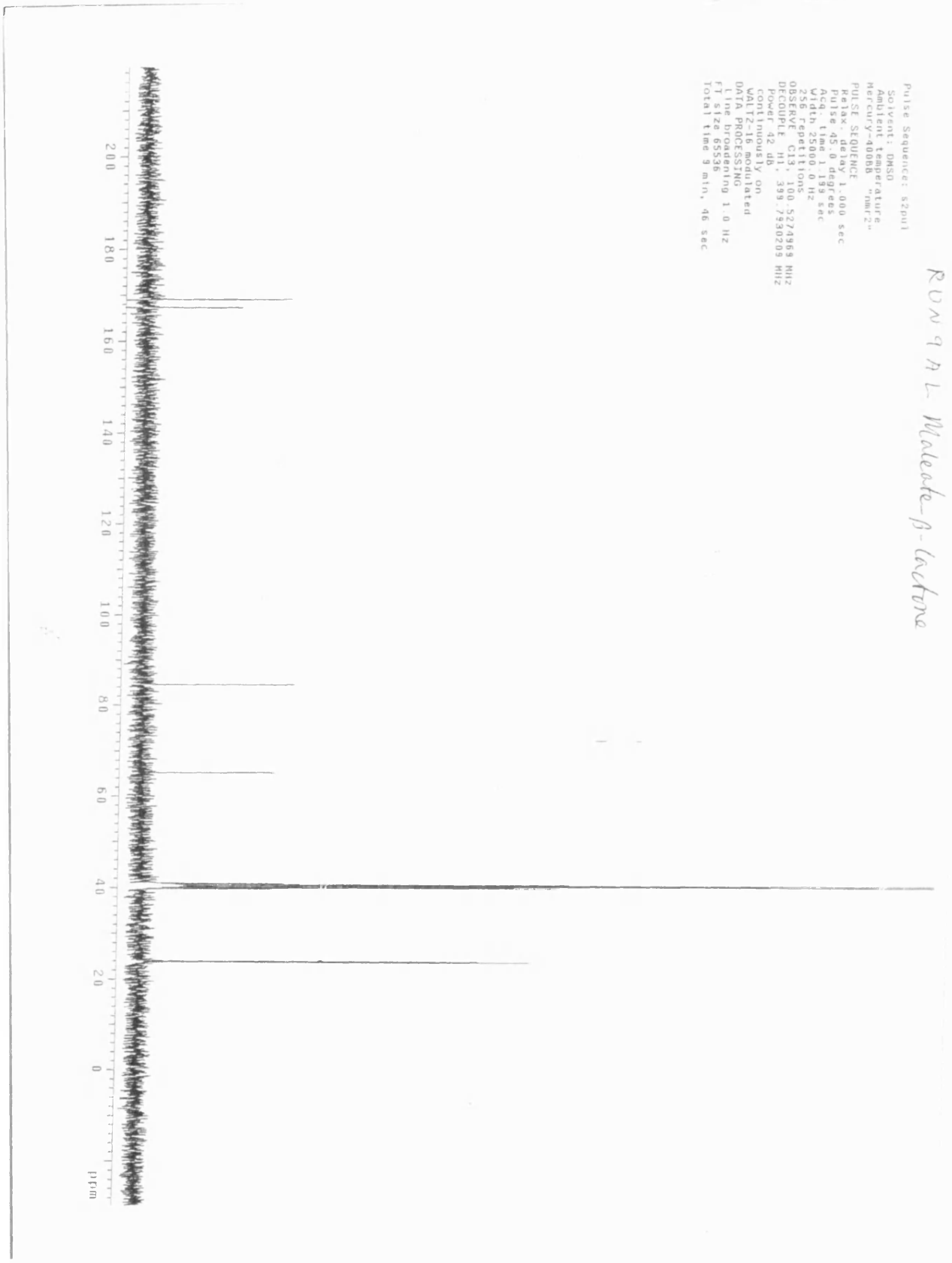

S4. Maleate bromo-β-lactone after recrystallisation COSY spectra

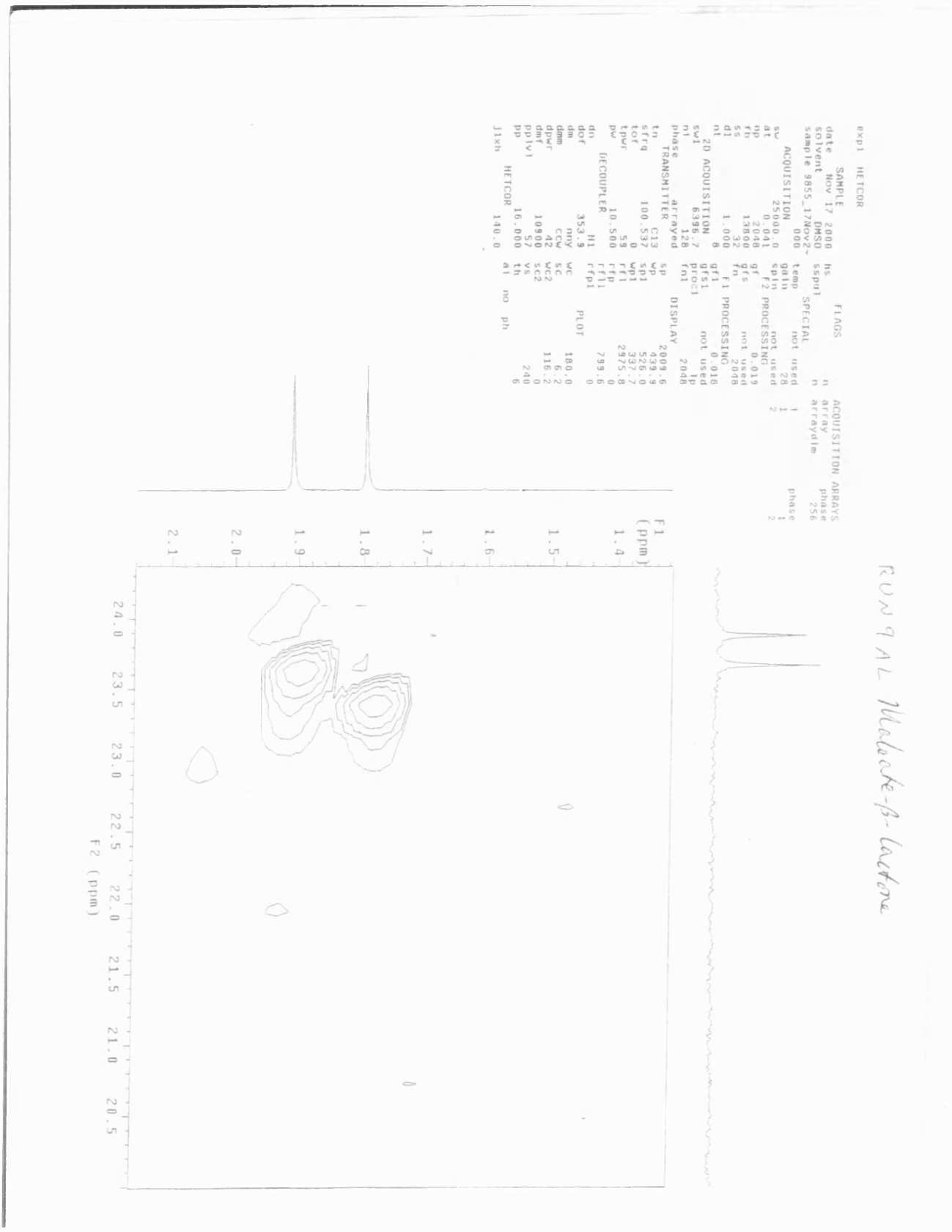

S5. F8x Fumarate bromo-β-lactone as isolated from crystallography

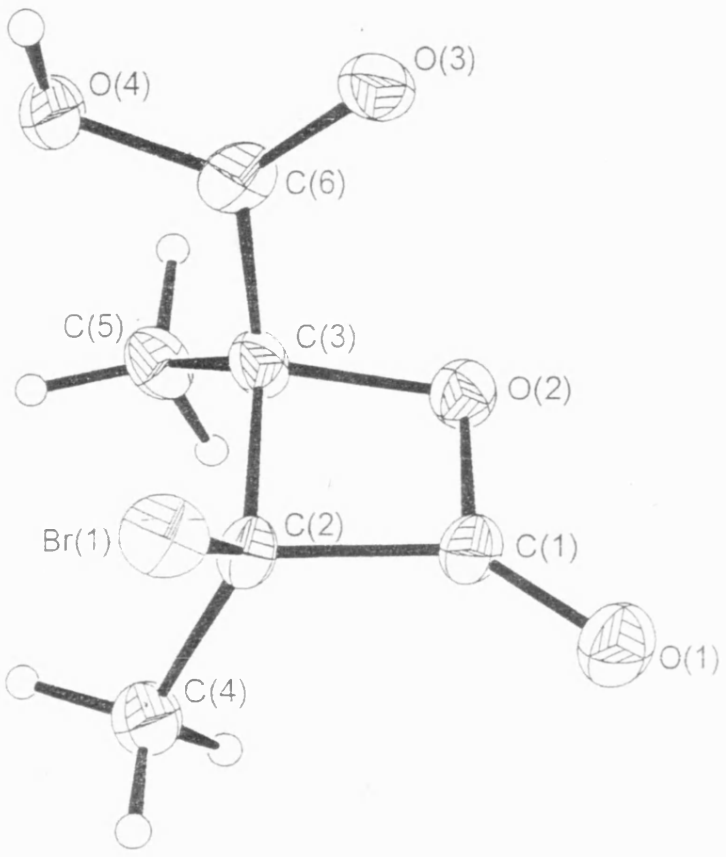

Fumarate-β-lactone

K00gb2

S6. Fumarate bromo-β–lactone after recrystallisation ^{1}H NMR

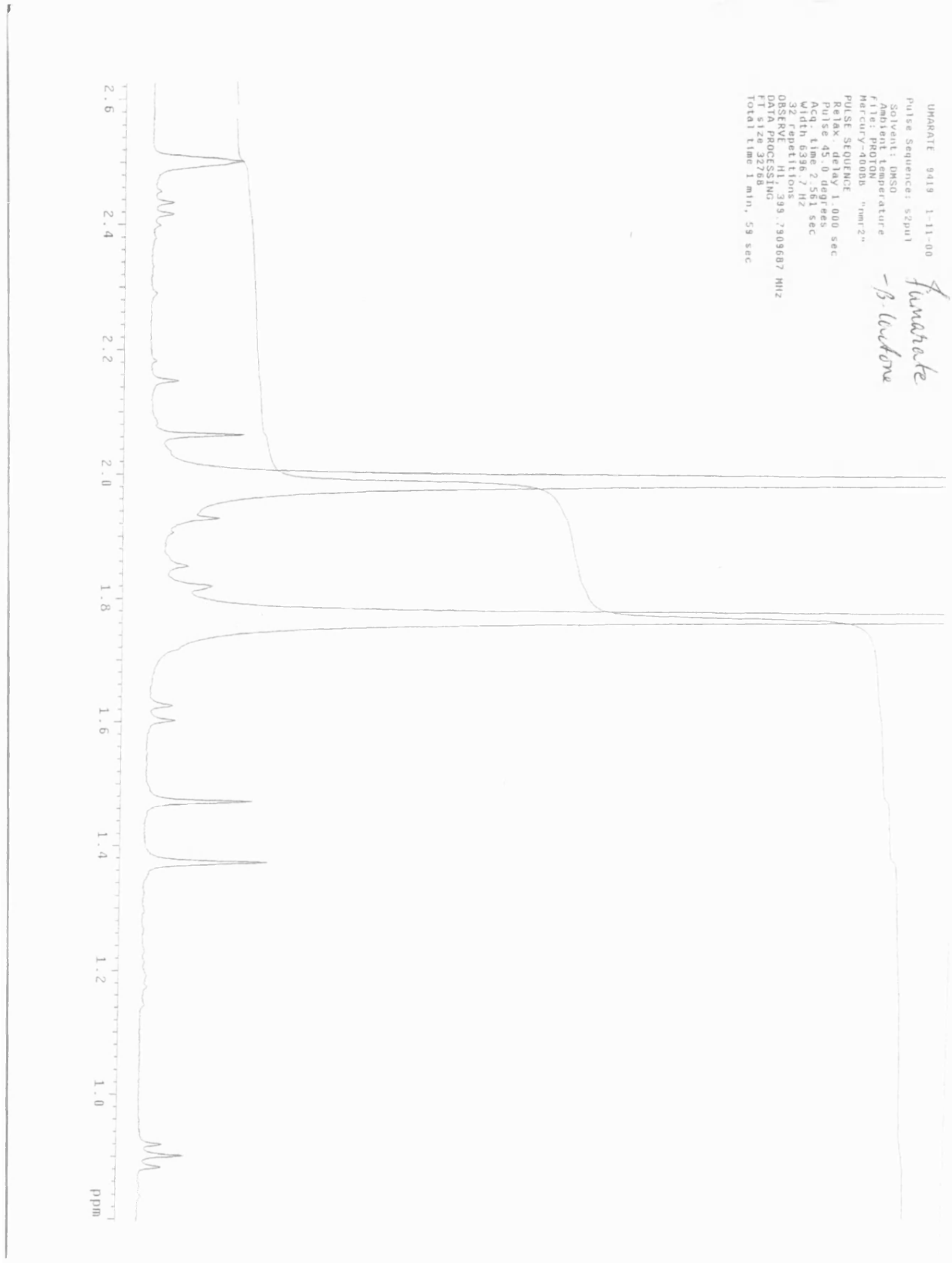

S7. Fumarate bromo-β-lactone after recrystallisation ^{13}C NMR

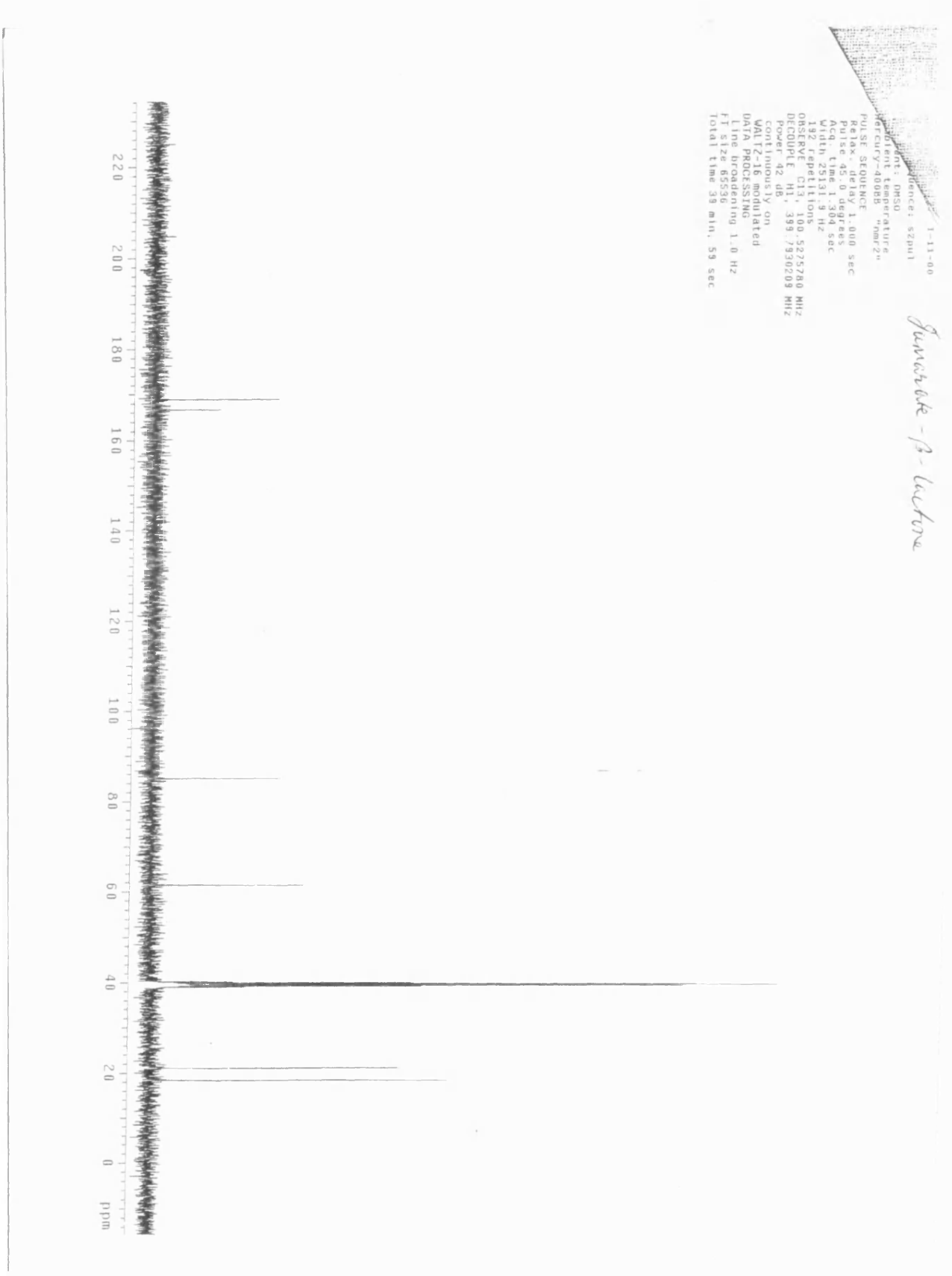

S8. Fumarate bromo-β-lactone after recrystallisation COSY NMR

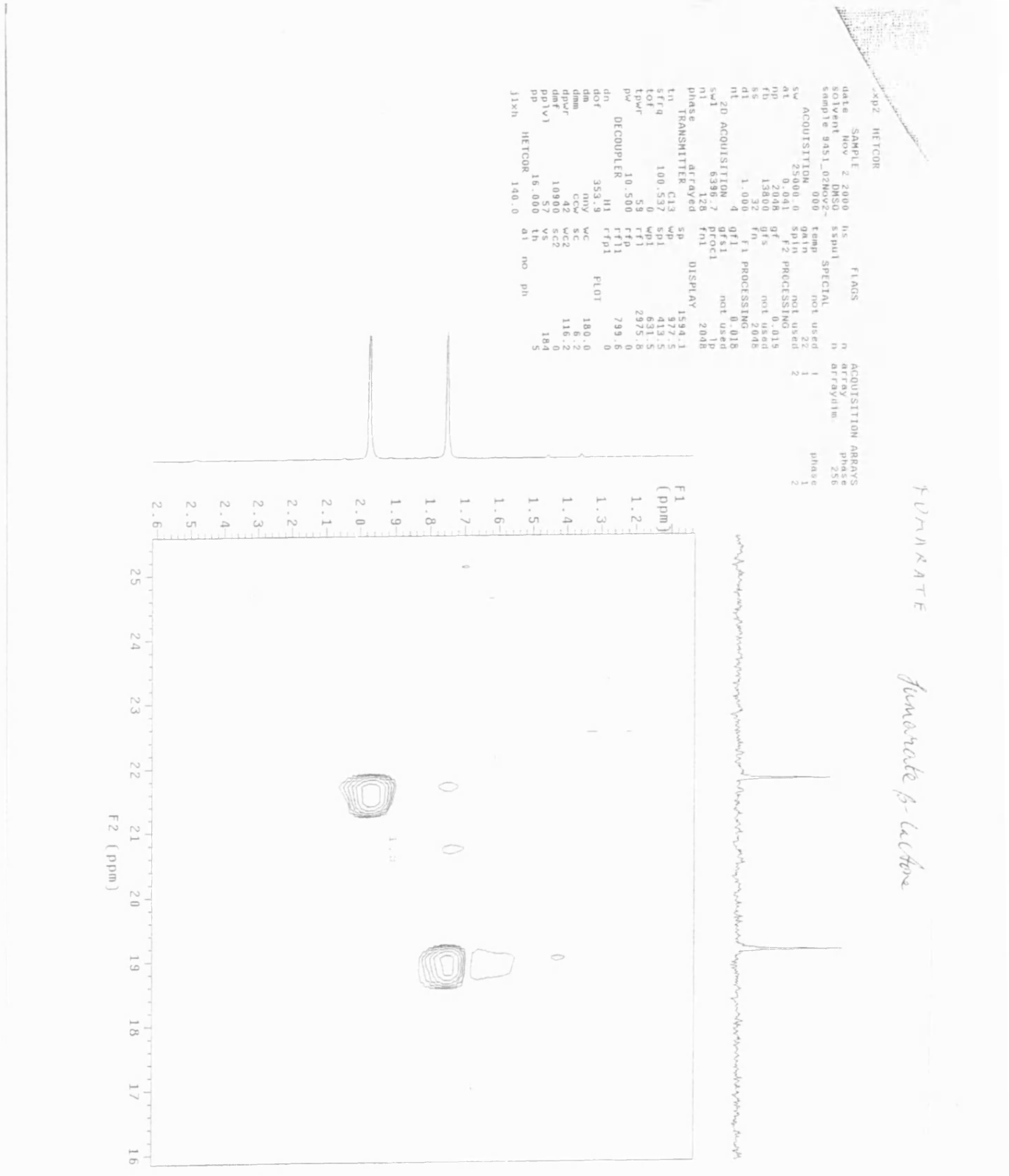

S9. Maleate bromo-β-lactone after recrystallisation, IR in nujol mull

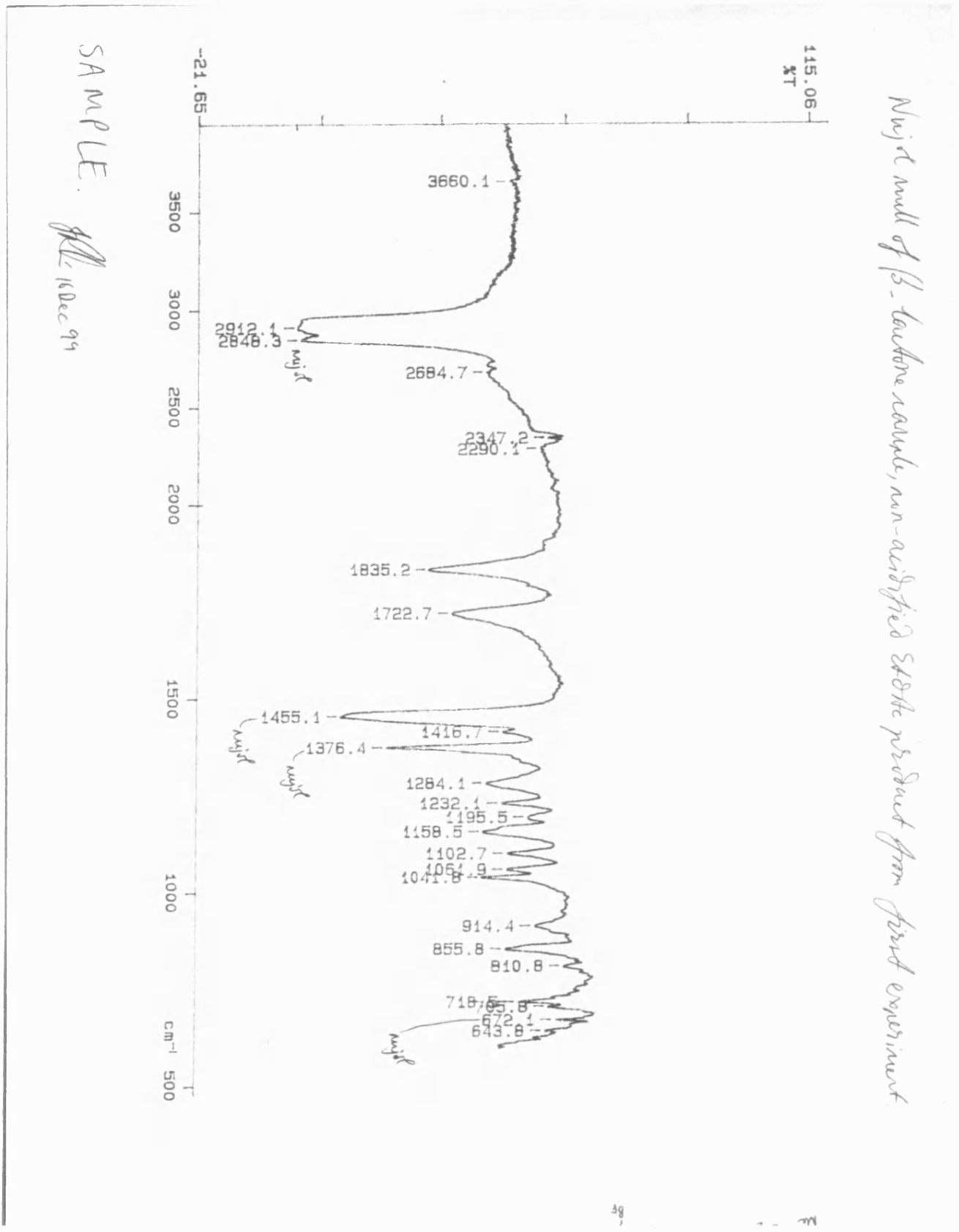

S10. Nujol blank IR spectra

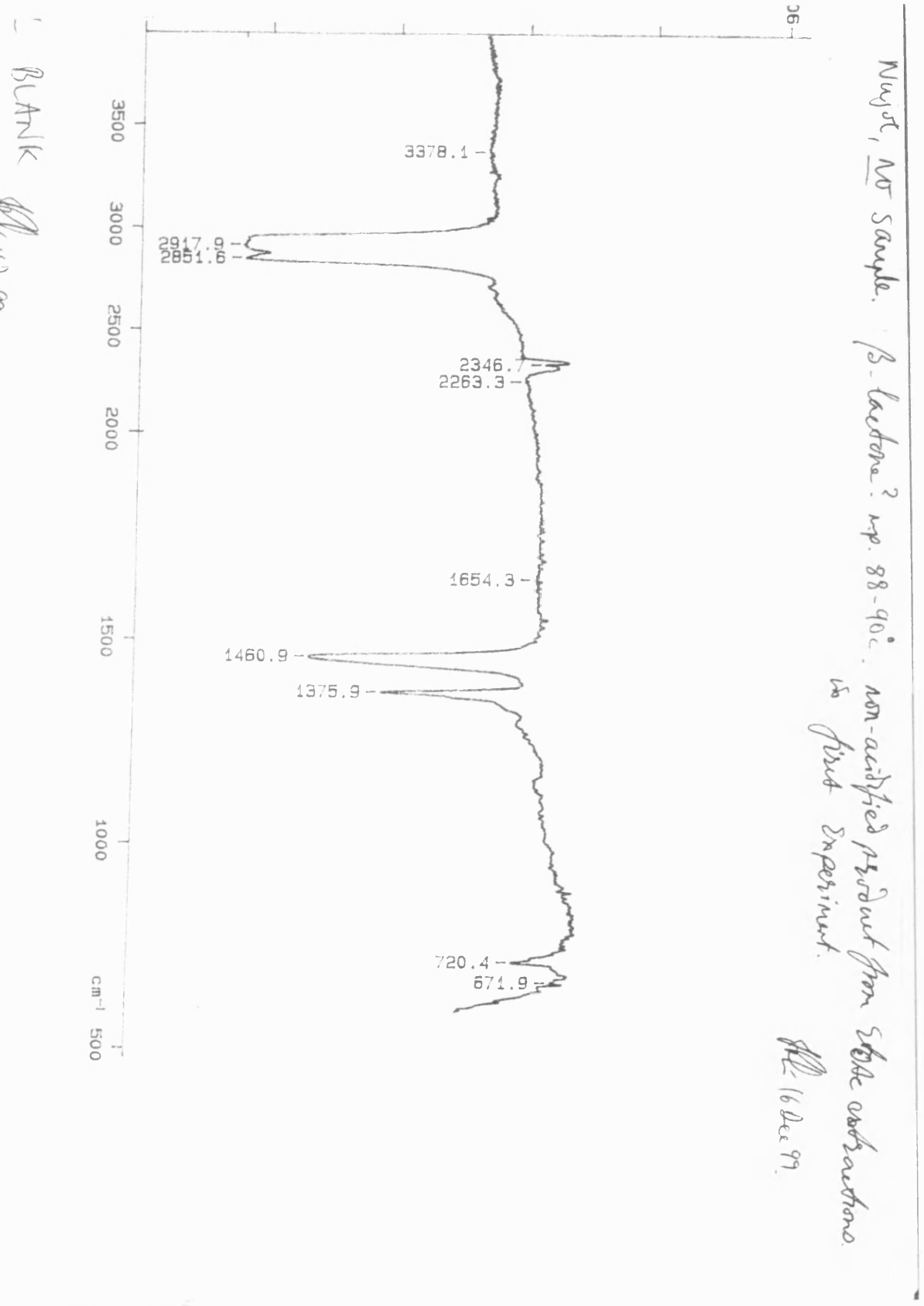

S11. Maleate crude product after acidification bromo-β-lactone ^{13}C NMR

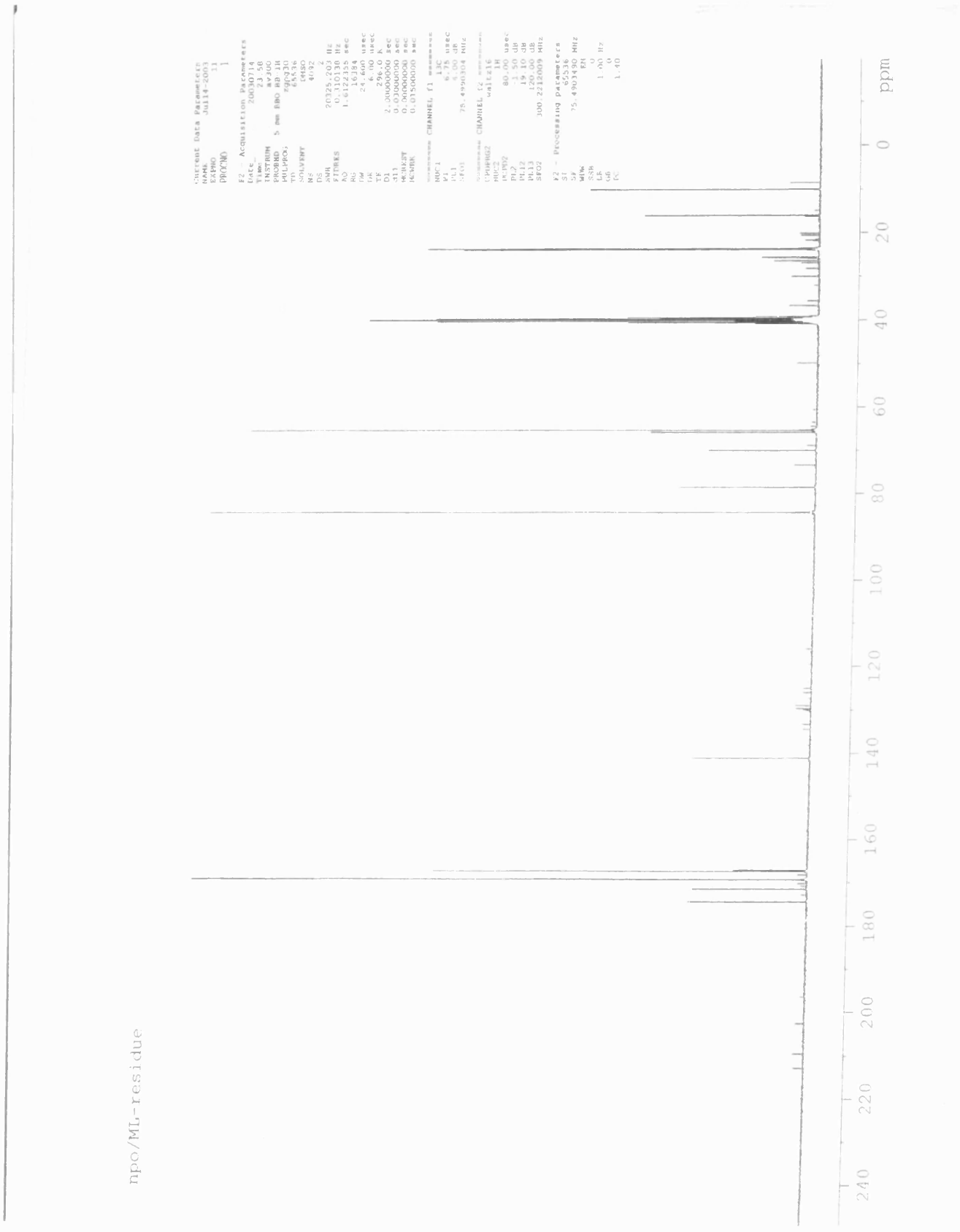

S12. Maleate acidified crude material 212 – 165 ppm ^{13}C NMR

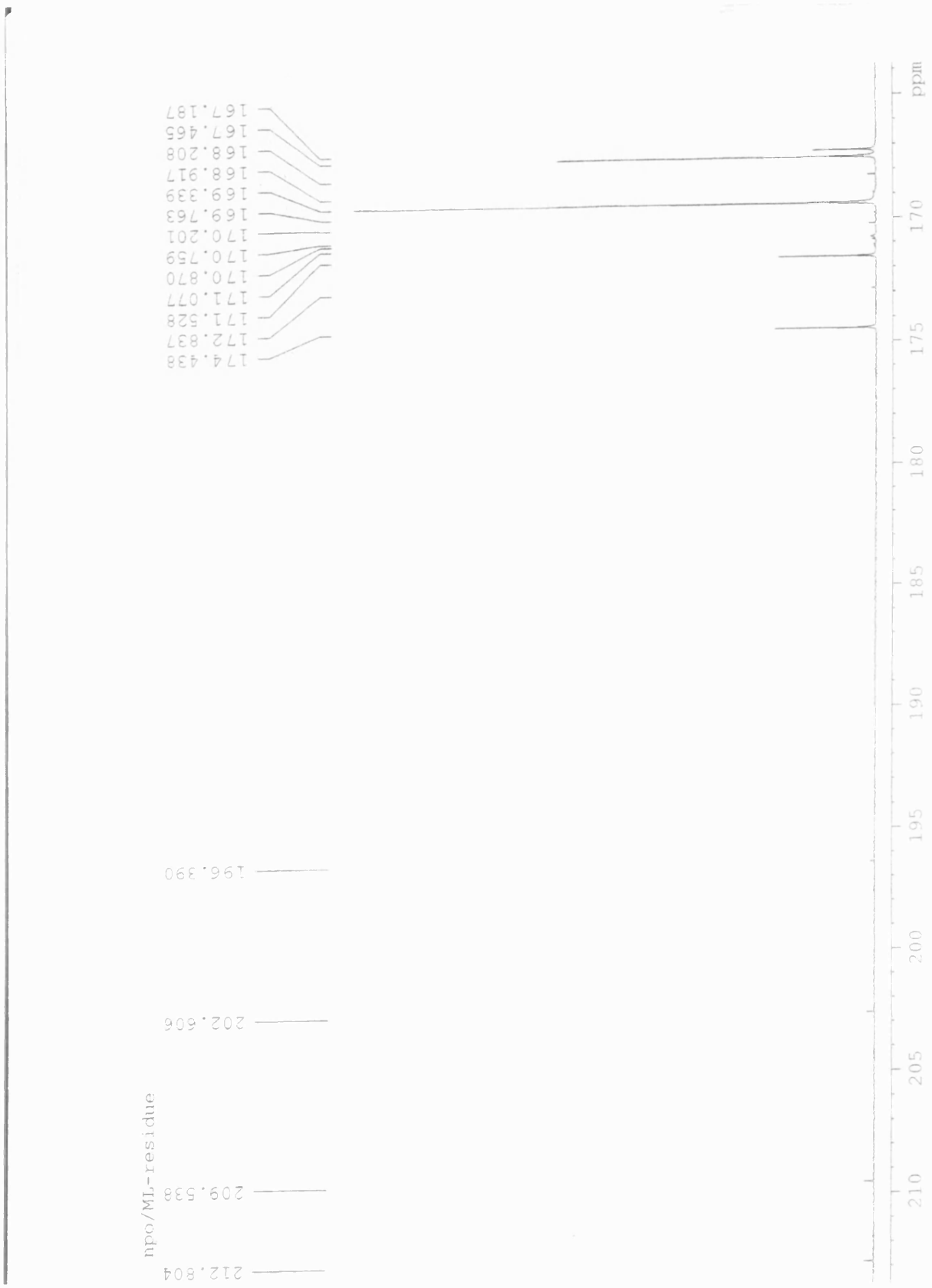

S13. Maleate acidified crude material 141 to 110 ppm ^{13}C NMR

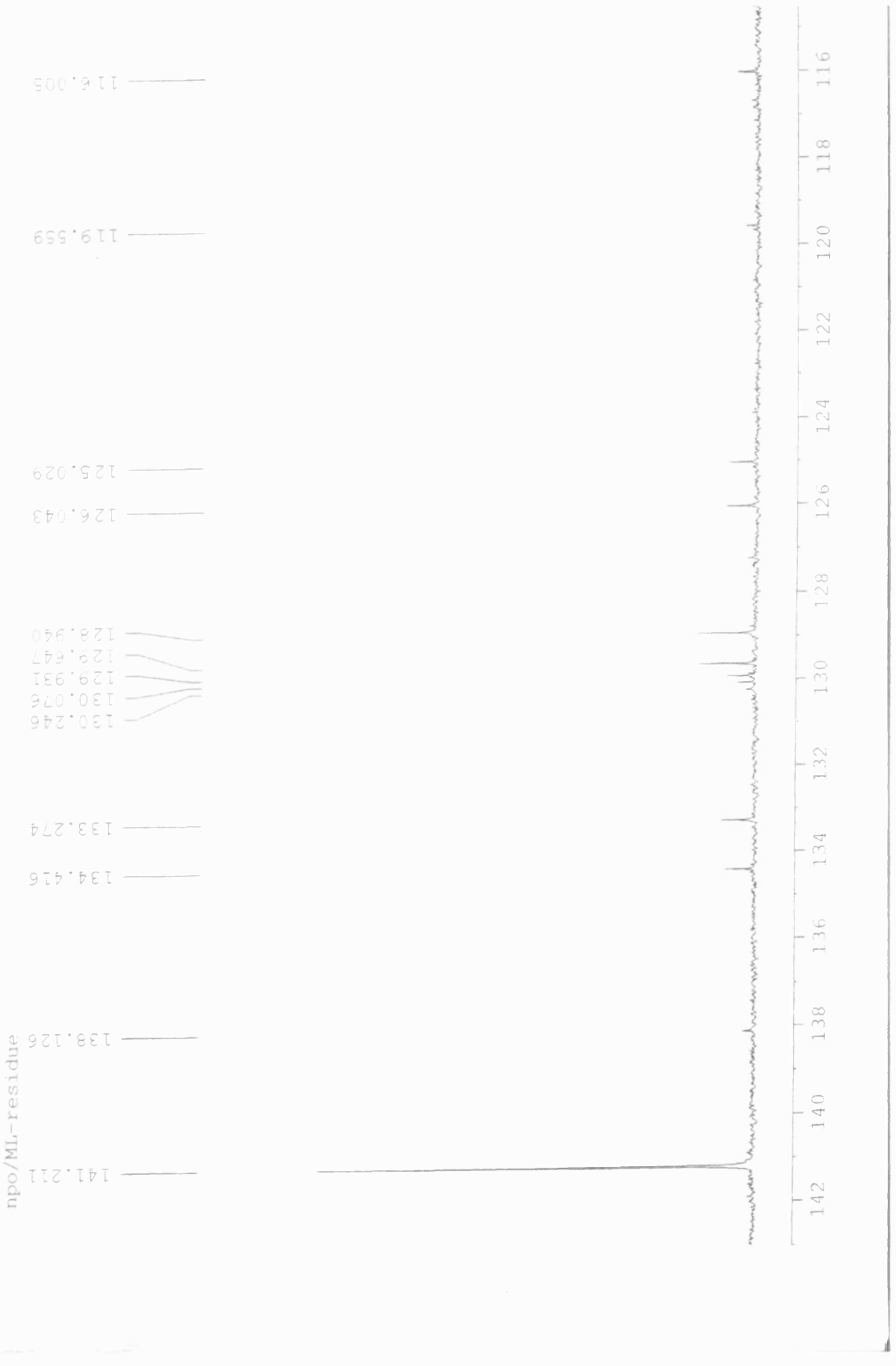

S14. Maleate acidified crude material 85 to 39 ppm ^{13}C NMR

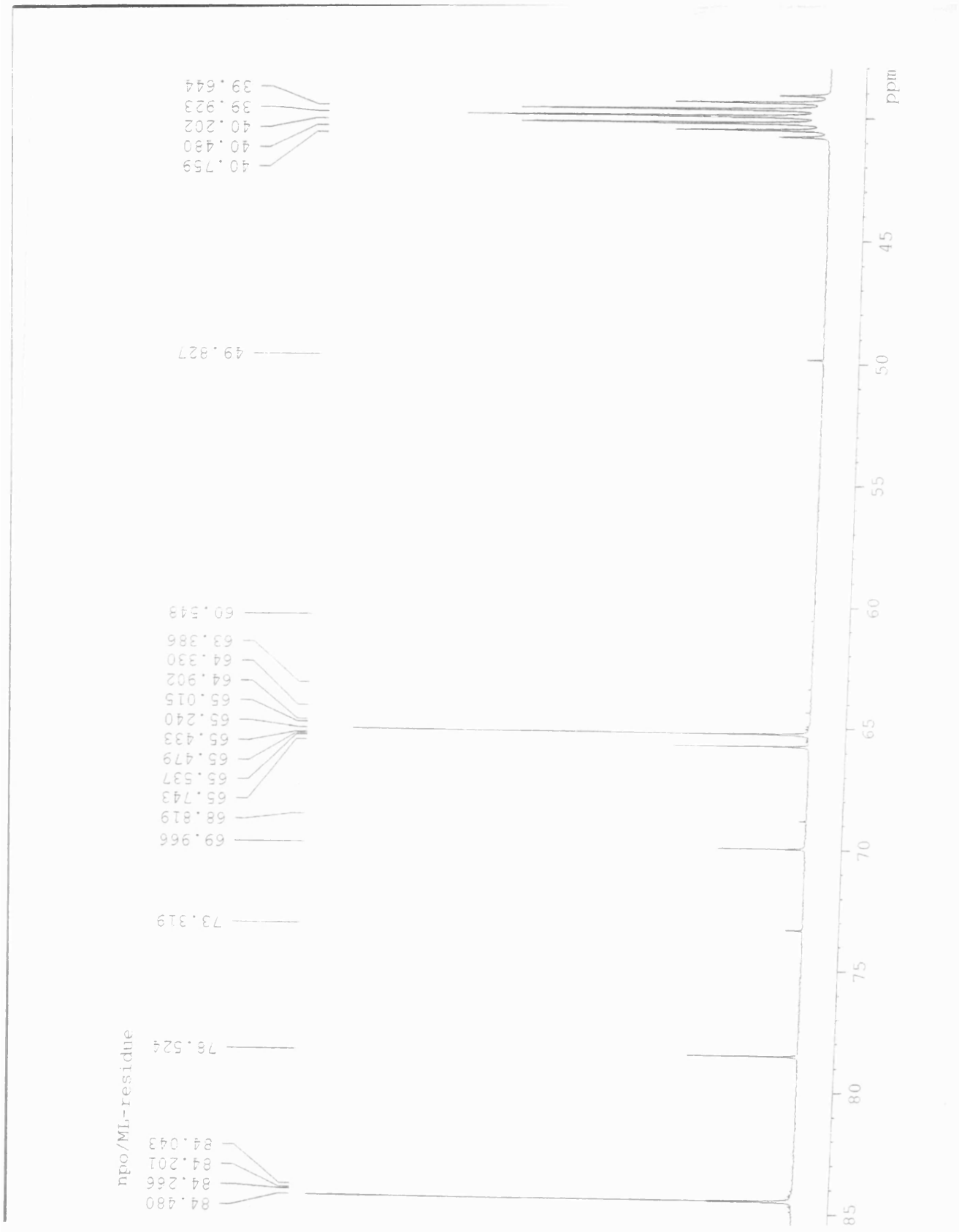

S15. Maleate acidified crude material 36 to 8 ppm ^{13}C NMR

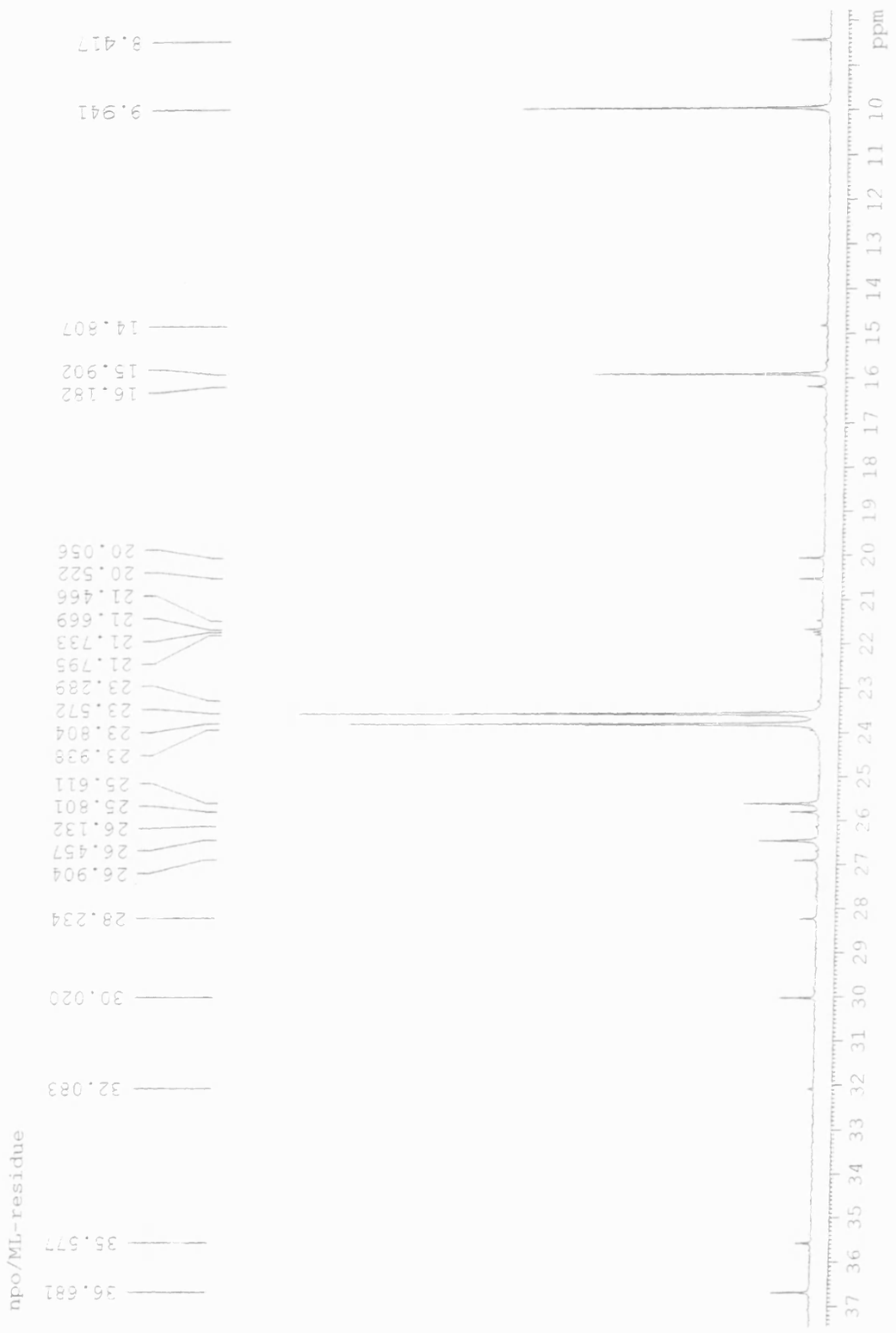

S16. Fumarate crude product after acidification bromo-β-lactone ^{13}C NMR

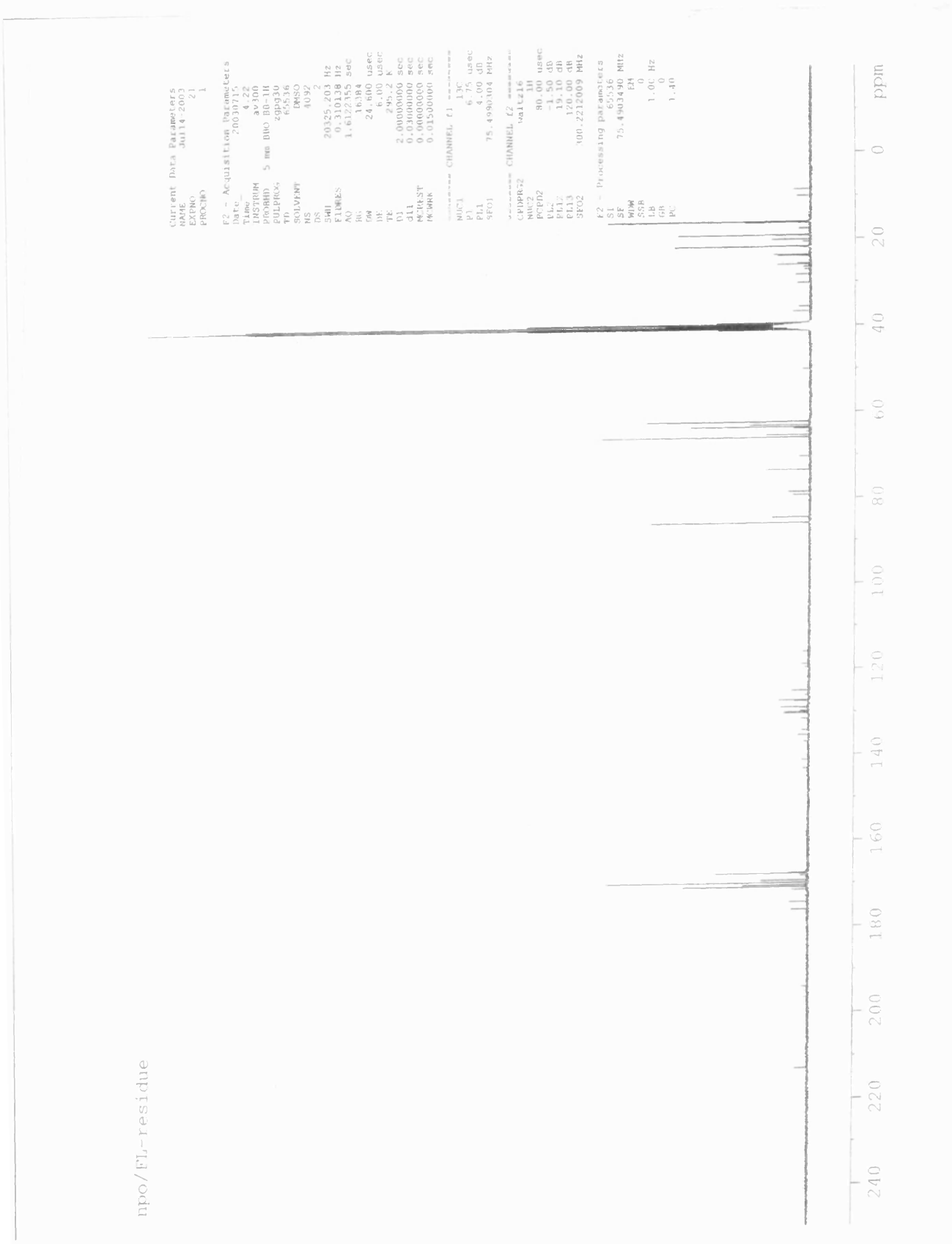

S17. Fumarate acidified crude material 213 to 167 ppm ^{13}C NMR

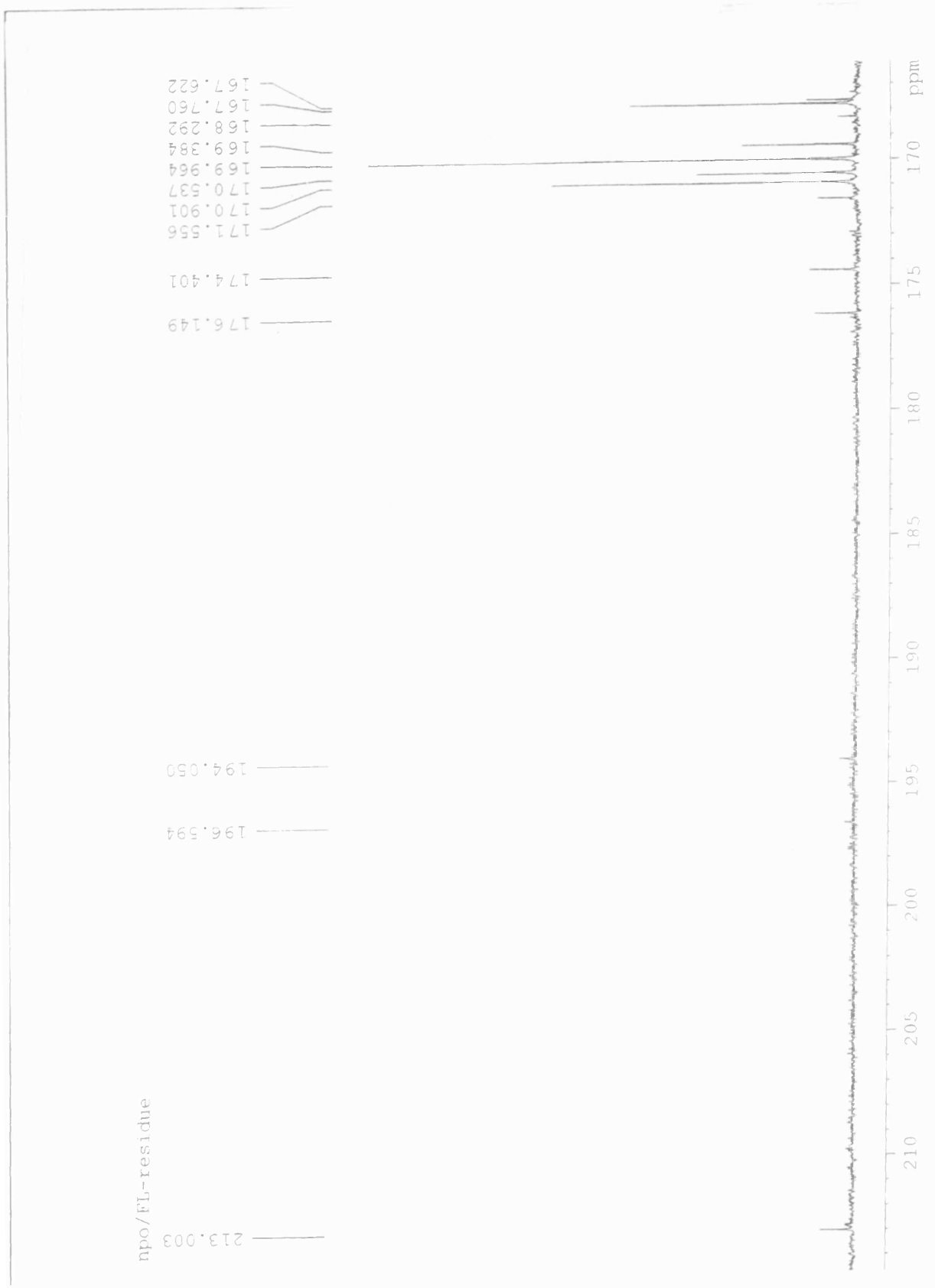

S18. Fumarate acidified crude material 143 to 116 ppm ^{13}C NMR

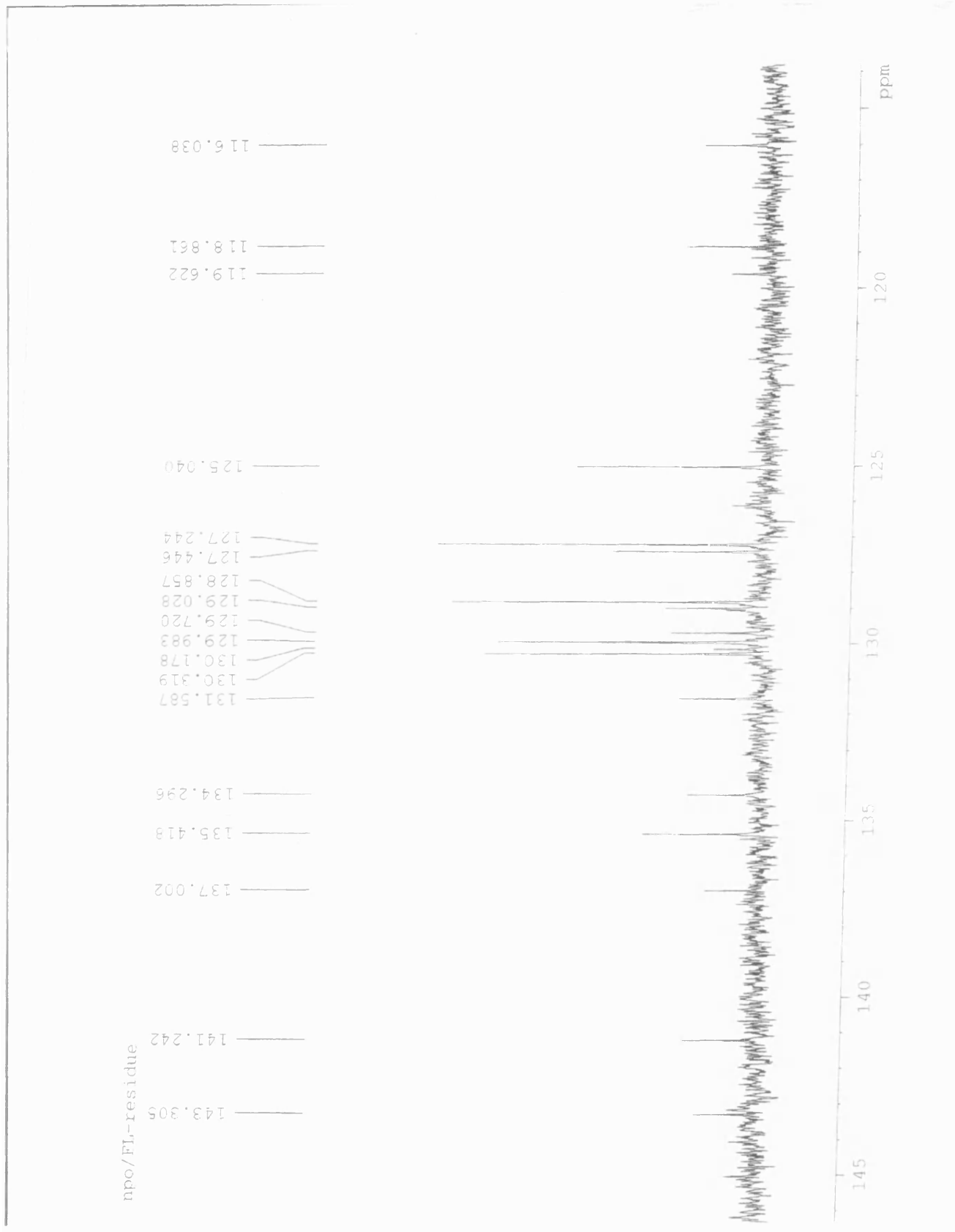

S19. Fumarate acidified crude material 85 to 39 ppm ^{13}C NMR

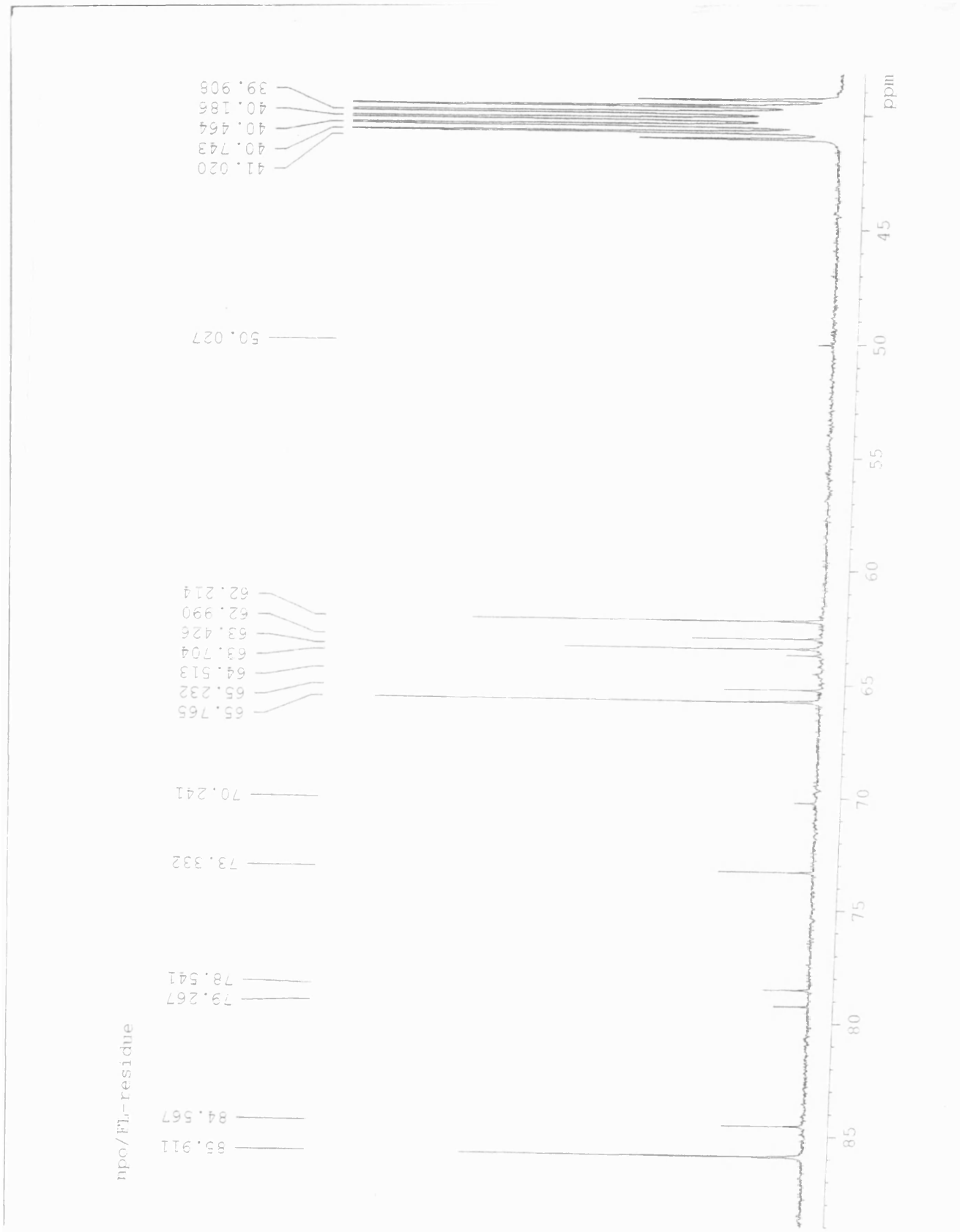

S20. Fumarate acidified crude material 36 to 8 ppm ^{13}C NMR

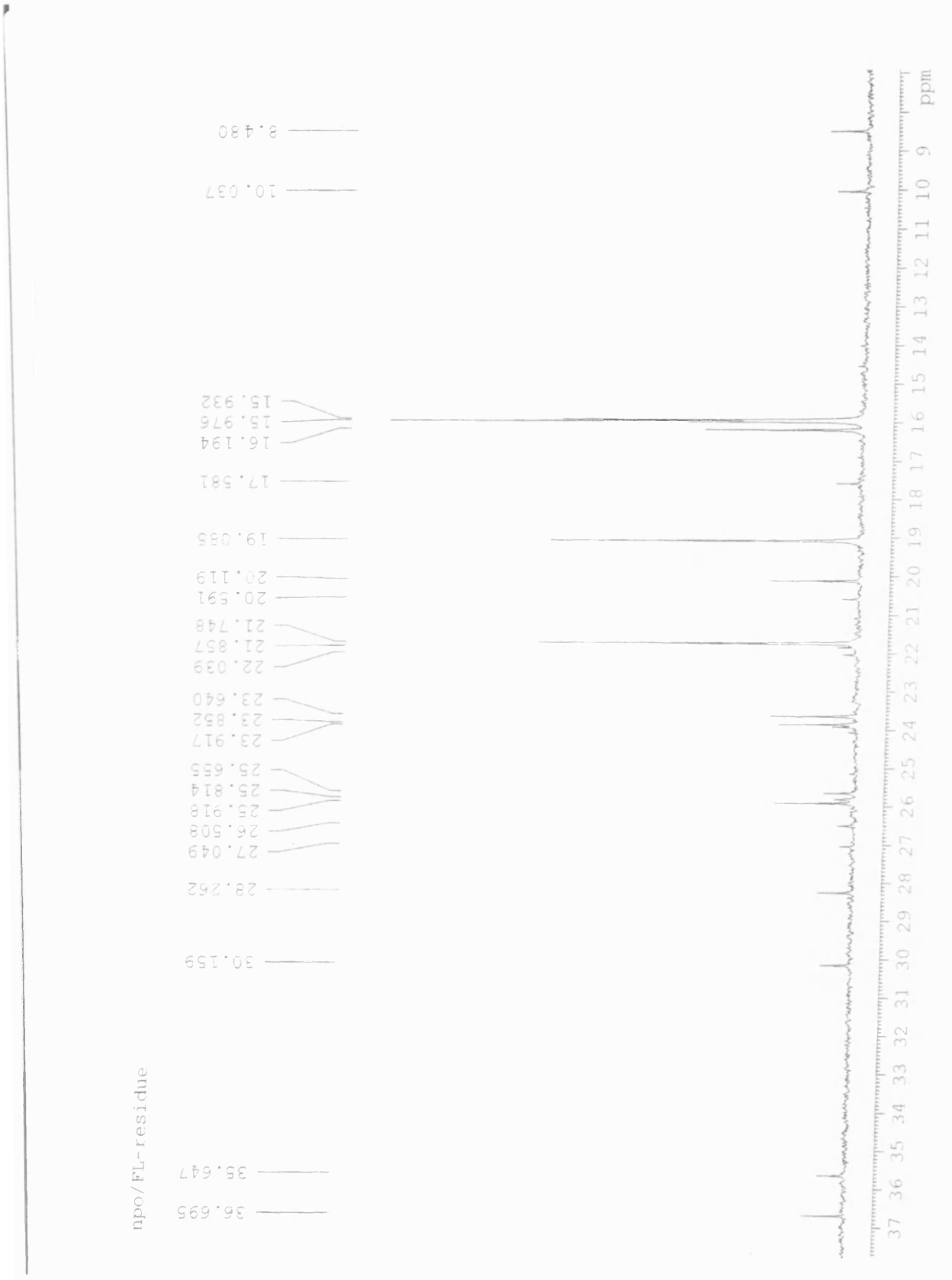

5. Computational Chemistry Introduction

5.1 Molecular modelling

The β-lactones isolated, [3R(3S),4R(4S)]-3-bromo-4-carboxy-3,4-dimethyloxetan-2-one [M8X] and [3R(3S),4S(4R)]-3-bromo-4-carboxy-3,4-dimethyloxetan-2-one [F8X], from aqueous bromination of 2,3-dimethylmaleate and 2,3-dimethyfumarate disodium salts, do not have stereochemistry suggested by Tarbell and Bartlett.[86,89,91,92] The obvious question to ask is why the stereochemistry of the bromo-β-lactones isolated is the way it is and not as that suggested by Tarbell and Bartlett. The answer may lie in the energetics of the reaction potential energy surface. Computational chemistry techniques provide calculations of energy for a given geometry; the results can then be used to construct a potential energy surface (PES) for a proposed reaction pathway to propose a minimum energy path (MEP) between reactants and isolated products and to test ideas.[93].

Calculations concerned with chemical reactions are normally concerned with locating the lowest energy path leading from one minimum through a saddle-point and to another minimum. Computational chemistry is concerned primarily with accurate energetic calculations. The properties of a given molecule are calculated by knowing how the electronic energy changes upon adding a perturbation. Perturbations may be a geometric change, e.g. bond stretching, or an external influence, e.g. approach of a solvent molecule. These calculations occur on a single molecule, experimental observations however are made on collections of molecules that may have a population of say 10^{23} molecules and a thermodynamic energy distribution as determined by a Boltzmann distribution.[94] So statistical thermodynamics is used to calculated macroscopic properties such as heat capacity.[95]

In molecular mechanic methods empirical data is fitted mathematically to features such as bond lengths, angles and dihedral angles.[96] These methods are suitable for systems where quantum chemistry methods

would simply take too long, such as minimising a protein model. Various partial charge methods are available that attempt to calculate partial charges based on atom types, nearest neighbours or scale the charges to provide a model to fit dipole moments. These methods are often used in molecular modelling, such as rational drug design.[97] Molecular mechanics methods do not model bond breaking and bond formation. Quantum mechanics and computational chemistry techniques must be used to model bond breaking/forming processes.

5.2 Self consistent field calculations.

All of the calculations used to relate chemical energetics and molecular geometry are approximate solutions of the Schrödinger wave-equation.[98] The Schrödinger wave equation is often written as $\hat{H}\Psi = E\Psi$ when applied to molecular systems. The energy **E** as derived, is an expectation (an observable) value that has physical significance, it can be measured. The systems energy, **E**, is the eigenvalue of the Hamiltonian operator, $\hat{H}$, corresponding to the allowed solutions of the wavefunction Ψ. The Hamiltonian is composed of kinetic energy **(T)** and potential energy terms **(V)**, where electrons are treated individually and each nucleus is treated as an aggregate. For an electron in 3 dimensional space, of coordinates **x**, **y** and **z**, and subject to an external field, say nuclear attraction, the time-independent Schrödinger equation which describes the energetic properties of the electron is represented below.[98,99,100,101,102]

$$\hat{H}\Psi_{(x,y,z)} = E\Psi_{(x,y,z)} \text{ where } \hat{H} = \frac{-h^2}{8\pi^2 m}\nabla^2 + V \text{ and } \nabla^2\Psi = \frac{\partial^2\Psi}{\partial x^2} + \frac{\partial^2\Psi}{\partial y^2} + \frac{\partial^2\Psi}{\partial z^2}$$

Where ***h*** is Planck's constant, ∇^2 is known as "del" squared and is a Laplacian operator, **V** that may depend upon position and the external field, is the potential energy of the electron and ***m*** is the mass of the electron.

In atomic units, the Hamiltonian for ***N*** electrons and ***M*** nuclei is shown below. The ratio of the mass of the nucleus, of atomic number **Za**, to the

mass of an electron is M_a. The distance between the ***i*th** electron and the ***a*th** nucleus is r_{ai}. The distance between the ***i*th** and ***j*th** electrons is r_{ij}. The distance between the ***a*th** nucleus and the ***b*th** nucleus is r_{ab}. The Laplacian operators ∇_i^2 and ∇_a^2 involve differentiation with respect to the coordinates of the ***i*th** electron and ***a*th** nucleus.[101] The wavefunction Ψ, is a mathematical description of the electrons and nuclei as calculated from quantum physics principles. Ψ in itself has no physical significance and has a conversion factor to SI units of $a_o^{-3/2}$ or 2.5978×10^{15} $m^{-3/2}$.[101]

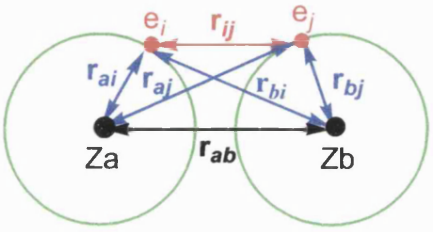

$$\hat{H} = \underbrace{-\sum_{i=1}^{N}\frac{1}{2}\nabla_i^2}_{\text{kinetic energy of electrons}} \underbrace{-\sum_{a=1}^{M}\frac{1}{2m_a}\nabla_a^2}_{\text{kinetic energy of nuclei}} \underbrace{-\sum_{i=1}^{N}\sum_{a=1}^{M}\frac{Z_a}{r_{ai}}}_{\text{coulombic attraction between electrons and nuclei}} + \underbrace{\sum_{i=1}^{N}\sum_{j>i}^{N}\frac{1}{r_{ij}}}_{\text{repulsion between electrons}} + \underbrace{\sum_{a=1}^{M}\sum_{b>a}^{M}\frac{Z_a Z_b}{r_{ab}}}_{\text{repulsion between nuclei}}$$

Kinetic energy, **T**

Potential energy, **V**

Fig. 68. A many bodied Hamiltonian.[101]

The Born interpretation of Ψ was to consider that it was related to the probability of an electron in a given volume of space. However, as Ψ has real and imaginary (complex) results, the probability of an electrons position must be related to $|\Psi|^2$. If an infinite volume of space from $-\infty<x,y,z<+\infty$ is considered, the electron must be in that space, so Ψ^2 can be considered to be unity.[104] The Hamiltonian operator is hermitian; $\hat{H}\Psi=\Psi\hat{H}$.[105]

$$E = = \frac{\int \Psi\, \hat{H}\Psi\, d\mathbf{r}}{\int \Psi\, \Psi\, d\mathbf{r}} = \frac{\langle \Psi|\hat{H}|\Psi\rangle}{\langle \Psi|\Psi\rangle}$$

The Variational Principle states that any approximate wave function has an energy above or equal to the exact ground state energy.[106] A proof relating the Schrödinger equation and energy, shows that even an approximate wave function will also have an energy above or equal to the exact ground-state energy of a calculated system.[107] There are a number of solutions to the Schrödinger equation from allowed wavefunctions (Ψ), and solutions where the energy is a minimum for an allowed solution of the wavefunction is the ground state energy of a molecular system and this is often the only solution desired. As nuclei are vastly heavier than electrons, nuclear velocities are much slower relative to electrons. This allows the energy to be separated into two terms, an electronic term that is solved with approximations of the Schrödinger equation and a nuclear term, which describes the nuclear wave function. This is referred to as the Born-Oppenheimer approximation.[108] If **R** denotes nuclear position and **r** electronic position then the following approximation may be made.[108] Thus computational chemists are concerned with solving Ψ for electronic wavefunctions.

$$\hat{H}(\mathbf{R})\Psi_i(\mathbf{R},\mathbf{r}) = E_i(\mathbf{R})\Psi_i(\mathbf{R},\mathbf{r}), \text{ where } i=1,2,3,4\ldots\infty$$

Where different wave functions Ψ are designated as *i* and *j* the solutions can be chosen to be orthogonal (mathematically distinct from each other) and normalised (satisfies boundary condition, normally $|\Psi_i^2|$ and $|\Psi_j^2|$ adjusted to unity), this yields orthonormal solutions.

$$\Psi_{total}(\mathbf{R},\mathbf{r}) = \sum_{i=1}^{\infty} \Psi_{nuclear}(\mathbf{R}).\ \Psi_{electronic}(\mathbf{R},\mathbf{r})$$

Using the adiabatic solution, $\int \Psi\ \Psi\ d\mathbf{r}$, which is often written as $\langle\Psi|\Psi\rangle$ in Dirac notation, can be normalised to unity. Inclusion of the Pauli exclusion principle and the Aufbau principles allows description where all electrons have unique quantum numbers and the electrons are indistinguishable; *none* of the quantum numbers for the electrons are

equal and electrons pair up with opposite spins, the solution of Ψ is restricted for closed shell systems.[109,110] So if an electron changes sign then so must the solution, this means Ψ is antisymmetric. The allowed antisymmetric solution to Ψ can be derived using Slater Determinants for **N** electrons and **N** spinorbitals.[111]

$$\Psi(r) = \frac{1}{\sqrt{N!}} \begin{vmatrix} \phi1(1) & \phi2(1) & \phi3(1) & \phi4(1) & \ldots\ldots\ldots\ldots\ldots\ldots\phi N(1) \\ \phi1(2) & \phi2(2) & \phi3(2) & \phi4(2) & \ldots\ldots\ldots\ldots\ldots\ldots\phi N(2) \\ \phi1(3) & \phi2(3) & \phi3(3) & \phi4(3) & \ldots\ldots\ldots\ldots\ldots\ldots\phi N(3) \\ \phi1(4) & \phi2(4) & \phi3(4) & \phi4(4) & \ldots\ldots\ldots\ldots\ldots\ldots\phi N(4) \\ \phi1(5) & \phi2(5) & \phi3(5) & \phi4(5) & \ldots\ldots\ldots\ldots\ldots\ldots\phi N(5) \\ \phi1(6) & \phi2(6) & \phi3(6) & \phi4(6) & \ldots\ldots\ldots\ldots\ldots\ldots\phi N(6) \\ . & . & . & . & \ldots\ldots\ldots\ldots\ldots\ldots \phi N(..) \\ \phi1(N) & \phi2(N) & \phi3(N) & \phi4(N) & \ldots\ldots\ldots\ldots\ldots\ldots\phi N(N) \end{vmatrix}$$

Fig. 69. A Slater determinant.[111]

Where $\langle\phi_i|\phi_j\rangle = \delta_{ij}$ or Kronecker delta.[112] The Kronecker delta function is part of linear algebra that allows matrix elements to be manipulated and eigenvectors and eigenvalues to be calculated. When $i=j$, then $\delta_{ij}=1$ and where $i\neq j$, then $\delta_{ij}=0$.

Even with the restrictions and approximations already made, it is impossible to solve for a many electron wave functions as shown in figure 68. A self-consistent field (SCF) approximation is used to replace the many electron Hamiltonian with a many one-electron Hamiltonian. In the SCF procedure, each electron no longer interacts with other electrons, but with an average field produced by the other electrons.

The columns in the Slater determinant are single electron wave functions, orbitals, whilst the electron co-ordinates are along the rows. The one-electron functions upon solving the Schrödinger equation thus become molecular orbitals, MO. These MO's are given as a product of a spatial orbital and a spin function where $\alpha_{spin}=\uparrow$ and $\beta_{spin}=\downarrow$ for electron spins. The orbitals are expanded into a basis, composed of mathematical functions.

$$\phi_i = \sum_{\mu=1}^{N} c_{vi}\chi_\mu \quad \text{and hence} \quad |\Psi_{(r)}\rangle = |\phi_1\phi_2\phi_3\phi_4..\phi_N\rangle \quad \text{and} \quad E = \langle\Psi(r)|\hat{H}|\Psi(r)\rangle$$

Where C_{vi} are the molecular orbital expansion coefficients. The arbitrary basis functions are χ_μ and χ_1 to χ_N are chosen to be normalised and ϕ_1 to ϕ_N are arbitrary molecular orbitals. Many software packages use gaussian function to describe gaussian-type atomic functions. Any functions may be used, but gaussian functions are popular and some packages use Slater functions.

$$g(\alpha,\check{r}) = C.x^n.y^m.z^l.\exp(-\alpha r^2) \quad \text{and} \quad \int[g(\alpha,\check{r})]^2\,\partial\tau = \langle g|g\rangle = 1$$

The constant α, determines the size of the function, so αr^2 is the radial extent, and $\check{r}$ is a vector composed of **x**, **y** and **z** components. For gaussian functions, $e^{-\alpha r^2}$, **C** is a constant and depends upon **α**, **n**, **m** and **l**.[113] Pople derived values for basis function constants by energy minimisation to yield variational energies.[114]

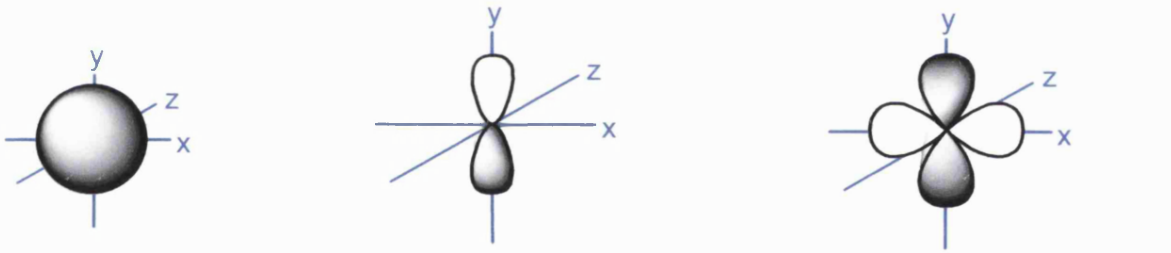

$g_s(\alpha,r) = (2\alpha/\pi)^{3/4}.e^{(\alpha r^2)}$ $g_{py}(\alpha,r) = (128\alpha^5/\pi^3)^{1/4}.y.e^{(\alpha r^2)}$ $g_{dxy}(\alpha,r) = (2048\alpha^7/\pi^3)^{1/4}.x.y.e^{(\alpha r^2)}$

Fig. 70. Atomic orbital function expressed as primitive gaussian functions.[115]

Primitive gaussian functions describe the atomic functions, so an **s**-type, p_y-type and d_{xy}-type functions for example are shown above in figure 70. Linear combinations of the primitive gaussian functions are used to form the actual basis functions used during the calculation, and form contracted basis functions. This is analogues to the method LCAO.[116] So for a set of **K** known basis functions $\{\phi_\mu(r)|\mu = 1,2,3...K\}$ and $i=1,2,3...K$

$$\chi_\mu = \sum_{\mu} d_{\mu p}.g_{prim} \quad \text{and as} \quad \phi_i = \sum_{\mu}^{K} c_{\nu i}\,\chi_\mu \quad \text{and so} \quad \phi_i = \sum_{\mu}^{K} c_{\nu i} \cdot \left(\sum_{prim} d_{\mu p}.g_{prim}\right)$$

The contracted basis functions contain constants $d_{\mu p}$, which are fixed constants within a basis set. The overlap between orbitals is calculated using $S_{\mu\nu}$ integrals and the electric field and electron interactions are calculated with $F_{\mu\nu}$ integrals. The problem now becomes how to find a solution for the set of molecular orbital expansion coefficients $C_{\nu i}$, so that the energy is a minimum, a solution corresponding to $\partial\varepsilon_i/\partial c_{\nu i} = 0$

$$\sum_{\nu=1}^{N} (F_{\mu\nu} - \varepsilon_i.S_{\mu\nu})\, c_{\nu i} = 0 \qquad \mu = 1,2,3....N$$

The Hartree-Fock equations may then be written as a set of matrices using Roothaan-Hall notation, where each element is a matrix.[117] The matrix element ε is a diagonal matrix of orbital energies each of its elements ε_i is the one-electron orbital energy of the molecular orbital ϕ_i.

$$FC = SC\varepsilon$$

$$C = \begin{bmatrix} C_{11} & C_{12} & C_{13} & \cdots & C_{1K} \\ C_{21} & C_{22} & C_{23} & \cdots & C_{2K} \\ C_{31} & C_{32} & C_{33} & \cdots & C_{3K} \\ \vdots & \vdots & \vdots & & \vdots \\ C_{K1} & C_{K2} & C_{K3} & \cdots & C_{KK} \end{bmatrix} \qquad \varepsilon = \begin{bmatrix} \varepsilon_1 & 0 & 0 & \cdots & 0 \\ 0 & \varepsilon_2 & 0 & \cdots & 0 \\ 0 & 0 & \varepsilon_3 & \cdots & 0 \\ \vdots & \vdots & \vdots & & \vdots \\ 0 & 0 & 0 & \cdots & \varepsilon_K \end{bmatrix}$$

C is a KxK square matrix of the expansion coefficients $C_{\upsilon i}$

ε is a diagonal matrix of the orbital energies, ε_i

The basis functions are not generally orthonormal to each other and thus overlap with a magnitude $0 \leq S_{\mu\nu} \leq 1$. The diagonal elements of the **S** overlap matrix are unity and off-diagonal elements in **S** are less than 1.

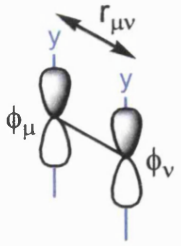

orbitals overlap
overlap element
in S is near unity

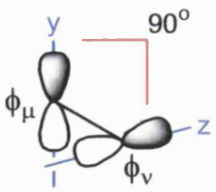

orbitals are orthogonal
overlap element in S is 0

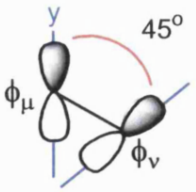

orbitals partially overlap,
overlap element 0<S<1
semi-empirical calc: uses parameters
ab initio calc: overlap is calculated.

$$s_{\mu\nu}=\int \phi_\mu(1)\phi_\nu(1)\, dr_{\mu\nu}$$

$$F_{\mu\nu}=\int \phi_\mu(1)f(1)\phi_\nu(1)\, dr_{\mu\nu}$$

Fig. 71. Orbital overlap terms are held in the **S** matrix.

The operator ***f*(1)**, is a one-electron operator, a set of one-electron function defines a matrix representation of this operator, which represents the first derivative of the electronic energy with respect to variations in the orbitals.[118]. The matrix element **F** is the Fock matrix and represents the average effects of the field of all the electrons on each orbital. For a closed shell system the Fock matrix elements is as follows[119]

$$F_{\mu\nu} = H^{core}{}_{\mu\nu} + \sum_{\lambda=1}^{N} \sum_{\sigma=1}^{N} P_{\lambda\sigma} [\langle\mu\nu|\lambda\sigma\rangle - \tfrac{1}{2}\langle\mu\nu|\lambda\sigma\rangle]$$

$$\langle\mu\nu|\lambda\sigma\rangle = \int \phi_\mu^*(1)\, \phi_\nu(1) r_{12}^{-1} \phi_\lambda^*(1)\, \phi_\sigma(1)\, dr_1 dr_2$$

C is matrix that holds the C_{vi} elements that need to be solved for. The $H^{corr}{}_{\mu\nu}$ Hamiltonian matrix represents the energy of a single electron in the field of bare nuclei, no electron correlation energy included and describes the kinetic energy and nuclear attraction of an electron.[119] The **<μν|λσ>** term is a four centre integral over the centres **μ**, **ν**, **λ** and **σ**, which represents the two-electron repulsion integral and each electron interacts with all other electrons in an average field and there is no instantaneous electron-electron interaction calculated. As there is a large number of two-electron integrals, the evaluation and manipulation of the **<μν|λσ>** is the major difficulty in Hartree-Fock calculations. For a basis set of size **K**, **<μν|λσ>** rises in proportion to **(K^4)/8**. For instance for a basis set of size **K =100**, there are 12753775

unique two-electron integrals. The effects of electron-electron interactions are, in general, called "electron correlation".[120]

$$P_{\mu v} = 2 \sum_{i=1}^{occupied=N/2} c_{\mu i} c_{vi^*}$$

The matrix element P is the density matrix. The coefficients are summed over all the occupied orbitals only and the factor of 2 is needed as each orbital in a closed shell system hold 2 electrons with opposing spins $\alpha_{spin}(\uparrow)$ and $\beta_{spin}(\downarrow)$.

All the matrix elements, **F**, **H**, **P**, **ε** and **S** depend upon the molecular orbital expansion coefficients $\mathbf{C_{vi}}$, held in matrix element **C**, so an iterative cycle is used to solve the problem and find $\mathbf{C_{vi}}$ values that represent an energy minimum. The procedure is described as a self-consistent field (SCF) method. The solution produced is a set of orbitals, both occupied (ϕ_i, ϕ_j....) and virtual or unoccupied orbitals (ϕ_a, ϕ_b.....). The total number of orbitals produced is equal to the total number of basis functions used. The energy E is then calculated from the following expression.[121]

$$E = \tfrac{1}{2} \sum_{\mu}^{N} \sum_{v} P_{\mu v} (H^{core}{}_{\mu v} + F_{\mu v}) = \langle \Psi(r) | \hat{H} | \Psi(r) \rangle$$

The overall scheme for minimising a self-consistent field calculation is shown below in figure 72.

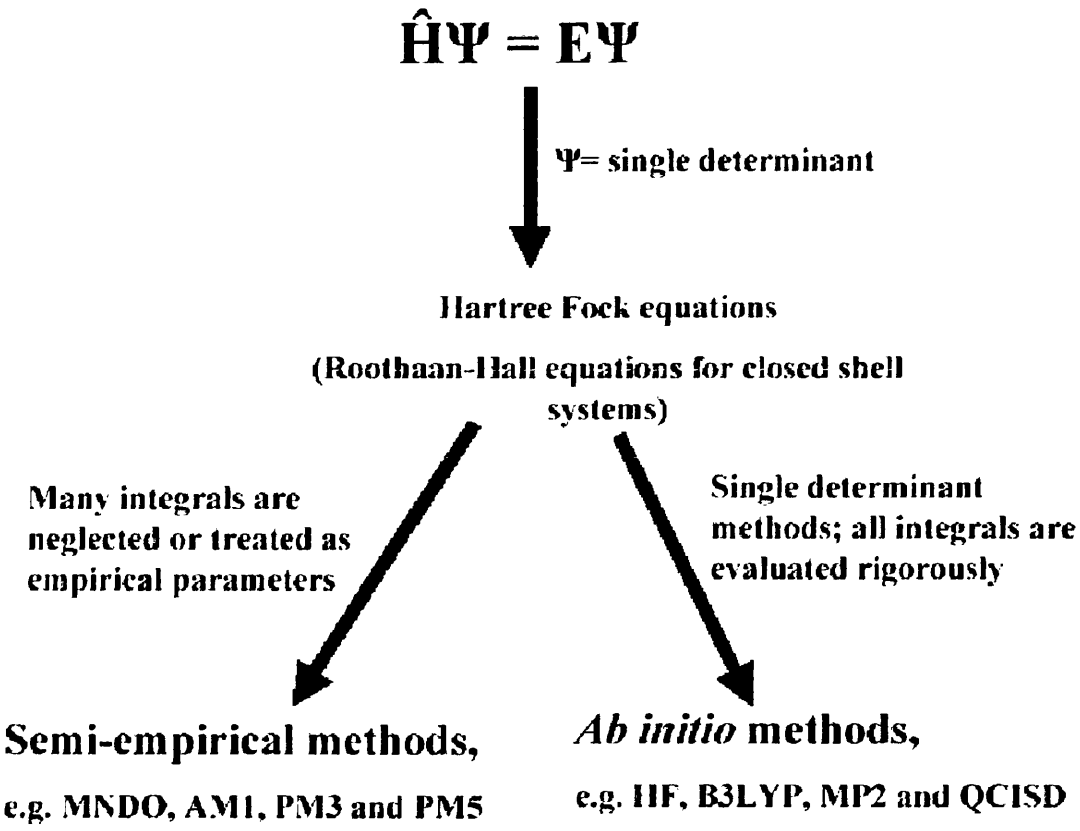

Fig. 72. General scheme for convergence of a wave-function using single determinants.[122]

The computational cost of performing Hartree-Fock calculations scales to the fourth power of the number of basis functions. This is reduced however, with Semi-empirical calculation methods, such as MNDO, AM1, PM3 and PM5.[123,124] The core assumption of semi-empirical methods is the Zero Differential Overlap (ZDO) approximation. The ZDO approximation neglects all products of basis functions depending upon the same electron co-ordinates when located on different atoms.[125] This approximation allows the cancellation of many multi-centre electron integrals in the off-diagonal elements in the overlap matrix S. To repair the deficiencies due to the number of approximations, parameters are introduced in place of some integrals.

Hartree-Fock calculations are also often referred to self-consistent field (SCF) calculations due to the presence of an average electric field. With

suitably large basis functions, the Hartree-Fock wave function will account for ~99% of the total energy of a molecular system. However the remaining ~1% is often critical for describing the energy of molecular systems, for instance the difference in energy between two conformations of the same molecule.

The difference in energy between Hartree-Fock results and the lowest possible energy in a given basis set is called the electron correlation energy.[126] Energies calculated with Hartree-Fock methods are variational, the exact energy, even if extended to the Hartree-Fock limit by using a large basis set, will always be a little bit lower than that calculated, this is due in part to the fact series expansion calculations will only yield approximate solutions. This is not an exact solution to the Schrödinger equation, only the best single determinant solution.

5.3. Hybrid Density Functional Theory.

Density functional theory (DFT) methods are attractive to computational chemists as they attempt to account for the effect of electron correlation; electrons in molecular system react to one another's motions and attempt to avoid each other. Density functional theory uses a different approach to that applied in Hartree-Fock (HF) calculation, instead of solving the Schrödinger equation; Hohenberg-Kohn equations are solved to provide solutions of the lowest ground state electron density.[127] The total number of electrons, **N**, is related to the total electron density, ρ. If r is a distance vector then, integration over all space gives

$$N = \int \rho(r)\, dr$$

As **N** is the number of electrons, the density for a Slater determinant is used, which is the exact eigenfunction for the non-interacting system, electron-electron correlation is ignored, within orbitals ϕ. As the electronic energy is related to the total electronic density, it is hence related to occupied orbitals, ϕ_i.

$$\rho(r)= \sum_{i=1}^{N} <\phi_i|\phi_i> \qquad \text{and} \qquad \hat{H}_i^{KS}.\ \phi_i = \varepsilon_i.\ \phi_i$$

The Kohn-Sham Hamiltonian is $\hat{H}_i^{KS}$ and allows the value of the orbitals ϕ_i that minimise the energy to be calculated, yielding pseudo-eigenvalues, ε_i. The Kohn-Sham method can provide solutions to the Hohenberg Kohn equation. To determine the Kohn-Sham orbitals, a similar approach to SCF procedures is adopted, where the orbital ϕ is expressed with a basis set of functions χ and the individual orbital coefficients are found by solving secular equations similar to that used in Hartree-Fock calculations.

DFT methods compute electron correlation using functionals of electron density. In 1965, Kohn and Sham suggested a practical way to solve the Hohenberg-Kohn theorem for a set of interacting electrons.[128] Their suggestion was that the exact total electronic energy (**E**) could be written as sum of terms, each dependent on the density:

$$E= E_T + E_V + E_J + E_{xc} = E[\rho(r)]$$

E_T is the kinetic energy of a system of non-interacting electrons with the same density as the real system. E_V is the potential energy term due to the interactions of the electrons with an external potential (typically due to the interaction of the electrons with the nuclei). E_J is the electron-electron repulsion term; is also known as the Hartree electrostatic energy, which arises from the classical interaction between two charge densities.

E_{xc} accounts for the difference between classical (coulombic) and quantum mechanical electron-electron repulsion. E_{xc} also includes terms that account for the difference in kinetic energy between the fictious non-interacting system and E_T in the real system. E_{xc} represents both the quantum mechanical exchange energy, which accounts for electron spin, and the dynamic correlation energy due to the concerted motion of individual electrons.[120] Classical analogies for E_{xc} do not exist.

The correlation energy in wave mechanics is defined as the difference between the exact energy and the corresponding Hartree-Fock value. The exchange energy is the total electron-electron repulsion minus the classical coulombic energy. The definitions of correlation and exchange energies in DFT are short-range (local) and related to electron density at a given point and in the immediate vicinity, via derivatives/gradients of the electron density.

The B3LYP method includes the Hartree-Fock terms and electron correlation and exchange terms, derived from modelling an electron-gas; a fictitious substance called jellium, in which the electronic distribution has a constant non-zero density.[129] Relating the uniform electron gas properties with energy does not mean that the energy expression is equivalent to assuming that the electron density of the molecule is a constant throughout space. The local spin density approximation, LSDA, assumes that the exchange-correlation energy density at every position in space for the molecule is the same as it would be for the uniform electron gas, having the same electron density as found in that position.

The B3LYP method is known as hybrid density functional theory method, mostly a method based upon pure DFT and containing Hartree-Fock SCF components. The B3LYP energy term has the form of:

$$E_{xc}^{B3LYP} = (1-a)E_x^{LSDA} + aE_x^{HF} + b\Delta E_x^{B} + (1-c)E_c^{LSDA} + cE_c^{LYP}$$

E_x terms are exchange energy terms. E_c terms are electron density gradient correction terms. The three parameters **a**, **b** and **c** were chosen to be **0.20**, **0.72** and **0.81** respectively. The name B3LYP implies it is a 3-parameter method that includes energy corrections related to the electron density gradient (GGA) and the correlation function **B** derived by Becke. The functional **LYP** was designed to compute the full correlation energy and is not a correction to the LSDA approximation. Of all the modern functionals, B3LYP has proven to be the most popular to date. Its overall performance is remarkably good, especially as the three parameters were not optimised.[130]

The key difference between DFT and Hartree-Fock theory is that DFT in its derived form is exact. Should the exchange energy, $\mathbf{E_x}$, be known as a function the electron density then an exact solution results. Hohenberg and Kohn proved that a functional of the density must exist, however there is no guidance to an exact mathematical relationship. So the exact form of the functionals used in DFT are unknown, many approximations and parameters are used. This does mean that DFT calculations that include $\mathbf{E_{xc}}$ give results that are not strictly variational. The hybrid B3LYP method does not give variational results. It is worth noting that Hartree-Fock calculations can be viewed as being similar to B3LYP calculation where $\mathbf{E_x}$ and $\mathbf{E_{xc}=0}$.

Some gradient corrected methods (GGA), such as B88 exchange and LYP correlation, contain parameters, which are fitted to give the best agreement with experimental atomic data. The semi-empirical method PM3 has 18 parameters for each atom whilst B88 exchange functional contains a single fitting constant valid for the whole of the periodic table.[132] Other functionals such as PBE1PBE, also known as PBEO, the exchange and correlation functionals are theoretical in derivation. [133]

The importance of electron correlation energy may be illustrated by considering helium, a simple 2 electron system. Taking a calculation to the HF SCF limit, which is converged with respect to the basis-set size for the number of digits reported, gives an energy of -2.86168 a.u. for helium.[134] The exact energy reported for helium is -2.90372 a.u.[135] The difference of 0.04204 a.u. is equivalent to 26.38 kcal mol^{-1}. At room temperature, 298 K, a change of 1.4 kcal mol^{-1} in free energy of a reaction will alter an equilibrium constant by an order of magnitude. Similarly, a change of 1.4 kcal mol^{-1} for a rate-determining free energy of activation will change the rate of reaction by an order of magnitude.

A similar scheme as that shown in figure 72 is used to converge a wave-function for DFT iteration scheme, however there are some important differences.[131] In the Kohn-Sham procedure the Hartree-Fock elements $\mathbf{F_{\mu\nu}}$ are replaced by the elements $\mathbf{K_{\mu\nu}}$.

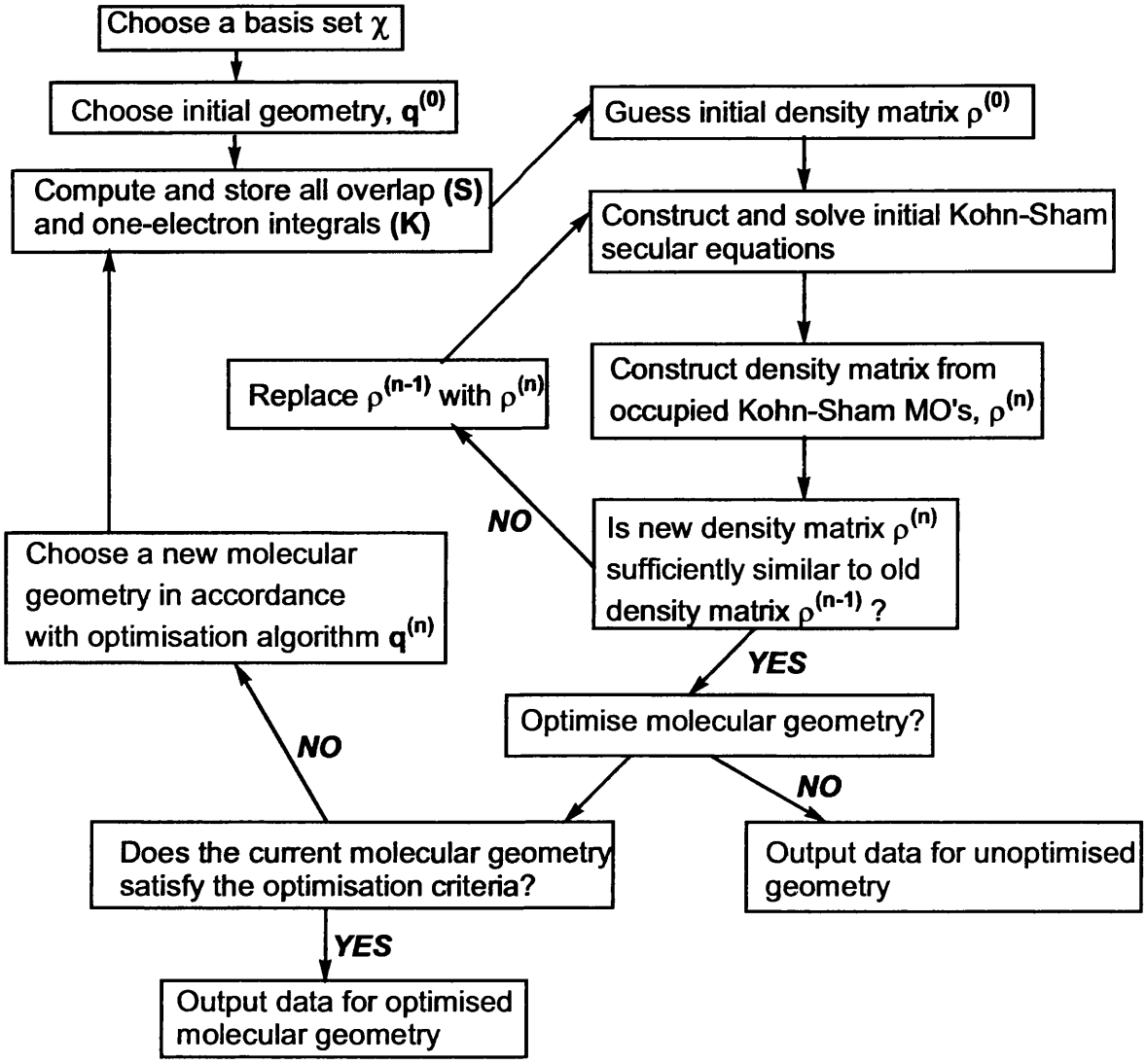

Fig. 73. Flow chart for Kohn-Sham SCF procedure.[131]

It should be noted that comparison of energies from *ab initio* calculations can be made using the relationship that 1 a.u. (hartree) is equal to **627.5095** kcal mol^{-1}. The B3LYP/6-31+G(d) method has been used extensively in this thesis and mean absolute error for energy calculation from the G2 test set is 5.9 kcal mol^{-1} with a maximum error of 35.9 kcal mol^{-1}.[136] Errors associated with AM1 calculation are higher, with a mean absolute error of 18.8 kcal mol^{-1}.[137] There is considerable debate over whether hybrid DFT methods are semi-empirical methods, however the energetic results of hybrid DFT results are superior to Hartree-Fock calculations.[130]

5.4. Basis Functions and Basis-Sets

The electronic wave function Ψ is calculated constructing a wave equation that is composed of many smaller simpler wave functions. This method is analogous to the method of LCAO, where molecular orbitals are constructed from linear combination of atomic orbitals. Basis sets must be defined as part of an *ab initio* calculation. The unknown molecular orbital, MO, which is being calculated, is expanded into a set of mathematical functions. Pople basis sets are popular and were designed from energy minimisation calculations.

A 6-31G basis set has six gaussian functions to describe the core electrons and four to describe the outer valence electrons: three gaussians for the inner valence region and one gaussian for the diffuse outer valence region. The 6-31G basis set is a split valence set, double zeta (2 functions for valence). The 6-311G basis set is a triple valence basis, set where the core orbitals are a contraction of six gaussians and the valence is split into three functions; represented by three, one and one gaussians respectively.

Polarisation functions are often added to basis sets. For instance a d function may be added to a 6-31G basis set by using 6-31G(d), sometimes denoted as 6-31G*. In this thesis the 6-31+G(d) basis set has been extensively used and some use has been made of the 6-311+G(2d,p) basis set to improve energetic calculations. The 6-311+G(2d,p) basis set adds 2d functions to heavy atoms and adds a p function to hydrogen atoms. The + function is a diffuse function.

Diffuse functions are normally s- and p- functions, normally denoted by + symbol. A single + function meaning s- and p- functions added to heavy atoms. A ++ symbol means adding s- and p- function to hydrogen's too. Little energetic gain is made by adding both + functions.[138] Anionic species require that additional functions be added to basis sets to improve the mathematical treatment of the electronic wave function with additional electrons for anions. Most of the calculations in this thesis

were performed on anions, containing even numbers of electron. Systems with even numbers of electrons are closed shell systems and all the electrons are paired in the ground state, having a multiciplicity of 1.

A closed shell (restricted) calculation with B3LYP/6-31+G(d) calculation on 2-bromo-2(methyl-3-oxiranyl)-propionate, say M2, $C_4H_6BrO_4$ and a charge of −1 has 55 $\alpha_{spin}\uparrow$ electrons and 55 $\beta_{spin}\downarrow$ electrons, is described by 236 basis functions and 431 primitive gaussian functions.

5.5. Implicit Solvation Methods

Laboratory and process chemistry normally involves the use of a support solvent to aid mixing, heat transfer and isolation of chemicals. Gas phase or *in vacuo* calculations may provide a suitable starting point, only the model of interest is examined, no solvation added to the calculation. However, most calculations are too big to include explicit solvation molecules, so implicit models are used to mimic solvation. A practical approach to calculate solvent effects is to use a continuum solvent model or self-consistent reaction field (SCRF) methods. The interaction between a solute molecule and the surrounding dielectric is represented by a term $\mathbf{V}_{int}$ that is added to the gas-phase electronic Hamiltonian operator for the molecule.[139]

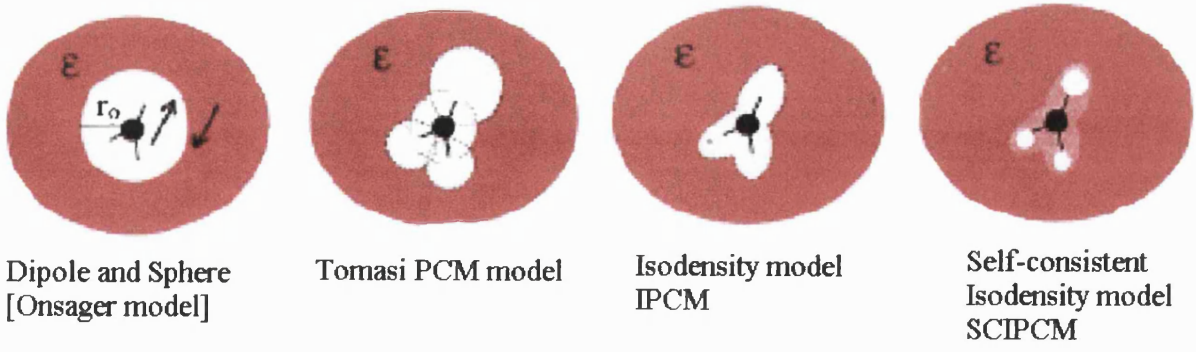

Fig. 74. SCRF models implemented within Gaussian98A.6 software.[140]

In the Onsager model, where a_o^3 is the spherical cavity radius in the solvent, μ is the dipole moment, g is the reaction field, and so for the Onsager dipole SCRF method the V_{int} term is [141]

$$V_{int} = -g.\mu.\langle\psi|\ \mu|\ \psi\rangle \text{ and } g = 2[(\varepsilon-1)/(2\varepsilon+1)]a_o^{-3}.$$

The electrostatic component of free energy of solvation is given by[141]

$$\Delta G_{electrostatic} = [(\varepsilon-1)/(2\varepsilon+1)].(\ \mu^2/\ a_o^3)$$

In the polarized continuum model (PCM), sometimes referred to as D-PCM method, of Tomasi, the cavity is still re-defined but treated more realistically as interlocking atomic spheres in which each nucleus is surrounded by a sphere of radius 1.2 times the van der Waals radius of that atom. The cavity is the volume occupied by these overlapping atomic spheres. The calculation of energy is composed of two cycles, an initial gas phase SCF calculation and then a continuum SCF calculation, including dipole and electrostatic terms. The effect of the solvent continuum is represented numerically, small tesserea surround the solute. The dipole of the solute induces a dipole in the continuum medium, the electric field induced by the solvent dipole in turn interacts with solute dipole this leading to net stabilisation.

The free energy of the solute is composed of a terms relating to the solute-solvent interactions and solute terms.[141]

$$\Delta G_{solvation} = \Delta G_{cavity} + \Delta G_{VDW} + \Delta G_{electrostatic}$$

ΔG_{cavity} is the energy to create the cavity. This is endothermic, requires energy and provides a destabilising contribution. ΔG_{VDW} is the dispersion, mainly van der Waals, energy between solvent and solute. This energy contribution is exothermic and provides stabilising contribution. $\Delta G_{electrostatic}$ is the effect on the solute due to the medium. The medium is polarized because of the solute electric charge distribution. This is another exothermic term and provides a stabilising contribution. The images shown in figure 75 illustrate how a probe is

used to build up the implicit solvent envelope and the *rhs* image was rendered from HyperChem5.01, coloured by partial charge, in an attempt to illustrate the "tesserae" used in a PCM calculation.

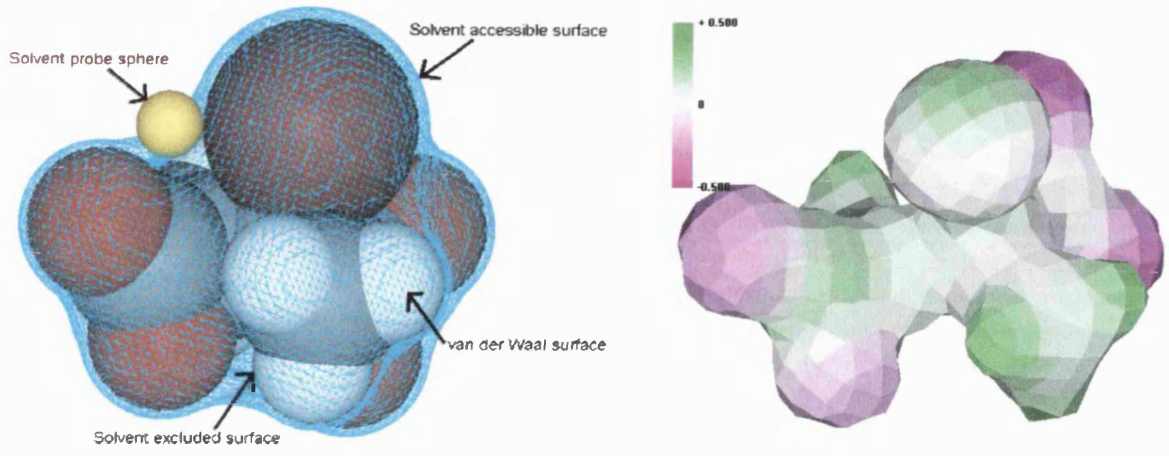

Fig. 75. A probe is used to construct the solvent accessible surface. (F2 used)

The PCM (D-PCM), CPCM and COSMO method construct an envelope around a solute and the SCF calculation is performed with inclusion of the energetic contributions the continuum envelope. In Gaussian98A.6, the PCM and CPCM methods performs two SCF cycles, initially a solute SCF calculation then a second SCF calculation is performed allowing for changes to the wave function caused by the influence of the implicit continuum solvent envelope.[142] The SCIPCM model performs an SCF energy calculation repeatedly within the SCRF SCIPM model, until convergence of the energy is obtained for a given molecule, hence only available for single-point energy calculations in Gaussian98A.6.[142]

The bromination of the unsaturated dianions reaction stoichiometry does not include incorporation of water molecules; bromohydrins were not isolated, which also indicates that potential hydrolysis and explicit water solvation need not be modelled when considering bromo-β-lactone formation. Implicit solvation models are use to model reactions in solution, and solvation does alter the reaction PES. A classic example is

the S_N2 reaction of chloromethane with chloride anion.[143] An example of a chemical reaction in both the gas phase and the liquid phase with the effects of solute-solvent interactions is the reaction of chloromethane with chloride anion to form a transition state and then products, a classic S_N2 reaction.[143] For the calculations in the liquid phase, the solute-solvent electrostatic and dispersion interactions were included along the reaction path. Results of the calculations are summarized in the figure 76 below, which shows the change in energy as a function of the reaction coordinate for this reaction in the gas phase, in solution with water, and in solution with dimethyl formamide (DMF).

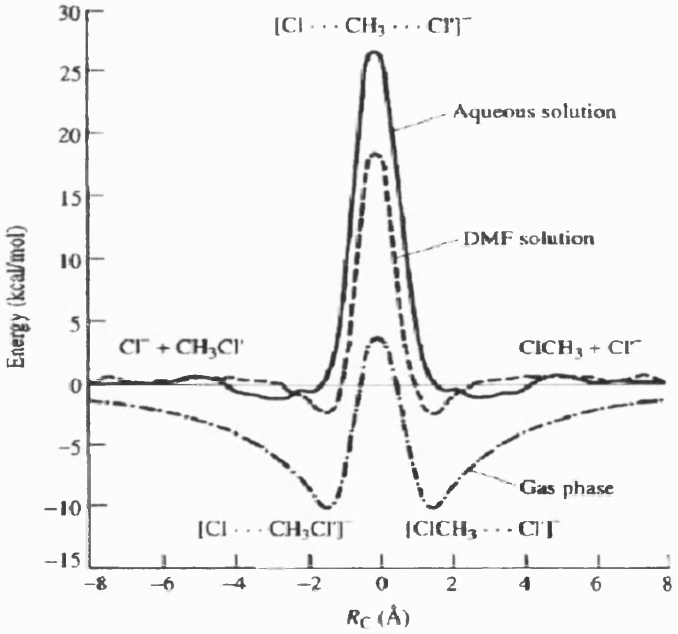

Fig.76. The energetic change of an S_N2 reaction energetic profile with differing solvents.[143]

In the gas phase, there are energy minima due to formation of an anion-dipole complex between chloride anion and methyl chloride, $[Cl^{\cdots\cdots}CH_3Cl]^-$ or $[CH_3Cl^{\cdots\cdots}Cl]^-$. Between these minima is an activation energy of about 13.9 kcal mol^{-1} to achieve a transition structure $[Cl^{\cdots\cdots}CH_3{}^{\cdots\cdots}Cl]^-$. In aqueous solution the chloride ion is solvated and no ion-dipole minima are observed. Any stabilisation due to formation of an

ion-dipole is offset by energy that would be lost in desolvation of the chloride anion. In water however, a much larger activation energy, ~ 26.3 kcal mol^{-1}, is observed for formation of the transition state. This energy is larger than observed for the gas phase because of poorer stabilisation by solvation of the transition state compared to stabilisation in the gas phase of the ion-dipole complex.

Comparison of experimental and calculated solvation data is not as numerous as comparison of energetics. Reaction rates and barrier heights are used to compare the energetic accuracy of many *ab initio* calculations. Comparison of pKa calculations and experimental data is often used to compare implicit solvation values. A comparison of mean absolute deviation of aqueous solvation free energies of 70 neutral and charged molecules at the HF/6-31+G(d)//B3LYP/6-31+G(d) using CPCM and the UAHF (Gaussian98) cavity method gave a total error of 2.95 kcal mol^{-1}, for neutral species the error was 1.43 kcal mol^{-1}, for anionic species the error was 3.86 kcal mol^{-1} and for cationic species the error was 4.32 kcal mol^{-1}.[144]

5.6. Finding Stationary points.

Stationary points such as energy minima or saddle points (cf. transition states) are all that normally concern computational chemists when investigation a potential energy surface. Gaussian98A.6 uses a powerful and robust algorithm called the Berny algorithm.[145] The Berny algorithm starts with an initial guess for second derivatives from using connectivity data and atomic radii using a simple valence forcefield. The hessian matrix initially derived from the forcefield model is updated with every optimisation step using computed first derivatives. Once stationary points have been identified, frequency calculations can be performed. Frequency calculations for minimum energy moieties should result in all real vibrational frequencies. Frequency calculations for a first order saddle point, a transition state, should result in only a single imaginary frequency. IRC, intrinsic reaction co-ordinate, calculations corresponding to a geometry perturbation along the eigenvector

corresponding to the imaginary frequency, are then used to provide starting points to optimise the structures to related minima. However, IRC calculations do not include kinetic energy terms and represent the theoretical minimum energy path for relating two minima stationary points with a single transition state.[145] Frequency calculations may be performed prior to optimisations and can be used instead of initial guesses from the simple valence force-fields.

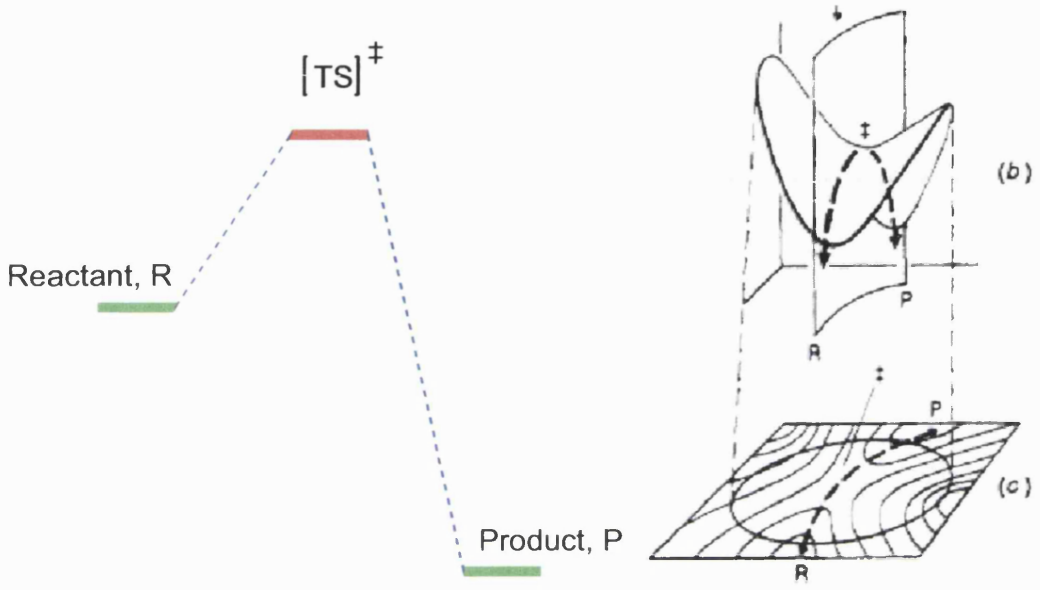

Fig. 77. A theoretical PES from reactant R to product P via a TS.[93]

First derivatives of the energy and the geometry of a structure, provides information of the overall gradient of the PES at a local stationary point. Energy gradients can be calculated by using a matrix $M_x = (x_1,x_2,x_3,...x_n)$ containing geometric information. If *i* is one geometric stationary point and *j* is another close geometric point, then the gradient at point *i*, with respect to small perturbations towards *j*, is $grad_{ij} = \partial E(Mx_i) / \partial Mx_i$ and the Hessian matrix can be calculated as $H_{ij} = \partial E(M_x) / \partial(M_{xi},M_{xj})$.[147] Diagonalisation of the Hessian matrix will yield force constants. Force constants are not the same as frequencies. Eigenvector following routines for optimisation attempt to solve the hessian matrix to yield eigenvalues that corresponds to the direction to take to minimise the internal forces for geometry optimisation. Transition state optimisations

attempt to optimise along a particular eigenvector to yield a species with one imaginary eigenvalue corresponding to a single imaginary vibration at a saddle point on the PES. Vibrational frequencies are computed by determining the second derivatives of the energy with respect to the cartesian nuclear coordinates and then transforming to mass-weighted coordinates. This transformation is only valid at a stationary point, whether that is an energy minimum or a transition state. Analytical methods are used for gas-phase stationary points. Numerical calculations of frequencies are used for solutes, when using implicit solvation models like PCM, as implemented in Gaussian98A.6. Small perturbations in the x, y and z cartesian co-ordinate space are made and energies are calculated at each point. For a species of N nuclei, for a non-linear molecule, there are 3N-6 (or 3N-5 for linear molecules) internal degrees of freedom only, so the translational and rotational contamination derived from numerical calculations must be removed at the end of a calculation. It must be stressed that quantum chemistry calculations involve complex mathematical operations broken down into computational algorithms; failure to optimise a structures does not mean it is not chemically relevant. Chemical understanding must be applied to the results; computational chemistry is applied mathematics and not real chemistry. Implicit solvation methods cannot describe hydrogen bonding and electron correlation cannot be treated to yield accurate energies. However, stationary points can be calculated and a potential energy surface constructed to relate reactants, transition states and products to allow the quantitative and qualitative testing of ideas. Relative energies suffice for testing ideas, provided potential errors are not ignored, leading to the construction of a potential energy surface. Software packages used included Mopac93® [148], CachePro6.1.1 (containing interfaces to Mopac2002 and DGauss)® [149], MOE® (2004.03) [150], HyperChem5.01® [151], Acceryls Viewer Pro® [152], Molekel® [153], GaussView® [154], Molden® [155] and Gaussian98A.6® and Gaussian03®.[142] Gaussian98A.6 was available on a multi-node SGI Origin 2000 with a queue submission facility and a maximum running time of 48 hours.[156]

6.Experimental results and discussion.

6.1 Isolated bromo-β-lactones and spectra

The result of the experiments, aqueous bromination of 2,3-dimethyl maleate and 2,3-dimethyl fumarate disodium salts, are that bromo-β-lactones are isolated, in agreement with Tarbell and Bartlett, however, the structures are not as they proposed.[91,92] Addition of bromine to 2,3-dimethyl maleate disodium salt results in the isolation of [3S(3R),4S(4R)]-3-bromo-4-carboxy-3,4-dimethyloxetan-2-one, M8. Where the methyl groups in 2,3-dimethyl maleate are *cis* in relation to each other in the reactant, the methyl groups are *trans* in relation to each other in the bromo-β-lactone product. Addition of bromine to 2,3-dimethyl fumarate disodium salt results in the isolation of [3R(3S),4S(4R)]-3-bromo-4-carboxy-3,4-dimethyloxetan-2-one, F8. Where the methyl groups in 2,3-dimethyl fumarate are *trans* in relation to each other in the reactant, the methyl groups are *cis* in relation to each other in the bromo-β-lactone product.

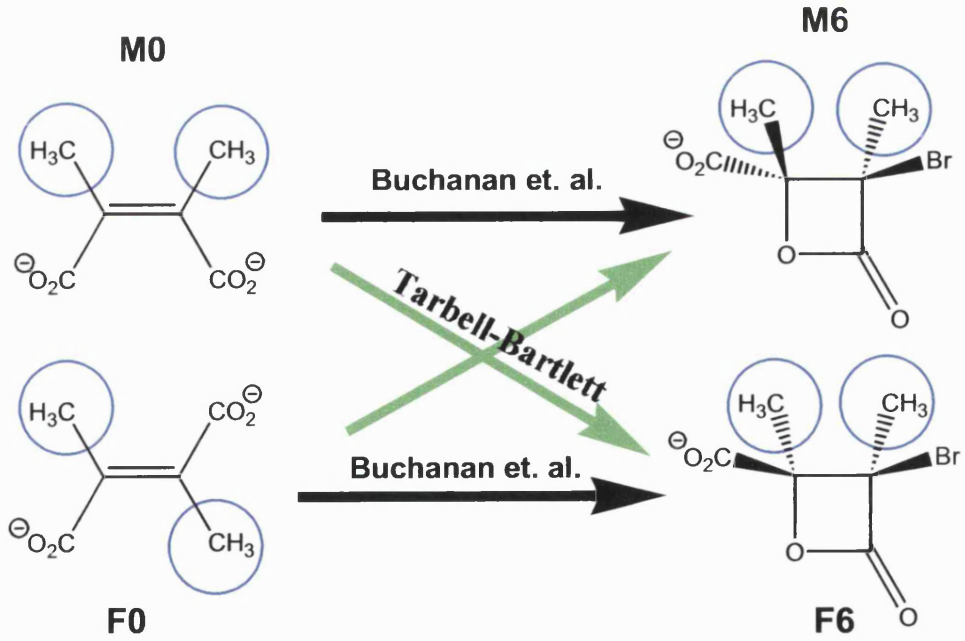

Fig. 78. Differences between Tarbell-Bartlett proposal and experimental results.[91]

The presence of some [3S(3R),4S(4R)]-3-bromo-4-carboxy-3,4-dimethyloxetan-2-one and 2,3-dimethyl maleic anhydride in the crude product prepared from aqueous bromination of 2,3-dimethyl fumarate disodium salt may be accounted for by the fact that prepared 2,3-dimethyl fumaric acid contained some 2,3-dimethyl maleic anhydride from which it was prepared. The aqueous bromination of 2,3-dimethyl maleate disodium salt and 2,3-dimethyl fumarate disodium salt are stereospecific. There is no cross-over; dibromoadducts, bromohydrins and mixtures of bromo-β-lactones were not isolated after recrystallisation. The bromination reaction as performed in the laboratory was investigated using computational chemistry, to provide a quantitative basis for a proposed mechanism. The reactants disodium salts are designated as M0 for 2,3-dimethyl maleate dianion and F0 for 2,3-dimethyl fumarate dianion. The product bromo-β-lactone isolated from M0, designated as M8X. The product bromo-β-lactone isolated from F0 designated as F8X, cf. figures 78 and 79. The bromo-β-lactone anions from calculations are designated as M6 from 2,3-dimethyl maleate and F6 from 2,3-dimethyl fumarate dianions.

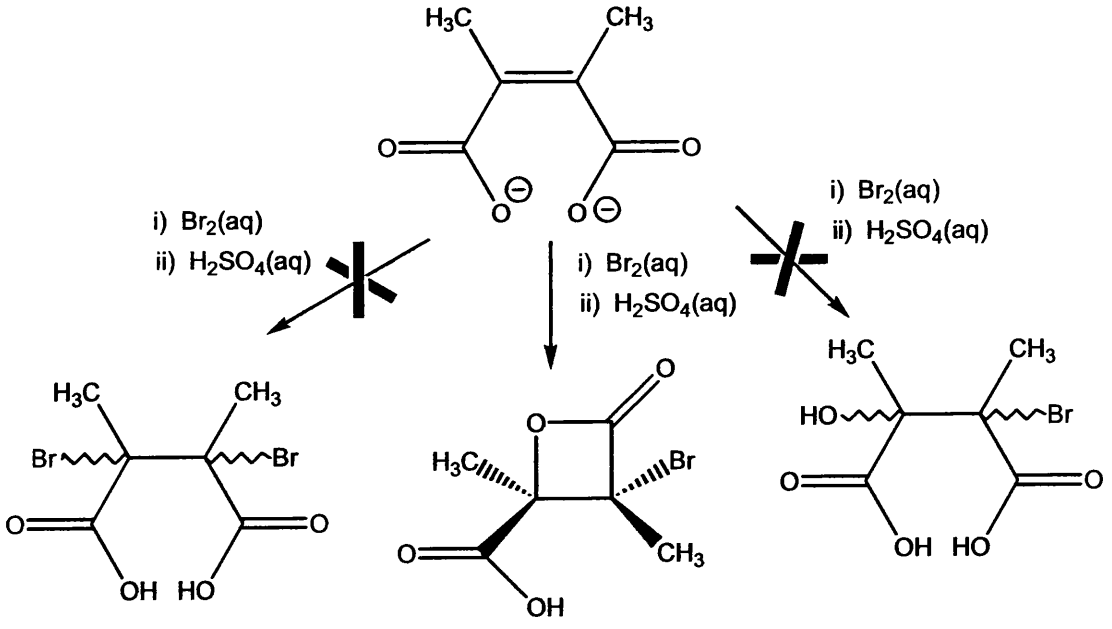

Fig. 79. Only bromo-β-lactones result from bromination of M0 and F0.[91]

The isolated bromo-β-lactones products are isolated from stereospecific reactions. The ^{13}C NMR data for the two recrystallised bromo-β-lactones shows close similarity to the spectral data for the crude material obtained after the reaction is acidified with dilute sulphuric acid.[91] Other researchers have isolated the bromohydrins from the recrystallised bromo-β-lactones and the bromohydrins from acid hydrolysis are different.[89]

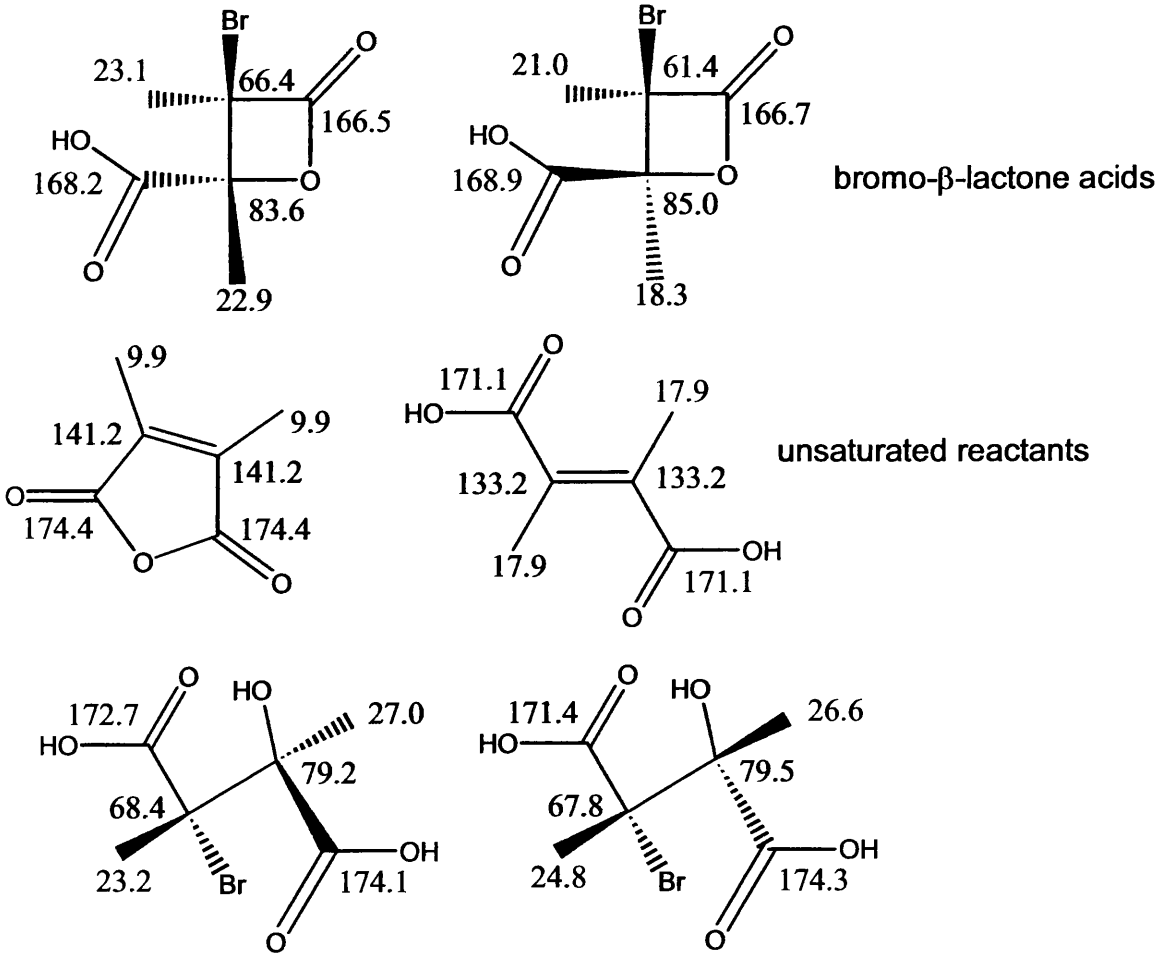

2,3-dimethyl maleate bromohydrin;
2S(R)bromo-2S(R)methyl-3S(R)hydroxy
-3S(R)methyl-butan-1,2-dioic acid

2,3-dimethyl fumarate bromohydrin;
2R(S)bromo-2R(S)methyl-3S(R)hydroxy
-3S(R)methyl-butan-1,2-dioic acid

Fig. 80. Measured δ_C $[(CD_3)_2SO]$ ^{13}C NMR chemical shifts, quoted in ppm.[89,91]

Tarbell and Bartlett were also mistaken about the nature of the bromohydrins.[86,89] It is possible to calculate ^{13}C NMR chemical shifts. The simple calculations can be made with programs such as ChemDraw Pro or *ab initio* Hartree-Fock calculations can be performed.[157]

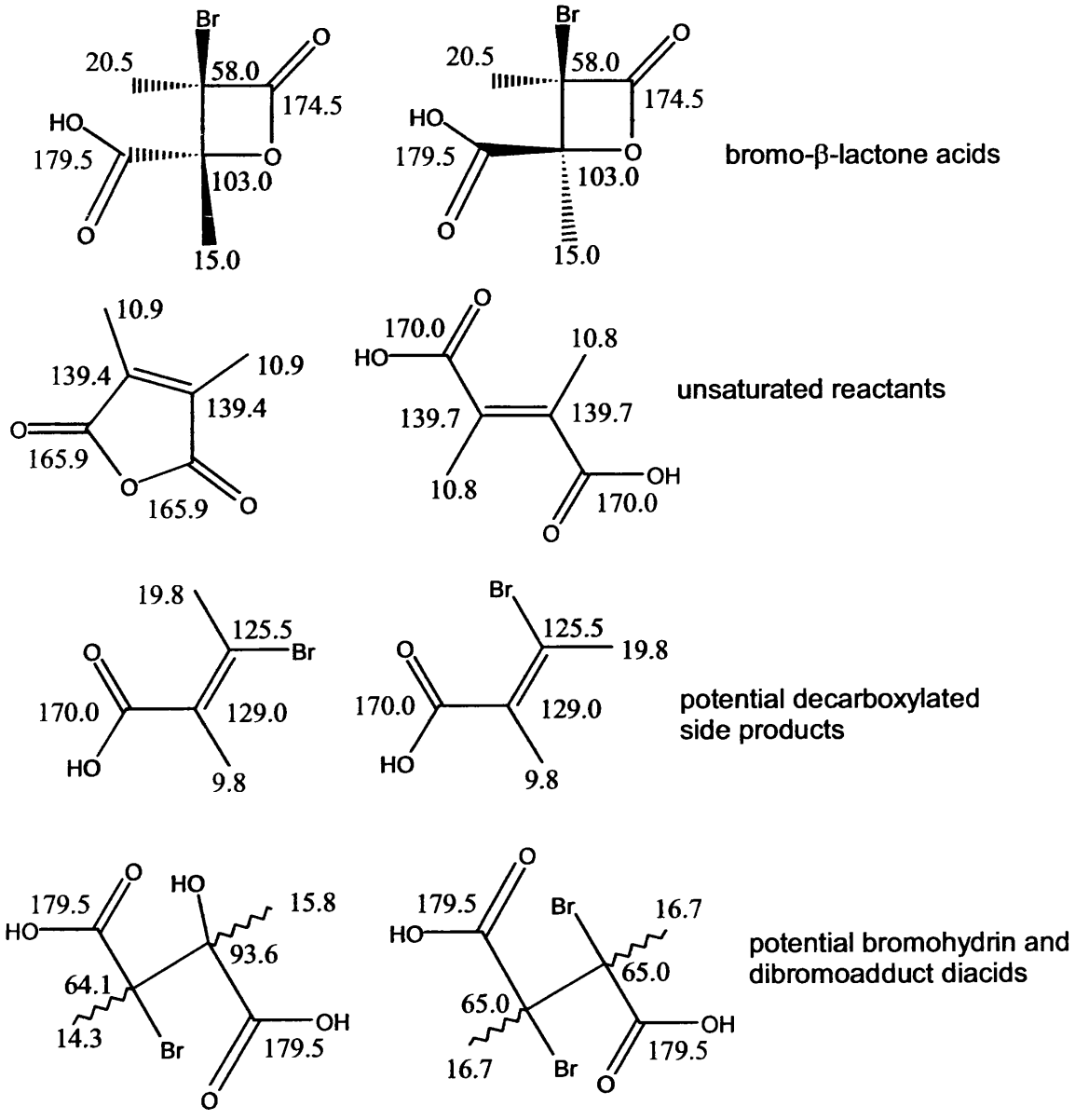

Fig. 81. ^{13}C NMR chemical shifts as predicted by ChemDraw Pro, δ_C quoted in ppm.

The 2,3-dimethyl maleic anhydride structure was optimised with PCM/B3LYP/6-31+G(d). The resultant geometry was subjected to a

single point calculation with rHF/6-311+G(2d,p) and NMR (GIAO) calculation.[142,158] The resultant anisotropic GIAO magnetic shielding tensors (ppm) were calculated as carbonyl carbon (C=O) as 161.5231 and 161.6164, the central alkene bond (C=C) carbons as 93.1282 and 93.4353 and the two methyl (-CH_3) carbons were 12.1101 and 12.1876 ppm. The ^{13}C NMR (δ_C) predictions made with ChemDraw Pro, using a look-up table with adjustment for neighbouring atom types, are closer to experimental values shown in figure 80, as opposed to the *ab initio* calculations performed with Gaussian98A.6. A similar *ab initio* calculation performed on an optimised bromo-β-lactone acid, M8, [3S(3R),4S(4R)]-3-bromo-4-carboxy-3,4-dimethyloxetan-2-one, and gave results that were not accurate as those predicted with ChemDraw Pro, as shown in figure 81.

The acidified crude ^{13}C NMR spectra from bromination of 2,3-dimethylmaleate shown as S13 on page 82 shows unassigned peaks at 129.647 ppm and 128.940 ppm which are similar to decarboxylated unsaturated side products as illustrated in figure 81. In spectra S15 on page 85 a peak at 15.902 ppm cannot be assigned, although similar to CH_3 signals predicted for saturated bromohydrin and/or dibromo-adduct shown in figure 81. In spectra S18 on page 87 a number of unassigned peaks appear from 130 ppm to 125 ppm, similar to decarboxylated unsaturated side products as predicted in figure 81. The *ab initio* GIAO and ChemDraw Pro calculations were conducted to test the use of implicit solvation models and see if unassigned peaks in the crude ^{13}C NMR spectra could be assigned to structures illustrated in figure 81. Gaussian based contracted basis functions do not properly describe the electron density close to nuclear centres. Accurate *ab initio* GIAO calculations of NMR shielding tensors must use large basis sets to obtain reasonable results.

It must be stressed that S12 on page 81 only shows signals for M8X, whereas S17 on page 86 shows signals for F8X and relatively weaker signals for M8X. The 2,3-dimethyl fumarate diacid was prepared from

2,3-dimethyl maleic anhydride, so the anhydride was also present in small amounts in the aqueous bromination of 2,3-dimethyl fumarate disodium salt. Hence, aqueous bromination of 2,3-dimethyl fumarate dianion appears to produce M8X and F8X acids in the crude products. The recrystallisation of the crude material prepared from F0 only contains F8X.

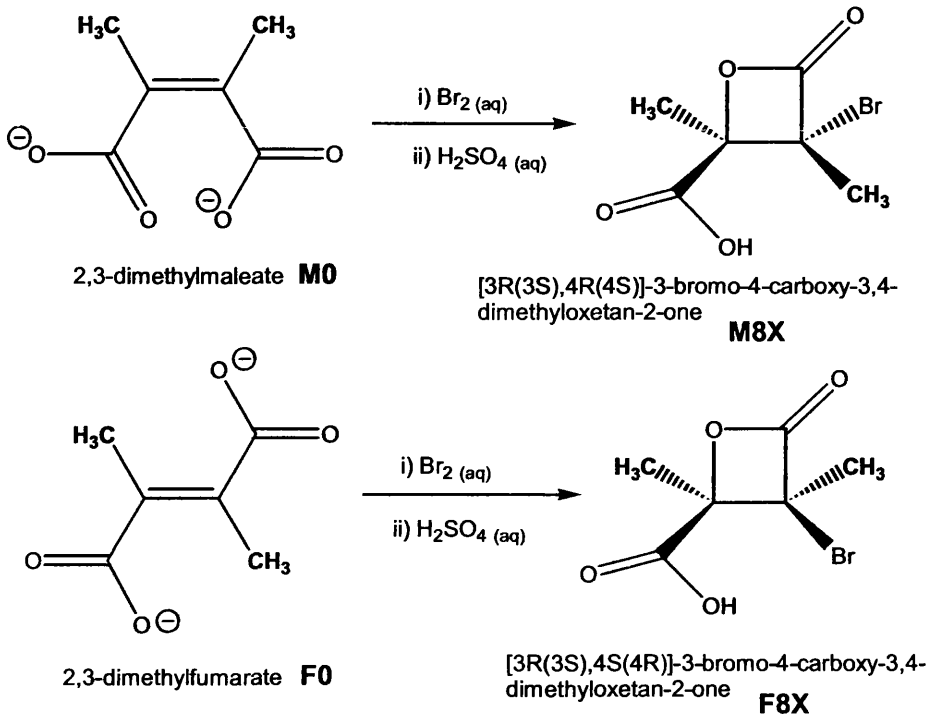

Fig. 82. Reaction examined using computational chemistry.[86,91,92]

Computational calculations were used to qualitatively and quantitatively test ideas for proposed structures and conditions to build reaction PES, to provide robust quantitative support for a proposed mechanism, to relate product bromo-β-lactones to the reactant dianions and bromine.

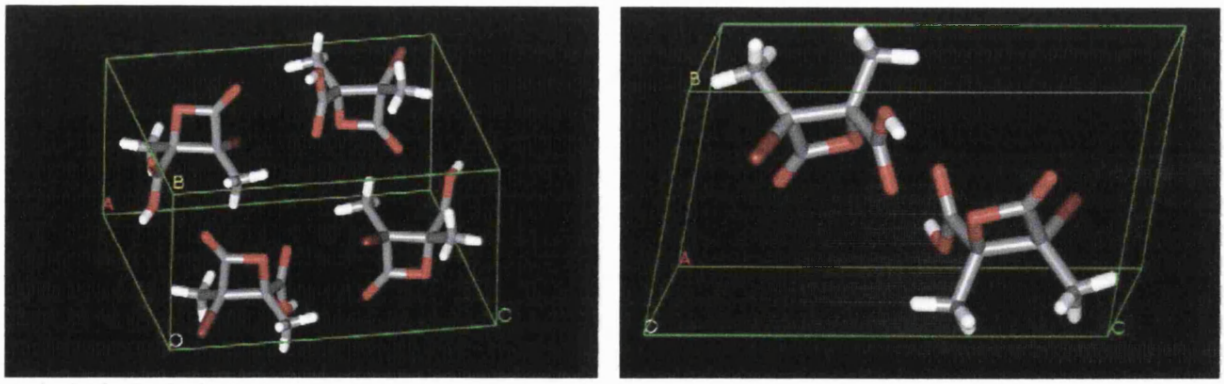

Fig. 83. bromo-β-lactones acids M8X and F8X captured from CIF files.[91]

The crystallographic structures for the [3S(3R),4S(4R)]-3-bromo-4-carboxy-3,4-dimethyloxetan-2-one(M8X) and [3R(3S),4S(4R)]-3-bromo-4-carboxy-3,4-dimethyloxetan-2-one (F8X) isolated from aqueous bromination were overlaid with the optimised PCM/B3LYP/6-31+G(d) structures (M8 and F8) using the rigid alignment method in MOE2004.3.[149] The crystallographic structures are in blue, M8X and F8X in figure 84. The differences between the M8X and M8 are less than they are for the differences between F8X and F8.

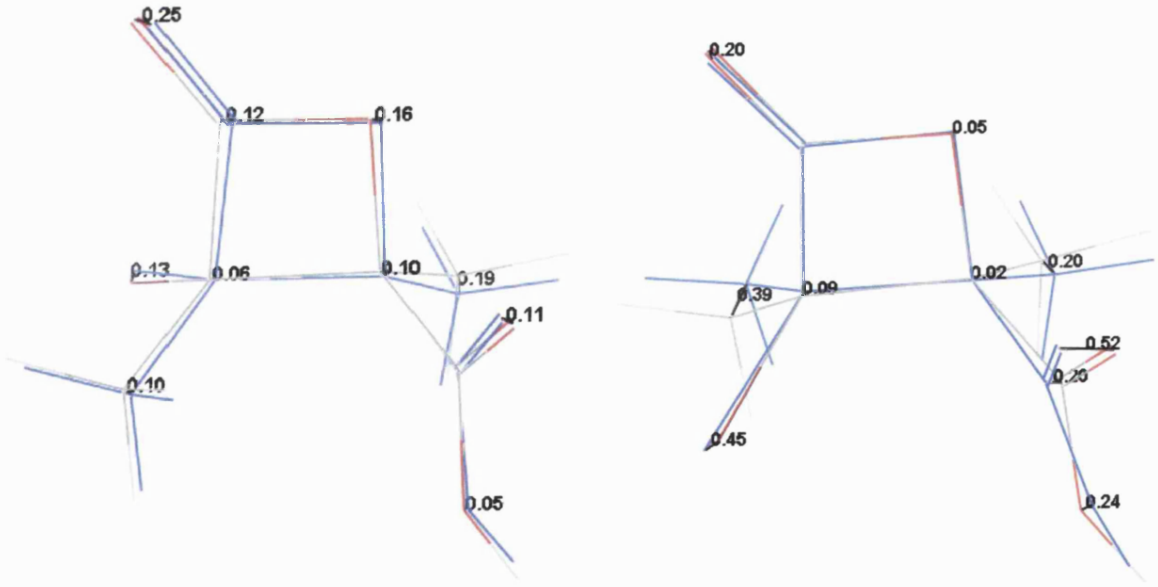

Fig. 84. Overlays of M8X and M8 (*lhs*) and F8X and F8 (*rhs*) as optimised with PCM/B3LYP/6-31+G(d).

The distances between heavy atoms are in black in Ångströms. The differences between hydrogen's atoms have been ignored; crystallographic structures usually calculate the position of hydrogen atoms rather than using measured electron density. The differences may be due to the fact that crystallographic structures are obtained from solid crystals so crystal packing effects cannot be ignored and the computational structures were optimised using PCM to treat implicit aqueous solvation. The qualitative similarity between the crystallographic structures and the optimised structures from PCM/B3LYP/6-31+G(d) calculations also confirmed the calculated method resulted in an acceptable qualitative structure for the bromo-β-lactone acid.

6.2 Mechanistic considerations

The product bromo-β-lactones form from ring closure, the intermediate preceding the formation of β-lactones need to be calculated and related to the reactants. Ring closure of halonium ions has been suggested by Tamelen, albeit for iodonium ions.[71] Considering the rate of ring closure of ω-bromo-alkylcarboxylates to lactones, cf. figure 41, the rate of ring closure for 4-membered rings is quicker than that for 3-membered rings, so β-lactone formation should be quicker compared to α-lactone formation for halolactonisation.[53] Other halolactones have been synthesised from halogenation of unsaturated acids and salts.[84]. Homsi and Rousseau found that β-lactones are formed directly with dialkyl substitution on the β-carbon.[58,59] The inductive effect of methyl group will aid cyclisation, referred to as the Thorpe-Ingold effect, where the formation of a transition state for ring closure is assisted by inductive alkyl groups.[30] The chlorination of maleic and fumaric salts investigated by Kuhn, Ebel and Wagner-Jauregg, does not lead to chloro-β-lactones but chlorohydrins that have been suggested to form from hydrolysis of cyclic chloronium ions and α-lactone intermediates. However, hydrolysis of α-haloacids indicate that 3-*Exo*-*Tet* processes occur rapidly and result in retention of configuration as found by Ingold, Winstein and

Chadwick.[35,32,33,79] Ring closures that may be pertinent are illustrated below.

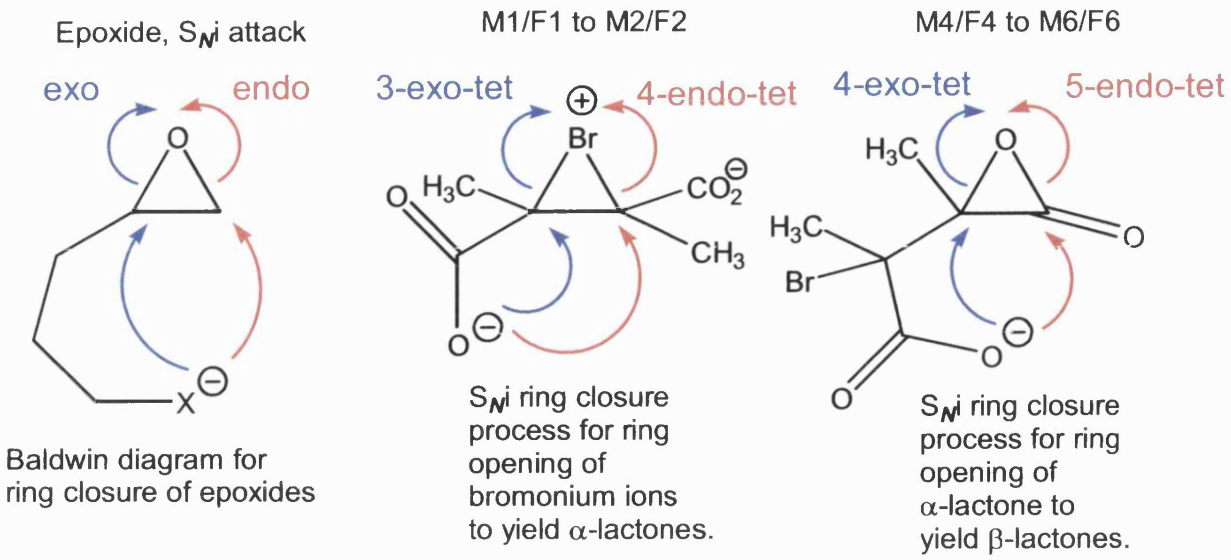

Fig. 85. Ring closure illustrated with Baldwin's nomenclature.[54]

The proposed mechanism of this thesis is that the cyclic bromonium ions leads to the formation of an α-lactone, by 3-*Exo-Tet* ring closure, that then undergoes a conformational change to facilitate 4-*Exo-Tet* ring closure to lead to bromo-β-lactone formation.[91] There are three mechanistic proposals:-

I. Tarbell and Bartlett; proposed the formation of open chain zwitterionic intermediates that undergo ring closure in the quickest possible succession.[86]
II. Roberts and Kimball; proposed initial formation of a cyclic bromonium intermediate that undergoes 4-*Exo-Tet* ring closure to yield bromo-β-lactones.[61]
III. Robinson, Buchanan and Williams et. al.; proposed initial formation of a cyclic bromonium intermediate that undergoes 3-*Exo-Tet* ring closure to yield α-lactones that undergo further conformational change to facilitate 4-*Exo-Tet* ring closure to yield bromo-β-lactones.[91]

In 1937, at a time of great interest in the mechanism of halogen addition to alkenes, Tarbell and Bartlett found the disodium salts of 2,3-dimethylmaleic acid and 2,3-dimethylfumaric acid reacts with aqueous bromine, $Br_{2(aq)}$, to give two different crystalline bromo-β-lactones, similar results were obtained with aqueous chlorine, $HOCl_{(aq)}$.[85] The stereospecific nature of the reaction implied that the addition of the two components to the alkene was concerted. Chlorination of maleic and fumaric acid salt solutions does not result in isolation of β-lactones, only halohydrins and dichloro compounds result, depending upon the conditions.[79,80,81,82]

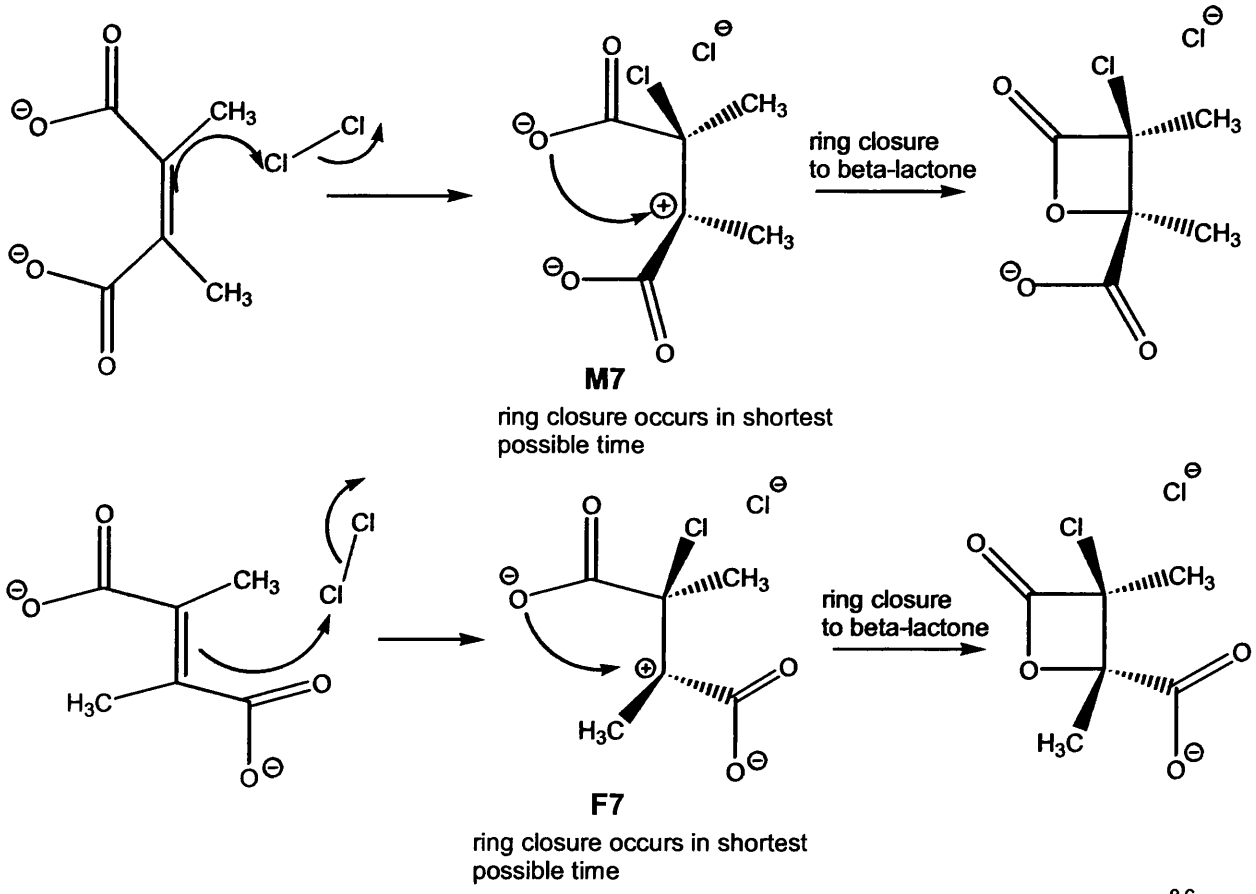

Fig. 86. Single step mechanism proposed by Tarbell and Bartlett.[86]

Tarbell and Bartlett explained their results by invoking a short lived anionic zwitterion intermediate where the halo-β-lactone formed directly from ring closure of the zwitterion, in the shortest possible time. The structure of the isolated halo-β-lactones was assigned based on this

mechanism proposed by Tarbell and Bartlett. However, the isolated crude and purified recrystallised products do not have stereochemistry as proposed by Tarbell and Bartlett.

The proposal of Roberts and Kimball invokes cyclic bromonium ion intermediates that would undergo ring closure to yield bromo-β-lactones in a simple step. The bromo-β-lactones isolated however, cannot form from a simple 4-*Endo-Tet* ring closure on the initial cyclic bromonium ions formed from the reactants dianions; this would yield stereochemistry opposite to that obtained experimentally. The proposal of Roberts and Kimball suggest that computational calculations should start with the modelling of cyclic halonium ions. This would provide a starting point for the construction of a PES relating to the known end-point, bromo-β-lactones, to the reactant unsaturated acid dianions.

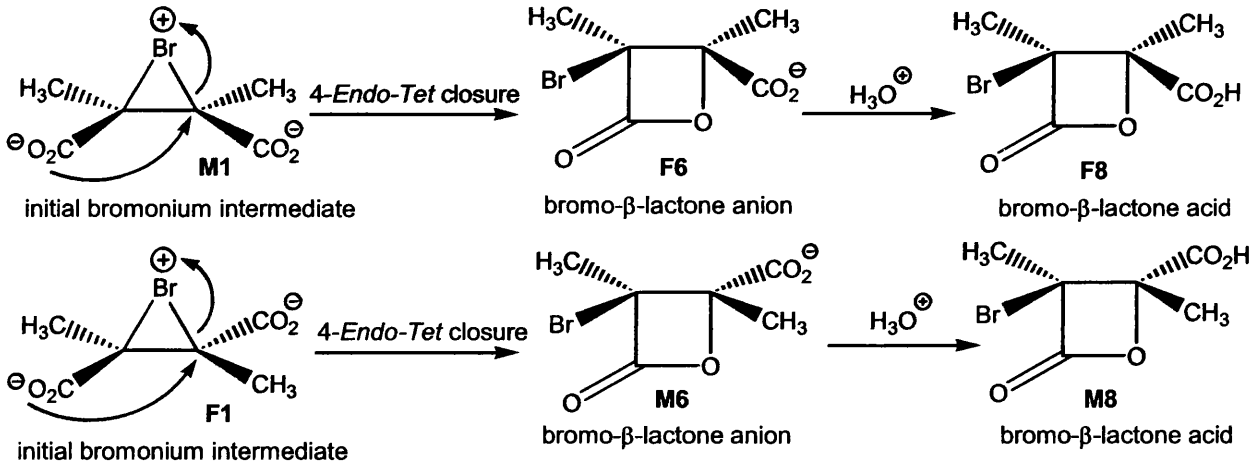

Fig. 87. Roberts and Kimball proposed that 4-*Endo-Tet* ring closure would lead to β-lactones.[61]

Alternative 3-*Exo-Tet* ring closure of the carboxyl group on the cyclic bromonium ions will give rise however to α-lactones, as proposed in this thesis.[91] The α-lactones were not isolated so a conformational change and subsequent 4-*Exo-Tet* ring closure would have to occur to result in bromo-β-lactones that correspond to the isolated products. The potential involvement of open chain zwitterions as suggested by Tarbell and

Bartlett must be examined carefully as the potential for hydrolysis and/or rotation about C-C single bonds may not be reconciled with experimental results; the reactions are stereospecific.

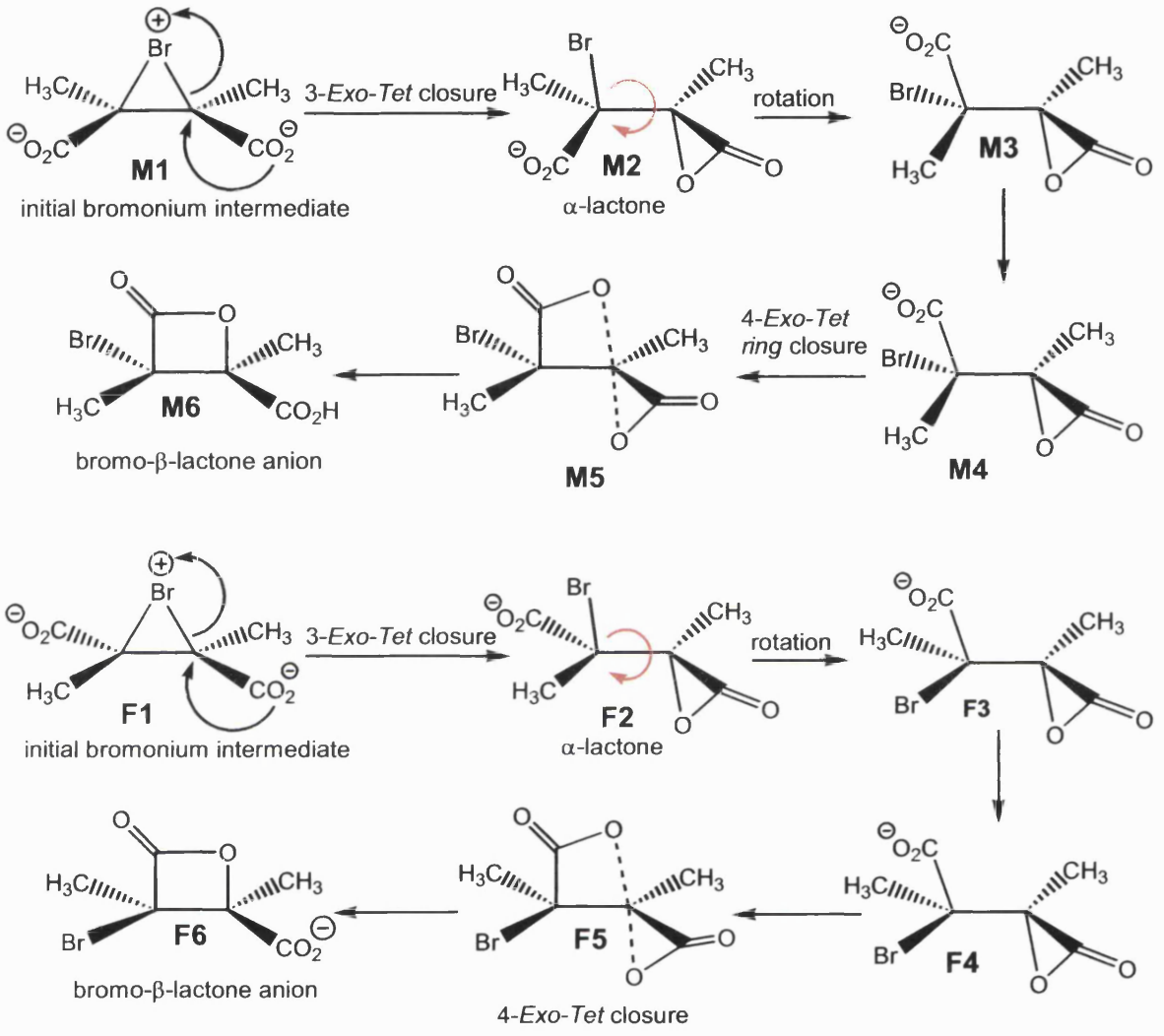

Fig. 88. α-lactone mechanism proposed in this thesis.[91]

The mechanism presented in figure 88, as proposed in this thesis, does not propose zwitterionic intermediates at any stage. A criticism of the above reaction PES scheme is that there is no connection to the reactant dianions and molecular bromine. In water and low bromine concentration, the dominant kinetic expression relates to Ad_E2 mechanism, cf. figure 51.

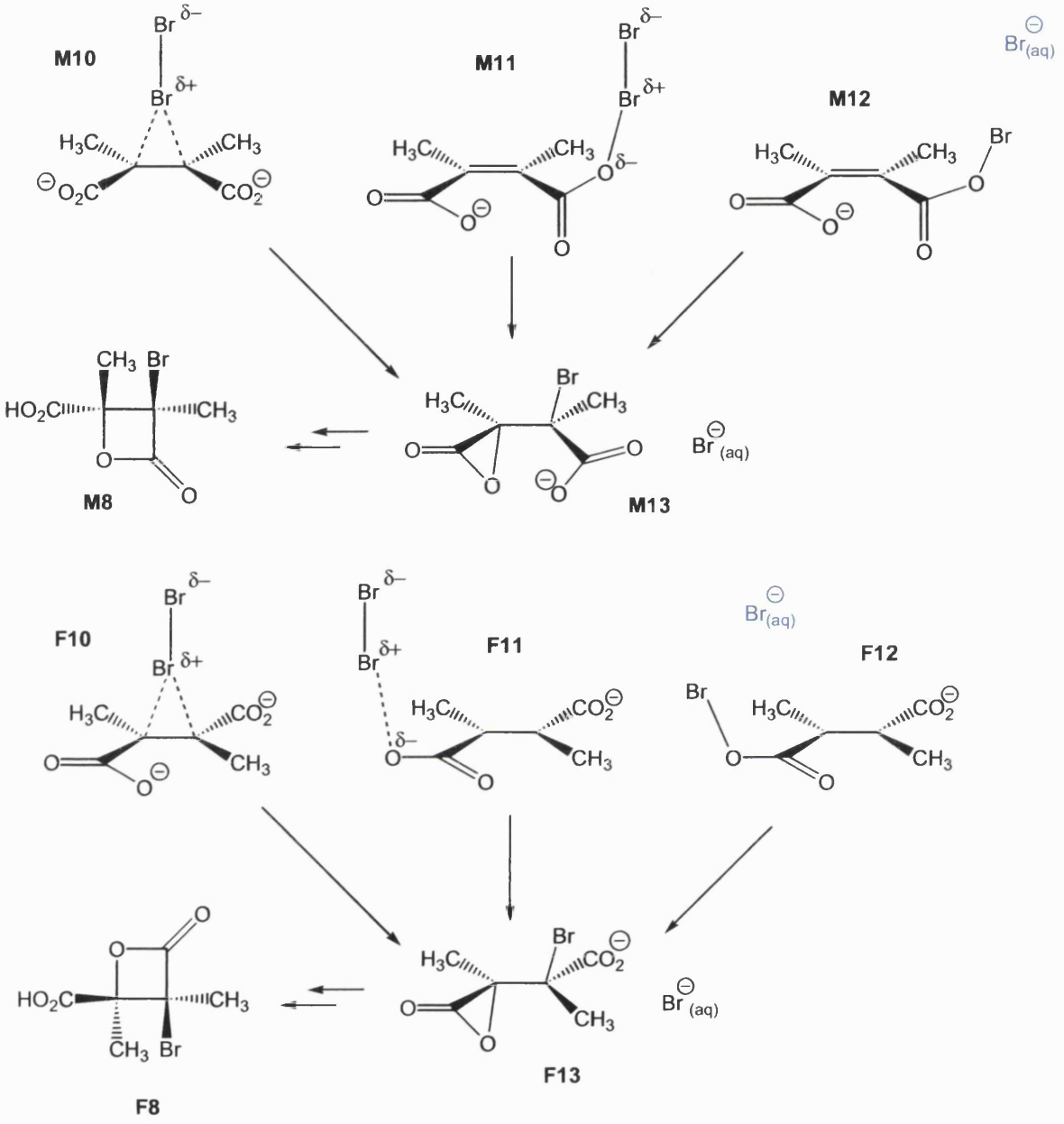

Fig. 89. Potential bromine-dianion complexes

The formation of cyclic bromonium ions in aqueous solutions, without initial concentrations of bromide ions may form from Ad_E2 mechanism, where the reaction rate would be expressed as $k_1[M0][Br_2]$ and $k_1[F0][Br_2]$. Atkinson and Bell have also suggested that the higher energy bromonium ion mechanism, the intermediate being $[RBr^+]$, predominates in the bromination of simple alkenes and intermediates that may give rise to α,β addition products, whereas the intermediate is

[RBr_2], predominates for reactions such as the bromination of diethyl fumarate.[83,159]

The possibility that some bromine dissociation will facilitate a small concentration of bromide ions and allow Ad_E3 mechanism to operate cannot be discounted. As bromine hardly dissociates in water, bromine molecules will have to be modelled to attack M0 and F0, as in Ad_E2 mechanism of bromination and the potential bromine-dianion complexes optimised.[160] Modelling interactions with bromine molecules will also test the proposal of Weiss.[83,84]

The bromination reaction is stereospecific; a similar mechanism is operating in both reactions, for 2,3-dimethylmaleate and 2,3-dimethylfumarate dianion aqueous bromination. The proposal that the α-lactones 2S(R)-bromo-2(2-methyl-3R(S)-oxiranyl)-propionate, M2, and 2R(S)-bromo-2(2-methyl-3R(S)-oxiranyl)-propionate, F2, are short-lived intermediates in water at ambient temperature is not a novel proposal.[29,31,33,42,43,45,46,47,58,59] The novel proposal is that hydrolysis and/or addition does not occur to yield *syn* addition products, such as bromohydrins or dibromoadducts, the α-lactones are stable enough to undergo a conformational change to facilitate 4-*Exo-Tet* ring closure to bromo-β-lactones.[91] Modelling with explicit water molecules may support the validity of such a claim, cf. figure 88, however such a calculation is not a simple undertaking, requiring considerable computational resource. Many different calculation methods and models were used to derive the reaction PES diagrams comparing relative energies.

The following discusses the calculated results and relates the experimental result of bromo-β-lactone isolated from aqueous bromination of the reactant dianions, to calculated structures and energies. Many calculations and methodologies were tried, however the results must be reconciled with the stereospecific experimental results.

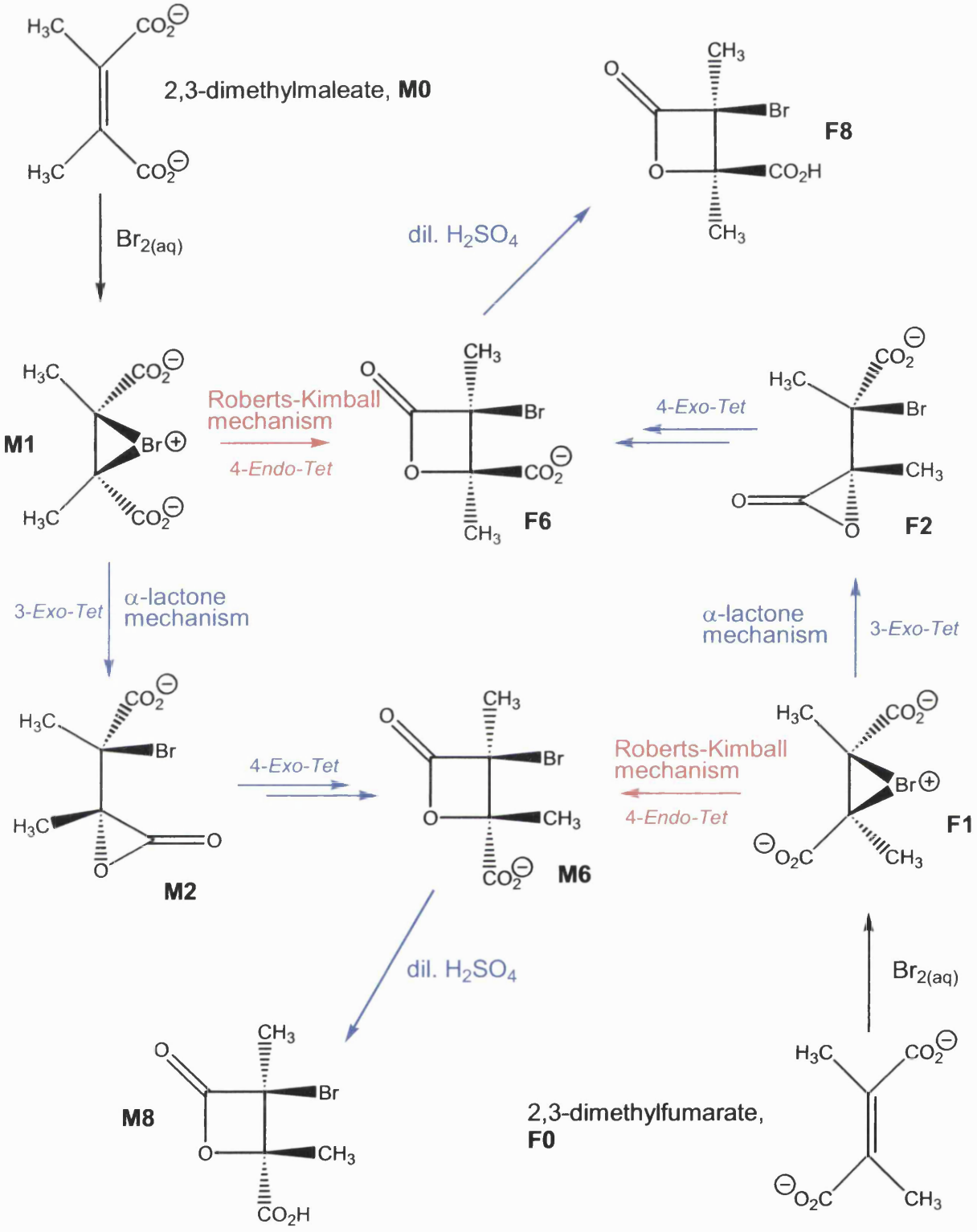

Fig. 90. Different mechanism from bromonium ions.[91]

The reaction PES from cyclic bromonium ions, calculated with PCM/B3LYP/6-31+G(d) in Gaussian 98A.6 support the mechanism proposed in this thesis.[91]

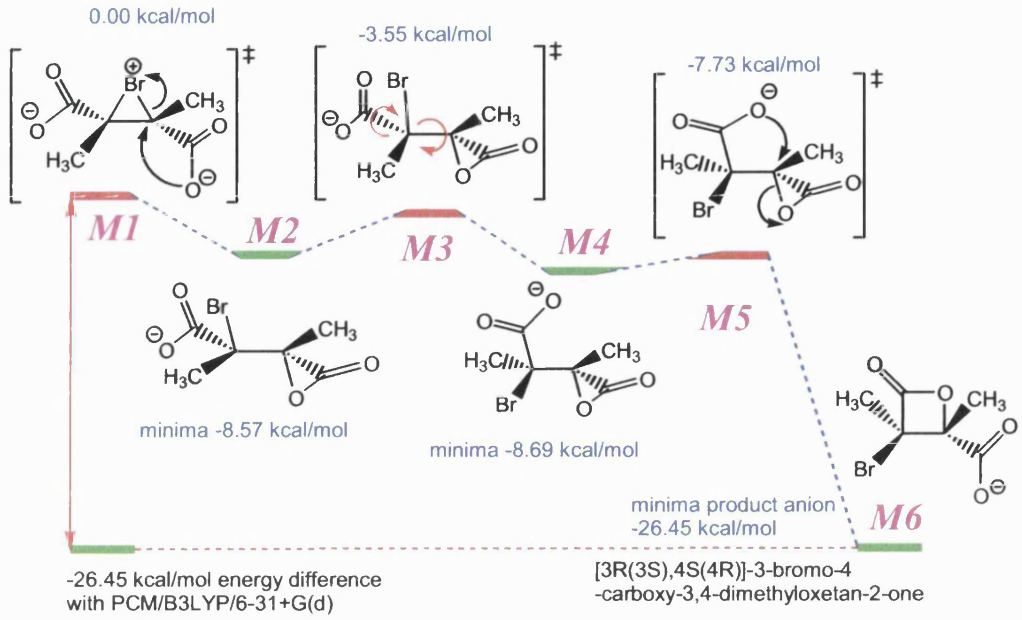

Fig. 91. PCM/rB3LYP/6-31+G(d) optimised reaction PES from M1 to M6.[91]

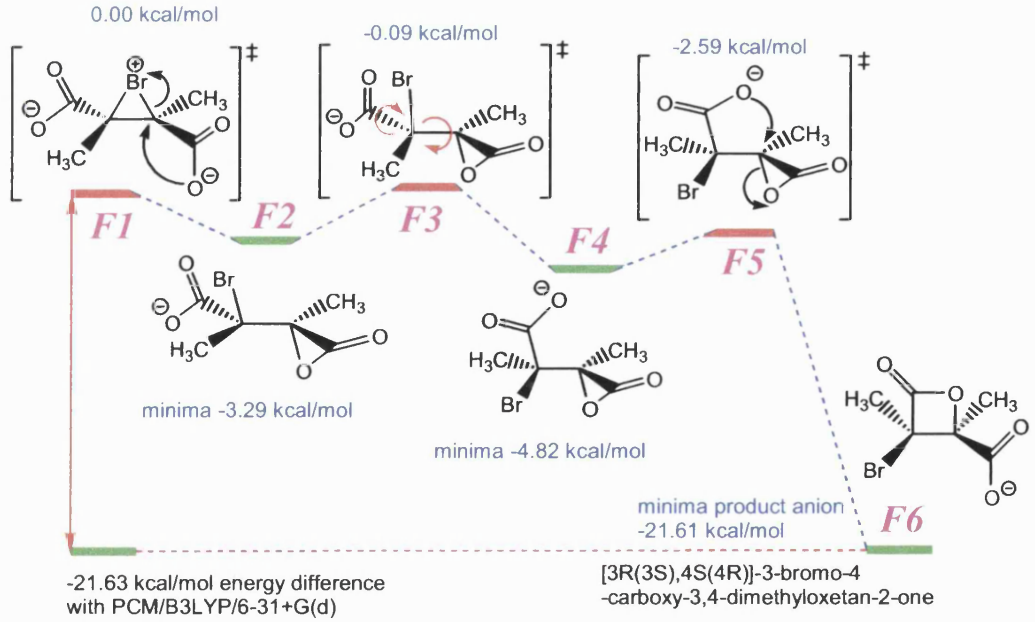

Fig. 92. PCM/B3LYP/6-31+G(d) optimised reaction PES from F1 to F6.[91]

7. Semi-empirical calculations

Initial modelling was performed with semi-empirical methods. Using AM1, in Mopac93, optimised the bromonium ions to Cs and C2 symmetrical species, for M1 and F1, in the gas phase to minimum energy species with all real vibrational modes. With Cosmo/AM1 solvation however, M1 and F1 are found to be transition states, with a single imaginary vibrational mode. Low gradient energy stationary points were found using the SIGMA algorithm. Force, IRC and optimisation calculations lead from bromonium ions M1 to a zwitterion Z1 with Cosmo/AM1 using Mopac93.

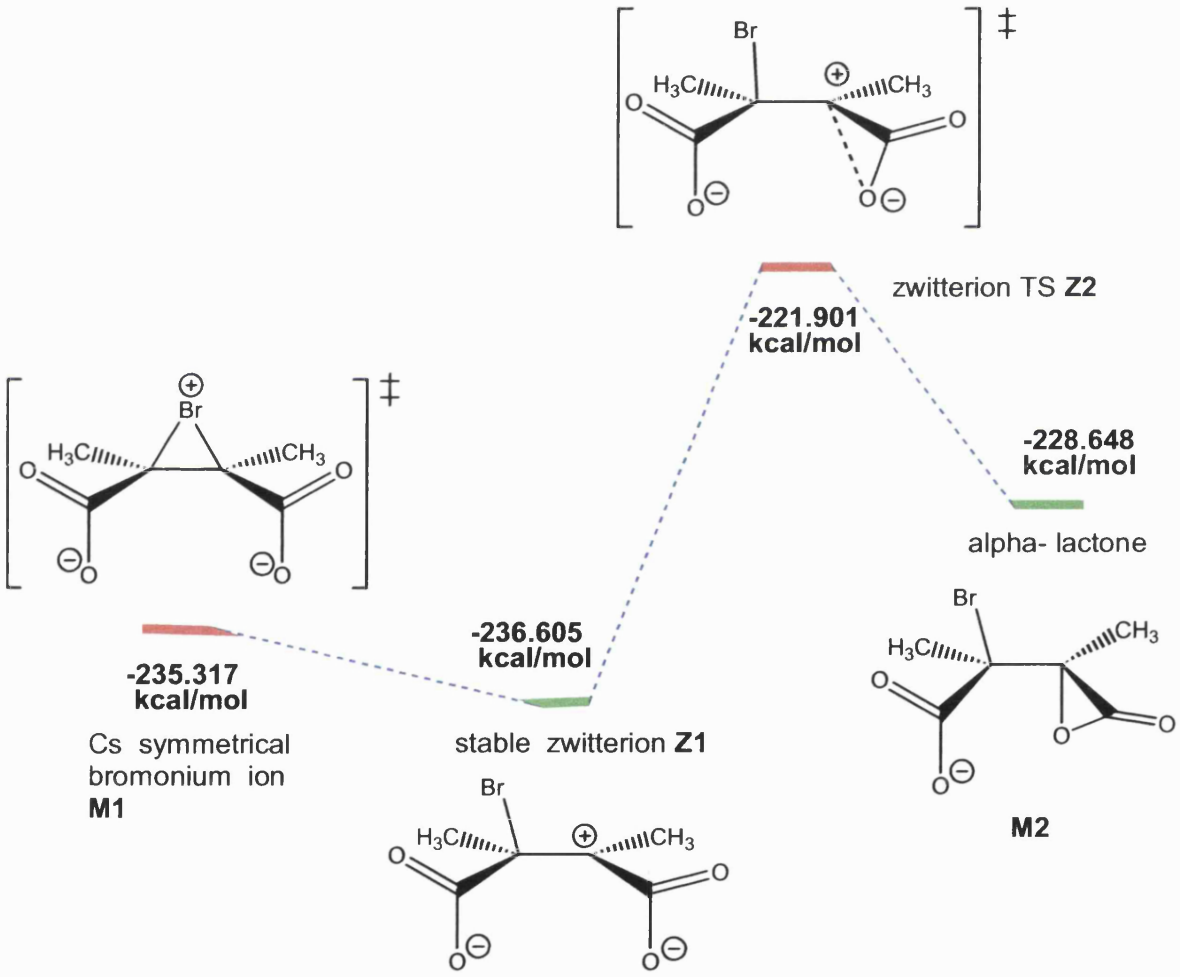

Fig. 93. Cosmo/AM1, bromonium collapse to zwitterion; M1 to Z2.

Species	H_f kcal/mol	Frequency
Bromonium M1	-235.288	31.4 *i* cm^{-1}
Zwitterion Z1	-236.605	all real
Zwitterion Z2	-221.901	460.2 *i* cm-1
α-lactone M2	-228.647	all real

Fig. 94. Cosmo/AM1 results with Mopac93, M1 to M2.

The bromonium ion F1 optimised with Cosmo/AM1 and having C2 symmetry has an optimised energy of -236.04 kcal mol^{-1} and the zwitterion from optimisation with F1 has an energy of -236.76 kcal mol^{-1}.

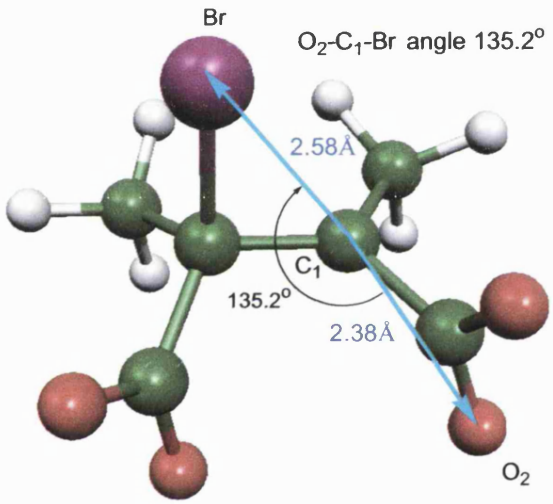

Fig. 95. Zwitterion Z1 from M1 from Cosmo/AM1 calculation.

The reaction is stereospecific and the results from Cosmo/AM1 calculations are not consistent with experimental results. The Cosmo/AM1 calculations suggest that zwitterions will form from bromination. The zwitterions will be susceptible to hydrolysis to yield bromohydrins or even potentially dibromoadducts. The aqueous

bromination of the reactant dianions are stereospecific, a zwitterionic intermediate cannot be reconciled with experimental results.

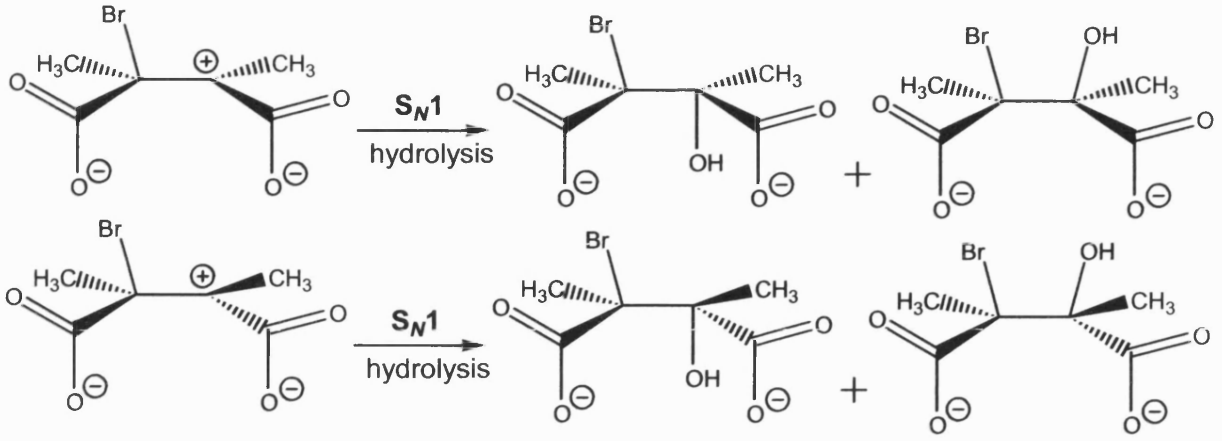

Fig. 96. S_N1 hydrolysis of zwitterions would yield bromohydrins

The conformational energy plot refers to the energy of the zwitterion against dihedral angle of the two methyl groups with respect to each other, by rotation about the central the C-C bond. The carboxyl groups were able to rotate too, albeit with constrained C-CO_2^- bond lengths and fixed O-C-O angles.

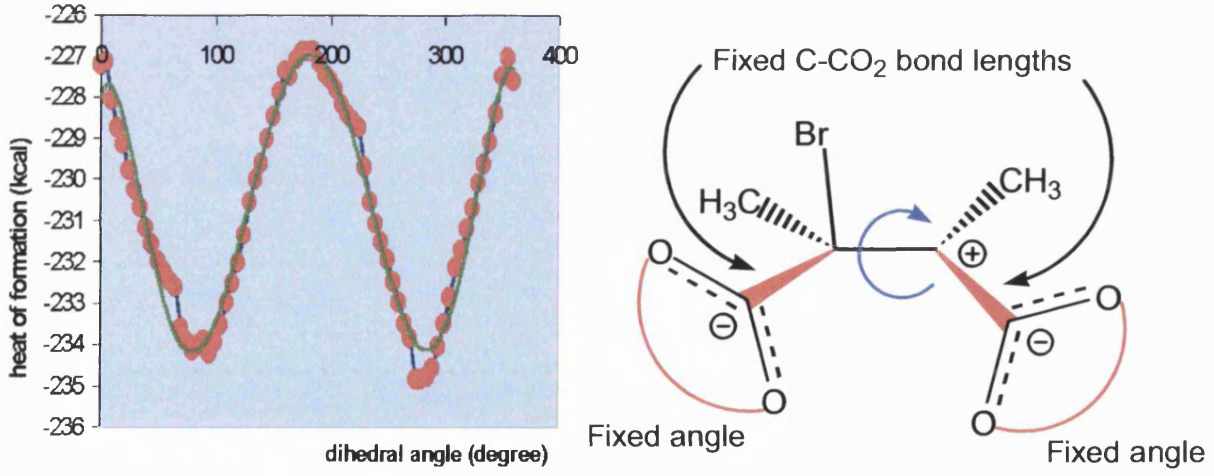

Fig. 97. Constrained zwitterion PES around central C-C bond.

The lowest energy structure was selected and constraints removed and reoptimised with Cosmo/AM1 to result in an optimised zwitterion Z3.

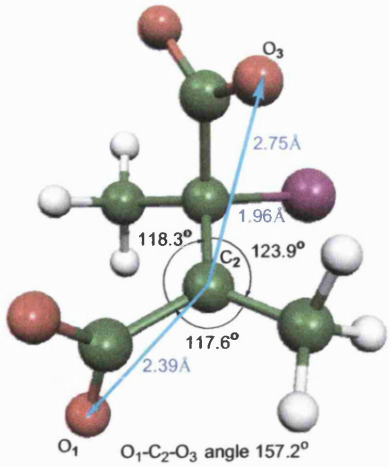

Fig. 98. Structure of the lowest energy zwitterion, Z3, from Cosmo/AM1 calculation. E =-236.677 kcal mol^{-1}.

The zwitterion Z3 has the lowest energy of an optimised zwitterion calculated with Cosmo/AM1. In figure 98 the C-Br length is 1.96Å and three bonds around carbon C_2 are nearly trigonal planar. The barrier for rotation about the central C-C bond of the zwitterion, albeit constrained, is calculated to be ~7 kcal mol^{-1}, whereas the barrier to α-lactone formation is ~14.7 kcal mol^{-1}. As the barrier to α-lactone formation is suggested to be relatively high, hydrolysis may be preferable to α-lactone formation is suggested by Cosmo/AM1 calculation.

The proposed mechanism for the relaxation of bromonium ions to α-lactones and finally to β-lactones does not involve explicit water molecules. To further test ideas, gas-phase optimisations with PM5 were performed to simply assess the energetics, in the absence of Cosmo solvation for implicit aqueous solvation, for the proposed mechanism shown in figure 88.[149]

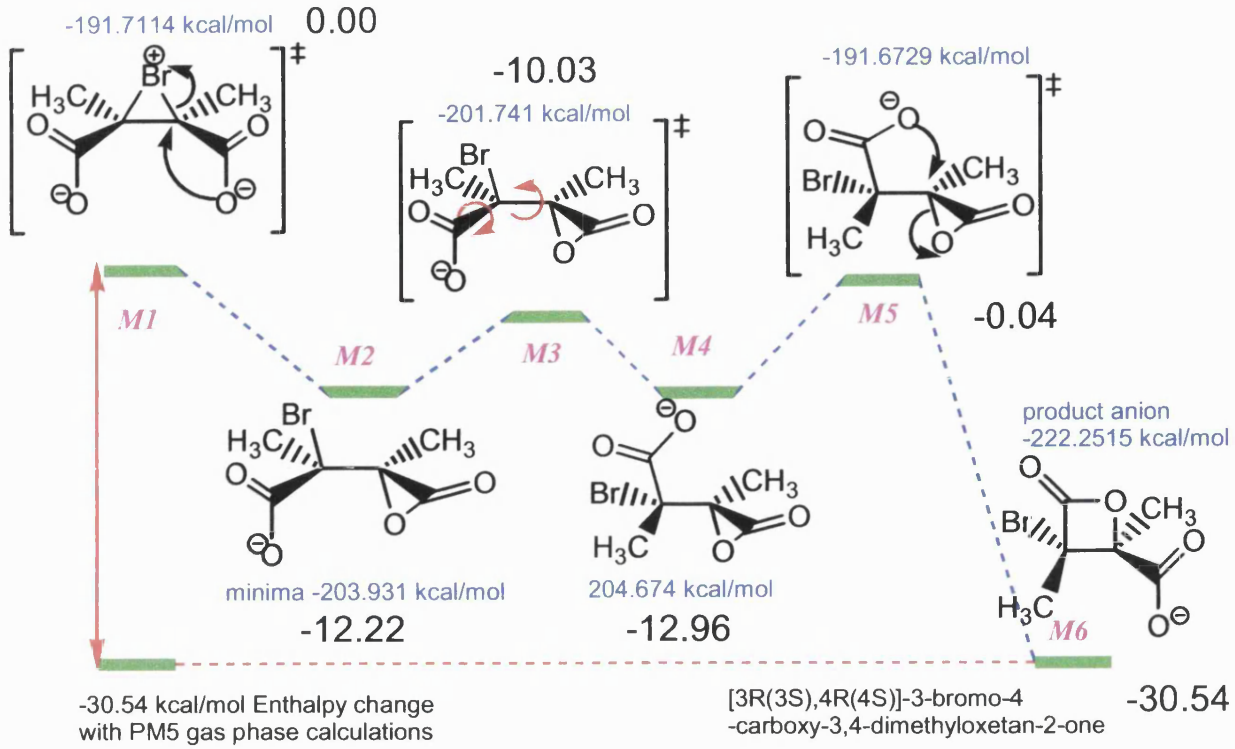

Fig. 99. PES from PM5 gas phase calculation to provide indication of energetic scheme.

The bromonium ion M1 was calculated to be a transition state in the gas phase with PM5, in contrast to the gas phase AM1 calculation, with heat of formation of –191.71 kcal mol^{-1}. The difference in energy between M1 and M2, with PM5 and with no implicit solvation is -12.22 kcal mol^{-1}. The gas phase PM5 potential energy surface of the α-lactones, M2, M3 and M4 indicate that M2 is higher in energy compared to M4, only by 0.73 kcal mol^{-1}. The gas phase PM5 calculations did not result in stable zwitterions at any stage.

The PM5 gas phase results provided starting coordinates for calculations performed with *ab initio* and hybrid DFT methods. The Cosmo/AM1 calculation results do mean that modelling solvation energetics is crucial when considering relative energies and constructive a reaction PES.

8. *Ab initio* and hybrid DFT calculation results

8.1 *Ab-initio* and DFT considerations

Hartree-Fock, DFT or even hybrid DFT, such as B3LYP calculations were alternatives that would not be too computationally demanding considering the computational resource available. To compare rB3LYP/6-31+G(d) calculations with Cosmo/AM1 results, the cyclic bromonium ions were modelled and α-lactones resulted, not zwitterions.

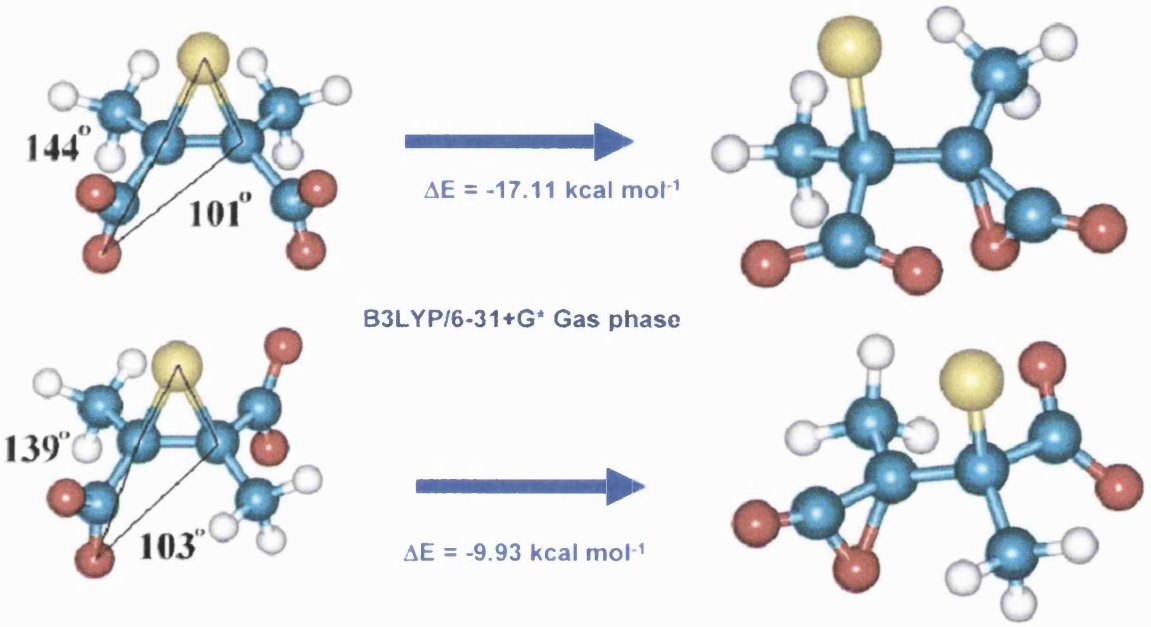

Fig. 100. Gas-phase rB3LYP/6-31+G(d) calculations for collapse of bromonium ions M1 and F1 to M2 and F2.[161]

The angles of attack of potential 3-*Exo-Tet* and 4-*Endo-Tet* attack are shown in figure 100 for the gas phase bromonium ion M1. However, gas phase calculations do not model the effects of solvated reactions, so the PCM implicit solvation model was used to model aqueous solvation in the *ab-initio* calculations conducted. M1 and F1 were optimised with PCM/B3LYP/6-31+G(d) and the resultant wave function tested with a stable calculation and no errors were reported. Gas phase HF/6-31+G(d) calculations gave similar results as shown in figure 100.

8.2 bromo-2,3-dimethylmaleate and bromo-2,3-dimethylfumarate

Calculations have shown that M1 and F1 are transition states that spontaneously relax to α-lactones, M2 and F2 by 3-*Exo-Tet* ring closure. To form the bromo-β-lactones with the experimentally observed stereochemistry, conformational change and must occur to facilitate 4-*Exo-Tet* ring closure. Both ring closure processes, 3-*Exo-Tet* and 4-*Exo-Tet*, are favourable in accordance with ring closure rules reported by Baldwin. Careful calculations with PCM/rB3LYP/6-31+G(d) allow optimisation of the following structures, facilitating the construction of a reaction PES from cyclic bromonium ions through to bromo-β-lactone anions.

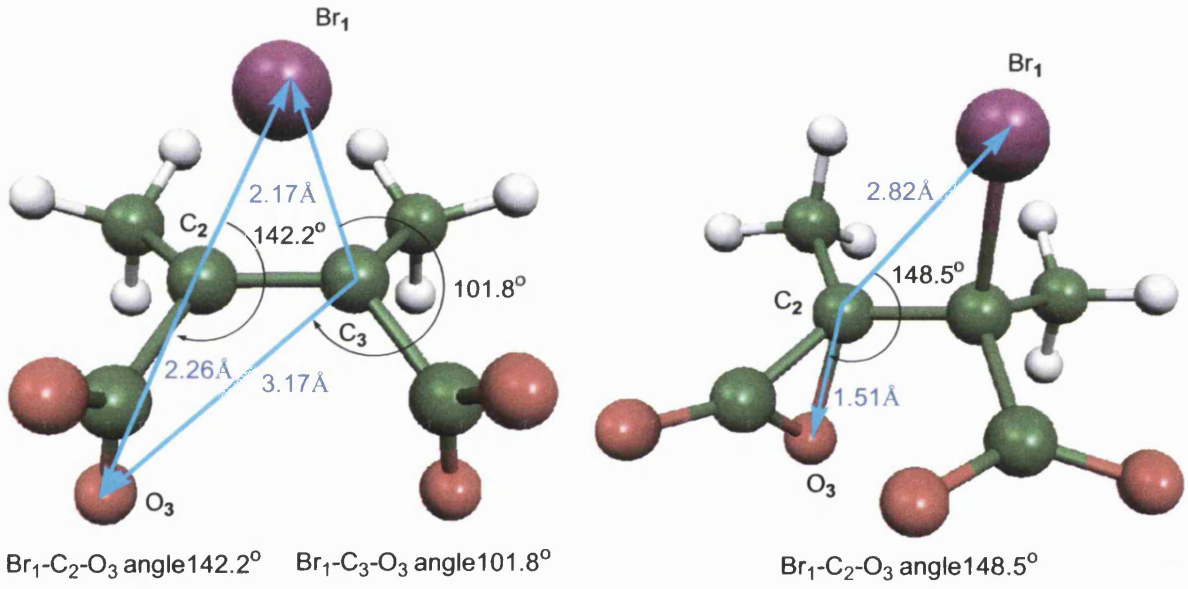

Fig. 101. M1 and M2 as optimised with PCM/B3LYP/6-31+G(d).

Animation of the single imaginary vibrational frequency of M1 indicates perturbation towards an asymmetric bromonium ion with lengthening of the C-Br bond corresponding with shortening of the C-O bond. IRC following the imaginary eigenvector and optimisation using GDIIS algorithm leads to the α-lactone M2. M4 was optimised and use in conjunction with M2 to find M3 from a QTS2 optimisation. M5 was also

found from PCM/HF/3-21G* scans by lengthening C_2-O_5, cf. figure 104 from M6.

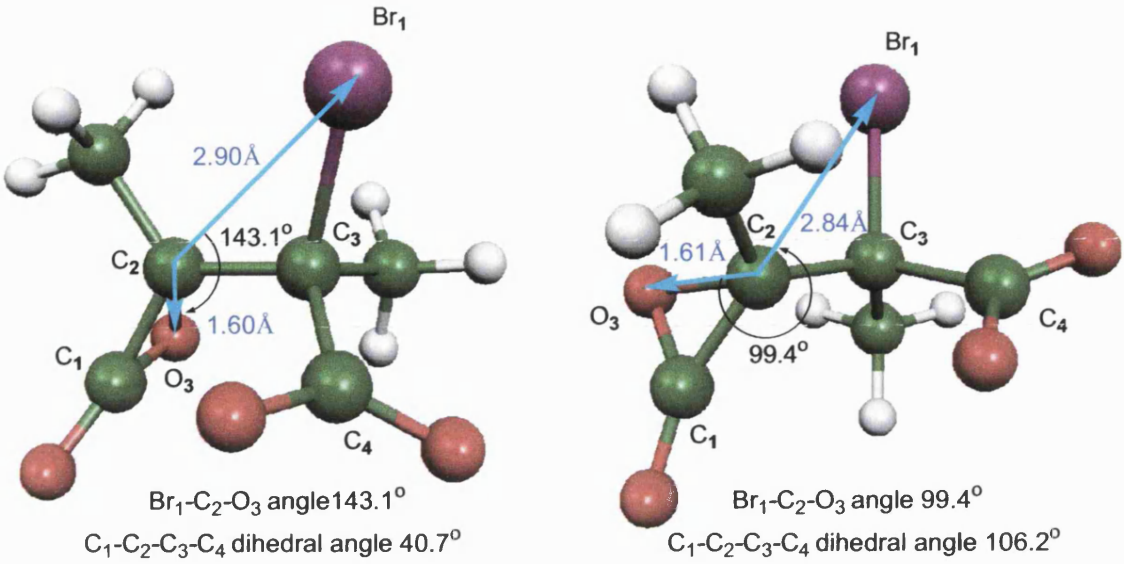

Fig. 102. M3 and M4 as optimised with PCM/B3LYP/6-31+G(d).

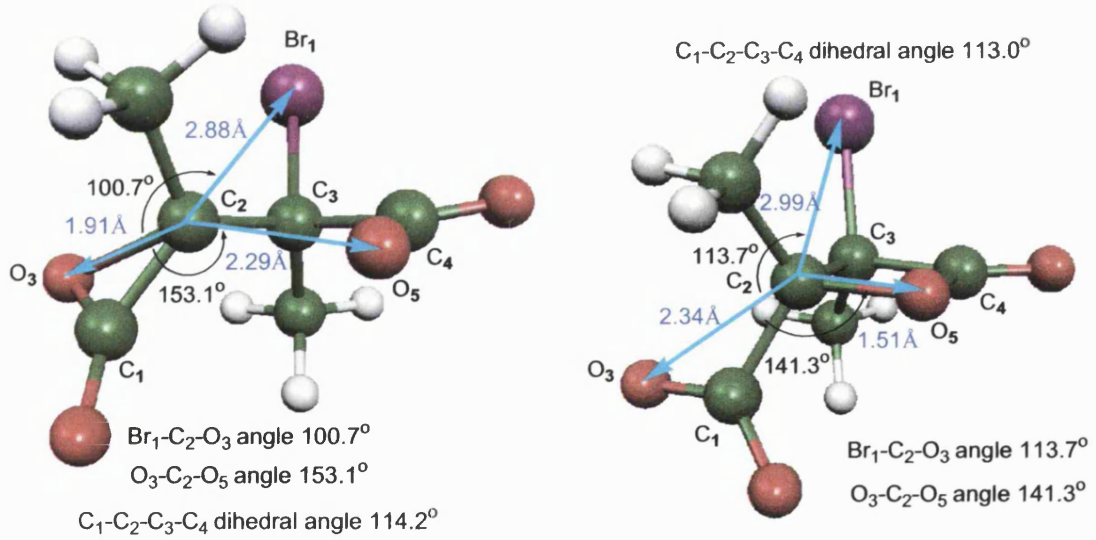

Fig. 103. M5 and M6 as optimised with PCM/B3LYP/6-31+G(d).

The structure M5 was also optimised from a QST2 calculation from M1 and M6 in an attempt to model the 4-*Exo-Tet* ring closure. An interesting feature is that C_2-O_3 bond length increases from m2 to M5. Using the optimised structures above, the reaction PES is shown below.

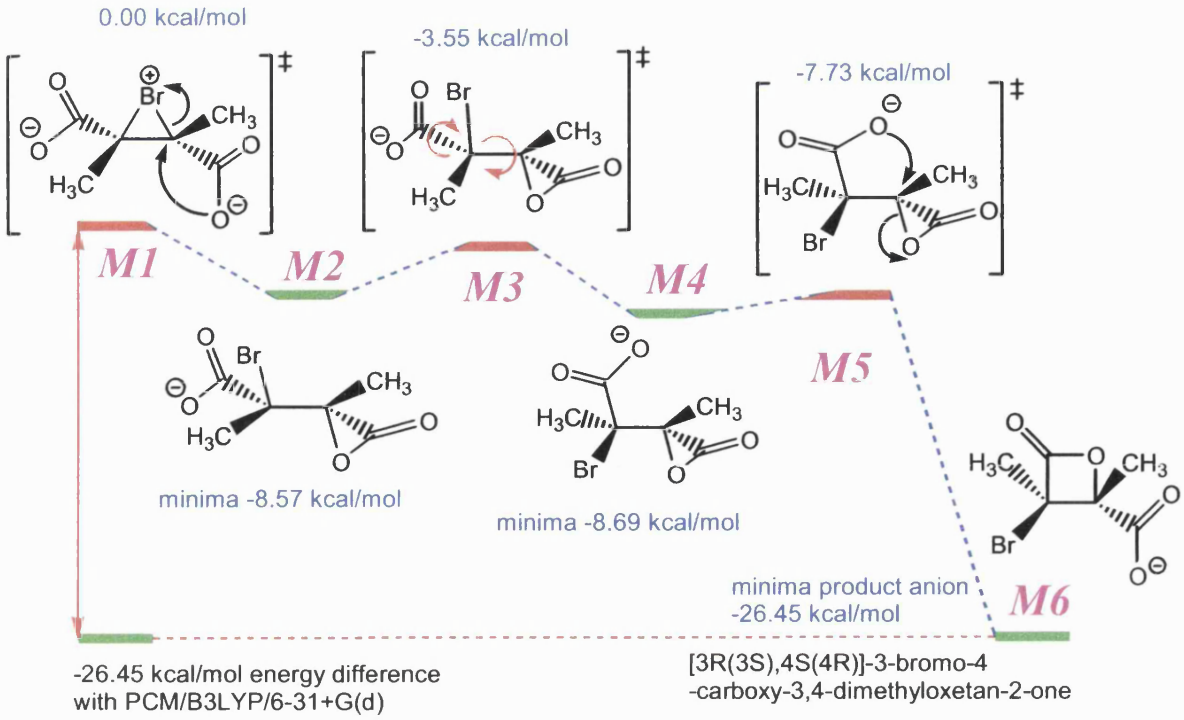

Fig. 104. PCM/rB3LYP/6-31+G(d) optimised reaction PES from M1 to M6.

Similar calculations with 2,3-dimethylfumarate series optimised the following structures with PCM/rB3LYP/6-31+G(d).

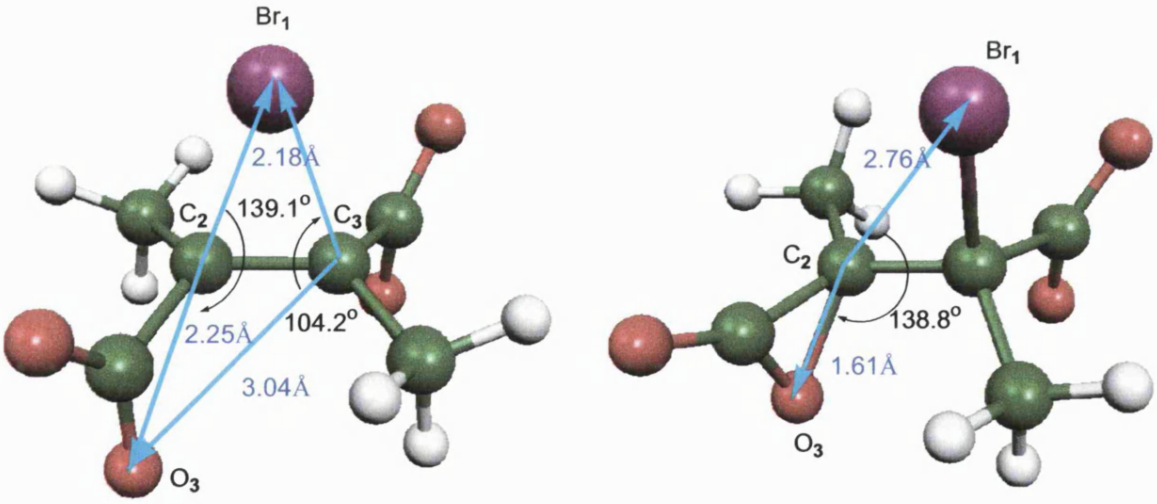

Fig. 105. F1 and F2 as optimised with PCM/B3LYP/6-31+G(d).

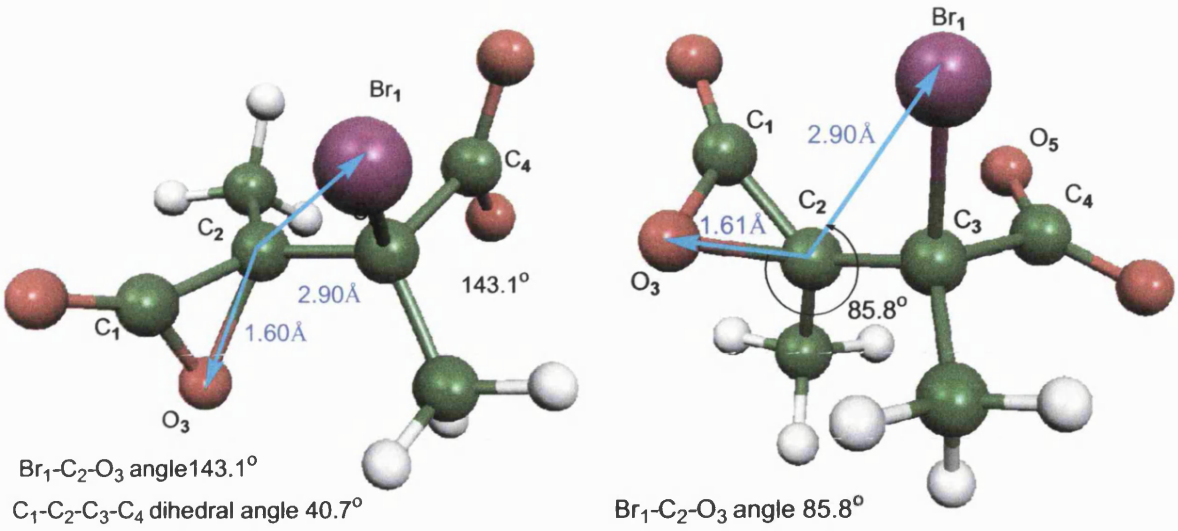

Fig. 106. F3 and F4 as optimised with PCM/B3LYP/6-31+G(d).

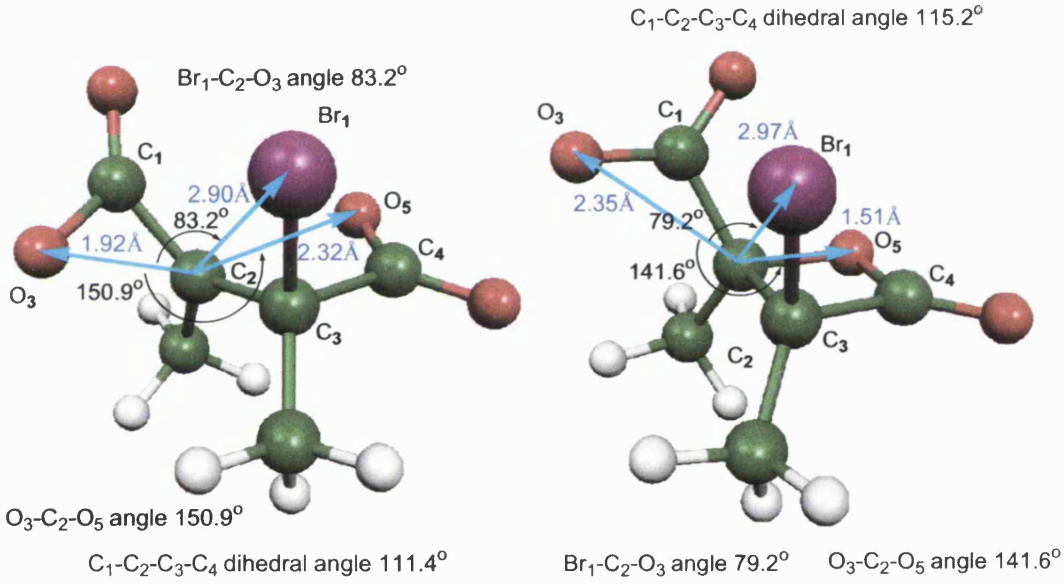

Fig. 107. F5 and F6 as optimised with PCM/B3LYP/6-31+G(d).

Using the optimised structures above, the reaction PES is shown below.

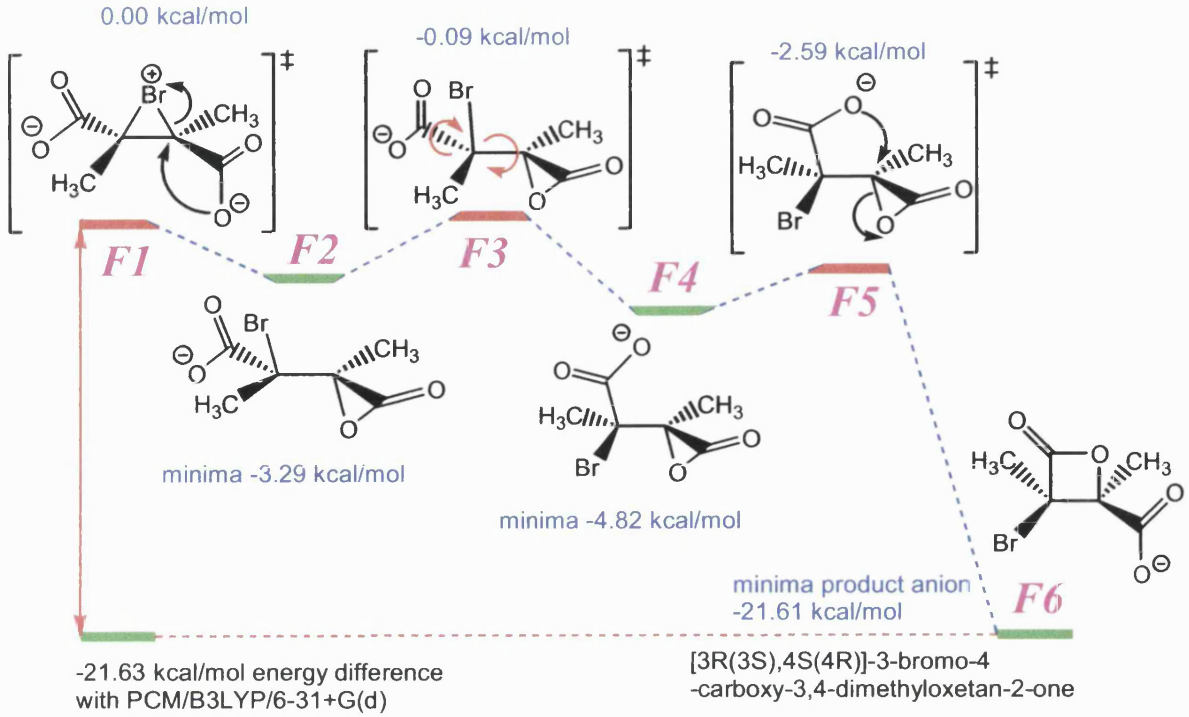

Fig. 108. PCM/B3LYP/6-31+G(d) optimised species, F1-F6, relative energy scheme.

Cartesian coordinates, in Ångströms are shown in Appendix1 on page 189. All the following results were calculated with Gaussian98A.6, on SGI irix 6.5 workstation, at Bath University, unless otherwise stated. Energies reported are total free energies in solution with non-electrostatic terms in a.u. (E in PCM). For TS, first-order saddle points, structures the single imaginary frequency is reported as a wave-number, minima structures were confirmed by possessing all real vibrations and are assigned as such. These results are from frequency calculations performed on fully optimised structures that had 4 YES optimisation flags from Gaussian98A.6 using default values of 0.000450 for Maximum Force, 0.000300 for RMS Force, 0.001800 for Maximum displacement and 0.001200 for RMS displacement. SCF energy convergences were set to *very-tight* with *maxcycle* specified to be 999 for structure optimisations and frequency calculations. Default values for SCRF PCM and CPCM continuum solvation calculations were used throughout to ensure energy comparisons with other calculations without having to

apply corrections for different PCM parameters. No temperature inputs were specified in the Gaussian input files so data reported is for default temperature of 298K.

Structures	E in PCM (a.u.)	Frequency	G=H-TS (a.u)	ZPE (kcal mol^{-1})
M1 bromonium TS	-3105.0223968	200.69 *i*cm^{-1}	-3104.947707	70.62459
M2 α-lactone	-3105.0360526	all real	-3104.959316	71.95104
M3 α-lactone TS	-3105.0280575	62.18 *i*cm^{-1}	-3104.950020	71.92530
M4 α-lactone	-3105.0362382	all real	-3104.963395	71.50831
M5 α/β-lactone TS	-3105.0347123	264.17 *i*cm^{-1}	-3104.959990	71.05860
M6 β-lactone	-3105.0645417	112.68 *i*cm^{-1}	-3104.985429	72.80950
M7 zwitterion TS	-3105.0164911	126.42 *i*cm^{-1}	-3104.942212	70.48375
M8x β-lactone acid	-3105.4235276	*N/A*	*N/A*	*N/A*
M8 opt β-lactone acid	-3105.5132466	all real	-3105.424175	80.03213

Table 109. Results of optimised structures for 2,3-dimethylmaleate series from frequency calculations on 4 YES flag optimised structures.

Structures	E in PCM (a.u.)	Frequency	G=H-TS (a.u)	ZPE (kcal mol^{-1})
F1 bromonium TS	-3105.0299809	87.96 *i*cm^{-1}	-3104.955462	70.55081
F2 α-lactone	-3105.0352178	all real	-3104.959172	71.70332
F3 α-lactone TS	-3105.0301368	50.00 *i*cm^{-1}	-3104.953196	71.51768
F4 α-lactone	-3105.0376595	all real	-3104.962180	71.61635
F5 α/β-lactone TS	-3105.0341203	271.10 *i*cm^{-1}	-3104.959828	70.75105
F6 β-lactone	-3105.0644133	all real	-3104.986344	72.73387
F7 α-lactone TS	-3105.0343747	276.65 *i*cm^{-1}	-3104.959674	71.00655
F8x β-lactone acid	-3105.4139103	*N/A*	*N/A*	*N/A*
F8 opt β-lactone acid	-3105.5141009	all real	-3105.426355	79.96470

Table 110. Results of optimised structures for 2,3-dimethylfumarate series from frequency calculations on 4 YES flag optimised structures.

The free energy, G=H-TS, is given as the sum of electronic and thermal free energy resulting from a frequency calculation in Gaussian98A.6 performed on stationary points. The ZPE scaling factor for B3LYP/6-31G(d) ZPE is 0.9806.[163] Calculated vibrational normal modes are often overestimated too, scaling factor can be applied to correct this error. Considering the bromonium ions of 2,3-dimethylmaleate (M1) and 2,3-dimethylfumarate (F1), a similar process of 3-*Exo-Tet* ring closure will yield bromo-α-lactones M2 and F2, an act of inversion. Conformational changes of the M2 and F2 would have to occur to facilitate 4-*Exo-Tet*

ring closure to give the bromo-β-lactones M6 and F6, giving rise to another act of inversion. Hence overall retention of configuration for the formation of bromo-β-lactones for bromination of the unsaturated dianions is the net stereochemical result, as is observed experimentally. Cyclic bromonium ions have been isolated and are the first formed intermediates in attack of chlorine, bromine and iodine upon simple alkenes.[160,163]

8.3 Calculations with explicit solvation and bromine

Consideration has to be made for the fact that molecular bromine is only slightly hydrolysed in water, >99% is $Br_{2(aq)}$ and only very small amounts of $BrOH_{(aq)}$ and $HBr_{(aq)}$ is present. The equilibrium for the dissolution of bromine in water, $Br_{2(aq)} + H_2O = H^+_{(aq)} + Br^-_{(aq)} + HOBr_{(aq)}$ has equilibrium constant K_e of 7.2×10^{-9} (4.2×10^{-4} for chlorine), the equilibrium concentration of [Br^-] and [HOBr] being 1.15×10^{-3} mol L^{-1} at 25°C (0.03 mol L^{-1} for chlorine). The equilibrium concentration of bromine $Br_{2(aq)}$ is 0.21 mol L^{-1} and for chlorine $Cl_{2(aq)}$ is 0.061 mol L^{-1}. Calculations with water and bromine molecules were performed. The bromine bond length from literature is 2.28Å.[174]

The semi-empirical method PM5 implemented in CachePro6.1.1 using Mopac2002 software is also combined to an algorithm called MOZYME that uses some regression analysis to assist in solving SCF equations for larger calculations.[148] The 2,3-dimethylmaleate dianion, bromine and explicit water molecules were optimised using MMFF94 forcefield using MOE2004.05, and then optimisation with PM5/MOZYME algorithm. For the structure shown in figure 112, more water molecules were added to the starting structure shown in figure 111 and minimised with MMFF94 forcefield in MOE2004.05. Rearrangement of water molecules accounted for the majority of energy changes during optimisation.

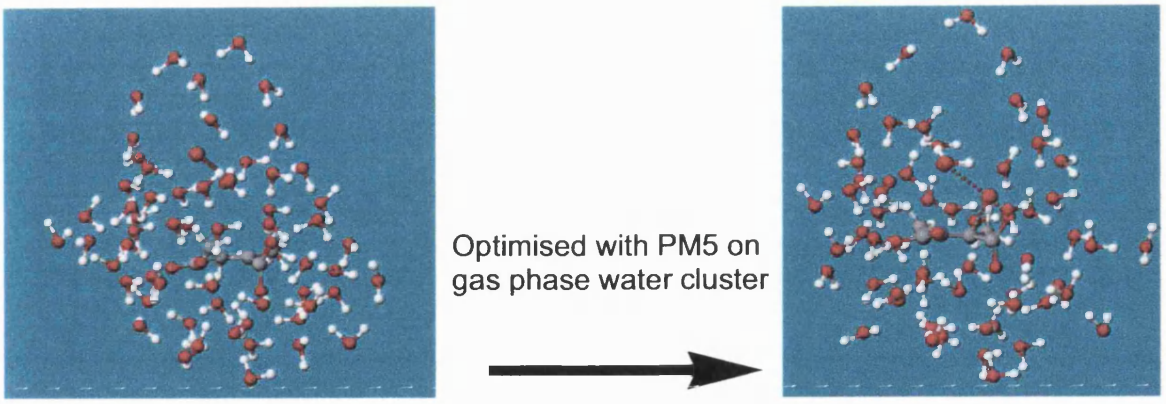

Fig. 111. From PM5 gas phase optimisation with explicit water cluster.

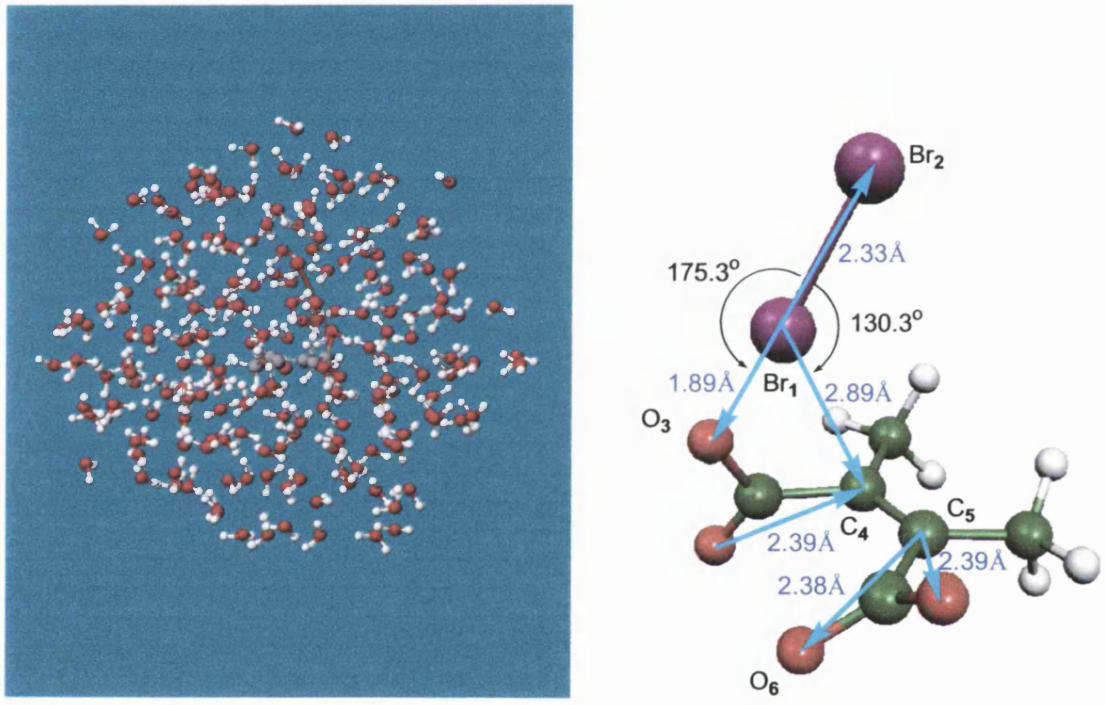

Fig. 112. PM5/MOZYME gas phase optimisation on water cluster.

In each case, the bromine molecule disrupts the carboxyl group bonding with explicit water, as shown in figure 111, a bromine-dianion complex forms with the bromine molecule being closely associated to a carboxyl group. The potential bromine-dianion complexes were modelled with PCM/B3LYP/6-31+G(d).

8.4. Electrophilic attack of bromine

Modelling the electrophilic attack of bromine, Br_2, upon the dianions produced interesting results, with PCM/B3LYP/6-31+G(d).

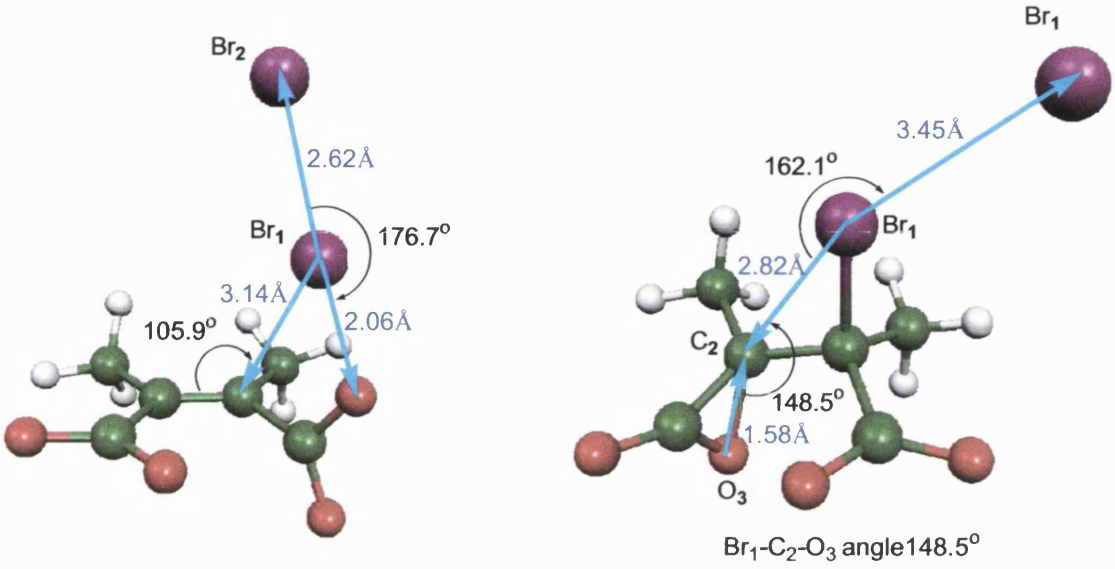

Fig. 113. Optimised geometries for M11 and α-lactone M13.

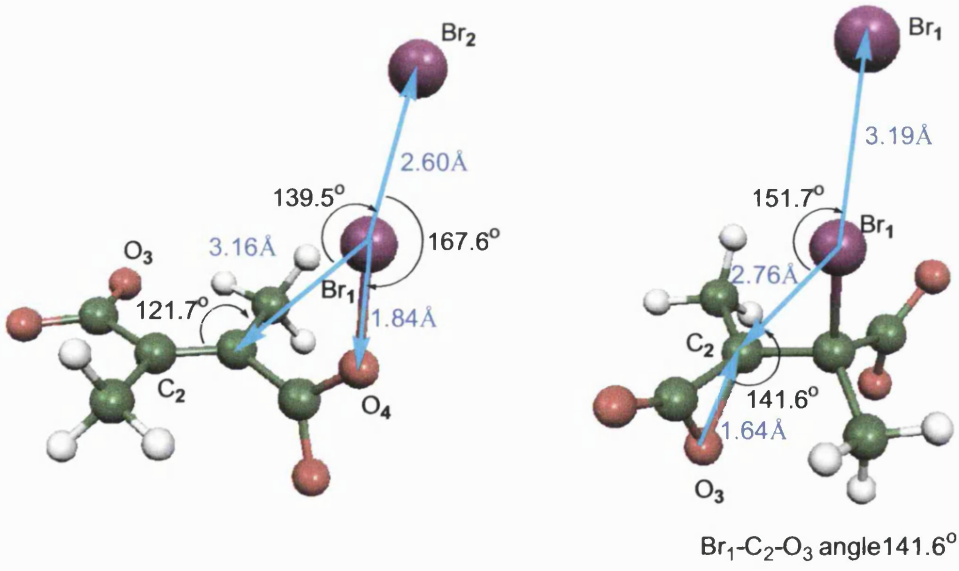

Fig. 114. Optimised geometries for F11 and α-lactone F13.

A frequency calculation on M11 indicates two imaginary vibrations, despite optimisation. Setting the furthest out peripheral bromine atom to a dummy atom X in M11 and F11, yields M12 and F12, cf. figure 118, to mimic potential solvation of the peripheral bromine atom. Performing optimisation on M12 and F12 results initially in a rotation of the free carboxyl group by 90 degrees for both structures shown in figure 113 and figure 114. As M11 will optimise to M2 and F11 did not optimise to F2, single point energies for M11 and F11 are reported when the outer bromine atom is changed to dummy atom using optimised structures for M11 and F11, having net charges of –1. A comparison with potential bromine-alkene complexes where the bromine molecules are association and the central C=C bond was made.

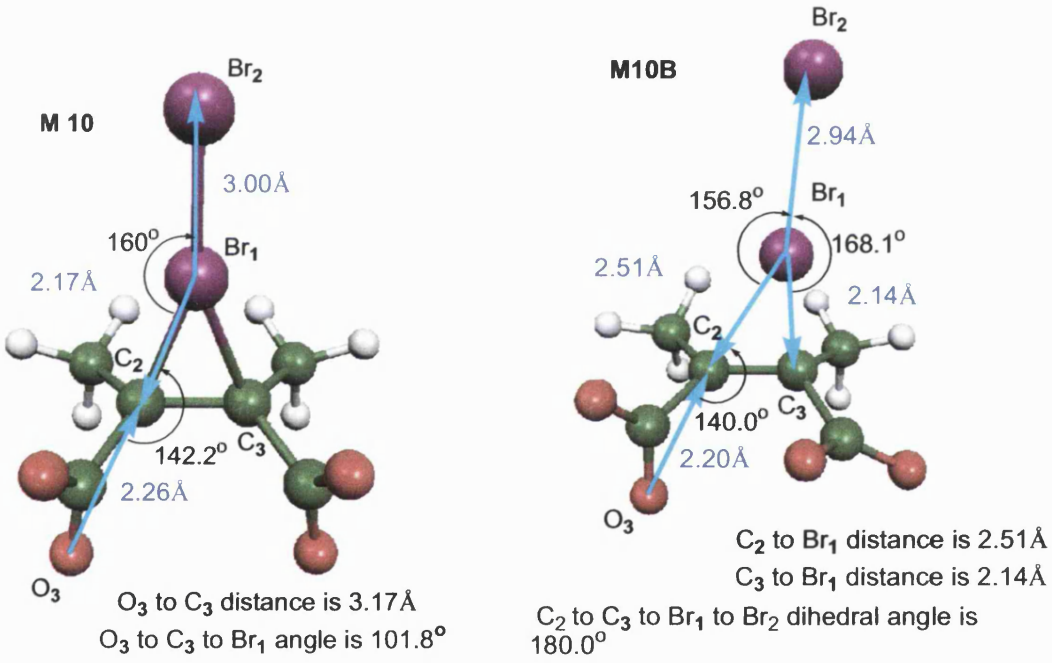

Fig. 115. Symmetrical and asymmetric bromine dianions M10 and M10B.

The structure M10 shown in figure 115, optimised with imposed Cs symmetry. The asymmetric structure M10B shown on the lhs in figure 115, was optimised with the constraint of C-C-Br-Br dihedral being set to 90° starting from M10. M10B has an energy of –5676.941072 au, lower in energy compared to the M10, but higher energy compared to M11.

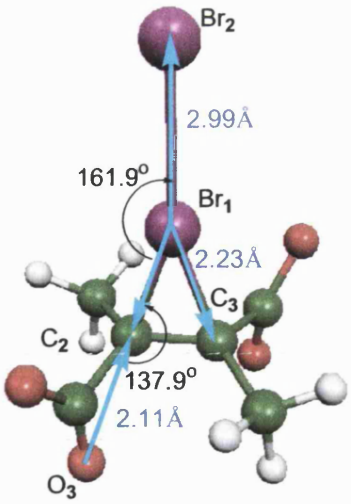

O_3 to C_3 distance is 2.82Å
O_3 to C_3 to Br_1 angle is 105.5°

Fig. 116. F10, bromine-dianion complex optimised without imposed symmetry.

For figure 113, M11 is the lowest energy bromine-dianion complex with the dianion portion having a similar structure to the optimised reactant dianion, M0 shown in figure 137. Gas phase calculation, with DGauss using BLYP/DZVP in CachePro6.1.1, of electrophilic susceptibility were performed on BLYP/DZVP optimised dianions.[149]

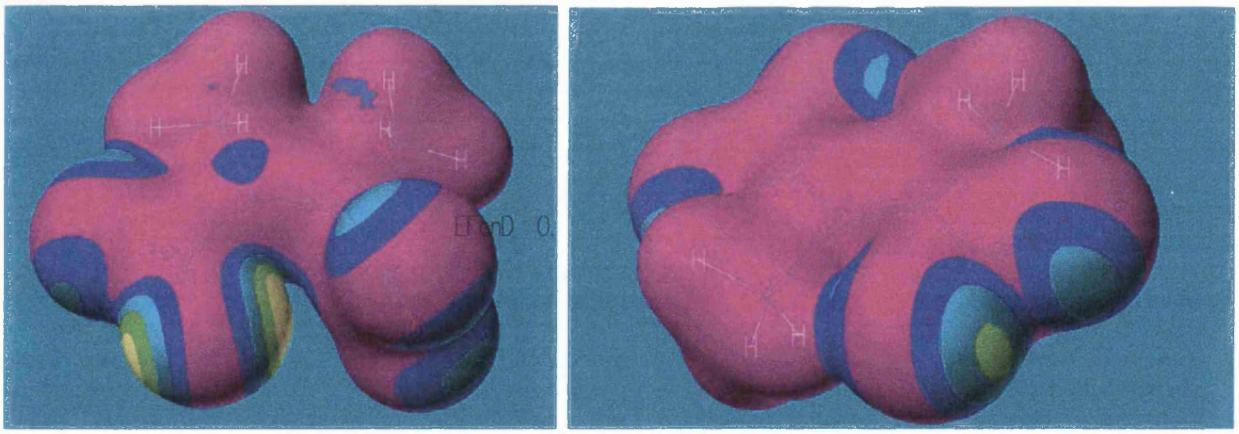

Fig. 117. The carboxyl groups have the highest electrophilicity (green/yellow) in M0(lhs) and F0(rhs).

The most susceptible area to electrophilic attack on M0 and F0 are the carboxyl groups. This is similar to the mechanism suggested by Weiss, initial electrophilic attack on the carboxyl groups.[83]

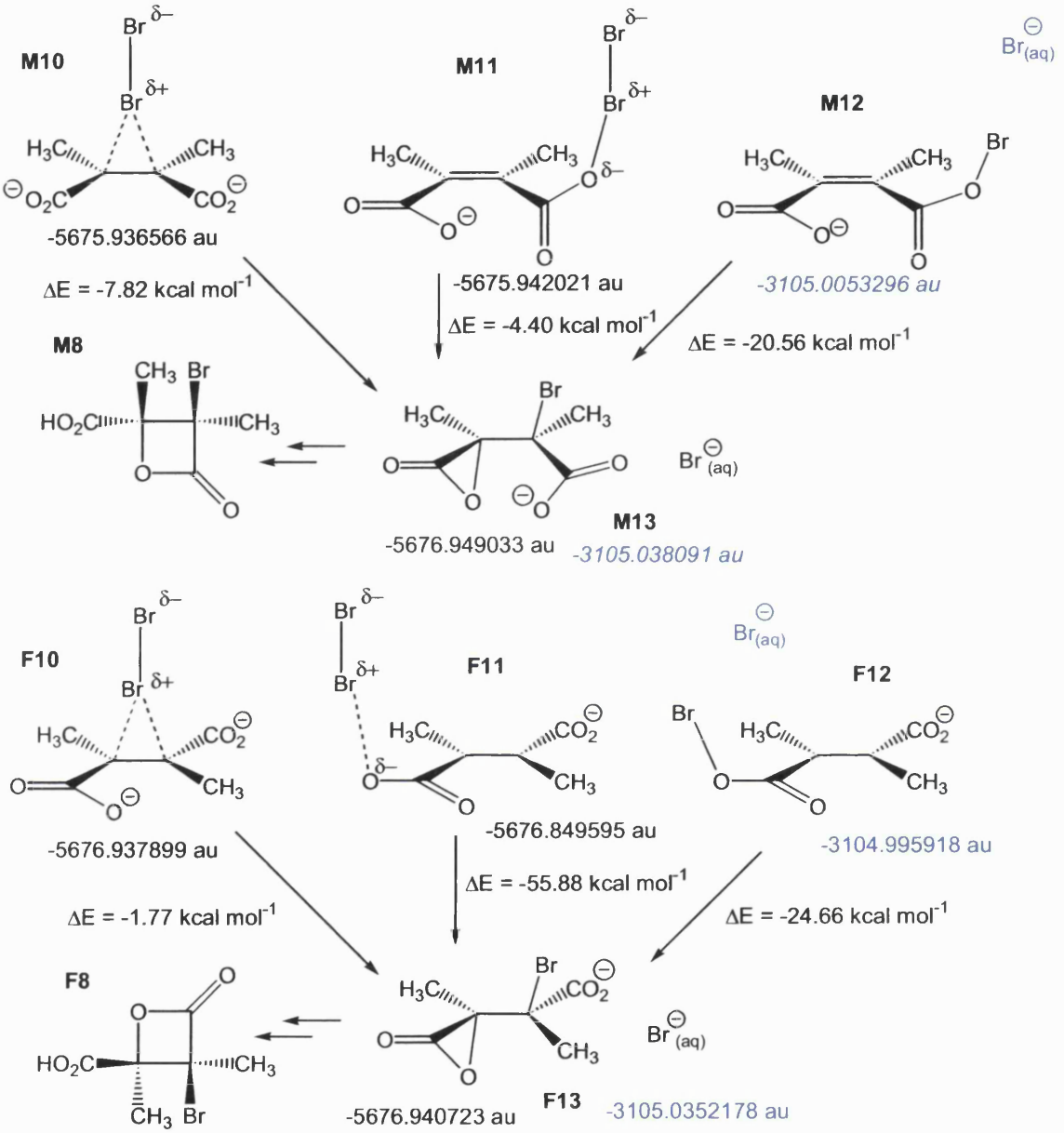

Fig. 118. Energies for bromine-dianion structures.

The calculations with Br_2 and dianions suggest that bromine attack on 2,3-dimethylmaleate dianion results in bromine-dianion complex where the bromine is coordinated towards the carboxyl groups. Potential

solvation of the peripheral bromine then facilitates collapse to M2 α-lactone. Modelling the attack of bromine on 2,3-dimethylfumarate dianion however suggests a bromine complex where the bromine molecules is coordinated towards the central carbon-carbon double bond, solvation of the peripheral bromine anion should yield the bromonium ion F1 which will collapse to F2 α-lactone.

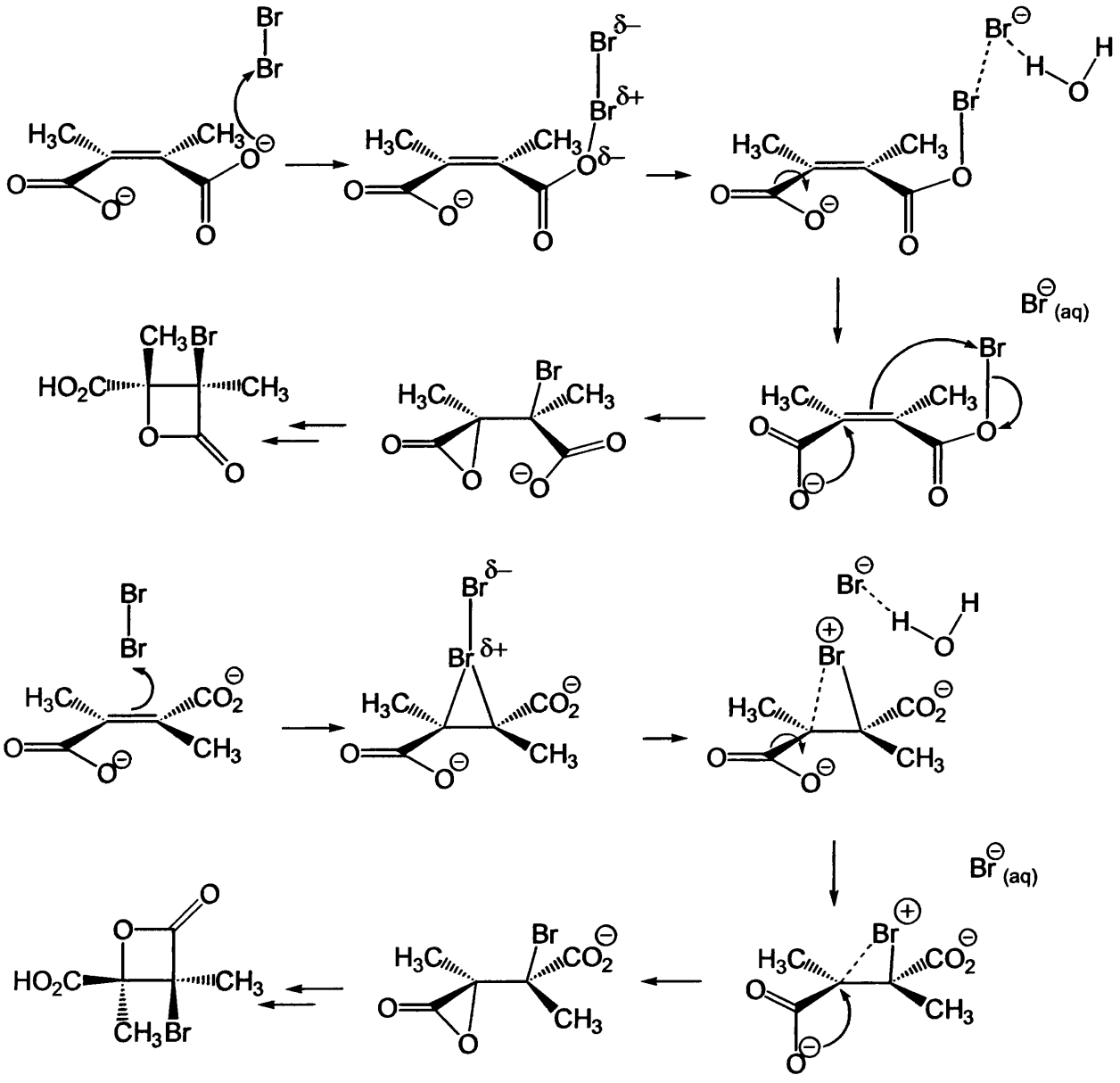

Fig. 119. Mechanism for β-lactone formation from electrophilic attack of bromine molecule.

A comparison of relative energies of models with explicit bromine and addition of $Br^-_{(aq)}$ ion may show differences. The energy of bromine anion calculated by PCM/B3LYP/6-31+G(d) is –2571.915835 au. The energy of bromine cation calculated by PCM/B3LYP/6-31+G(d) is –2571.268171 au. Bromine, $Br_{2(aq)}$ calculated by PCM/B3LYP/6-31+G(d) has a bond length of 2.321Å and an energy of –5143.425755 au.

E (a.u.) and bromine	E (a.u.) with $Br^-_{(aq)}$	Difference (kcal mol^{-1})
M10 -5675.936566	M1+Br^- -5676.938232	-628.55
M11 -5675.942021	M1+Br^- -5676.938232	-625.13
M12 -3105.0053296	M1 -3105.0223968	-10.71
M12+Br^- -5676.921165	M1+Br^- -5676.938232	-10.71
M13 -5676.949033	M2+Br^- -5676.951888	-1.79
F10 -5676.937899	F1+Br^- -5676.945816	-4.97
F11 -5676.849595	F1+Br^- -5676.945816	-60.38
F12 -3104.995918	F1 -3105.0299809	-21.37
F12+Br^- -5676.911753	F1+Br^- -5676.945816	-21.37
F13 -5676.940723	F2+Br^- -5676.951053	-6.48
M0 + Br_2 -5676.914679	M0+Br^+ -3104.757095	N/A
F0 + Br_2 -5676.913032	F0+Br^+ -3104.755448	N/A

Table 120. Relative energies with bromine and with $Br^-_{(aq)}$ from PCM/B3LYP/6-31+G(d) calculations

No counterpoise corrections have been applied to eliminate potential basis set superposition error for the bromine-dianion complexes and the α-lactone and bromide moieties.

8.5. QM/MM (GAMESS/CHARMM) collapse of chloronium ion

As modelling with explicit bromine molecule had occurred, explicit water molecules were included to model chloronium ion collapse to an α-lactone. The 2,3-dimethylmaleate chloronium F1Cl was optimised with PCM/B3LYP/6-31+G(d) and found to be a transition state, IRC and optimisation resulted in F2Cl. The packages GAMESS-UK and CHARMM

were used to perform QM/MM optimisation, TIP3P-water/B3LYP/6-31+G(d), of chloronium ion F1Cl, using coordinates from PCMB3LYP/6-31+G(d) optimisation, surrounded by a 15Å radius of explicit water molecules minimised in MOE with a fixed solute using CHARMM. The *ab initio* calculation on the solute was performed with B3LYP/6-31+G(d) calculation using GAMESS-UK.[172] The explicit solvent water molecules were treated with the CHARMM forcefield, with dynamic sampling of the solvent between *ab initio* optimisation steps.[173]

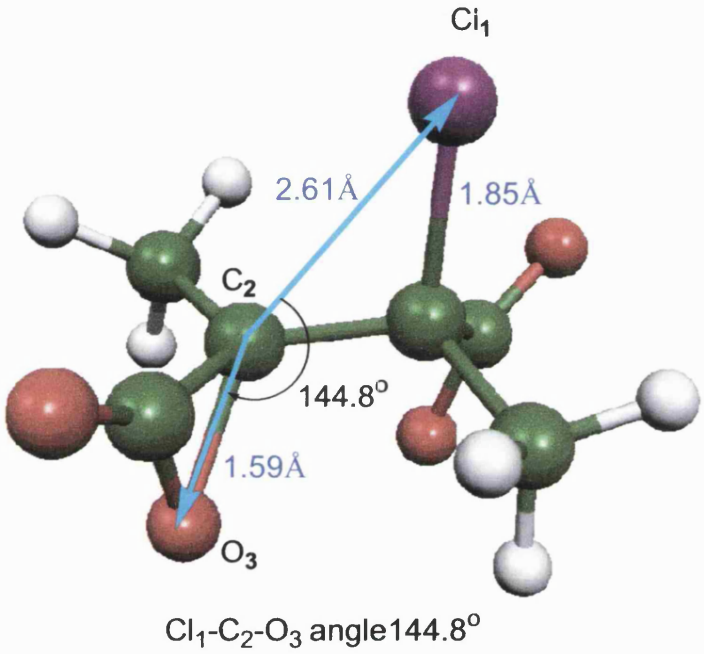

Fig. 121. F2Clqm optimised with GAMESS/CHARMM from F1Cl.

Unlike Oniom calculations the advantage of QM/MM calculations is that the optimisation is dependent upon the solute energy changes, not on the whole assembly, the gradient utilised is for the full system. The final optimised structure was a chloro-α-lactone, not a zwitterion. The GAMESS-UK software did not contain a basis set definition 6-31+G(d) for bromine, so chlorine was used.

9.Discussion of calculated results

The calculated result support the proposed mechanism that cyclic bromonium ions M1 and F1 are transition states that collapse to α-lactones and that bromine-dianion complexes are higher in energy compared to α-lactones and bromine anions. The conclusion is that the first formed intermediates are α-lactones.

9.1. Difference between Cosmo/AM1 and PCM/B3LYP/6-31+G(d) results

The Cosmo/AM1 calculations resulted in the optimisation of a zwitterion, Z3, cf. figure 95. Optimisation with PCM/rB3LYP/6-31+G(d) using the coordinates from Z3, obtained from Cosmo/AM1 calculation, result in spontaneous decarboxylation and formation of an alkene, *E*-2-bromo-3-carboxy-but-2-ene. This result demonstrates the qualitative and quantitative difference between Cosmo/AM1 and PCM/B3LYP/6-31+G(d) calculations upon the zwitterion shown in figure 91.

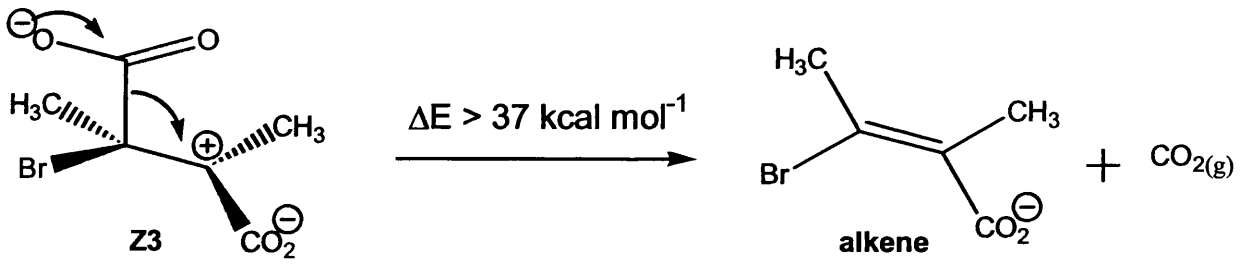

Fig. 122. Optimisation of Z3 with PCM/rB3LYP/6-31+G(d) results in spontaneous decarboxylation. $\Delta E > -37.00$ kcal mol^{-1}.

The PCM envelope did not suffice to prevent spontaneous decarboxylation and CO_2 loss during the calculation. The calculation was terminated when the rate of energy change became low, so is not strictly a complete optimisation. This calculation does suggest that decarboxylation may lead to monocarboxyl-brominated alkenes, as shown in figure 122. The estimates of ^{13}C NMR chemical shifts were made to see if the experimental ^{13}C NMR spectra of the crude material contained any potential decarboxylated alkene products. The ^{13}C NMR

spectra do contain unassigned signals but these cannot be unambiguously assigned to alkene products, bromohydrins or dibromoadducts. The alkenes A1 and A2 were optimised with Gaussian03 using PCM/B3LYP/6-31+G(d).[142]

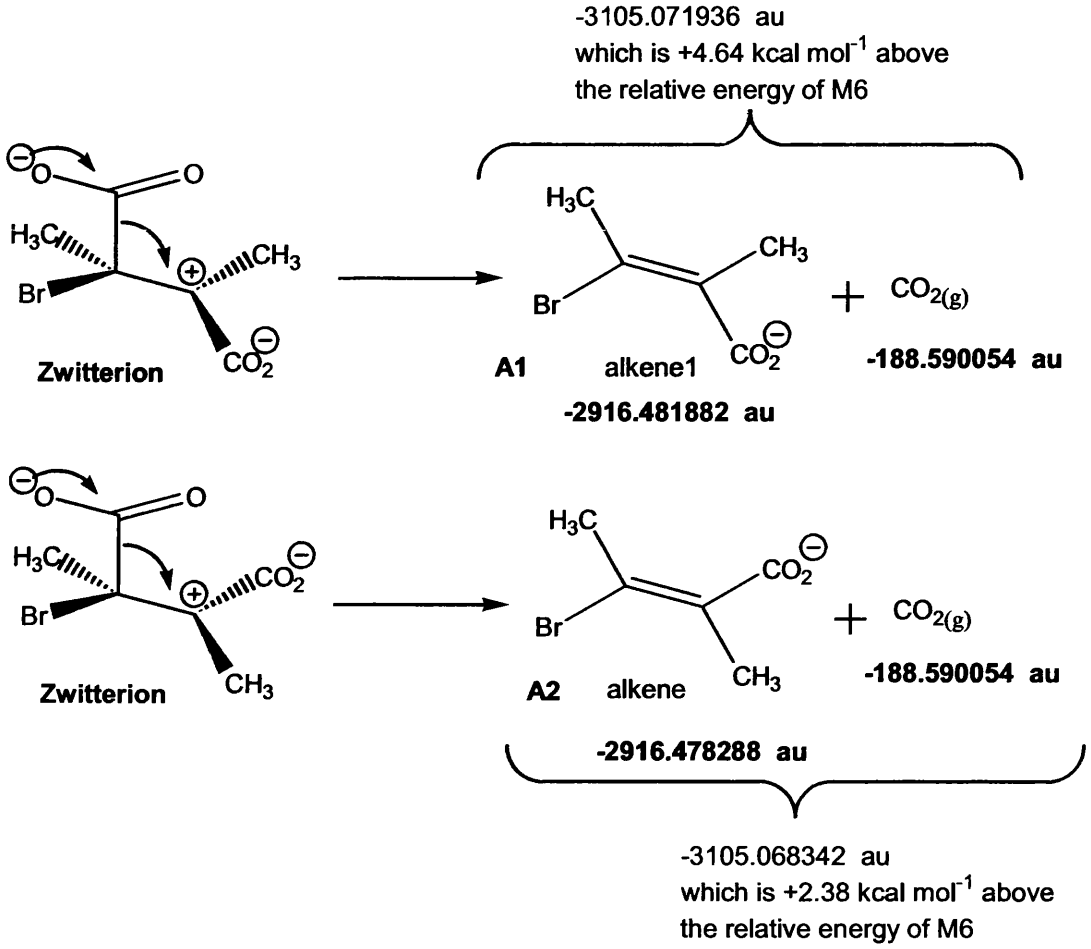

Fig. 123. Decarboxylation may lead to alkene formation.

The symmetry for the cyclic bromonium ion M1 (Cs) and F1 (C2) had to be imposed by using z-matrices with dummy atoms between the central C-C bond in the dianions and relating all dihedrals to the dummy atom when performing optimisation with Gaussian98A.6.

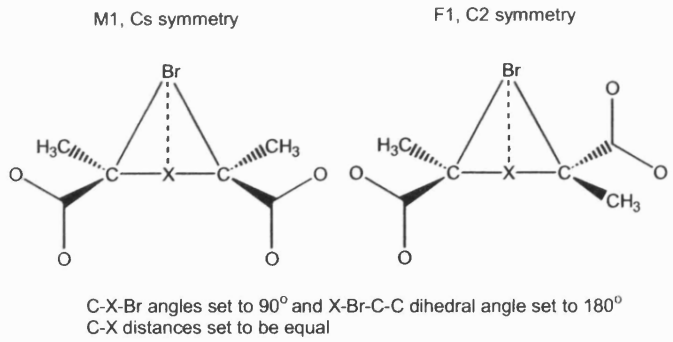

Fig. 124. Schematic representation of the Z-matrices used to optimise M1 and F1 with PCM/B3LYP/6-31+G(d).

Placing a dummy atom, X, in the central C-C bond and fixing some angles and all dihedral angles and relating as many variable dihedral angles, as possible to the dummy atom and using the NOSYMM keyword, did ensure that Gaussian98A.6 used symmetry in the optimisations of cyclic bromonium ions. The wavefunction for the optimised cyclic bromonium ions were subjected to a TEST calculation and no errors were returned. Optimisation of M10 with PCM/uB3LYP/6-31+G(d) and a multiplicity of 3 gave an energy higher than a PCM/B3LYP/6-31+G(d) optimisation.

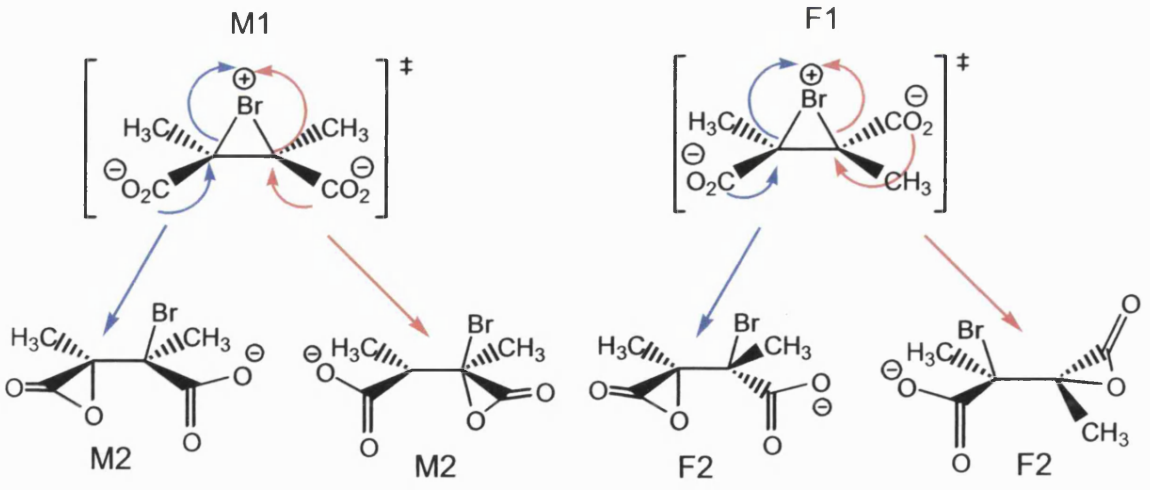

Fig. 125. Spontaneous relaxation of bromonium ions to α-lactones from PCM/B3LYP/6-31+G(d) calculations by 3-*Exo-Tet* ring closure.

The electronic description of oxiranone indicate the C-O acyl bond to be quite polar and extended when modeled with SCI-PCM/MP2/6-31+G(d).[37,92] The correct energetic description of this bond will influence predictions for solvent stabilisation contributions. The Cosmo/AM1 may contain energetic errors from either a systematic error in the AM1 method, possibly an over-estimation of α-lactone ring strain or Cosmo implicit solvation methods over-estimate the solvent cavity and zwitterion charges interaction and hence overestimates the electrostatic energy contribution, leading to solvent stabilised zwitterions. The energetic difference between the two gas phase AM1 optimisations of M1 and M2 is -12.8 kcal mol^{-1}. Including Cosmo solvation energy contributions, the difference between M1 and M2 is actually endothermic, by +4.45 kcal mol^{-1} with an associated difference in dipole moment of 3.7D. The difference in energy calculated with PCM/B3LYP/6-31+G(d) is exothermic for the difference between optimised bromonium ion M1 and M2 bromo-α-lactone, is -8.57 kcal mol^{-1} with an associated difference in dipole moment of 2D. The energy difference between the bromonium ion F1 and F2 bromo-α-lactone, is -3.29 kcal mol^{-1}.

Dianion	Cosmo/AM1 1SCF, μ	PCM/B3LYP/6-31+G(d), μ
M1	16.8	17.3
M2	13.1	19.3
Difference	3.7	2.0

Table 126. Calculated dipole moments, in Debye (D).

Hartree-Fock calculations overestimate the magnitude of dipole moments.[141] A reaction with a zwitterionic intermediate with the potential for S_N1 hydrolysis will yield a racemic mixture of bromohydrin products. The PCM/B3LYP/6-31+G(d) calculations have a smaller difference in dipole moment compared to the AM1 calculations. The relationship between dipole moment and solubility for neutral solutes is utilised in dipole moment measurements. Dipole moments are measured in non-polar solvents such as carbon tetrachloride and cyclohexane.

Corrections must be applied for solute concentrations and equations derived from the Debye-Clausius-Mosotti models are used to calculate the square of the dipole moment from dielectric and concentration relationships.[162]

The α-lactones M2 and F2 are asymmetric so they may form from asymmetric transition states. Modelling the spontaneous collapse of symmetrical cyclic bromonium ions to α-lactones does not indicate the presence of asymmetric transition states. Recently Ruggiero and Williams, at Bath University, performed PCM/B3LYP/6-31+G(d) calculations on halo-acrylate species and the results indicated that the cyclic chloronium and bromonium adducts of acrylate anion were not intermediates but transition structures for the degenerate rearrangement of halomethyl-α-lactones.[37,91]

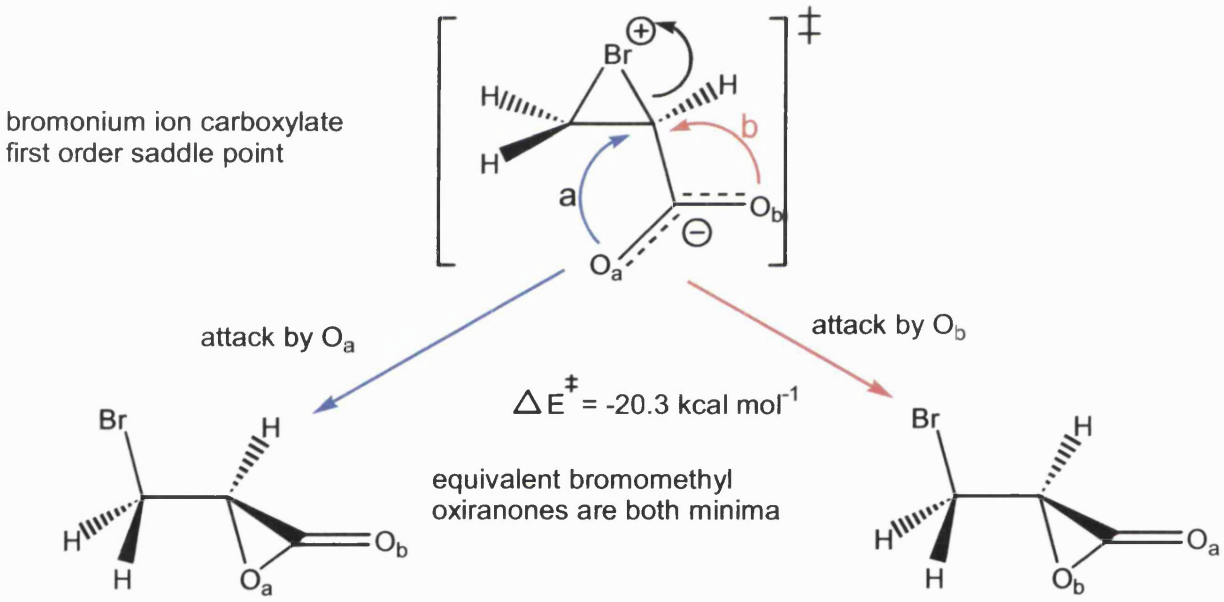

Fig. 127. α-lactone formation from bromonium ion of bromonium ion of acrylate anion.[91]

9.2 chloro-2,3-dimethylmaleate and chloro-2,3-dimethylfumarate

Simply replacing the bromine atom with chlorine and re-optimisation enabled the following relative energies to be calculated after

optimisation with PCM/B3LYP/6-31+G(d). The highest energy species along the reaction path are chloronium ions M1Cl and F1Cl. The conformational α-lactone TS, M3Cl and F3Cl are slightly lower in energy. The profile of the reaction from chloronium ions M1Cl and F1Cl are similar to the reaction PES profile from M1 and F1 to M6 and F6.

Chloro M series	E in PCM a.u.	Relative Energy in kcal mol^{-1}
M1Cl	-993.482096	0.00
M2Cl	-993.501492	-12.17
M3Cl	–993.493355	-7.07
M4Cl	–993.501785	-12.36
M5Cl	-993.500539	-11.57
M6Cl	–993.532359	-31.54

Table. 128. Energies for M1Cl to M6Cl relative to M1Cl optimisation.

Chloro F series	E in PCM	Relative energy in kcal mol^{-1}
F1Cl	-993.487178	0.000
F2Cl	-993.5002021	-8.173
F3Cl	-993.4954361	-5.182
F4Cl	-993.501937	-9.261
F5Cl	-993.4986469	-7.197
F6Cl	-993.530376	-27.107

Table 129. Energies for F1Cl to F6Cl relative to F1Cl optimisation.

The structures of the optimised chloro species are similar to optimised bromo species, with C-Cl bonds being shorter than C-Br bonds. Calculations performed with $HOCl_{(aq)}$, $HCl_{(aq)}$ and $Cl_{2(aq)}$ have not been attempted.

9.3 Accuracy of energetic barriers.

The bromination reaction occurs in a few minutes, so high energetic barriers along the reaction PES will indicate lengthened reaction time.

Post Hartree-Fock calculations such as Møller-Plesset (e.g MP2), Hartree-Fock with Configuration interation (CI) and couple-cluster calculations (e.g. CCSD) are computationally demanding.[114] Hartree-Fock theory often over-estimates barriers for chemical reactions whereas pure DFT underestimates them. The popular hybrid DFT B3LYP method with 20% Hartree-Fock exchange systematically underestimates barrier heights.[181] As many DFT and hybrid DFT functionals and methods are available, a different methodology was used to compare the B3LYP results. The mean unsigned error associated with barrier height calculations for B3LYP/6-31+(d,p) has been reported as 4.8 kcal mol^{-1} in one study by Truhlar and coworkers.[165]Another study by Kobayashi and co-workers found that B3LYP calculations systematically underestimate barrier heights.[166] The MPW1K methodology has been suggested to have a mean unsigned error of 1.5 kcal mol^{-1} for barrier height calculation, developed against a database of energies of activation and hydrogen–atom transfer reactions.

Calculation method	E in PCM
M1 B3LYP/6-31+G(d) no solvation	-3104.9227099 au
M1 MPW1K/6-31+G(d) no solvation	-3104.957738 au
M1 PCM/B3LYP/6-31+G(d)	-3105.0223968 au
M1 PCM/MPW1K/6-31+G(d)	-3104.9577380 au
M2 PCM/B3LYP/6-31+G(d)	-3105.0360526 au
M2 PCM/MPW1K/6-31+G(d)	-3104.9775524 au
M1 to M2 with PCM/B3LYP/6-31+G(d) in kcal mol^{-1}	-8.57
M1 to M2 with PCM/MPW1K/6-31+G(d) in kcal mol^{-1}	-12.43

Table 130. Comparison of B3LYP and MPW1K relative energies in PCM for M1 and M2, using default PCM settings and 6-31+G(d) basis set.

The MPW1K method increases the percentage of Hartree-Fock contributions in the density functional method by a factor of 2.[167] Poater and co workers have reoptimised B3LYP parameters in order to minimise differences between computed electron densities from this modified DFT

level and those calculated at the QCISD level of theory. It was noticed that different molecular systems require different levels of exact Hartree-Fock exchange for optimal agreement between different models.[168] As is shown in table 130, differences between energetic calculations with identical basis set and identical implicit solvation lead to different energies. The calculations on M1 maintained imposed Cs symmetry. The comparison shown in table 130, may be more valid in the gas phase as Truhlar and co-workers report calculation with MPW1K in the gas phase and even slight differences in the PCM cavity of the solvent and calculated dipole moment for a solute, will result in energetic differences. The conformation of the free carboxyl group in M2 will greatly influence the barrier height between M1 and M2.

Despite the fact that reaction barrier heights can be estimated, making predictions about reaction kinetics, which would be useful for estimating residence times in reactors, is still a difficult task.[169,170,171]

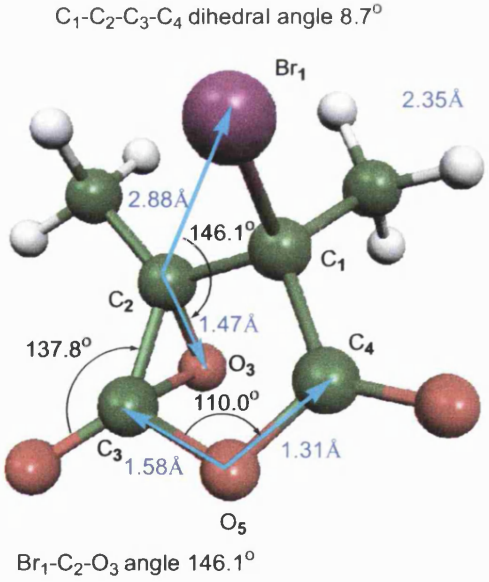

Fig. 131. M9 optimised with PCM/rB3LYP/6-31+G(d), E in PCM was –3105.0299278 a.u.

The attempt to optimise M2 using MPW1K/6-31+G(d) in the gas phase failed as the calculation tended towards a structure denoted as M9. The

structure M9 was first encountered during erroneous optimisation with Cosmo/AM1. The structure M9 was re-optimised with PCM/rB3LYP/6-31+G(d) and is shown below. M9 is an anhydride derived, potentially, from 5-*Endo-Tet* ring closure, cf. figure 85, of the free carboxyl group oxygen attacking the carbonyl carbon of the oxiranone ring in M2. The structure M9 does not fit into the overall mechanistic scheme and was noted for interest only and has a relative energy 3.84 kcal mol^{-1} higher compared to the α-lactone M2. However, the barrier between M2 and M4, via the M3 transition state is 5.02 kcal mol^{-1}. The structure M9 is probably an artefact from PCM solvation and is a dead-end mechanistically. Implicit solvation models cannot model hydrogen bonding to explicit solvent water molecules.[143] Explicit solvation may well hold the free carboxyl group in M2, inhibiting rotation about the C-CO_2^- bond and prevent 5-*Endo-Tet* ring closure to M9. M9 did not result during optimisation of M10, M11, M12 and M13.

9.4 Modelling with explicit water molecules

Energetic differences between implicit solvation models such as PCM/B3LYP and explicit solvation models such as QM/MM calculation have be noted by other researchers.[143] Calculations with explicit water molecules were tried. Oniom calculations employing two layers such as B3LYP/6-31+G(d) for solute and molecular mechanics (UFF), PM3, HF/sto-3G* and HF/3-21G* were tried for explicit water. Optimised structures resembled the PCM results. Oniom and QM/MM calculations do not allow charge transfer between solute and solvent layers.

The optimisation of F2Clqm species did not result in an intermediate zwitterion. The calculation took a number of months to complete. A single point energy calculation with PCM/B3LYP/6-31+G(d) in Gaussian98A.6, using the resultant coordinates of F2Clqm, results in an energy of –993.5090073 au for the structure shown in figure 121. An overlay of F2Cl and F2Clqm is shown below in figure 131. The structure of F2Cl as optimised with PCM/B3LYP/6-31+G(d), is higher in energy

compared to F2Clqm, as optimised with TIP3P-water/B3LYP/6-31+G(d) as calculated using GAMESS-UK/CHARMM, the difference being 4.4 kcal mol^{-1}.

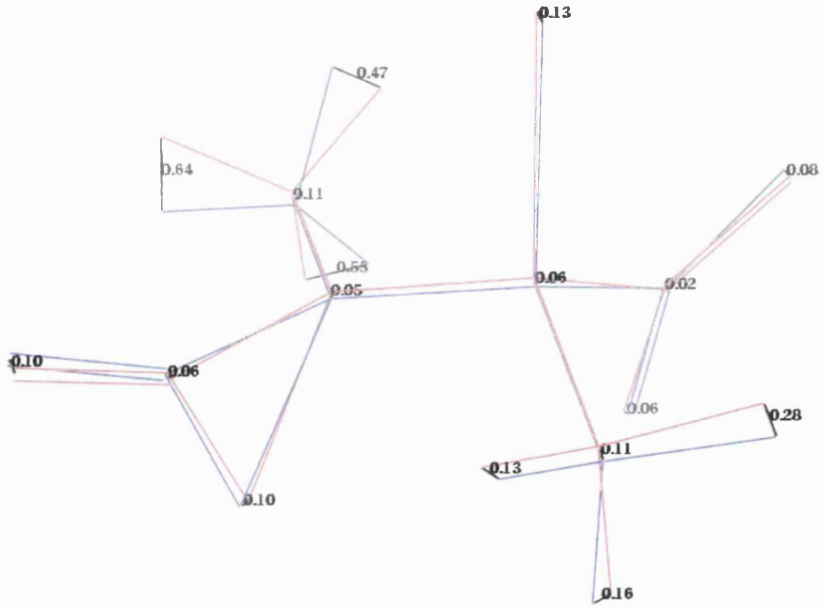

Fig. 132. Overlay of F2Cl and F2Clqm optimised structures, from MOE.

The QM/MM calculation on F1Cl also indicates that explicit solvation will lower the energy of the chloronium F1Cl by perturbing the structure toward an asymmetric chloronium ion and the optimisation finished with an optimised chloro-α-lactone, F2Cl. No intermediate zwitterion was optimised. In figure 132 the distance between similar atoms are shown in Ångströms, the rigid alignment tool in MOE was used to maintain geometries of the two structures overlaid. The biggest qualitative difference between F2Cl and F2Clqm is the conformation of the methyl group adjacent to the oxiranone ring.

Attempts to model the α-lactones in the present of a few explicit water molecules within a dipole/Onsager sphere proved interesting. Some calculations resulted in α-lactones, ring-opened zwitterions and even five-membered ring-closed structures. Optimisation will often yield a local energy minima and adequate number of water molecules must be used to incorporate hydrogen bonding within the explicit solvent

molecules as well as modelling solute-solvent interactions. Many more explicit water molecules are needed in the calculation shown in figure 133. Calculations with HyperChem5.01 using the periodic box set up for aqueous solvation provided ideal starting structures for optimisation with Gaussian98.

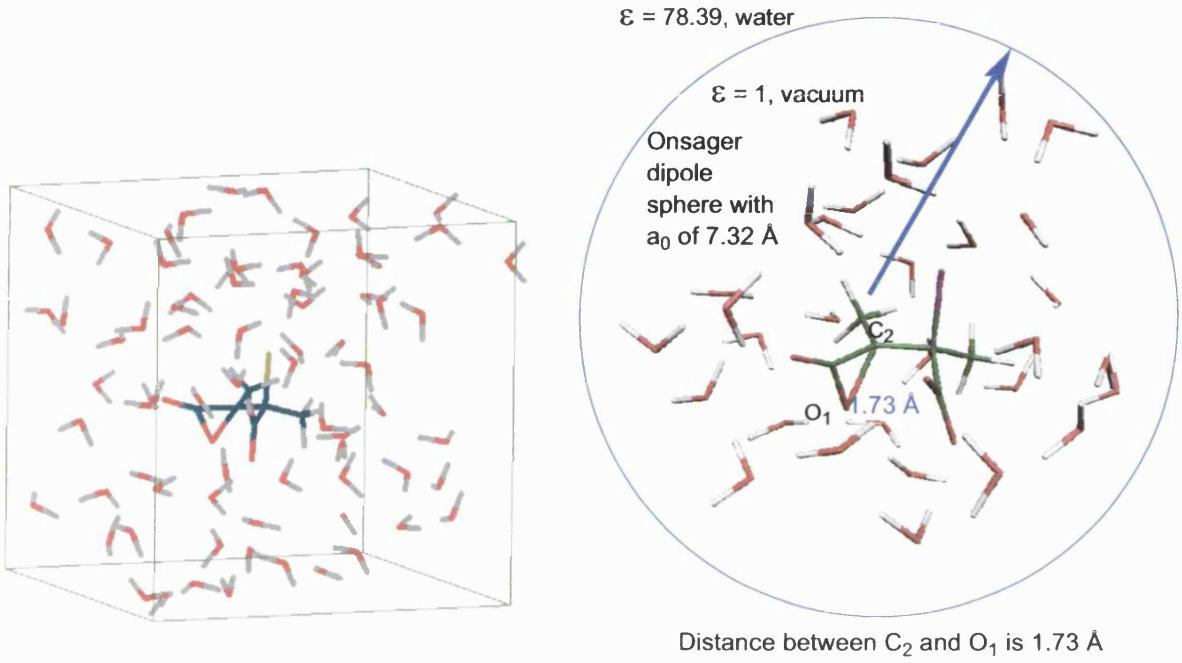

Fig. 133. optimisation with explicit water molecules

Optimisation with PM3 and periodic box condition containing water in HyperChem5.01 resulted in α-lactones, even when the gradient was less than 0.1 from eigenvector following routines. The structure on the rhs in figure 133 was obtained from Dipole/B3LYP/3-21G* optimisation when the Maximum Force reached 0.002618, not quite converged. The O-acyl bond was stretched to 1.73Å, the energy and the maximum force did diminish during optimisation, however after many tens of cycles the calculation crashed with coordinate problems. Restarting failed to rectify this. It is unlikely that a halohydrin will result from optimisation, but elongation of the O-acyl bond is not unexpected. The computational resource and time was unavailable to run Dipole/B3LYP/6-31+G(d)

and/or PCM/B3LYP/6-31+G(d) calculations including a reasonable number of explicit water molecules.

9.5 Modelling 4-*Endo-Tet* mechanism

To test the proposal on a zwitterionic intermediate as suggested by Tarbell and Bartlett, cf. figure 90 and figure 87, a QST2 calculation between M1 and F6 was performed and M7 was optimised. The transition state M7 relates the conversion of an α-lactone, M2, to a β-lactone, F6.

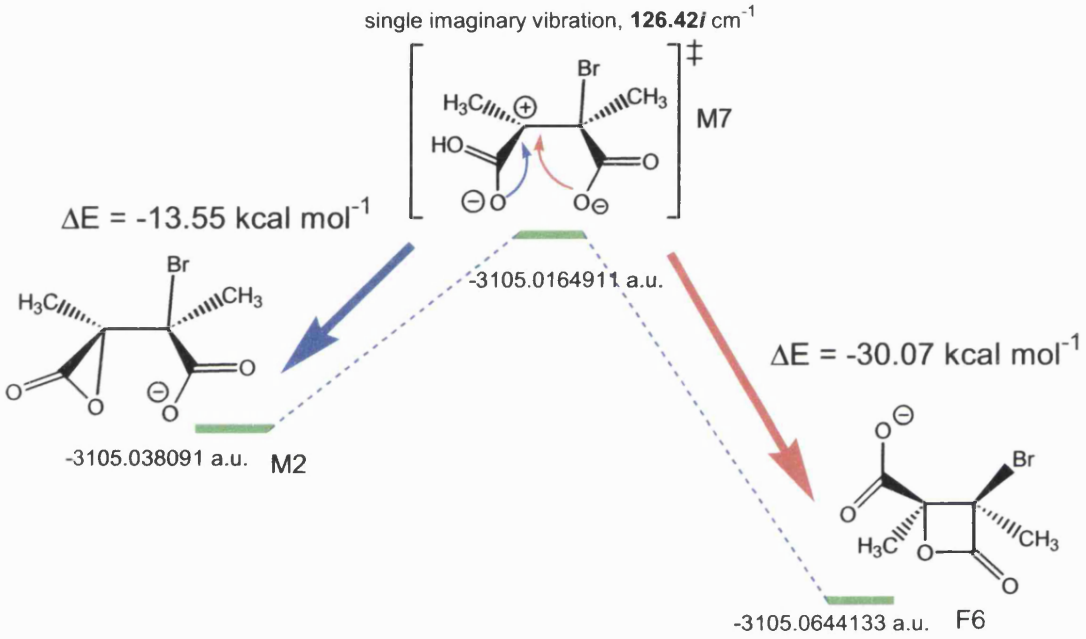

Fig. 134. PCM/B3LYP/6-31+G(d) profile for M7 TS collapse to α-lactone, M2 and β-lactone, F6.

The structure optimised for M7, shown in figure 135, is from a QST3 calculation using coordinates for M1 and F6 and the resultant structure from a calculation with PCM/rHF/3-21G* QST2 calculation using M1 and F6 to give a guess for M7. M7 was then optimised with PCM/B3LYP/6-31+G(d) and conducting IRC and optimisation from M7, leads forward to α-lactone (enantiomer of M2, not M1 bromonium ion) and back to a bromo-β-lactone (F6). The dihedral angle around C1 with closest three carbon atoms is 178.8° in M7.

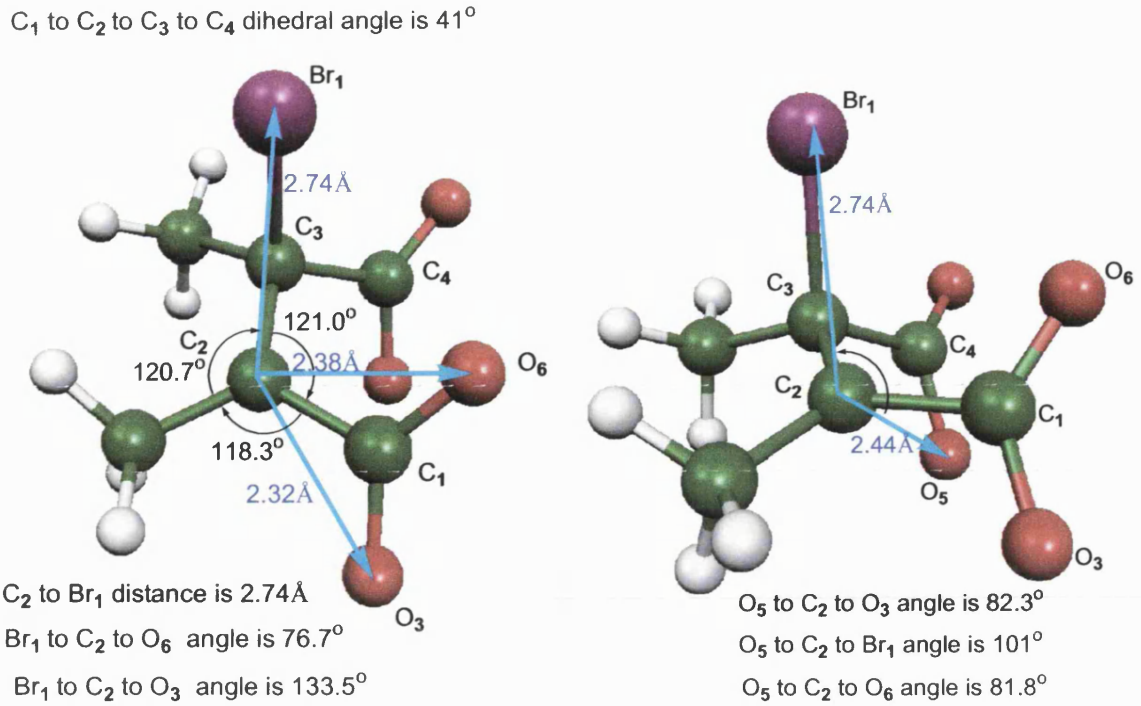

Fig. 135. M7 transition state from PCM/B3LYP/6-31+G(d)

The mechanism proposed by Tarbell and Bartlett suggested a zwitterionic intermediate, the PCM/B3LYP/6-31+G(d) calculation suggest that any zwitterions are unstable when compared to α-lactones. The proposed mechanism of Roberts and Kimball does not agree with the calculated reaction PES. The mechanism proposed by this thesis is in agreement with calculations.[91,92] How the α-lactones form is a problem that may not be easily answered.

The conformational change from M2 to M4 via M3, also F2 to F4 via F3, involves overcoming a conformational barrier of a few kcal mol^{-1} and the rotated α-lactones M4 and F4 are lower in energy than the initial α-lactones, M2 and F2, but only by less than 2 kcal mol^{-1}. Modelling with explicit solvation methods may result in energetic differences for this trend in comparison with implicit solvation modelling. Single-step 4-*Endo-Tet* ring closure from bromonium ions to yield β-lactones directly involves a higher energy transition state relative to bromonium ions; + 3.70 kcal mol^{-1} for 2,3-dimethylmaleate single-step TS $[M7]^{\ddagger}$. A similar

zwitterion TS for single step β-lactone (M6) formation from 2,3-dimethyl fumarate bromonium ion (F1) found by calculation closely resembled the transitions state M5. Formation of α-lactone is energetically preferred, -8.57 kcal mol^{-1} for 2,3-dimethylmaleate α-lactone formation and -3.29 kcal mol^{-1} for 2,3-dimethylfumarate α-lactone formation from potential cyclic bromonium transition states.

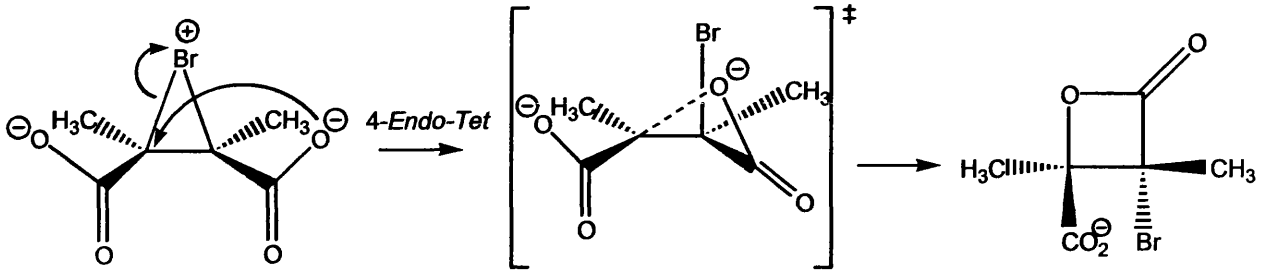

Fig.136. Front-side 4-*Endo-Tet* ring closure on bromonium ion M1

Attempts to model the 4-*Endo-Tet* ring closure on bromonium ion M1 using a QST2 PCM/B3LYP/6-31+G(d) calculation, with M6 resulted in M5. M1 modelled with implicit solvation is a transition state that collapses to an α-lactone not a zwitterion. All attempts to calculate alternatives to the α-lactone mechanism have failed to lead to calculated reaction PES that can be reconciled with the experimental results.

9.6 Modelling the reactant dianions

The reactant dianions M0 and F0 were modelled with PCM/B3LYP/6-31+G(d). The optimised structure of 2,3-dimethylmaleate dianion does resemble the crystal structure of maleate ligand in the crystal structure of 1ASE.pdb, a wild type E.Coli Aspartate Aminotransferase enzyme.[175] The structure of 2,3-dimethylfumarate is similar to that for fumarate dianion in the crystal structures 1GZ3.pdb and 1GZ4.pdb, human (oxidoreductase) mitochondrial NADP dependent malic enzyme.[56]

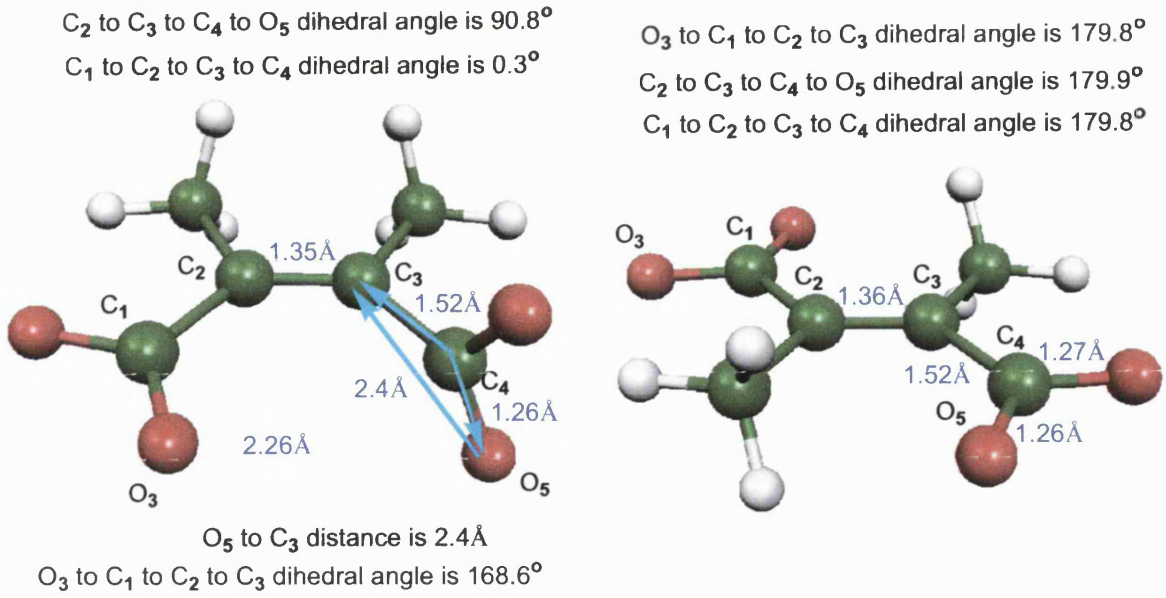

Fig. 137. Structure of optimised reactant dianions

The structure of the optimised 2,3-dimethylfumarate dianion is interesting in that is planar with respect to the two carboxyl groups and the central carbon-carbon double bond.

Dianion	E(RB+HF-LYP)	E in PCM
M0 2,3-dimethylmaleate	-533.4935235	-533.488924
F0 2,3-dimethylfumarate	-533.6560275	-533.487277

Table. 138. Optimised unsaturated dianions from PCM/B3LYP/6-31+G(d) reactants.

9.7 Calculation of pKa

The bromination of M0 and F0 is carried out on disodium salts. Slight changes in the pH of reactant solutions will affect the outcome of the reaction. If too much bromine is used, hydrobromic acid will form and the reactants may be protonated, affecting the mechanism. The two pKa values of 2,3-dimethylfumaric acid can be determined experimentally. However, the two pKa values of 2,3-dimethylmaleic acid cannot be determined, as in acidic aqueous solution 2,3-dimethylmaleic acid will spontaneously ring close to 2,3-dimethylmaleic anhydride, an aqueous

stable anhydride. Calculation of pKa is demanding as an error of 1.36 kcal mol^{-1} when calculating ΔG° free energy changes, will result in an error of 1 pKa unit. QSPR and *ab initio* methods have been used by other researchers. The CPCM implicit solvation model has been used for accurate energy calculation for deriving pKa.[176,177,178] Comparison of experimentally determined haloacid pKa with theoretical calculations may also offer insight into selecting an appropriate level of theory to calculate the reaction energy profiles with more certainty.

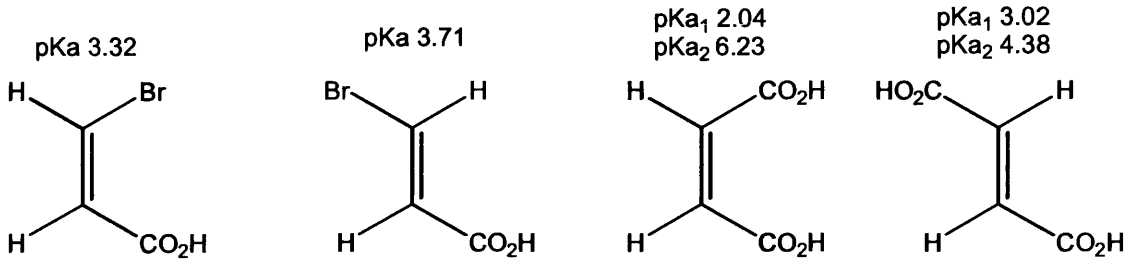

Fig. 139. Empirical pKa data for unsaturated acids.[179]

The first pKa of 2,3-dimethylmaleic acid may be similar to that for maleic acid, as shown in figure 139. An attempt was made using the B3LYP/6-311+G(2d,p) level of theory and CPCM method for implicit solvation to calculate the first pKa of 2,3-dimethylmaleic acid, to test the implicit solvation and B3LYP methodology. The optimisation and subsequent frequency calculation of the aqueous mono-anion reveal that the structure is a TS, with a single imaginary vibrational mode of 755.6 $i cm^{-1}$. The result of the pKa calculation is consistent with experimental data; anhydride formation is spontaneous in acidic aqueous media. Animation of the imaginary mode suggests ring closure to the anhydride with elimination of a hydroxide anion. Using the thermodynamic data obtained, from the four CPCM/B3LYP/6-311+G(2d,p) calculations and without applying vibrational or ZPE scaling factors, the calculated first pKa value of 2,3-dimethylmaleic acid is 7.03.

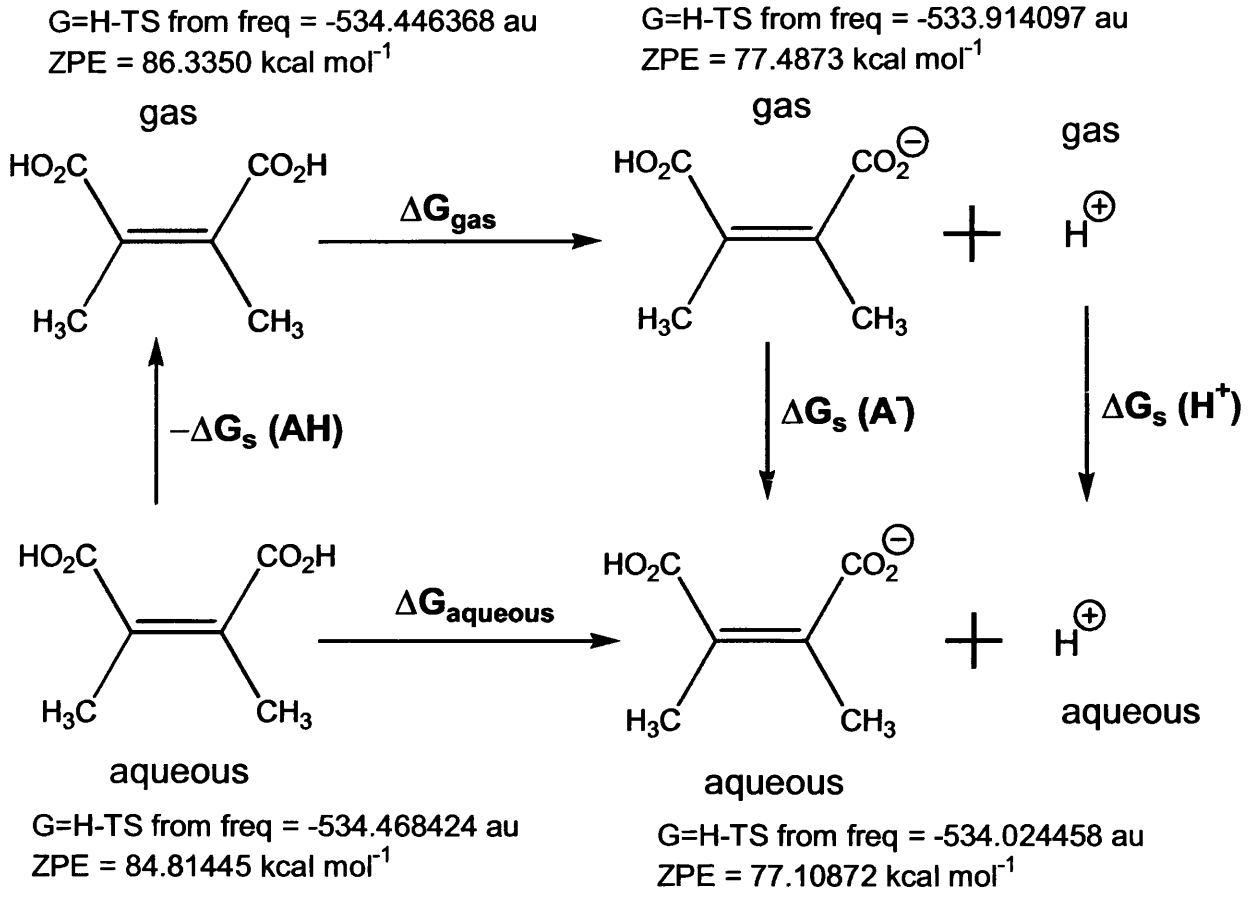

$pK_a = [G(A^-_{gas}) - G(AH_{gas}) + \Delta G_s(A^-) - \Delta G_s(AH) - 269.0] / 1.3644 = 7.03$ [no scaling]

Fig. 140. Calculation of pKa from CPCM/B3LYP/6-311+G(2d,p)

9.8. Calculation of halomaleic and halofumaric salts

Roberts and Kimball suggested that the first formed intermediate during halogenation of alkene is a cyclic halonium ion. The work of McKenzie can be explained by examining the products of back-side attack upon the initially formed halonium ion by a halide anion.[61] Bromination of maleic acid leads to *threo* products that can be resolved using morphine salts. Bromination of fumaric acid leads to a *meso* (*erythro*) product that cannot be resolved.

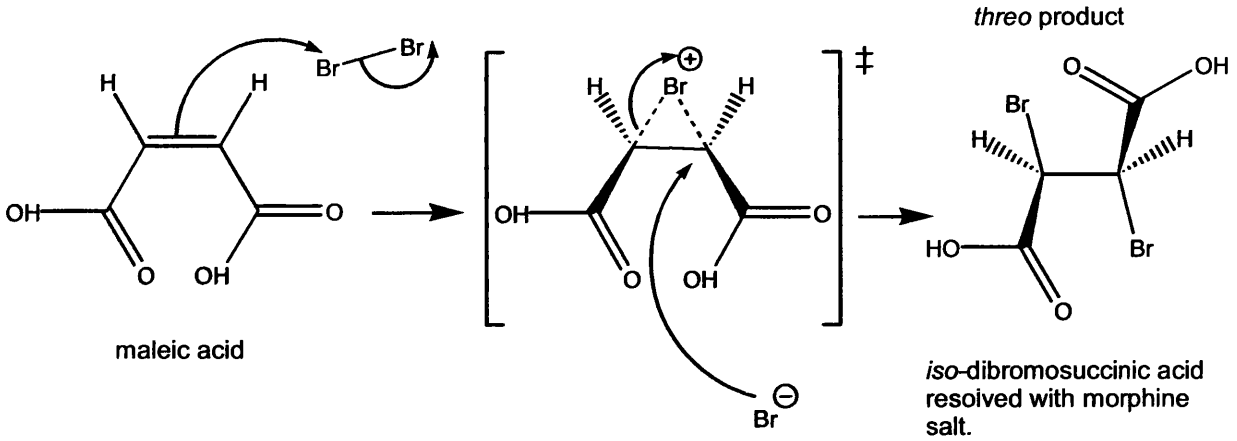

Fig. 141. Bromination of maleic acid in ether.[75,60.]

However chlorination of maleic acid disodium salt as examined by Kuhn and Ebel does not lead to dichloroadducts as proposed by Terry and Eicehelberger, chlorohydrins are formed.

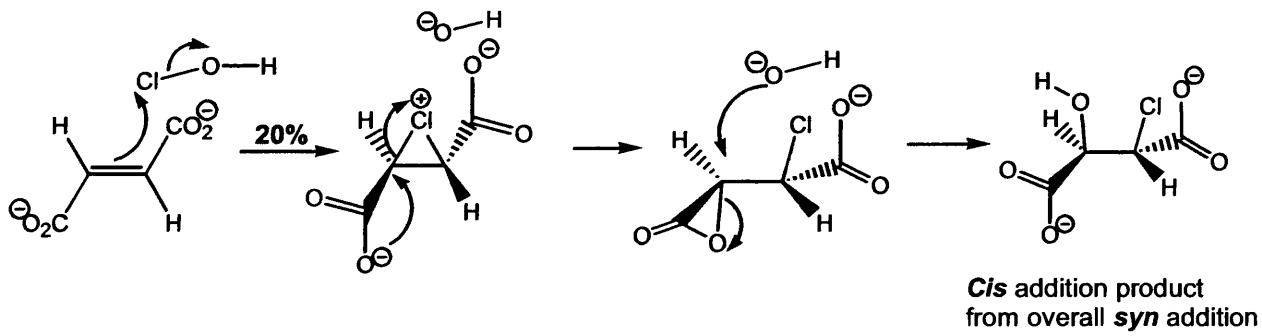

Fig. 142. KEF2Cl 80% chlorohydrins form from backside attack on chloronium ion and 20% from hydrolysis of α-lactone, for fumaric acid disodium salt.[79]

Terry and Eichelberger used added excess chloride ions in their experiments. The chlorohydrins resulting from chlorination of maleic acid are *cis* addition products.[81] This stereochemical result is opposite to that noted for bromination of maleic acid.[78,79] In light of the experimental results by Kuhn and Ebel and the suggestion of Badea, halomaleic and halofumaric species were examined using PCM/B3LYP/6-31+G(d) method.[78,79] The symmetrical maleic bromonium ion KEM1Br, was optimised and a frequency calculation resulted in a single imaginary vibrational mode of 32.12 $i$cm^{-1}. Cs symmetry was imposed by using

appropriate z-matrices with dummy atoms between the central C-C bond. The maleate cyclic bromonium ion is a TS and IRC and optimisation results in an α-lactone KEM2Br. Similar results were obtained when modelling the symmetrical maleate chloronium ion KEM1Cl, which relaxed to an α-lactone, KEM2Cl.

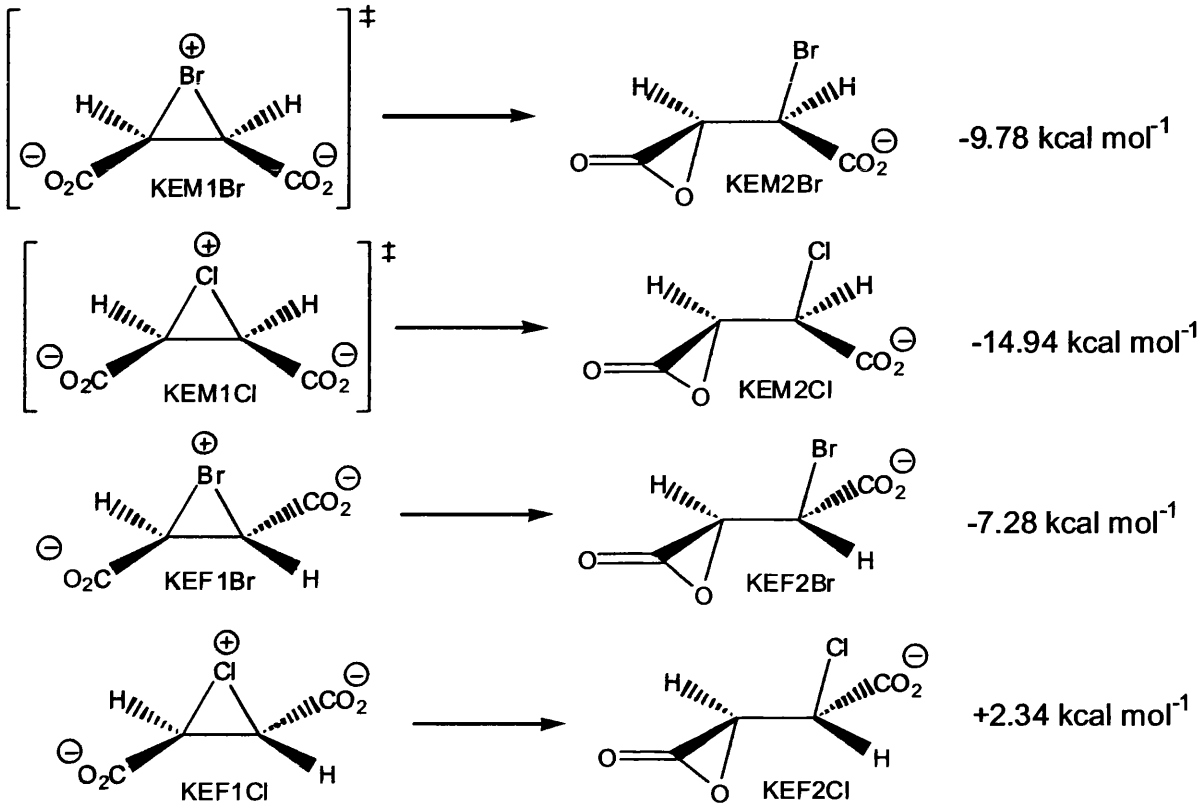

Fig. 143. Relative energies for maleic and fumaric moieties, PCM/B3LYP/6-31+G(d).

The symmetrical fumaric bromonium ion KEF1Br, was not a transition state, a frequency calculation with PCM/B3LYP/6-31+G(d) gave all real vibration modes for KEF1Br. The optimisation of the bromo-fumarate α-lactone, KEF2Br, proved problematic. The C-H bonds have lengths of 1.096Å and 1.099Å in gas phase. Using implicit solvation, PCM/B3LYP/6-31+G(d) causes the calculation to optimise to a structure with extended C-H bond lengths. Numerous attempts to optimise the structure of KEF2Br, failed using PCM explicit solvation, so best

guesses were chosen for KEF2Br and KEF2Cl. The fumarate chloronium ion KEF1Cl, could not be optimised to give 4 YES optimisation flags, so a best guess of non-symmetrical structure was chosen for KEF1Cl. Optimising the potential α-lactone, KEF2Cl, from the fumaric chloronium ion proved difficult, the C-H bonds elongated to 1.93Å. Constrained C-H bonds were set to 1.09Å and a best guess was optimised. The chloronium ion, KEF1Cl, may be lower in energy compared to the potential α-lactone KEF2Cl.

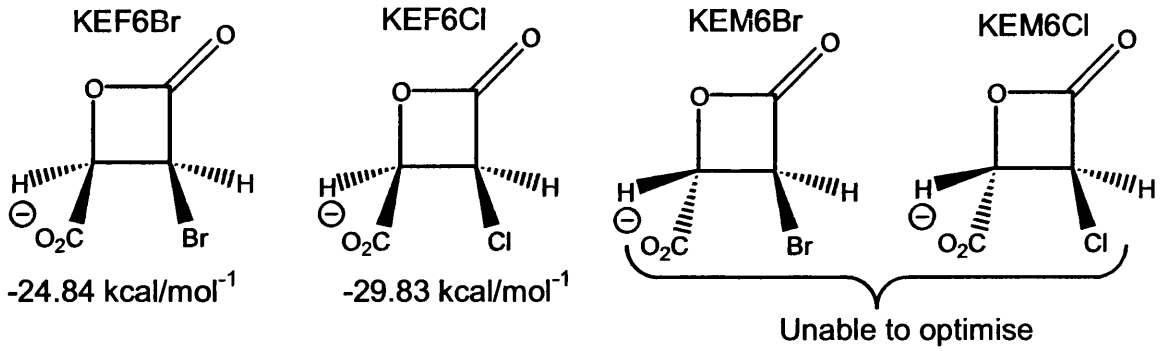

Fig. 144. Potential β-lactones from maleic and fumarate dianions.

The potential β-lactones KEF6Br and KEFCl6 optimised with ease, energies reported in figure 144 are relative to cyclic halonium ions KEF1Br and KEF1Cl. All attempts to optimise the potential β-lactone KEM6Br and KEM6Cl failed, a variety of methods were tried PCM/HF/3-21G*, PCM/B3LYP/6-31+G(d) and CPCM/B3LYP/6-311+G(2d,p).

The empirical results of Weiss, Kuhn, Ebel and Wagner-Jauregg show differences in bromination and chlorination.[75,81] Bromination of disodium fumarate affords 93% of the *meso*-dibromosuccinate salt. Calculation suggest that potential cyclic halonium ions of maleic dianion are less stable compared to potential cyclic halonium ions of fumarate dianion and this does support the proposal of Badea.[79] Badea proposed that chlorohydrin formation from disodium maleate operated by a chloro-α-lactone ion that underwent hydrolysis, to give *cis* addition products from overall *syn* addition. Whereas the chlorination of disodium fumarate

gives rise to a chlorohydrin from hydrolysis of the cyclic chloronium ion.[79] The bromination of maleic acid reported by McKenzie gave two *threo*-dibromosuccinic acids that could be resolved. The bromination of fumaric acid results in a *erythro* products and hence a *meso*-dibromosuccinate that cannot be resolved.[75,84] Bromination of fumaric disodium salts results in a *meso* and *racemic* dibromoadducts. Bromination of diethyl-esters of maleic and fumaric acids also results in *meso*-dibromoadducts.

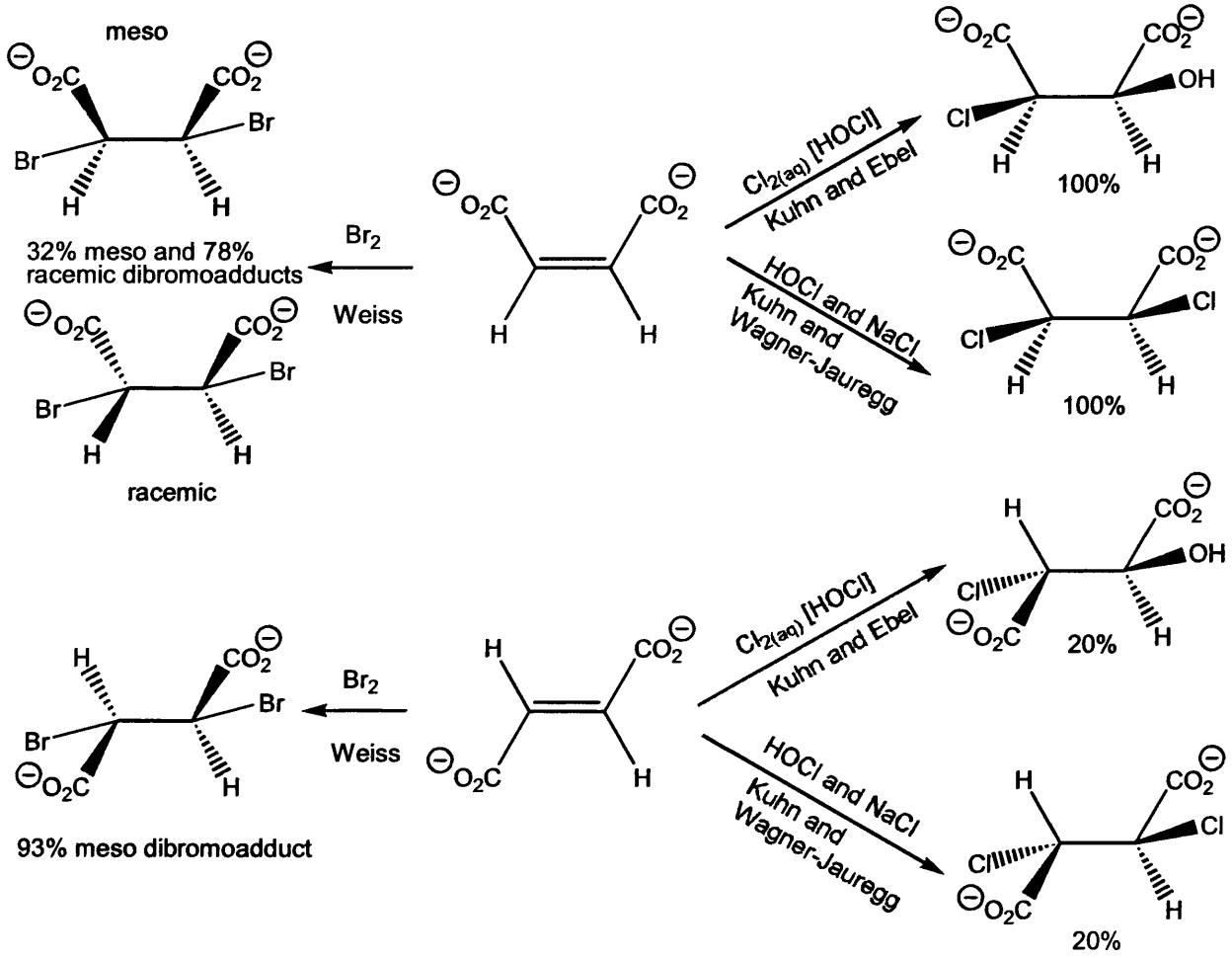

Fig. 145. Experimental results from halogenation of maleic and fumaric salts.

The question of whether the α-lactone mechanism is operating in the case of bromination of maleic disodium salts remains unanswered.

9.9 Attack of acetate anion on a monocarboxylbromonium ion

The coordinates for M1 were used to place an acetate anion carboxyl oxygen atom where one of the lower M1 oxygen's had been to give the starting structure of M1hoac. The calculation was an attempt to estimate the energetic differences between the angle of attack of an acetate anion from the same position as the 3-*Exo-Tet* ring closure for M1 and a more energetically favourable position from a relaxed scan calculation. This would allow a quantitative comparison of angles of attack, albeit with fixed C-OAc distances of 2.258Å.

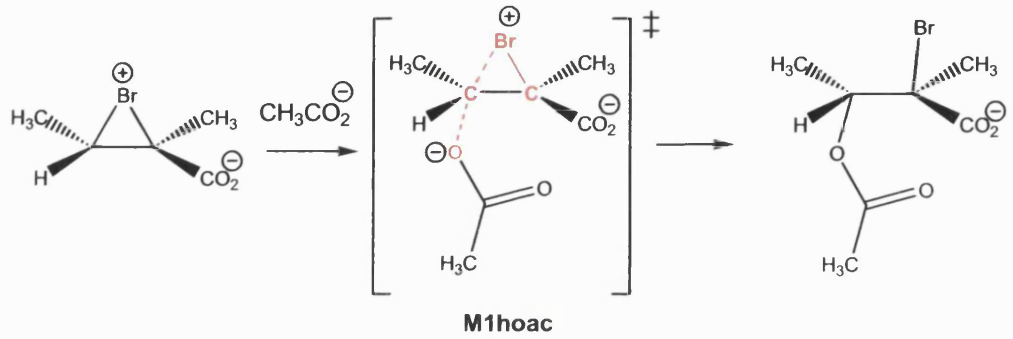

Fig. 146. Attacks of acetate anion on a bromonium ion similar to M1, dihedral9 angle for scan, shown in red.

The dihedral angle coloured red in figure 146 was scanned in a relaxed manner, the bromonium ion was held fixed.

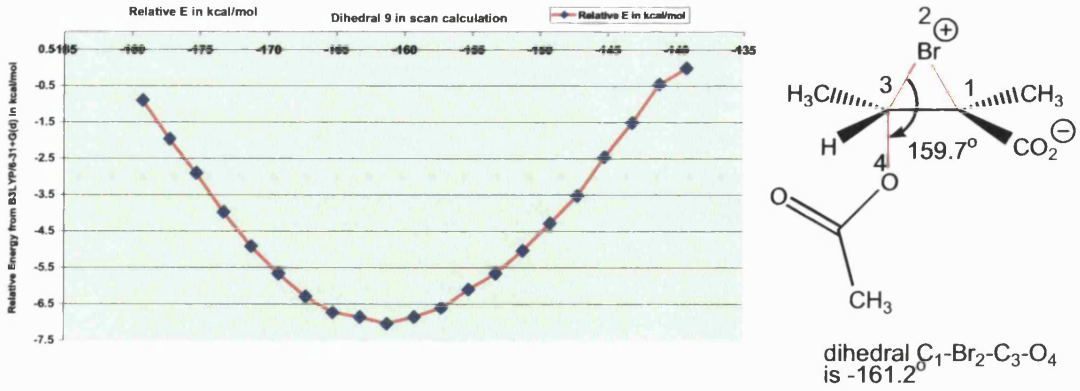

Fig. 147. B3LYP/6-31+G(d) energy and geometries from a relaxed scan through dihedral angle shown in red in fig. 146.

The initial AcO-C-Br-C dihedral angle was -139.2°. The C-O bond was held fixed at 2.25Å between the bromonium ion and the acetate anion. The energy was a minimum with a dihedral angle of -161.2° and the unconstrained AcO-C-Br angle of 159.7° as shown above. The lowest energy point on the relaxed dihedral angle scan corresponds to a Br-C-OAc angle of 159.7°. The attack of a nucleophile on the bromonium ion M1 has an angle of attack that is more favourable compared to the 3-*Exo-Tet* ring closure.

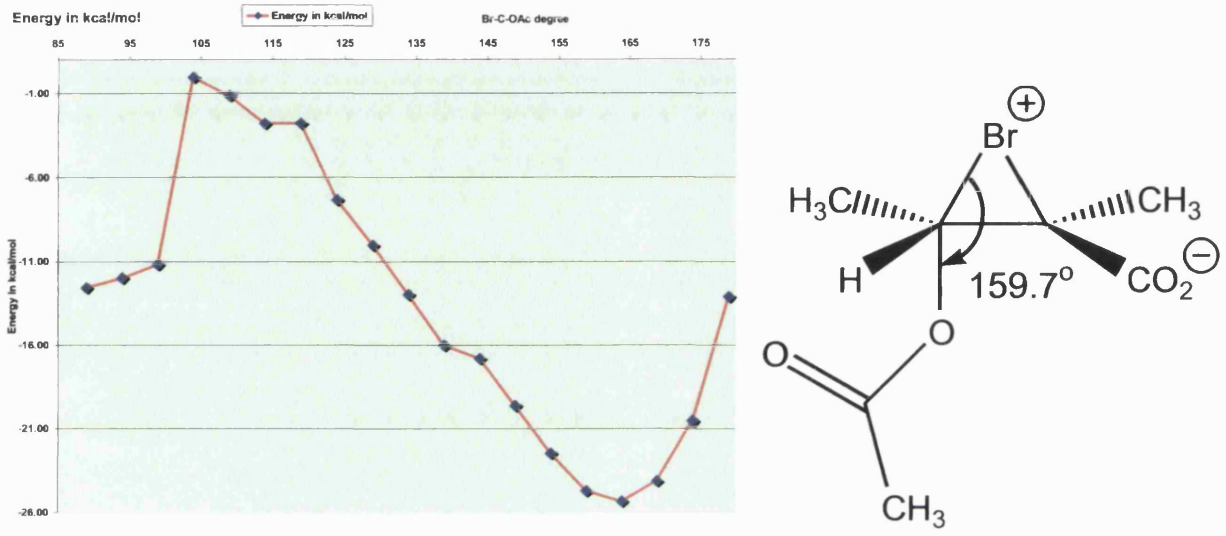

Fig. 148. Relative energies from B3LYP/6-31+G(d), relaxed scan of angle Br-C-OAc angle from 179° to 89° in the gas-phase.

However, the carboxyl group oxygen in M1, has an angle of attack that is 142.2° and a distance of 2.26Å. Any attacking nucleophile would have to overcome the electrostatic repulsion of the bromonium anion M1 and at least approach to with 2.26Å to compete with 3-*Exo-Tet* ring closure. Water is a weaker nucleophile compared to carboxyl oxygen.

10. Conclusion

The work of Walden had dispelled the primitive notion that substitution occurs in a homofacial manner. The excellent work of Holmberg and McKenzie had also provided an insight into substitution reactions, neighbouring group effects, lactone hydrolysis and the fact that addition reactions to unsaturated systems yielded *trans* addition products. The explanation for the work of McKenzie was provided by Roberts and Kimball by the proposal of a halonium intermediate. The work of Kuhn, Ebel, Wagner-Jauregg, Kenyon and Phillips provided more evidence for reactions that did not occur in a homofacial fashion. The work of Cowdrey, Hughes and Ingold laid the foundation for mechanistic designation of S_N1, S_N2 and S_Ni reactions.

Tarbell and Bartlett proposed that aqueous bromination of 2,3-dimethylmaleic acid disodium salts would facilitate the isolation of [3R(3S),4S(4R)]-3-bromo-carboxy-3,4-dimethyloxetan-2-one and that aqueous bromination of 2,3-dimethylfumaric acid disodium salt would facilitate [3S(3R),4S(4R)]-3-bromo-4-carboxy-3,4-dimethyloxetan-2-one. Tarbell and Bartlett were mistaken and the actual products from the bromination reaction are opposite to those initially proposed. The aqueous bromination of 2,3-dimethylmaleic acid disodium salt results in the production of [3S(3R),4S(4R)]-3-bromo-4-carboxy-3,4-dimethyloxetan-2-one. The aqueous bromination of 2,3-dimethylfumaric acid disodium salt results in the production of [3R(3S),4S(4R)]-3-bromo-carboxy-3,4-dimethyloxetan-2-one.

The bromination and chlorination of α,β-unsaturated carboxyl salts in most cases leads to initial α-lactone intermediates. Attempts to calculate alternative pathways lead to higher energy moieties or higher energy zwitterions. Calculations on 2,3-dimethyl maleate and 2,3-dimethyl fumarate dianions result in two inversion processes; 3-*Exo-Tet* ring closure to α-lactone and 4-*Exo-Tet* ring closure that results in isolation of halo-β-lactones. Calculations with maleic and fumaric dianions

results, in most cases, that the α-lactones is lower in energy compared to parent cyclic halonium ions, except for chloro-fumarate moieties. The lack of inductive methyl groups means that halo-β-lactones are not formed. Hydrolysis to yield halohydrins occurs in the absence of excess halide ions.

Optimisation of structures and comparison of relative energies facilitates the construction of reaction PES for bromination of M0 and F0 to M6 and F6. Calculation with PCM/B3LYP/6-31+G(d) from cyclic bromonium ions M1 and F1 result in spontaneous collapse to α-lactones M2 and F2 by 3-*Exo-Tet* ring closure. The first formed intermediate in the aqueous bromination of 2,3-dimethylmaleate and 2,3-dimethylfumarate disodium salts are α-lactones. The α-lactones undergo rotation about the central C-C bond and this facilitates 4-*Exo-Tet* ring closure to yield β-lactone M6 and F6. Spectroscopic analysis by ^{13}C NMR shows the reactions are stereospecific and that both crude and recrystallised products contain bromo-β-lactones, not bromohydrins or dibromoadducts/dibromosuccinic acids. Alkenes formation by decarboxylation may be present in acidified crude material. The yield of bromo-β-lactone is low, so other side products are formed. Calculation with PCM/B3LYP/6-31+G(d) from cyclic chloronium ions M1Cl and F1Cl result in spontaneous collapse to α-lactones M2Cl and F2Cl by 3-*Exo-Tet* ring closure. A QM/MM calculation on F1Cl resulted in optimisation of F2Cl and not a zwitterion. The α-lactones undergo rotation about the central C-C bond and this facilitates 4-*Exo-Tet* ring closure to yield β-lactone M6Cl and F6Cl. The 2,3-dimethyl fumarate was prepared from 2,3-dimethyl anhydride, giving rise to the presence of 2,3-dimethyl maleate in the reactants and explains why some [3S(3R),4S(4R)]-3-bromo-4-carboxy-3,4-dimethyloxetan-2-one is present in the crude acidified material of [3S(3R),4S(4R)]-3-bromo-4-carboxy-3,4-dimethyloxetan-2-one

As bromine is weakly hydrolysed in water calculations with PCM/B3LYP/6-31+G(d) on bromine molecules and unsaturated dianions M0 and F0 result in bromine-dianion complexes. The bromine-2,3-

dimethylmaleate dianion complex has a structure where the bromine associated with carboxyl groups. The bromine-2,3-dimethylfumarate dianion complex has a structure where the bromine associated with the central C=C bond. Removal of the peripheral bromine atom and optimisation with PCM/B3LYP/6-31+G(d) results in α-lactones. Optimisation of the α-lactones with bromide anions with PCM/B3LYP/6-31+G(d) results in structures that are lower in energy compared to bromine-dianion complexes. Experimental and theoretical evidence suggests that bromination of even simple alkenes is a complex process and mechanism can alter in relation to solvation characteristics.[75,163] Polymeric bromo species such as Br_3^- are often involved.

The unanswered question is how the intermediate α-lactones form. Do bromine-dianion complexes collapse to α-lactones or do cyclic bromonium ions form from Ad_E2 electrophilic attack of bromine, hydrobromic acid, hypobromite or polymeric bromine moieties? Calculation with bromine cations and bromine molecules both yield α-lactones. Hydrogen bonding between carboxyl groups and water molecules may mean that QM/MM calculation may differ from PCM/B3LYP/6-31+G(d) models in terms of structure and relative energies.[143]

The stability of the α-lactones in the presence of explicit solvation has not been examined by calculation. The acidic and basic hydrolysis of α-bromopropanoic acid result in inversion. The pH neutral hydrolysis of α-bromopropionate anion results in retention of configuration; cf. figure 20.[26,27] There is experimental evidence of isolated α-lactones and intermediate α-lactones. There is recent experimental evidence for similar isolated 3,3-di-*tert*-butyl-thiirane-2-thione and 3,3-di-*tert*-butylthiirane-2-thione S-oxide.[180] The PCM/B3LYP/6-31+G(d) calculations on M2, M2Cl, F2 and F2Cl do not answer the question of whether α-lactones have formal bonds or are zwitterionic as suggested by Ingold.

The reactions are known to be complete in a few minutes, but exact kinetic data is lacking. Comparison of reaction PES and kinetic data may assist in answering exactly how the α-lactones form. Hartree-Fock theory usually overestimates barrier heights, whereas pure DFT (e.g. BLYP) often underestimate barrier heights. Hybrid DFT methods such B3LYP also underestimates barrier heights, so comparison with kinetic data may offer an insight whether a better method can be chosen to estimate the barrier heights for the bromo-β-lactone formation from the reactant dianions.[181]

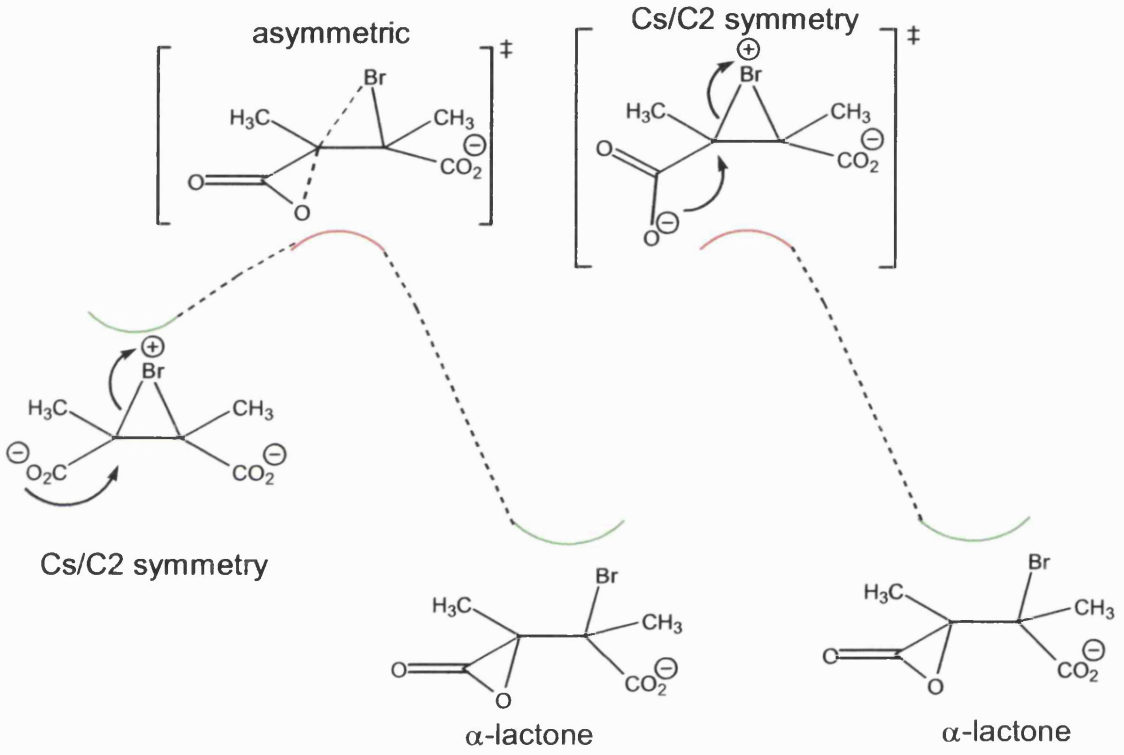

Fig. 149. LHS; potential explicit water model and RHS, calculated implicit solvation model for bromonium ion collapse to α-lactone.

The potential role of explicit water molecules has not been fully investigated. The calculations using implicit solvation methods indicate that cyclic symmetrical bromonium ions are transition states. The α-lactones however are asymmetric, so the cyclic bromonium ions when modelled with explicit water solvent molecules may be intermediates

with only a small barrier height to an asymmetric transition state. The hydrogen bonding of the carboxyl groups to water molecules may provide a small energetic barrier to 3-*Exo-Tet* ring closure to α-lactone. The reaction PES from α-lactone to β-lactone does not contain large energetic barriers so the reactions are rapid.

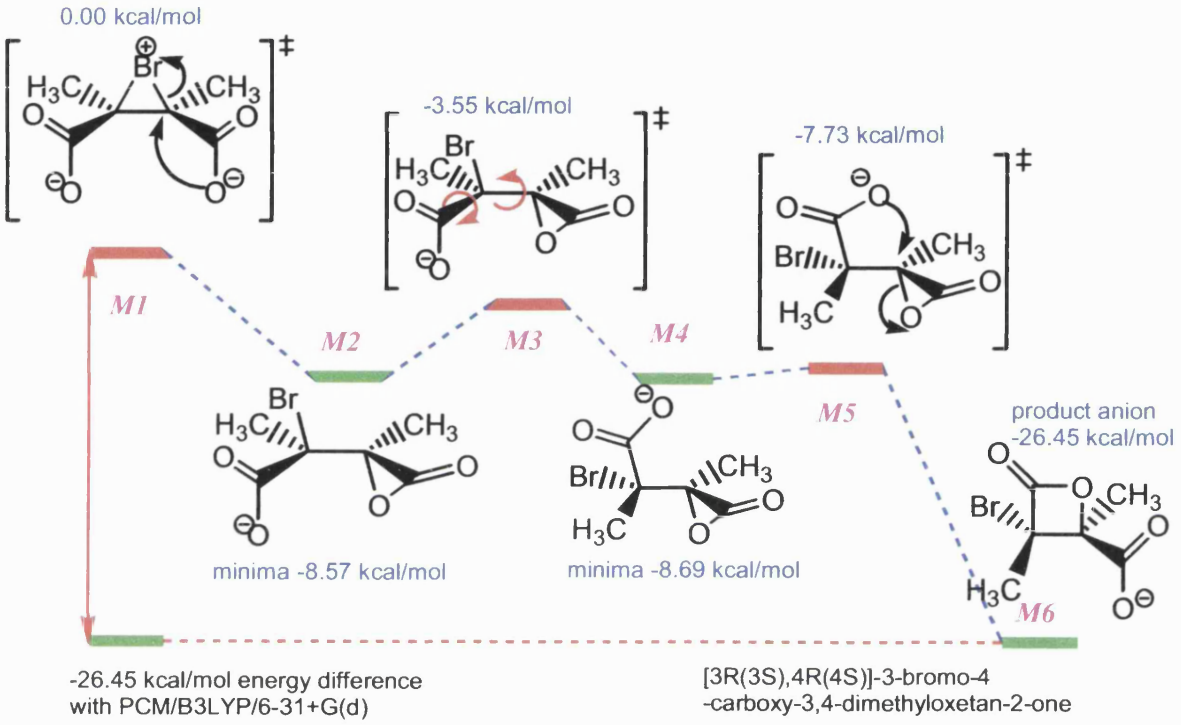

Fig. 150. PCM/B3LYP/6-31+G(d) energetic pathway from M1 to M6.

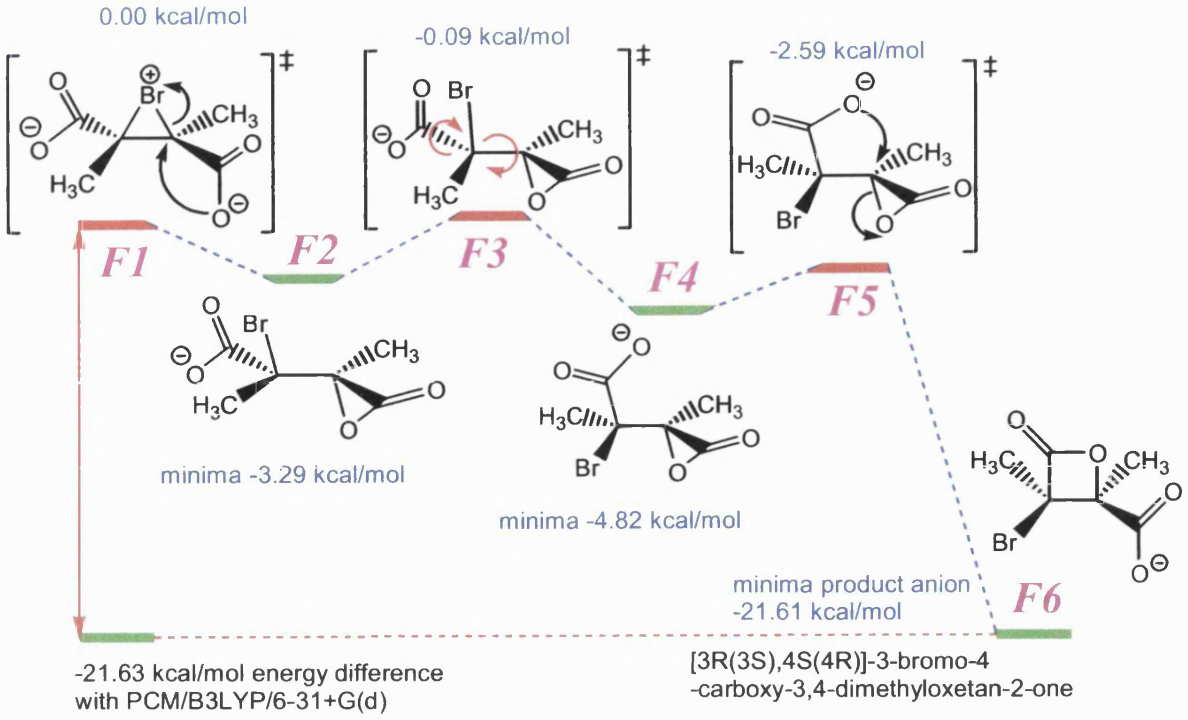

Fig. 151. PCM/B3LYP/6-31+G(d) energetic pathway from F1 to F6.

The rate-determining step for halo-β-lactone formation may be prior to α-lactone formation; collapse of halogen-dianion complexes or dissociation of halogens to halide and hypohalide species. The reaction PES diagrams have been drawn from initial cyclic bromonium transition states M1 and F1. However, the collapse of bromine-dianion complexes to α-lactone and bromine dianion is energetically favourable so the structure M1 may have no role in the reaction. The cyclic bromonium F1 may however have a role in the reaction PES. Potential transition states between bromine-dianion complexes have not been identified.

The α-lactone intermediates M2 and F2 form from 3-*Exo-Tet* ring closure, in aqueous solvent are not attacked by water, or by bromide anions, but undergo a conformational change to facilitate 4-*Exo-Tet* ring closure to β-lactones, promoted by the Thorpe-Ingold effect. The bromo-β-lactones form from two acts of inversion from S_Ni ring closures. Water is a weak nucleophile so hydrolysis of α-lactone to yield *syn* bromohydrins does not occur to any observable extent.

11. Suggested Future work

The unanswered question of whether bromonium ion (M1 and F1) collapse and/or solvation of a bromide anion from a dianion-bromine complex (M10 and F13) proceed to α-lactone formation (M2 and F2) is a problem that would not be easy to answer. Polymeric bromo species such as Br_3^- may be involved. The bromonium ions M1 and F1 have been characterised by imposing symmetry, higher levels of theory, MP2 for instance, may yield optimised stationary points for asymmetric bromonium ions M1 and F1.

Explicit solvation modelling must be performed to model the initial electrophilic attack of bromine upon the dianions M0 and F0. Even though the bromine-dianion complex species been modelled, potential transition states have not been identified. Potential charge transfer between bromine and close proximity explicit solvent water molecules may mean a QM/MM approach must include some water molecules in the QM partition. However, non-bonded interactions are difficult to model and B3LYP may not be best for describing the polar α-lactone and hydrogen bonding to water.[182] It is likely that results from QM/MM, with a number of water molecules included in the QM partition, calculations will have differing conformations compared to the PCM/B3LYP/6-31+G(d) results.

If the solvated bromide anion is in proximity to M2 and/or F2, what is the probability of the bromide anion attacking the O-acyl bond of the α-lactone to yield *syn* addition of bromine? In comparison with the work by Grunwald, Winstein, Chadwick and Pacsu, would added bromide anions produce a mass law affect? Would an increases or decrease in pH result in bromohydrin formation from hydrolysis of the α-lactone and would β-lactone formation be retarded at elevated pH? The crude ^{13}C NMR spectra contain unassigned signals that may indicate small amounts of side products. Decarboxylation of zwitterions as modelled by PCM/B3LYP/6-31+G(d) suggests alkene formation and CO_2 evolution as

a potential side reaction. No effervescence was observed during the synthesis of the bromo-β-lactones. Chromatographic techniques such as HPLC or LC/MS may aid in identifying the small amounts of side products. Starting reactant disodium salts, M0 and F0, will benefit from purification to eliminate contamination from impurities prior to halogenation.

Kinetic measurements for the aqueous bromination of M0 and F0 may assist and comparison to the proposed mechanism and computed reaction PES may provide some insight. An improved computational approach using implicit or explicit solvation models and perhaps a different hydrid DFT (e.g. PBE1PBE) or *ab initio* (post Hartree-Fock method such as MP2, QCISD(T) or HF with CI) methodology, may be suggested by comparing calculations of pKa for M8, F0 and F8 with experimental determination of pKa of M8, F0 and F8.

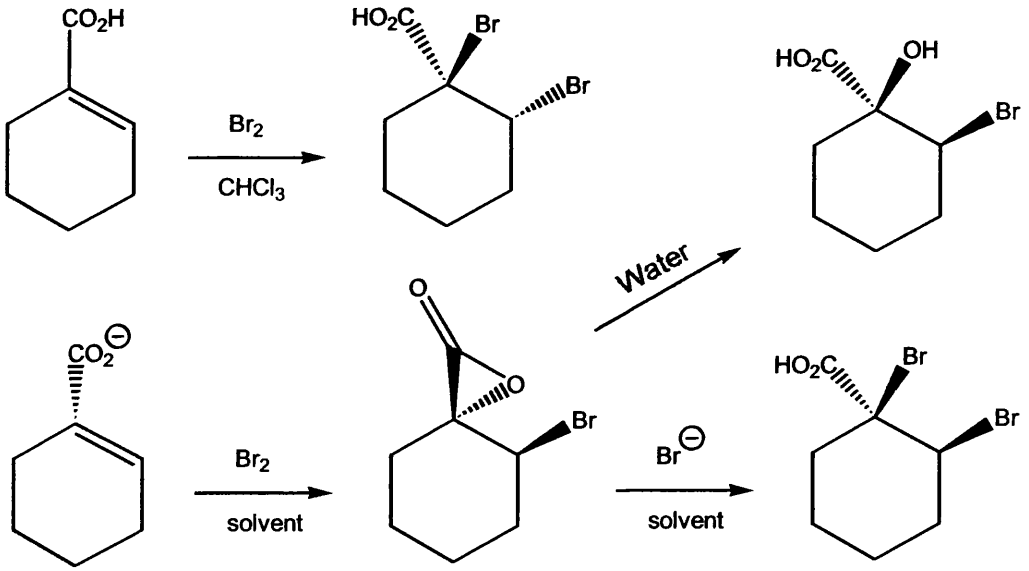

Fig. 152. Bromination without β-lactone formation.

The 3-Cyclohexene-1-carboxylic acid was brominated with bromine in chloroform, cf. figure 38. What would the results be if 1-Cyclohexene-1-carboxylic sodium salt was brominated in water, would a β-lactone or halohydrin form? The reaction illustrated in figure 152 has the potential

to produce a β-lactone or a *syn* bromohydrin may result. The cyclopentyl ring is not as flexible as a cyclohexane ring, so the carboxyl groups cannot rotate with respect to each other. This would investigate the nature of possible competition between α-lactone formation by 3-*Exo-Tet* ring closure and β-lactone formation by 4-*Endo-Tet* ring closure. Hydrolysis of potential cyclic bromonium ion may also occur.

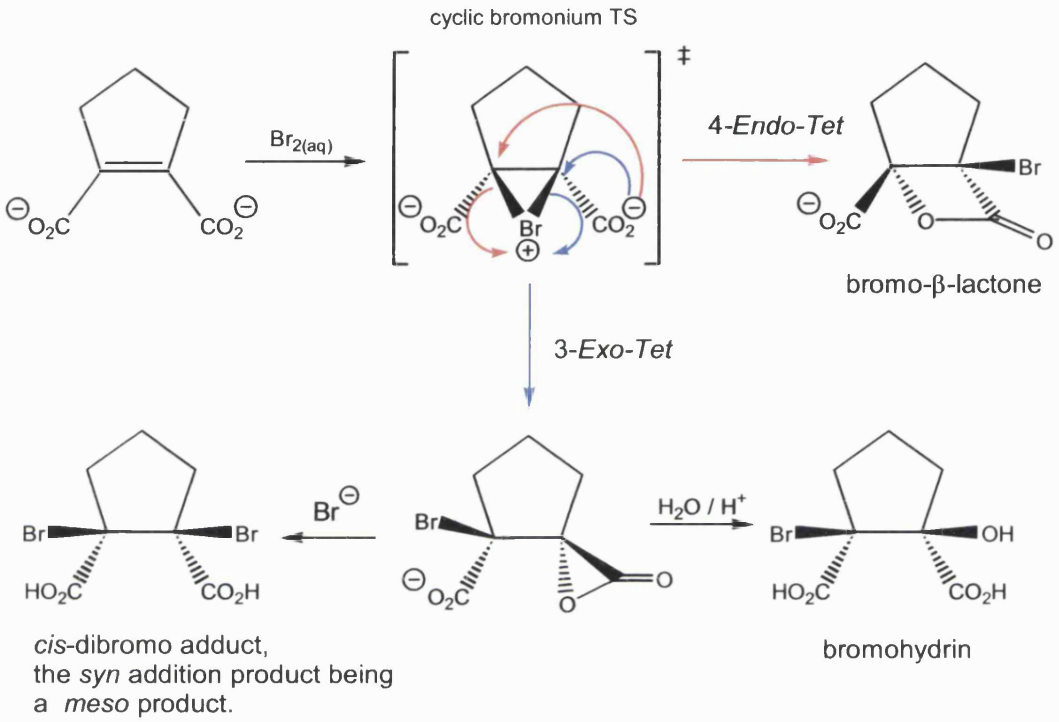

Fig. 153. Aqueous bromination of cyclopent-1-ene-1,2-dicarboxylic disodium salt would not involve conformational change.

A perfluorinated cyclopentyl ring disodium salt, $C_7F_6O_4Na_2$, may promote an α-lactone intermediate and a *cis* bromohydrin may result from overall *syn* addition. The perfuorinated unsaturated acid shown in figure 154 is commercially available, 2,3,4,5,5,5-hexafluoro-4-trifluoromethyl-2-pentenoic acid has CAS code of 103229-89-6. The potential α-lactone may form from 3-*Exo-Tet* ring closure on a bromonium ion.

CAS No: 103229-89-6

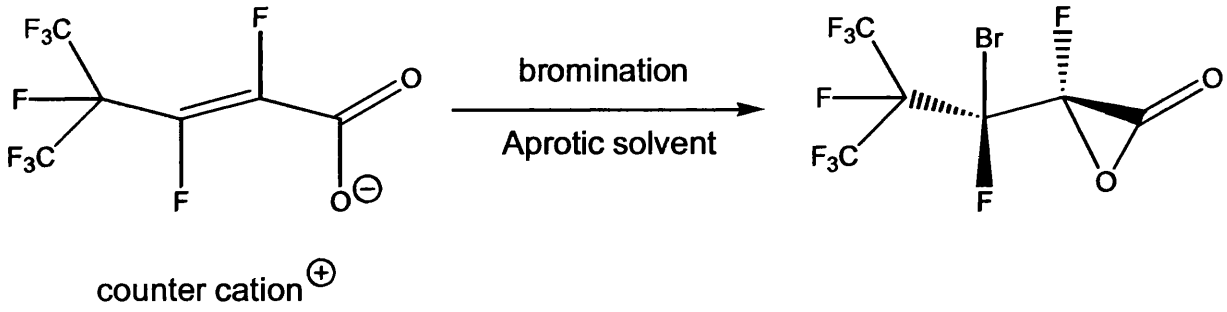

counter cation ⊕

Fig. 154. bromination of the perfluorinated unsaturated acid salt may yield an isolable β-bromo-α-lactone.

Other perfluorinated α,β-unsaturated acids have been prepared.[183] An alternative to using molecular bromine to conduct the bromination, may be (diacetoxyiodo)benzene-lithium bromide which may be used in THF solvent.[184] Aqueous bromination my result in a *cis* adduct bromohydrin.

Chlorination of disodium salt of 2,3-dimethylmaleic and 2,3-dimethylfumaric acids should yield similar β-lactones as bromination did, however an experimental analysis of the products is desirable to confirm this.[85,90,91] The work reported by Kingsbury may benefit from computational chemistry to suggest the mechanism for β-lactone formation.

12. References

1. F. A. Carey and R. J. Sundberg, *Advanced Organic Chemistry, Part A.* Plenum Press, 1990, p. 89.
2. A. Modro, G. H. Schmid and K. Yates, *J. Org. Chem.,* 1977, 42, 3673. Also see reference 1, p. 92.
3. E. Eliel and M. N. Rerick, *J. Amer. Chem. Soc.*, 1960, 82, 1367. See also reference 1, p.93.
4. C. K. Ingold, *Mechanism in Organic Chemistry*, Cornell University Press: Ithaca, 1953, p. 421.
5. See reference 1, p. 257.
6. P. Sykes, *A Guidebook to Mechanism in Organic Chemistry*, 1986, Longman, p. 77.
7. See reference 1, p. 89.
8. See reference 1, p. 90.
9. L. F. Fieser and M. Fieser, *Organic Chemistry*, Rheinhold, 1956, p. 340.
10. F. A. Carroll, *Perspectives on Structure and Mechanism in Organic Chemistry*, Brooks/Cole, 1998, p. 489.
11. P. Walden, *Ber.*, 1897, 30, 3146.
12. P. F. Frankland, *J. Chem. Soc.,* 1913, 103, 713.
13. B. Holmberg, *Ber.*, 1912, 46, 1713. See also B. Holmberg, *J. Prakt. Chem.*, 1913, 88, 553. See also B. Holmberg, *Brit. Chem. Abstr.*, 1914 825.
14. A. R. Olson and R. J. Miller, *J. Amer. Chem. Soc.,* 1938, 60, 2687.
15. R. Olson and J. L. Hyde, *J. Amer. Chem. Soc.*, 1941, 63, 2459. See also A. R. Olson and P. V. Youle, *J. Amer. Chem. Soc.,* 1951, 73, 2468. See also Reference 10, p. 440.
16. J. Kenyon and H. Phillips, *J. Chem. Soc., Trans. Farad. Soc.*, 1930, 26, 451.
17. Reference 10, p. 455.
18. T. H. Lowry and K. S. Richardson, *Mechanism and Theory in Organic Chemistry,* Harper and Row, 1981, p. 294 and p. 338.

19. Reference 4, p. 431.
20. Reference 10, p. 464.
21. J. Steigman and L. P. Hammett, *J. Amer. Chem. Soc.*, 1937, 59, 2536. See also reference 18, p. 317.
22. E. D. Hughes, F. Juliusberger, S. Masterman, B. Topley and J. Weiss, *J. Chem. Soc.*, 1935, 1525.
23. E. S. Gould, *Mechanism and Structure in Organic Chemistry,* Holt, Rinehart and Winston, New York, 1959, p. 266.
24. Reference 6, p. 82 and reference 4, p. 430.
25. Reference 9, p. 340.
26. W. A. Cowdry, E. D. Hughes and C. K. Ingold, *J. Chem. Soc.*, 1937, 1208.
27. J. Hine, *Physical Organic Chemistry,* McGraw-Hill, 1962, p. 143.
28. Reference 4, p. 524. See also reference 23, p. 270 and Reference 6, p. 95.
29. M. Bean, J. Kenyon and H. Phillips, *J. Chem. Soc.*, 1936, 303.
30. E. Eliel, S. H. Wilden and M. P. Doyle, *Basic Organic Stereochemistry*, Wiley Interscience, 2001, p. 433. See also J. Jager, T. Graafland, H. Schenk, A. J. Kirby and J. B. F. N. Engberts, *J. Amer. Chem. Soc.*, 1984, 106, 139.
31. S. Winstein and H. J. Lucas, *J. Amer. Chem. Soc.*, 1939, 61, 1576. See also S. Winstein and H. J. Lucas, *J. Amer. Chem. Soc.*, 1939, 61, 1581.
32. E. Grunwald and S. Winstein, *J. Amer. Chem. Soc.*, 1948, 70, 842.
33. A. F. Chadwick and E. Pacsu, *J. Amer. Chem. Soc.*, 1943, 65, 392.
34. Reference 23, p. 271.
35. Antolovic, V. J. Shiner and E. R. Davidson, *J. Amer. Chem. Soc.*, 1988, 110, 1375.
36. E. Milligan and M. E. Jacox, *J. Chem . Phys.*, 1962, 35, 2911. See also G. B. Kistiakowsky and K. Sauer, *J. Amer. Chem. Soc.*, 1958, 86, 1066.

37. G. D. Ruggiero and I. H. Williams, *J. Chem. Soc. Perkins Trans II,* 2001, 2, 733. See also I. H. Williams and C. F. Rodriguez, *J. Chem. Soc., Perkin Trans. II,* 1997, 956.
38. Kovacs and J. E. Jackson, *J. Phys. Chem. A.*, 2001, 105, 7579.
39. D. Schroder, N. Goldberg, W. Zummack, H. Schwarz, J. C. Poutsma and R. R. Squires, *Int. J. Mass. Spec.*, 1997, 165, 71.
40. J. F. Liebman and A. Greenburg, *J. Org. Chem.,* 1974, 39, 2, 123.
41. L'abbé, *Angew. Chem. Int. Ed. Eng.*, 1980, 19, 4, 276.
42. O. L. Chapman, P. W. Wojtkowski, W. Adam, O. Rodriguez and R. Rucktäschel, *J. Amer. Chem. Soc.,* 1972, 94, 1365
43. R. Wheland and P. D. Bartlett, *J. Amer. Chem. Soc.,* 1970, 92, 6057
44. P. L. Coe, I. R. Owen and A. Seller, *J. Chem. Soc., Perk. Trans. I*, 1989, 1097.
45. S. C. Reed, G. J. Capitosti, Z. Zhu and D. A. Modarelli, *J. Org. Chem.,* 2001, 66, 287.
46. E. A. Pritchina, N. P. Gritsan, A. Maltsev, T. Bally, T. Autrey, Y. Liu, Y. Yang and J. P. Toscano, *Phys. Chem. Chem. Phys.,* 2003, 5, 1010. See also B. M. Showalter, D. A. Brady, C. A. Kenesky and J. P. Toscano, *Phys. Chem. Chem. Phys.*, 2003, 5, 1059. See also B. M. Showalter and J. P. Toscano, *J. Phys. Org. Chem.,*2004, 17, 743. Also private communication with J. P. Toscano.
47. M. dP. Garcia-Santos, E. Calle and J. Casado, *J. Amer. Chem. Soc.,* 2001, 123, 7506.
48. G. Bordwell and A. C. Knipe, *J. Org. Chem.,* 1970, 35, 2956. See also F. G. Bordwell and A. C. Knipe, *J. Org. Chem.,* 1970, 35, 2959. Similar work earlier conducted by B. Holmberg, *Chem. Abstr.*, 1913, 6, 2072 and B. Holmberg, *J. Prakt. Chem.*, 1913, 88, 553.
49. R. W. Guthrie, R. W. Kierstead, F. A. Mennona and A. C. Sullivan, US Patent, 1982, 4312885 and *Chem. Abstr.,* 1983, 99, 38304. See also R. E. Dolle, A. Gribbe, T. Wilkes, L. I. Kruse,

D. Eggleston, B. A. Saxty, T. N. C. Wells and P. H. Groot, *J. Med. Chem.,* 1995, 38, 537. See also C. W. Perry, A. Brossi, K. M. Dietcher, W. Tuatz and S. Tietel, *Synthesis*, 1977, 492.

50. Shibata, M. Toyota, A. Baba and H. Matsunda, *J. Org. Chem.,* 1990, 55, 2487.

51. S. Terashima and S. Jew, *Tetrahedron Lett.,* 1997, 1005.

52. K. Krajewski, Z. Ciunick and I. Z. Siemon, *Tetrahedron: Asymm.*, 2001, 12, 455.

53. M. Casedei, G. Galli and L. Mandolini, *J. Amer. Chem. Soc.,* 1984, 106, 1051. See also G. Illumati and L. Mandolini, *Acc. Chem. Res.,* 1981, 14, 95 and C. Galli and L. Mandolini, *Eur. J. Org. Chem.,* 2000, 3117.

54. E. Baldwin, *J. Chem. Soc., Chem. Comm.,* 1976, 734.

55. S. England and S. P. Colowick, *J. Biol. Chem.,* 1956, 221, 1019. Pig sequence P10173 used, as held in SwissProt database, 2003. A. Bairoch, B. Boeckman, S. Ferro and E. Gasteiger. *Brief. Bioinform.* 2004, 5, 39. Model built with MOE 2003.04, using Blosum62 sequence scoring and MMFF94 forcefield. 100 models built and best intermediate chosen. Template used was 1YFM.pdb having 67.6% amino acid residue homology using Blosum62 scoring. For 1YFM.pdb see T. Weaver, M. Lees, V. Zaitsev, I. Zaitseva, E. Duke, P. Lindley, S. McSweeny, A. Svensson, J. Keruchenko, I. Keruchenko, K. Gladilin and L. Banaszak, *J. Mol. Biol.,* 1998, 280, 431.

56. Z. Yang, C. W. Lanks and L. Tong, *Structure*, 2002, 10, 951.

57. Y-F. Li, Y. Hata, T. Fujii, T. Hisano, M. Hishihara, T. Kurihara and N. Esaki, *J. Biol. Chem.,* 1998, 24, 273, 15035.

58. Nardi-Die, T. Kurihara, C. Park, M. Miyagi, S. Tsunasawa, K. Soda and N. Esaki, *J. Biol. Chem.,*1999, 30, 274, 20977. See also R. M. de Jong, W. Brugman, G. J. Poelarends, C. P. Whitman and B. W. Dijkstra, *J. Biol. Chem.*, 2004, 12, 279, 11546. See also P. Paneth, *Acc. Chem. Res.,* 2003, 36, 120. See also G. J. Poelarends, H. Seranno, W. H. Johnson and C. P. Whitman, *Biochem.*, 2004, 43, 4082.

59. F. Homsi and G. Rousseau, *J. Org. Chem.*, 1999, 64, 81. See also S. Robin and G. Rousseau, *Eur. J. Org. Chem.*, 2002, 3099.
60. M-C. Roux, R. Paugam and G. Rousseau, *J. Org. Chem.,* 2001, 66, 4304.
61. I. Roberts and G. E. Kimball, *J. Amer. Chem. Soc.,* 1937, 59, 947.
62. P. W. Atkins, *Physical Chemistry,* Oxford University Press, 1988, p. 823.
63. I. Teberekidis and M. P. Sigalas, *Tetrahedron,* 2002, 58, 6171. See also S. Kozhushkov, T. Späth, T. Fiebig, B. Gallard, M-F. Ruasse, P. Xavier, Y. Apeloig and A de Meijere, *J. Org. Chem.,* 2002, 67, 4100.
64. R. S. Brown, *Acc. Chem. Res.,* 1997, 30, 131.
65. W. Larsen and A. V. Metzner, *J. Amer. Chem. Soc.*, 1972, 94, 1614.
66. F. Freeman, *Chem. Rev.,* 1975, 4, 439.
67. P. D. Bartlett and D. S. Tarbell, *J. Amer. Chem. Soc.*, 1936, 58, 466.
68. S. A. Wolf, S. Ganguly and E. Berliner, *J. Org. Chem.*, 1985, 50, 1053.
69. W. G. Young, R. T. Dillon and H. J. Lucas, *J. Amer. Chem. Soc.,* 1929, 51, 2528. See also J. H. Rolston and K. Yates, *J. Amer. Chem. Soc.,* 1969, 91, 1469, 1477.
70. R. M. Carmen, R. P. Derbyshire, K. A. Hansford, R. Kadirvelraj and W. T. Robinson, *Austral. J. Chem.*, 2001, 54, 117
71. E. E. Tamelan and Shama, *J. Amer. Chem. Soc.,* 1954, 76, 2315 and see M. D. Dowle and D. I. Davies, *Chem. Soc. Rev.* 1979, 171.
72. Reference 12, p. 331. See also reference 4, p. 357.
73. S. R. Merrigan and D. A. Singleton, *Org. Lett.,* 1999, 1, 327.
74. Reference 4, p. 355.
75. M-F. Rausse and J. E. Dubois, *J. Org. Chem.,* 1977, 42, 16, 2689. See also M-F. Rausse, *Adv. Phys. Org. Chem.,* 1993, 28, 207.

76. A. McKenzie, *J. Chem. Soc.,* 1912, 6, 2072.
77. S. Chatterjee, V. R. Pedireddi and C. N. Roa, *Tetrahedron Lett.*, 1998, 39, 2843.
78. T. Ogino, H. Yaezawa, O. Yoshida and M. Ono, *J. Chem. Soc., Org. Biomol. Chem.*, 2003, 1, 2771.
79. R. Kuhn and F. Ebel, *Ber.*, 1925, 58, 919.
80. F. Badea, *Reaction Mechanism in Organic Chemistry,* Abacus Press, 1977, 496.
81. E. M. Terry and L. Eichelberger, *J. Amer. Chem. Soc.*, 1925, 47, 1067.
82. R. Kuhn and T. Wagner-Jauregg, *Ber.*, 1928, 61, 481.
83. H. Weiss, *J. Amer. Chem. Soc.*, 1977, 99, 5, 1670.
84. R. P. Bell and M. Pring, *J. Chem. Soc. B,* 1966, 11, 19.
85. C. A. Kingsbury, *J. Org. Chem.*, 1968, 33, 3247.
86. D. S. Tarbell and P. D. Bartlett, *J. Amer. Chem. Soc.,* 1937, 59, 407.
87. A. R. Olson and F. A. Long, *J. Amer. Chem. Soc.,* 1936, 58, 393.
88. J. Young and A. R. Olson, *J. Amer. Chem. Soc.,* 1936, 58, 1157.
89. J. G. Buchanan and I. H. Williams at Bath University, UK and N. Pirinççioğlu at University of Dicle, Turkey.
90. E. Ott, *Ber.*, 1928, 61, 2131. The german paper of Ott was translated by Dr. T. Langer, formerly with EvotecOAI now currently with Astra-Zeneca. See also R. E. Lutz and R. J. Taylor, *J. Amer. Chem. Soc.*, 1933, 55, 1589.
91. J. J. Robinson, J. G. Buchanan, M. H. Charlton, R. G. Kinsman, M. F. Mahon and I. H. Williams, *J. Chem. Soc., Chem. Comm.,* 2001, 5, 485.
92. J. G. Buchanan, M. H. Charlton, M. F. Mahon, J. J. Robinson, G. D. Ruggiero and I. H. Williams, *J. Phys. Org. Chem.*, 2002, 15, 9, 642.
93. I.H. Williams, *Chem. Soc. Rev.,* 1993, 22, 4, 277.
94. Reference 64, p.6.

95. F. Jensen, *Introduction to Computational Chemistry,* 1999, John Wiley and Son, p.4.
96. Reference 94, p.8. See also U. Dinur and A. T. Hagler, *Rev. Comput. Chem.,* 1991, 2, 99.
97. A. R. Leach, *Molecular Modelling: principles and applications*, 2001, Prentice Hall, p. 308. For an example see N. M. Howarth, A Purohit, J. J. Robinson, N. Vicker, M. J. Reed and B.V.L. Potter, *Biochem.*, 2002, 41, 14801.
98. C. W. N. Cumper, *Wave Mechanics for Chemists*, Heinemann, 1962, p.26. See also E. Schrödinger, *Ann. Physik*, 1926, 79, 361. See also J. Simmons, *J. Phys. Chem.,* 1991, 95, 1017.
99. A. J. Cramer, *Essentials of Computational Chemistry*, 2002, John Wiley and Sons, p. 97.
100. J. B. Foresman and Æleen Frisch, *Exploring Chemistry with Electronic Structure Methods*, Gaussian Inc., 1996, Second edition, p. 254.
101. A. Szabo and N. Ostlund, *Modern Quantum Chemistry*, 1989, Dover Publications, p. 41.
102. R. McWeeny, *Coulson's Valence*, 1979, Oxford University Press, p. 53.
103. Gill, *Orbitals in Chemistry,* 2000, Cambridge University Press, p.38. See also P. L. Lang and M. H. Towns, *J. Chem. Educ.*, 1998, 75, 506.
104. Reference 102, p. 20. See also reference 103, p. 11. See also M. Born and J. E. Mayer, *Z. Phys.*, 1932, 1, 75.
105. Reference 101, p. 7. Reference 103, p. 20.
106. Reference 102, p.60. See also reference 99, p. 98 and reference 101, p. 31.
107. J. K. L. MacDonald, *Phys. Rev.*, 1933, 43, 10, 830. See also reference 95, p. 407.
108. Reference 95, p. 53. See also W. Kolos and L. Wolniewics, *J. Chem. Phys.*, 1964, 41, 3663. See also B. T. Sutcliffe, *Adv. Quantum. Chem.,* 1997, 28, 65.

109. Reference 95, p. 58. Reference 101, p. 45. Reference 99, p. 113.
110. Reference 101, p.39. Reference 102, p.101.
111. Reference 101, p.89. Reference 95, p. 58. Reference 97, p. 42. J. C. Slater, *Phys. Rev.*, 1955, 98, 1038. *Ibid* 1930, 36, 57.
112. Reference 101, p.3. Reference 99, p. 97.
113. Reference 101, p. 155. Reference 95, p. 150. See also S. F. Boys, *Proc. Roy. Soc. (London) A*, 1950, 200, 542.
114. See reference 95, p. 159. J. S. Binkey and J. A. Pople, *J. Amer. Chem. Soc.*, 1980, 102, 939. M. J. Frisch, J. A. Pople and J. S. Binkey, *J. Chem. Phys.* 1984, 80, 3265. J. Simmons, *J. Phys. Chem.*, 1991, 95, 1017.
115. Reference 100, p.262. See also reference 99, p. 67.
116. Reference 102, p. 63 and reference 115.
117. Reference 100, p. 116. Reference 102, p.136 .See also C. C. J. Roothaan, *Rev. Mod. Phys*, 1951, 23, 2,
118. Reference 101, p. 137
119. Reference 101, p. 141
120. Reference 99, p. 190. See also reference 101 p. 61, 139 and 231.
121. Reference 100, p. 150.
122. Reference 95, p. 68.
123. J. S. Dewar, E. G. Zoebisch and E. F. Healy, *J. Amer. Chem. Soc.*, 1985, 107, 3902. See also reference 99, p.121.
124. J. J. P. Stewart, *J. Comp. Chem.*, 1989, 10, 221. See also J. J. P. Stewart, *Int. J. Quant. Chem.*, 1996, 58, 113. For a recent application using PM5 see H. I. Omar, Y. Odo, Y. Shigemitsu, T. Shimo and K. Somekawa, *Tetrahedron,* 2003, 59, 8099. See also M. P. Repasky, J. Chandrasekhar and W. Jorgensen, *J. Comp. Chem.*, 2002, 23, 16, 1601.
125. Reference 99, p. 121. Reference 95, p. 81.
126. Reference 95, p. 98.
127. Reference 99, p. 236. See also P. Hohenberg and W. Kohn, *Phys. Rev.*, 1964, 136, B864.

128. Reference 99, p. 239. See also W. Kohn and L. Sham, *J. Phys. Rev.,* 1965, B13, 4274. See also W. Kohn and L. Sham, *Phys. Rev.,* 1965, 140, A1133.
129. Reference 99, p. 234. See also A. D. Becke, *J. Chem. Phys.*, 1993, 98, 5648 and P. J. Stevens, J. F. Devlin, C. F. Chabalowski and M. J. Frisch, *J. Phys. Chem.*, 1994, 98, 11623.
130. Reference 99, p. 251.
131. Reference 99, p. 245.
132. Reference 95, p. 192.
133. J. P. Perdew, K. Burke and M. Ernzerhof, *Phys. Rev. Lett.*, 1996, 77, 3865 and *J. Chem. Phys.,* 1996, 105, 9982. See also A. D. Becke, *J. Chem. Phys.*, 1993, 98, 5648. See also Y. Zhao and D. G. Truhlar, *J. Phys. Chem. A,* 2004, 108, 33, 6908.
134. Reference 98, p. 122. See also E. Clementi and C. Roetti, *At. Data Nucl. Data Tables*, 1974, 14, 177.
135. C. L. Perkeris, *Phys. Rev.*, 1959, 115, 1216.
136. Reference 99, p. 262. See also L. A. Curtiss, K. Raghavachari, G. W. Trucks and J. A. Pople, *J. Chem. Phys.,* 1991, 94, 7221. The G2 test set consisted of 55 molecules with 1st and 2nd row elements.
137. Reference 99, p. 147.
138. Reference 95, p. 160.
139. S. Miertus, E. Scrocco and J. Tomasi, *Chem. Phys.*, 1982, 65, 239. See also J. Tomasi and M. Persico, *Chem. Rev.* 1994, 94, 2027. See A. Klamt, *J. Chem. Soc., Perkin Trans II,* 1993, 799.
140. Reference 99, p. 237.
141. I. Morao, B. Lecea, A. Arrieta and F. P. Cossio, *J. Amer. Chem. Soc.,* 1997, 119, 816. Also J. Sponer, J. Leszcynski, P. Hobza, *J. Phys. Chem.,* 1996, 100, 1965 and see also G. Roa, J. M. Ugalde and F. P. Cossio, *J. Phys. Chem.,* 1996, 100, 9619. See also reference 95, p. 392.
142. Gaussian 98, Revision A.6; M. J. Frisch, G. W. Trucks, H. B. Schlegel, G. E. Scuseria, M. A. Robb, J. R. Cheeseman, V. G. Zakrzewski, J. A. Montgomery, Jr., R. E. Stratmann, J. C.

Burant, S. Dapprich, J. M. Millam, A. D. Daniels, K. N. Kudin, M. C. Strain, O. Farkas, J. Tomasi, V. Barone, M. Cossi, R. Cammi, B. Mennucci, C. Pomelli, C. Adamo, S. Clifford, J. Ochterski, G. A. Petersson, P. Y. Ayala, Q. Cui, K. Morokuma, D. K. Malick, A. D. Rabuck, K. Raghavachari, J. B. Foresman, J. Cioslowski, J. V. Ortiz, B. B. Stefanov, G. Liu, A. Liashenko, P. Piskorz, I. Komaromi, R. Gomperts, R. L. Martin, D. J. Fox, T. Keith, M. A. Al-Laham, C. Y. Peng, A. Nanayakkara, C. Gonzalez, M. Challacombe, P. M. W. Gill, B. Johnson, W. Chen, M. W. Wong, J. L. Andres, C. Gonzalez, M. Head-Gordon, E. S. Replogle and J. A. Pople, Gaussian Inc., Pittsburgh PA, 1998. Gaussian 03, revision B.04, M. J. Frisch, G. W. Trucks, H. B. Schlegel, G. E Scuseria, M. A. Robb, J. R. Cheesemen, J. A. Montgomery, Jr., T. Vreven, K. N. Kudin, J. C. Burant, J. M. Millam, S. S. Iyengar, J. Tomasi, V. Barone, B. Menucci, M. Cossi, G. Scalmani, N. Rega, G. A. Petersson, H. Nakatsuji, M. Hada, M. Ehara, K. Toyota, R. Fukuda, J. Hasegawa, M. Ishida, T. Nakajima, Y. Honda, O. Kitao, H. Nakai, M. Klene, X. Li, J. E. Knox, H. P. Hratchian, J. B. Cross, C. Adamo, J. Jaramillo, R. Gomperts, R. E. Stratman, O. Yazyev, A. J. Austin, R. Cammi, C. Pomelli, J. W. Ochterski, P. Y. Ayala, K. Morokuma, G. A. Voth, P. Salvador, J. J. Dannenberg, V. G. Zakrzewski, S. Dapprich, A. D. Daniels, M. C. Strain, O. Farkas, D. K. Malick, A. D. Rabuck, K. Raghavachari, J. B. Foresman, J. V. Ortiz, Q. Cui, A. G. Baboul, S. Clifford, J. Cioslowski, B. B. Stefanov, G. Liu, A. Liashenko, P. Piskorz, I. Komaromi, R. L. Martin, D. J. Fox, T. Keith, M. A. Al-Laham, C. Y. Peng, A. Nanayakkara, M. Challacombe, P. M. W. Gill, B. Johnson, W. Chen, M. W. Wong, C. Gonzalez and J. A. Pople, Gaussian Inc., Pittsburgh PA, 2003.

143. J. Chandraekhar and W. L. Jorgensen, *J. Amer. Chem. Soc.*, 1985, 107, 2974. See also G. Vayner, K. N. Houk, W. L. Jorgensen and J. I. Bruaman., *J. Amer. Chem. Soc.*, 2005, 126,

9054. See also O. Acevedo and W. L. Jorgensen, *Org. Lett.*, 2004, 6, 17, 2881.

144. Y. Takano and K. N. Houk, *J. Chem. Theory Comp.*, 2005, 1, 70.

145. B. Schegel, *Theor. Chim. Acta.*, 1984, 66, 33. See also C. Peng, P. Y. Ayala, H. B. Schlegel and M. J. Frisch, *J. Comp. Chem,* 1995, 17, 1, 49.

146. Reference 99, p. 181. See also, S. S. Shaik, H. B. Schlegel and S. Wolfe, *Theoretical Aspects of Physical Organic Chemistry: The S_N2 mechanism*, Wiley, New York, 1992, p. 50. See also H. P. Hractchian and H. B. Schlegel, *J. Chem. Theory Comp.*, 2005, 1, 61.

147. Reference 95, p. 316. See also reference 101, Appendix C on p. 437.

148. Mopac93; J. J. P. Stewart, ©Fujitsu Ltd, Tokyo, Japan.

149. CAChe Worksystem Pro6.1.1, Mopac2002 and DGauss contained therein; © 2000-2003, Fujitsu Ltd, Tokyo, Japan also © 1989-2000 Oxford Molecular Ltd, Oxford, UK.

150. MOE 2004.03 software; Chemical Computing group, 1010 Sherbrooke Street, Suite 910, Montreal, Quebec, Canada. http://www.chemcomp.com

151. HyperChem 5.01, © 1996, HyperCube Inc. CA, USA.

152. DS Viewer Pro 5.0 © Acceryls Inc., San Diego, CA, USA.

153. Molekel 4.3; S. Portman and H. P. Lüthi, *Chimica,* 2000, 54, 766.

154. GaussView; Gaussian Inc., Pittsburgh PA, 1998.

155. Molden; G. Schaftenaar, J. H. Noordik, *J. Comput. Aid. Mol. Des.*, 2000, 14, 123.

156. Silicon Graphics Origin 2000 supplied by SGI Inc., USA.

157. CS ChemDraw Pro, © 1985-1997, CambridgeSoft Corp., Cambridge, MA, USA.

158. Reference 95, p. 252.

159. J. R. Atkinson and R. P. Bell, *J. Chem. Soc.,* 1963, 3260.

160. D. Lenoir and C. Chiappe, *Chem. A. Eur. J.*, 2003, 5, 9, 1036.

161. B3LYP/6-31+G(d) calculations performed with Gaussian98A.6 but the images were rendered with HyperChem5.01.
162. I. F. Halverstadt and W. D. Kulmer, *J. Chem. Amer. Soc.*, 1943, 64, 2988. Also Dr. T. G. Nevell, Portsmouth University, UK.
163. C. Chiappe, D. Lenoir, C. S. Pomelli and R. Bianchini, *Phys. Chem. Chem. Phys.*, 2004, 6, 3235. See also R. Herges, A. Papafilippopoulos, K. Hess, C. Chiappe, D. Lenoir and H. Detert, *Angew. Chem. Int. Ed.*, 2005, 44, 1412. See also J. March, *Advanced Organic Chemistry*, fourth edition, p. 738.
164. Reference 99, p.548, 564 and 565.
165. B. J. Lynch and D. G. Truhlar, *J. Phys. Chem. A.*, 2001, 105, 2936. See also S. Parthiban, G. de Oliveira and J. M. L. Martin, *J. Phys. Chem. A.*, 2001, 105, 895. See also A. Dybala-Defratyka, P. Paneth, J. Pu and D. G. Truhlar, *J. Phys. Chem. A.*, 2004, 108, 2475.
166. Y. Kobayashi, M. Kamiya and K. Hirao, *Chem. Phys. Lett.*, 2000, 319, 695.
167. B. J. Lynch, P. L. Fast, M. Harris and D. G. Truhlar, *J. Phys. Chem. A.*, 2000, 104, 21, 4811. See also Reference 99, p. 251
168. Reference 99, p. 251. See also J. Poater, M. Duran and M. Solà, *J. Comp. Chem.*, 2001, 22, 1666.
169. T. Ziegler, *J. Chem. Soc., Dalton Trans.*, 2002, 642. See also O. A. Kurnysheva, N. P. Gritsan and Y. P. Tsentalovich, *Phys. Chem. Chem. Phys.*, 2001, 3, 3677.
170. E. A. Moelwyn-Hughes, *The kinetics of reaction in solution,* Oxford, 1950, p. 135.
171. H. S. Fogler, *Elements of Chemical Reaction engineering,* Prentice-Hall, 1992, p. 109.
172. F. Guest, J H. van Lenthe, K. Schoffel, P. Sherwood, R. J. Harrison, R. D. Amos, R. J. Buenker, M. Dupuis, N. C. Handy, I. H. Hillier, P. J. Knowles, V. Bonacic-Koutecky, W. von Niessen, V. R. Saunders and A. J. Stone, GAMESS-UK, Daresbury Laboratory, Daresbury, 1995-99.

173. B. R. Brooks, R. E. Bruccoleri, B. D. Olafson, D. J. States, S. Swaminathan, M. Karplus, *J. Comp. Chem.*, 1983, 4, 187.
174. F. A. Cotton and G. Wilkinson, *Advanced Inorganic Chemistry,* John Wiley and Sons, 1988, p. 545, 564 and 565.
175. 1ASE.pdb, PDB data bank. H. M. Berman, J. Westbrook, Z. Feng, G. Gilliland, T. N. Bhat, H. Weissig, I. N. Shindyalov, P. E. Bourne, *Nucleic Acids Research,* 2000, 28, 235.
176. K. R. Adam, *J. Phys. Chem. A.*, 2002, 106, 11963.
177. M. D. Shields and G. C. Shields, *J. Amer. Chem. Soc.*, 2001, 123, 7314. See also M. D. Liptak, K. C. Gross, P. G. Seybold, S. Feldgus and G. C. Shields, *J. Amer. Chem. Soc.*, 2002, 124, 22, 6421.
178. Y. H. Jang, L. C. Sowers, T. Cağin and W. A. Goddard III, *J. Phys. Chem. A.*, 2001, 105, 274.
179. Reference 3, p. 356. See also E. P. Serjent and B. Dempsey, *Ionisation Constants of Organic Acids in Aqueous solution,* Pergammon, New York, 1979.
180. K. Okuma, T. Shigetomi, Y. Nibu, K. Shioji, M. Yoshida and Y. Yokomori, *J. Amer. Chem. Soc,* 2004, 126, 9508.
181. Y. Zhao, J. Pu, B. J. Lynch and D. G. Truhlar, *Phys. Chem. Chem. Phys.*, 2004, 6, 673.
182. Y. Zhao and D. G. Truhlar, *J. Chem. Theory Comput.*, 2005, 1, 415.
183. D. C. England and C. G. Krespan, *J. Amer. Chem. Soc.*, 1966, 88, 5582.
184. D. C. Braddock, G. Cansell and S. A. Hermitage, *Synlett*, 2004, 3, 461.

12.1. Appendices A.

Cartesian coordinates of M1 to F8 optimised to four YES optimisation default flags with PCM/B3LYP/6-31+G(d) in Gaussian98A.6. The coordinates for M8 and F8 are those as optimised with PCM/B3LYP/6-31+G(d) as the coordinates for the experimentally obtained bromo-β-

lactone acid. The structures M8x and F8X as isolated in the laboratory and obtained by X-ray crystallography, can be obtained from the CIF file that may be downloaded from reference 91 on the Royal Society of Chemistry website;
http://www.rsc.org/is/journals/current/chemcomm/CC001005.htm

The coordinates for M12 and F12 may be obtained from M11 and F11 by removing the most periphery bromine or replacing the peripheral Br by X. The coordinates for M10 and F10 are similar to M1 and F1 however an extra bromine needs to be attached to the Br present and having a C-C-Br-Br dihedral of 180°.

M1			
Br	0.00000	0.45969	1.51762
C	0.73855	0.45969	-0.51937
C	1.53125	1.71405	-0.76408
C	1.48595	-0.85117	-0.84334
C	-0.73855	0.45969	-0.51937
C	-1.48595	-0.85117	-0.84334
C	-1.53125	1.71405	-0.76408
O	1.67314	-0.87514	-2.08375
O	-1.67314	-0.87514	-2.08375
O	-1.81468	-1.64694	0.05144
O	1.81468	-1.64694	0.05144
H	1.05264	2.61448	-0.37424
H	2.53016	1.61786	-0.32642
H	1.64630	1.82073	-1.85078
H	-1.05264	2.61448	-0.37424
H	-2.53016	1.61786	-0.32642
H	-1.64630	1.82073	-1.85078

M2			
Br	0.00000	0.00000	1.52818
C	0.73501	0.00000	-0.52510
C	1.47472	1.30806	-0.84335
C	1.50157	-1.26415	-0.77809
C	-0.73501	0.00000	-0.52510
C	-1.47472	-1.30806	-0.84335
C	-1.50157	1.26415	-0.77809
O	2.02107	1.97880	0.04751
O	-2.02107	-1.97880	0.04751
O	1.41669	1.47099	-2.08809
O	-1.41669	-1.47099	-2.08809
H	1.64576	-1.33916	-1.86415
H	-1.64576	1.33916	-1.86415
H	0.96700	-2.15528	-0.43765
H	-0.96700	2.15528	-0.43765
H	2.48586	-1.21370	-0.30158
H	-2.48586	1.21370	-0.30158

M3			
C	0.38877	-1.18401	0.40332
C	0.05572	-0.00602	-0.52614
C	0.71680	-0.13456	-1.88949
C	-0.47028	-2.35821	0.39726
C	1.43844	-1.09941	1.47539
C	-1.49174	0.27030	-0.56641
H	0.50339	0.75760	-2.48136
H	1.80036	-0.26043	-1.79482
H	0.30530	-0.99954	-2.41946
O	0.53886	-2.53337	-0.44618
O	-1.39919	-3.01614	0.78169
H	1.62583	-2.09113	1.89848
H	2.37282	-0.68689	1.08027
H	1.08148	-0.44399	2.27728
O	-2.08616	0.12060	0.52847
O	-1.96223	0.61502	-1.67535
Br	0.79004	1.68910	0.28676

M4			
C	1.61316	0.79880	-1.31569
C	0.78981	0.15864	-0.20719
C	1.55520	-1.07906	0.38282
O	2.59984	-0.85040	1.02599
Br	0.59830	1.56776	1.22359
C	-0.61443	-0.24661	-0.58932
C	-1.57993	-0.72781	0.46523
O	-1.31770	0.80401	-1.58045
C	-0.96267	-0.40266	-1.99356
O	-1.04386	-1.03109	-3.01543
O	1.04126	-2.18157	0.06629
H	1.13248	1.69609	-1.71471
H	2.59674	1.06406	-0.92045
H	1.75845	0.07660	-2.13146
H	-1.03552	-1.27386	1.23869
H	-2.33892	-1.38959	0.03703
H	-2.07832	0.13205	0.92576

M5			
O	-1.34463	0.14409	2.02923
C	-0.86386	-0.05942	0.19350
O	-0.05123	-1.25423	-1.58728
C	0.92188	-0.48888	-1.29154
C	0.60668	0.22893	0.05031
O	-1.61572	-2.08477	1.48303
C	-1.32671	-0.91507	1.30107
Br	0.88369	2.20064	-0.15265
C	-1.90223	0.64357	-0.62623
H	-1.48097	0.98345	-1.57444
H	-2.75043	-0.02054	-0.82016
H	-2.26329	1.52189	-0.07902
O	1.99410	-0.31333	-1.88317
C	1.51367	-0.23867	1.17619
H	2.55331	-0.04337	0.89941
H	1.39057	-1.31993	1.32681
H	1.28475	0.27628	2.11266

M6			
C	-1.03977	-0.13570	-1.66733
C	-0.40411	0.12335	-0.31902
C	1.14627	0.16374	-0.15866
C	1.84163	-0.62831	0.92594
C	-0.34145	1.56554	0.16833
O	-1.13566	2.44707	0.38981
O	0.99624	1.59803	0.29955
Br	-1.34395	-0.94617	1.06454
C	1.91171	0.06536	-1.50450
O	2.39259	1.11571	-1.98434
O	1.96372	-1.10935	-1.94893
H	-2.10063	0.13194	-1.63568
H	-0.54771	0.47518	-2.43426
H	-0.93692	-1.18757	-1.94672
H	2.89741	-0.33437	0.96302
H	1.39221	-0.44358	1.90609
H	1.78952	-1.69632	0.69789

M7			
O	0.56739	-2.19850	0.12070
C	-0.81334	-0.28015	-0.47993
C	0.66024	-0.09178	-0.65279
C	1.30864	-1.16649	0.22706
O	2.37844	-1.02162	0.82589
H	1.01740	-1.14573	-2.50046
C	1.21077	-0.15448	-2.07324
H	2.29268	0.00492	-2.03960
H	0.77104	0.60829	-2.72120
Br	0.92689	1.78337	-0.01158
C	-1.41466	-0.58672	0.89986
O	-2.38653	-1.37294	0.83198
O	-0.88920	-0.02629	1.88342
H	-1.59976	-1.05678	-2.24626
C	-1.72375	-0.15035	-1.62328
H	-1.44238	0.68949	-2.27221
H	-2.76829	-0.09784	-1.31265

M8			
Br	0.34286	-0.68575	-1.80886
O	0.34286	-0.68575	1.75059
O	2.49464	-0.68575	0.93164
O	-2.21416	1.74609	0.90864
H	-2.59640	2.52030	1.41421
O	-0.97166	1.46733	2.77784
C	1.33099	-0.40454	0.85885
C	0.41711	0.32384	-0.12328
C	-0.70483	-0.06235	0.90867
C	0.73154	1.77732	-0.41266
H	0.80370	2.35293	0.51887
H	-0.04431	2.22035	-1.04405
H	1.69404	1.84499	-0.92959
C	-1.77147	-1.07682	0.54728
H	-1.31218	-1.99320	0.16808
H	-2.44222	-0.66979	-0.21459
H	-2.35952	-1.32294	1.43864
C	-1.29522	1.13540	1.65777

M10			
C	0.80134	-2.49601	0.12705
C	-0.46682	-2.18729	-0.19988
C	1.92593	-2.11443	-0.82336
O	3.10995	-2.39066	-0.47656
O	1.58411	-1.53437	-1.89735
C	-0.87398	-1.67431	-1.55418
O	-1.14840	-0.38852	-1.71991
O	-1.19450	-2.46476	-2.44832
C	-1.65808	-2.53333	0.66285
C	1.15365	-3.17374	1.42841
Br	-0.60159	0.95098	-0.25762
Br	0.02568	2.76397	1.52121
H	-1.40689	-2.49829	1.72812
H	-2.01871	-3.54784	0.43569
H	-2.49516	-1.84670	0.48499
H	0.89041	-2.55473	2.29859
H	2.22824	-3.36603	1.46415
H	0.62554	-4.13023	1.54360

F1				F2				F3			
Br	0.00000	0.00000	1.52818	C	-0.93777	0.39516	-2.09687	C	-0.30482	0.48727	-1.93508
C	0.73501	0.00000	-0.5251	C	-0.99936	0.46395	-0.59615	C	-0.22963	0.49144	-0.41084
C	1.47472	1.30806	-0.84335	Br	1.56961	0.39156	0.42239	C	1.19591	0.55862	0.14043
C	1.50157	-1.26415	-0.77809	C	-0.21667	-0.54217	0.23487	C	1.60942	1.66419	1.07280
C	-0.73501	0.00000	-0.5251	O	-1.18630	-2.41877	-0.74498	H	0.96579	1.6395	1.96138
C	-1.47472	-1.30806	-0.84335	C	-0.06111	-1.91034	-0.50838	H	1.48227	2.63948	0.59428
C	-1.50157	1.26415	-0.77809	O	1.07673	-2.35653	-0.76137	H	2.64734	1.53283	1.39265
O	2.02107	1.97880	0.04751	C	-1.57102	1.62667	0.05753	O	2.32382	0.31066	-1.00258
O	-2.02107	-1.97880	0.04751	O	-2.50736	0.70895	-0.07266	O	2.57364	-1.61503	0.31095
O	1.41669	1.47099	-2.08809	O	-1.48331	2.74193	0.50645	C	2.10760	-0.56071	-0.04117
O	-1.41669	-1.47099	-2.08809	C	-0.74462	-0.75833	1.64767	Br	-0.96383	-1.30345	0.17601
H	1.64576	-1.33916	-1.86415	H	-1.46168	-0.50164	-2.44388	O	-1.95588	1.38106	1.07251
H	-1.64576	1.33916	-1.86415	H	-1.73151	-1.22813	1.59296	C	-1.11727	1.64649	0.18728
H	0.96700	-2.15528	-0.43765	H	0.10806	0.31949	-2.41681	O	-0.83438	2.7543	-0.33162
H	-0.96700	2.15528	-0.43765	H	-0.82222	0.17929	2.20799	H	-1.35429	0.43584	-2.24089
H	2.48586	-1.21370	-0.30158	H	-1.38261	1.28252	-2.55599	H	0.12438	1.41711	-2.31898
H	-2.48586	1.21370	-0.30158	H	-0.06806	-1.42895	2.18686	H	0.23185	-0.36069	-2.36705

F4				F5				F6			
C	-0.01791	-0.02951	-0.02345	C	0.00000	0.00000	0.00000	C	0.02930	-0.05625	-0.02811
C	-0.02810	0.12414	1.47665	C	0.00000	0.00000	1.50069	C	0.07914	-0.10477	1.47961
C	1.29989	-0.02166	2.18932	C	1.32319	0.00000	2.21665	C	1.42373	0.09618	2.21171
C	2.31237	1.03729	1.79507	C	2.34819	1.00670	1.73403	C	2.47969	1.07527	1.75317
O	-0.87744	1.41953	1.91768	C	-1.27750	0.21758	2.19466	C	-1.25087	0.12968	2.19101
C	-1.29327	0.18637	2.17858	O	-2.16847	-0.46070	2.67590	O	-1.87486	-0.80676	2.71191
O	-2.26068	-0.31665	2.68696	O	-1.09266	1.48045	2.03791	O	-1.50589	1.38214	2.25176
C	1.78790	-1.51021	2.02313	C	1.71824	-1.50542	2.08850	C	1.59227	-1.38710	2.07540
O	3.02350	-1.67964	1.94809	O	2.88395	-1.86474	2.30081	O	2.48848	-2.16561	2.32896
Br	1.01648	0.15027	4.17548	Br	1.07043	0.26271	4.18232	Br	1.14040	0.39900	4.16216
O	0.86464	-2.36060	1.99386	O	0.70524	-2.19540	1.75422	O	0.35910	-1.60813	1.66694
H	0.57565	0.76752	-0.48536	H	0.13644	1.02684	-0.36160	H	0.02383	0.99025	-0.36315
H	-1.03524	0.00931	-0.42348	H	-0.94722	-0.38486	-0.38885	H	-0.88937	-0.53383	-0.38322
H	0.42235	-0.99513	-0.29114	H	0.82136	-0.60662	-0.38987	H	0.89413	-0.55409	-0.47470
H	2.54654	0.94877	0.72735	H	2.53780	0.86696	0.66203	H	2.70058	0.93007	0.68753
H	3.23999	0.88433	2.35002	H	3.28835	0.84728	2.26917	H	3.40453	0.91173	2.31635
H	1.92953	2.04353	1.99438	H	2.00076	2.03111	1.90220	H	2.13820	2.10205	1.90846

F7				F8				F10			
C	0.00000	0.00000	0.00000	C	0.00000	0.00000	0.00000	C	1.91223	-1.90346	0.54122
C	0.00000	0.00000	1.52059	C	0.00000	0.00000	1.51070	C	0.58960	-1.85859	0.29283
Br	1.90826	0.00000	2.11940	Br	1.85838	0.00000	2.18333	C	0.03102	-1.82719	-1.09407
C	-0.73909	1.12069	2.20307	C	-0.74475	1.10253	2.25851	O	-0.52863	-0.77149	-1.67578
C	-1.51151	2.07238	1.38268	O	-0.75269	2.30163	2.27525	O	-0.01010	-2.78565	-1.86244
O	-0.42230	2.73089	1.21187	O	-1.51228	0.24783	2.98913	C	-0.44044	-1.93009	1.35932
C	-0.74298	-1.23633	2.09297	C	-0.94831	-0.94900	2.32455	C	2.91095	-1.74631	-0.54951
O	-1.84183	-0.84986	2.60463	C	-0.30005	-1.84799	3.37831	H	0.07648	-2.08789	2.33906
C	-0.56475	1.42889	3.65817	O	0.18838	-2.95137	2.80859	H	-1.01236	-0.99353	1.39797
O	-0.28721	-2.38066	1.97891	C	-2.02184	-1.68693	1.54294	H	-1.14252	-2.75414	1.18556
O	-2.66859	2.22411	1.02965	O	-0.27287	-1.59610	4.56337	H	3.45044	-0.79799	-0.41797
H	-1.03470	0.00948	-0.36933	H	0.47498	-0.90977	-0.38121	H	3.65537	-2.5531	-0.51456
H	0.52894	0.86821	-0.40135	H	0.55472	0.86862	-0.36863	H	2.47069	-1.74221	-1.55577
H	0.48288	-0.91393	-0.35721	H	-1.02300	0.05868	-0.38794	Br	-0.81910	0.77747	-0.71983
H	-1.51482	1.75880	4.09144	H	-2.72486	-2.15959	2.23860	C	2.51762	-2.13565	1.93968
H	-0.19753	0.55547	4.20163	H	-1.56982	-2.46658	0.92207	O	3.76616	-2.19836	2.06109
H	0.16762	2.23675	3.77336	H	-2.58175	-0.99497	0.90660	O	1.77649	-2.29313	2.94652
				H	0.57652	-3.55531	3.49946	Br	-1.40797	2.68580	0.02069

13. Acknowledgements

I would like to express my gratitude and deep thanks to the following:

Prof. J. Grant Buchanan and Prof. Ian. H. Williams of the Chemistry Department of Bath University for support, encouragement and good critique and for making me think about chemistry in a new light. Dr. N. Pirinççioðlu, University of Dicle, Turkey for help with crude lactone and bromohydrin spectra. Dr. G. Ruggiero, Dr. G. Rickard, Dr. S. Husbands and Dr. M. Russell who shared my frustrations and useful tips.

Dr. P. Page, Dr. M. Polywka, Dr. E. Moses, Dr. A. Baxter, Mr. M. Melvin, Dr M. Charlton and Dr. J. Knight for the support and acknowledgement of a good idea at EvotecOAI plc.

Dr. K. Hahnfeld for providing initial inspiration (this is all his fault!); " *he is lucky he is stupid* ". Would like to thank my parents; Mr I. Robinson and Ms C. Hahnfeld BA(HONS), for thinking this was all absurd, but encouraging me to do it nonetheless.

Dr. J. Meeks, Dr. B. Slater-Duke, Dr. D. Osguthorpe, Dr. J. Williams, Dr. S. Parker, Dr P. Plucinski, Dr. R. Lawrence, Dr. D. Fox, Dr M. Karabon, Mr. M. T. Blackman, Mrs. M. Curtis, Dr. W. Ford, Dr. T. G. Nevell and Mr. R. M. Stevens. Mr. I. Riddick, Dr A. Otteridge, Dr M. Paul and Dr A. Medhurst, for encouragement during the years. Miss O. Howlett for coffee and stealing my lighter.

Mr. A. J. Pegler and Mrs. "Peggy" Pegler for providing a sofa on some nights. Mr. R. Li and Mrs. M. Li for their friendship, humour and excellent food. Thank you my dearest friends.

Miss A. Rivett for her understanding, wit and laughter. I couldn't squeeze the word *loggerhea* in anywhere.

Dr James J. Robinson BSc(HONS) PhD MRSC., EvotecOAI plc.